Intercell Interference Mitigation in Long Term Evolution (LTE) and LTE-Advanced

A Thesis
submitted to
University of Technology, Sydney
by

Ameneh Daeinabi

In accordance with
the requirements for the Degree of

Doctor of Philosophy

Faculty of Engineering and Information Technology
University of Technology, Sydney
New South Wales, Australia

February 2015

CERTIFICATE OF ORIGINAL AUTHORSHIP

I certify that the work in this thesis has not previously been submitted for a degree nor has it been submitted as part of requirements for a degree except as fully acknowledged within the text.

I also certify that the thesis has been written by me. Any help that I have received in my research work and the preparation of the thesis itself has been acknowledged. In addition, I certify that all information sources and literature used are indicated in the thesis.

Ameneh Daeinabi

Date: 17.02.2015

ACKNOWLEDGMENT

I would like to express my special appreciation and thanks to my supervisor, A/Prof. Dr. Kumbesan Sandrasegaran, who has been a tremendous mentor for me with his priceless advice on both research and on my career. Also I would like to thank him for encouraging my research and for allowing me to grow as a researcher.

I would also like to thank to my close friends and all CRIN members for their friendly support and caring.

A special thanks to my mother, father, mother-in law and father-in-law. They were always supporting and encouraging me with their best wishes.

At the end I would like to express appreciation to my beloved husband Pejman Hashemi was my support in all times. He was always there cheering me up and stood by me through the good times and bad. Without his encouragement, it would have been impossible for me to complete this research work.

TABLE OF CONTENTS

LIST OF FIGURES

LIST OF TABLES

LIST OF ACRONYMS

4G	Fourth Generation
ABCS	Adaptive Offset Configuration Strategy
ABS	Almost Blank Subframe
ACK	Acknowledgement
AWGN	Additive White Gaussian Noise
BLER	Block Error Rate
BW	Bandwidth
CA	Carrier Aggregation
CC	Component Carriers
CCE	Control Channel Element
CCU	Cell Centre UE
CDF	Cumulative Distribution Function
CDMA	Code Division Multiple Access
CEU	Cell Edge UE
CFI	Control Format Indicator
CG	Correlative Group
Ch	Chromosome
CINR	Channel to Interference and Noise Ratio
CoMP	Coordinated Multi-Point
CQI	Channel Quality Indicator
CRE	Cell Range Expansion
C-RNTI	Cell Radio Network Temporary Identifier
CRS	Common Reference Signal
CS	Common Subband
CSB	Common Subband
DFFR	Dynamic Fractional Frequency Reuse
DL	Downlink
DwPTS	Downlink Pilot Time Slot
EESM	Exponential Effective Signal to interference and noise ratio Mapping
eICIC	Enhanced Intercell Interference Coordination
eNB	Evolved NodeB
EPDCCH	Enhanced-PDCCH

EPS	Evolved Packet System
E-UTRAN	Evolved Universal Terrestrial Radio Access Network
FB	Full Buffer
FDD	Frequency-Division Duplex
FFR	Fractional Frequency Reuse
FLS	Fuzzy Logic System
FQL	Fuzzy Q-Learning
GBR	Guaranteed Bit Rate
GP	Guard Period
HARQ	Hybrid Automatic Repeat Request
HeNB	Home eNBs
HetNet	Heterogeneous Network
HII	High Interference Indication
HoL	Head-of-Line
HS	High Subband
HSPA	High-Speed Packet Access
IAF	Interference Avoidance Factor
IAR	Interference Avoidance Request
IASB	Interference Avoidance Subband
ICI	Intercell Interference
ICIC	Intercell Interference Coordination
IMT	International Mobile Telephony
ISI	Inter-Symbol Interference
ITU	International Telecommunication Union
IZ	Interference Zone
LLCS	Lightly Loaded Control Channel Transmission Subframe
LP-ABS	Low Power ABS
LS	Low Subband
LTE	Long Term Evolution
MCS	Modulation and Coding Scheme
MIB	Master Information Block
MIMO	Multiple –Input Multiple-Output
MME/GW	Mobility Management Entity/Gateway
NACK	Non-Acknowledgement
NCL	Neighbouring Cell List
NEFFR	Novel Enhanced Fractional Frequency Reuse

NP	Nondeterministic Polynomial
NRT	Neighbour Relation Table
OFDM	Orthogonal Frequency Division Multiplexing
OFDMA	Orthogonal Frequency Division Multiple Access
OI	Overhead Indication
PAPR	Peak-to-Average Power Ratio
PBCH	Physical Broadcast Channel
PCFICH	Physical Control Format Indicator Channel
PDCCH	Physical Downlink Control Channel
PDF	Probability Density Functions
PDN	Packet Data Networks
PDSCH	Physical Downlink Shared Channel
PFR	Partial Frequency Reuse
PGW	PDN Gateway
PHICH	Physical Indicator Channel
PLR	Packet Loss Rate
PPP	Poisson Point Process
PRB	Physical Resource Block
PSB	Priority Subband
PSF	Protected Subframes
PUSCH	Physical Uplink Shared Channel
QAM	Quadrature Amplitude Modulation
QCI	QoS Class Identifier
QoS	Quality of Service
QPSK	Quadrature Phase Shift Keying
RAN	Radio Access Network
RB	Resource Block
RE	Resource Element
RE UE	Range Expanded UEs
REG	RE Groups
RF1	Reuse Factor 1
RF3	Reuse Factor 3
RNC	Radio Network Controller
RNTP	Relative Narrowband Transmit Power
RR	Round Robin
RRC	Radio Resource Control

RSRP	Reference Signal Received Power
RSS	Received Signal Strength
SAE	System Architecture Evolution
SC-FDMA	Single Carrier Frequency Division Multiple Access
SDF	Service Data Flow
SerFR	Softer Frequency Reuse
SFFR	Soft Fractional Frequency Reuse
SFR	Soft Frequency Reuse
SGW	Serving Gateway
SINR	Signal to Interference plus Noise Ratio
TB	Transport Block
TDD	Time-Division Duplex
TDM	Time Division Multiplexing
TD-SCDMA	Time Division Synchronous Code Division Multiple Access
TTI	Transmission Time Interval
UE	User Equipment
UL	Uplink
UpPTS	Uplink Pilot Time Slot
VoIP	Voice over Internet Protocol
VS	Video Streaming
WCDMA	Wideband Code Division Multiple Access
ZP-ABS	Zero Power ABS

LIST OF SYMBOLS

$\rho_{m,n}$	Indicator of RB allocation to UE_m
$C_{m,n}$	Maximal bits supported by PRB_n for UE_m
o_{κ_0}	Variance
P_n^i	Transmission power from the serving eNB_i
P_n^j	Transmission power from the interfering picocell j
P_n^k	Transmission power from the interfering macrocell k
$H_{n,m}^i$	Channel gain from the serving eNB i
$H_{n,m}^j$	Channel gain from the interfering picocell j
$H_{n,m}^k$	Channel gain from the interfering macrocell k
ς_{eff}	Effective SINR
Λ	Calibration by means of link level simulations to fit the compression function to the AWGN BLER result
$Hol_m^{'}$	Normalized value of *HoL*
$I_m^{'}$	Normalized value of the interference level
$Q_m^{'}$	Normalized value of *QCI*
$\mu_{L_i^n}$	Membership function for the n^{th} FLS input and the rule i
χ	Learning rate
ϑ	Discount factor
$O_P^{\max}$	Maximum outage probability for picocell
$O_P^{\min}$	Minimum outage probability for picocell
θ_m	Minimum required data rate for macro UE
θ_p	Minimum required data rate for UEs located in picocell basic coverage area
θ_{RE}	Minimum required data rate for RE UE
a	Scalar parameter
a_i	Fuzzy action
b	Scalar parameter
BW_c	Bandwidth allocated to cell centre
BW_e	Bandwidth allocated to cell edge

c	Scalar parameter
$c_{i,n}$	Doppler coefficient of process i of the n^{th} sinusoid
d	Gaussian central value
D	Delay
D^*	The maximum allowed delay for sending data
d_0	Shadow fading correlation distance
D_c	Encoding delay
dir_i	Direction of UE_i
$d_{p,k}$	Delay of the p^{th} packet of UE_k
f_i	The desired objective functions
$f_{i,n}$	Discrete Doppler frequency of process i of the n^{th} sinusoid
f_{max}	Maximum Doppler frequency
$G(t)$	Gaussian random variable
h	Fast fading power gain from the serving eNB
I_M	Interference from neighbouring macro eNBs
I_m	Interference level of UE_m from neighbouring eNBs
I_{max}	Maximum interference
I_p	Interference from neighbouring pico eNBs
K	Vector of actions
L	Offset value
L_i	Modal vector of rule i
L_i^n	Fuzzy label corresponding to a distinct fuzzy set defined in the domain of the n^{th} component S^n
L_m	Pathloss between a macro eNB and UE
loc_i	Location of UE_i
L_p	Pathloss between a pico eNB and UE
M	Transmission power reduction
m	Next state
mc	Number of interfering macrocells
m_{ch}	Number of chromosomes
N	Number of FLS inputs
N_a	Number of ABSs
N_i	Number of sinusoids of process i
N_m	Number of UEs located in macrocell
N_p	Number of UEs located in picocell basic coverage area
N_{packet}	Fixed number of packets

N_{PRB}	Total number of PRBs
N_{RB}	Number of RB allocated to each UE
N_{RE}	Number of UEs located in cell range expanded area
N_s	Number of subframes in each frame
N_U	Total number of UEs in macrocell and its picocells
N_{UE}	Ratio of RE UEs to macro UEs
o_i^k	k^{th} output action for rule i
o_j	Fuzzy output value
O_T	Acceptable outage probability
P	Set of rules
P^*	Maximum packet loss tolerance for video streaming traffic
P_C	Transmission power of *CS*
pc	Number of interfering picocells
P_H	Transmission power of *HS*
P_L	Transmission power of *LS*
P_m	Transmission power of macro eNB
P_N	Noise power
Pos_k	Locations of neighbouring eNB_k
Pos_l	Locations of serving eNB_l
P_p	Transmission power of pico eNB
P_{rf}	Power reduction factor
p_s	Total size of all packets (in bits) arrived into the eNB buffer of UE_k
P_T	Maximum transmission power of each eNB
q	Q-value function
Q	Q-value for the input state vector
Q_m	QCI priority
R	Distance of UE from its serving eNB
r	Distance from serving eNB
r_m	Minimum required data rate
R_m^*	The required transmission rate of macro UEs
R_p^*	The required transmission rate of pico UEs
s	Set of fuzzy rules
S	State vector
$SINR_{RE}$	5 % of CDF of SINR of pico UEs
S_n	n^{th} Subframe
S_p	Size of a packet

t	Time
T	Regular time interval
T^*	The required throughput of macro UEs
$T_{arrival}$	Time that the packet arrives to the buffer
Thr_m	Average throughput of macro UEs
T_{max}	Maximum allowable packet delay
T_{oj}	Output fuzzy set
T_s	Total simulation time
T_{xi}	Input fuzzy set
v_i	Speed of UE_i
w_i	Weighting coefficients
X	Vector
x_i	Fuzzy input value
z	SFR parameter
α	Pathloss
α_i	Degree of truth of rule i
α_m	Macrocell pathloss
α_p	Picocell pathloss
B	Offset value
γ_0	Outage threshold
Δ_{ABS_value}	Output of ABS value module
Δ_{offset_value}	Output of CRE offset value module
ΔP	Additional transmission power
ΔQ	Difference between the old and new values of Q
ε	Greedy parameter
η	Ratio of UEs schedules on ABS
$\theta_{i,n}$	Doppler phase of process i of the n^{th} sinusoid
κ_n	Correlated filtered white Gaussian noise with zero mean of the n^{th} sinusoid
λ_m	Density of macro eNBs
λ_p	Density of pico eNBs
λ_u	Density of UEs
μ	Membership degree
μ_ap_i	Approximated uncorrelated filtered white Gaussian noise
σ	Gaussian standard deviation
ς_i	Vector of the per-RB SINR values
φ	Shadow fading

ψ_i	Shadow fading autocorrelation function
ω	Shadow fading standard deviation

ABSTRACT

Bandwidth is one of the limited resources in Long Term Evolution (LTE) and LTE-Advanced (LTE-A) networks. Therefore, new resource allocation techniques such as the frequency reuse are needed to increase the capacity in LTE and LTE-A. However, the system performance is severely degraded using the same frequency in adjacent cells due to increase of intercell interference. Therefore, the intercell interference management is a critical point to improve the performance of the cellular mobile networks. This thesis aims to mitigate intercell interference in the downlink LTE and LTE-A networks.

The first part of this thesis introduces a new intercell interference coordination scheme to mitigate downlink intercell interference in macrocell-macrocell scenario based on user priority and using fuzzy logic system (FLS). A FLS is an expert system which maps the inputs to outputs using "IF...THEN" rules and an aggregation method. Then, the final output is obtained through a deffuzifaction approach. Since this thesis aims to mitigate interference in downlink LTE networks, the inputs of FLS are selected from important metrics such as throughput, signal to interference plus noise ratio and so on. Simulation results demonstrate the efficacy of the proposed scheme to improve the system performance in terms of cell throughput, cell edge throughput and delay when compared with reuse factor one.

Thereafter, heterogeneous networks (HetNets) are studied which are used to increase the coverage and capacity of system. The focus of the next part of this thesis is picocell because it is one of the important low power nodes in HetNets which can efficiently improve the overall system capacity and coverage. However, new challenges arise to intercell interference management in macrocell-picocell scenario. Three enhanced intercell interference coordination (eICIC) schemes are proposed in this thesis to mitigate the interference problem. In the first scheme, a dynamic cell range expansion (CRE) approach is combined with a dynamic almost blank subframe (ABS) using fuzzy logic system. In the second scheme, a fuzzy q-learning (FQL) approach is used to find the optimum ABS and CRE offset values for both full buffer traffic and video streaming traffic. In FQL, FLS is combined by q-learning approach to optimally select the best consequent part of each FLS rule. In the third proposed eICIC scheme, the best location

of ABSs in each frame is determined using Genetic Algorithm such that the requirements of video streaming traffic can be met. Simulation results show that the system performance can be improved through the proposed schemes.

Finally, the optimum CRE offset value and the required number of ABSs will be mathematically formulated based on the outage probability, ergodic rate and minimum required throughput of users using stochastic geometry tool. The results are an analytical formula that leads to a good initial estimate through a simple approach to analyse the impact of system parameters on CRE offset value and number of ABSs.

Chapter 1

INTRODUCTION

The demand for mobile broadband services with higher data rates and better Quality of Service (QoS) is growing rapidly and this demand has motivated 3GPP to work on two parallel projects: Long Term Evolution (LTE) and System Architecture Evolution (SAE). One of the main goals was to define a simple protocol which involves both the Radio Access Network (RAN) and the network core [1]. LTE/SAE, also called the Evolved Packet System (EPS), can obtain the peak rates of 100 Mb/s and a radio-network delay of less than 5 ms while improving the spectrum efficiency and supporting flexible bandwidth [2]. Moreover, LTE has been introduced as a smooth evolution from earlier 3GPP systems such as Time Division Synchronous Code Division Multiple Access (TD-SCDMA), Wideband Code Division Multiple Access/High-Speed Packet Access (WCDMA/HSPA), and Code Division Multiple Access (CDMA) 2000 towards International Mobile Telephony (IMT)–Advanced as shown in Figure 1.1. The LTE Release 8 has many of the features considered for Fourth Generation (4G) systems [3].

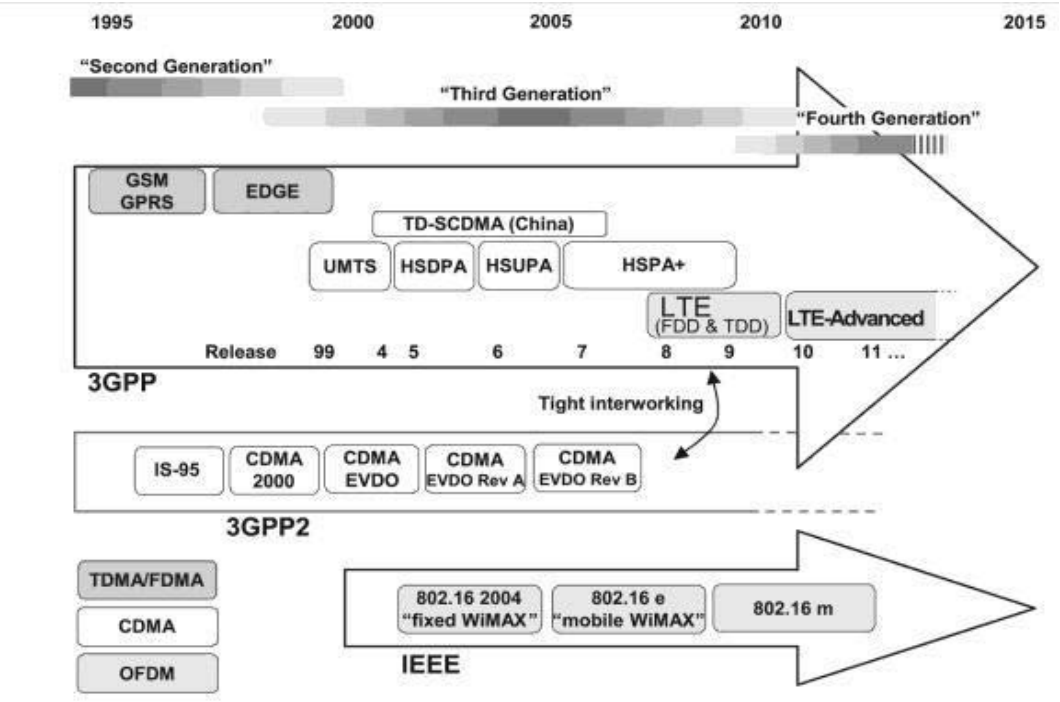

Figure 1.1. Approximate timeline of the mobile communications standards landscape [4]

LTE is based on the new technical principles to satisfy the required data rate, capacity, spectrum efficiency, and latency [5]. The main radio access technologies considered for downlink (DL) and uplink (UL) are Frequency Division Multiplexing Access (FDMA) [1]. However, the multiple access technologies on the air interface are different in DL and UL of LTE systems; Orthogonal Frequency Division Multiple Access (OFDMA) is the DL multiple access technology while for UL, Single Carrier Frequency Division Multiple Access (SC-FDMA) is deployed [5]. OFDM is used to improve the performance of high-speed systems through removing the inter-symbol interference (ISI). Moreover, LTE supports Frequency-Division Duplex (FDD), Time-Division Duplex (TDD) and a wide range of system bandwidths which enables the system to work in a number of different spectrum allocations [3]. The following sub-sections discuss several requirements and key features of LTE.

1.1. LTE Requirements

For LTE systems, 3GPP gathered a set of requirements that must be met by evolved Universal Terrestrial Radio Access Network (e-UTRAN) (see Table 1 [4]). Based on the information in Table 1.1, a significant improvement can be obtained in terms of capacity and user experience from 3G to 4G evolution [4].

1.2. System Description

This sub-section provides the system's description and architecture deployed for 4G networks.

1.2.1. LTE Architecture

The flat architecture of LTE consists of two types of nodes called evolved NodeB (eNB) and Mobility Management Entity/Gateway (MME/GW) [2]. In LTE, a simplified e-UTRAN architecture is used which only comprised of eNBs. In contrast to the hierarchical architecture of the 3G system, the intermediate Radio Access Network (RAN) have been removed from LTE architecture and therefore the LTE eNBs are connected to the core network without using the RAN [6]. The function of RAN has

been performed by eNBs. The main functions of eNB are header compression, ciphering, reliable delivery of packets, admission control and radio resource management. The new flat network architecture can reduce latency better than 3G because eNBs are directly connected to the core network and also the radio network control processing load is contributed into multiple eNBs [2].

Table 1.1. LTE Requirements [4]

	Parameter	Requirement
Downlink	Peak transmission rate	> 100 Mbps
	Peak spectral efficiency	>5bps/Hz
	Average cell spectral efficiency	>1.6-2.1 bps/Hz/cell
	Cell edge spectral efficiency	>0.04-0.06 bps/Hz/cell
	Broadcast spectral efficiency	>1bps/Hz
Uplink	Peak transmission rate	> 50 Mbps
	Peak spectral efficiency	>2.5 bps/Hz
	Average cell spectral efficiency	>0.66-1.0 bps/Hz/cell
	Cell edge spectral efficiency	>0.02-0.03 bps/Hz/cell
System	User plane latency (two way radio delay)	<10 ms
	Connection setup latency	<100 ms
	Operating bandwidth	1.4-20 MHz

All the network interfaces in the LTE architecture are based on IP protocols. An eNB is connected to other eNBs through an X2 interface and its connection to MME/GW entity is performed by an S1 interface which supports a many-to-many relationship between MME/GW and eNBs [2]. Figure 1.2 represents a simple LTE architecture. In addition, two logical gateway entities called the Serving Gateway (SGW) and the Packet data network Gateway (PGW) are defined in LTE. The SGW is a local mobility anchor which forwards and receives packets to/from the eNB serving users. The PGW interfaces with external Packet Data Networks (PDNs) (such as the Internet) and performs several IP related functions such as address allocation, policy enforcement, packet filtering and routing. The MME is a signalling entity which grows the network capacity for signalling and traffic independently. The main functions of MME are: 1) idle-mode UE reachability including the control and execution of paging retransmission, tracking area list management, roaming, authentication, authorization, PGW/SGW

selection, and 2) bearer management including dedicated bearer establishment, security negotiations, and so on [2], [7].

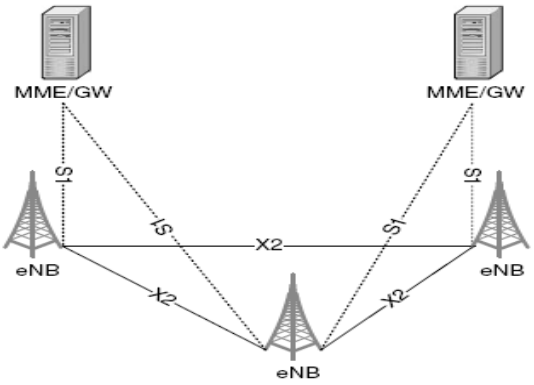

Figure 1.2. LTE architecture [2]

1.2.2. Orthogonal Frequency Division Multiplexing

Multiple access technology is developed to handle multiple users at any given time in cellular network systems. The different fundamentals of multiple access technologies can change the smallest unit, known as radio resources, assigned and distributed among the entities (e.g. power, time slots, frequency bands/carriers or codes). OFDM is a kind of multicarrier transmission technique where available spectrum is split into multiple carriers named subcarriers. Each of these subcarriers is independently modulated by a low rate data stream (see Figure 1.3.). The downlink transmission scheme for e-UTRA FDD and TDD modes is based on OFDMA which is an OFDM-based multiple access technique. OFDM has a lot of benefits described as follows:

1) A multiple carrier transmission technique significantly leads to decrease or even remove the ISI because the symbol time can be made substantially longer than the channel delay spread and the user of cyclic prefix. In other words, the width of each subcarrier is much smaller than the coherence bandwidth of the channel; therefore each user experiences flat fading on each subcarrier. Consequently, OFDM is robust against frequency selective fading.

2) The access to OFDMA implies a high degree of freedom to the scheduler because the radio resource can be dynamically allocated in time and frequency domains based on a selected resource allocation policy.

3) Its spectrum flexibility leads to smooth evolution from already existing radio access technologies to LTE [8].

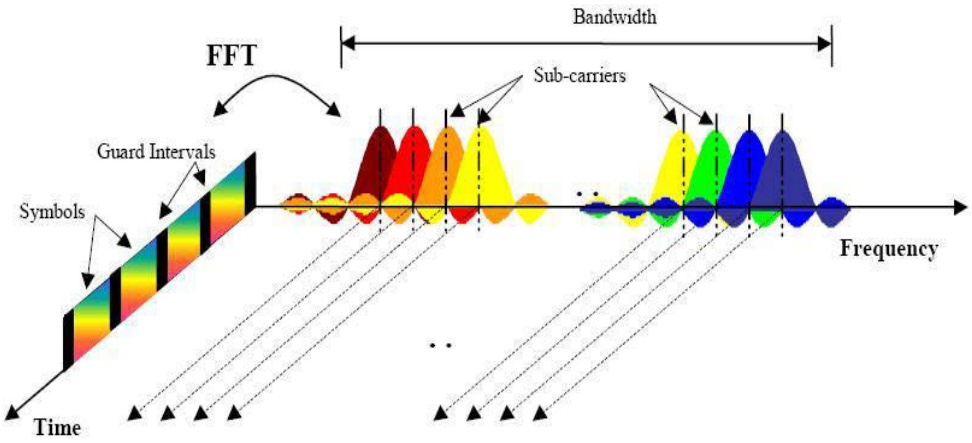

Figure 1.3. Illustration of the OFDM transmission technique [5]

1.2.2.1. Orthogonal Frequency Division Multiple Access

In OFDMA, the multiple access technology is performed by the dynamic subcarrier allocation among different users at each time while for OFDM, each subcarrier is assigned to one specific user for the duration of a call. In OFDMA, a specific time-frequency resource is assigned to each user based on the dynamic bandwidth and adaptive resource allocation technique for multi-user scenario. Dynamic bandwidth allows select different bandwidth based on the particular purposes. For example, the smaller bandwidth leads to easy deployment of a LTE system through GSM bands purchased by a service provider. In addition, the wider bandwidth can be deployed to enhance data rates when the amount of traffic increases. Consequently, OFDMA is deployed in LTE downlink networks. Figure 1.4 illustrates the difference between OFDM and OFDMA.

As an essential principle of e-UTRA, a new scheduling decision is made to determine which users should be allocated to which time/frequency resources for current Transmission Time Interval (TTI) [5]. However, a subcarrier level granularity in resource allocation is difficult due to practical limitations. Therefore, the resources are partitioned in time and frequency domain resources to minimize signalling and simplify resource allocation [9]. In OFDMA, there is a minimal multi-path interference due to

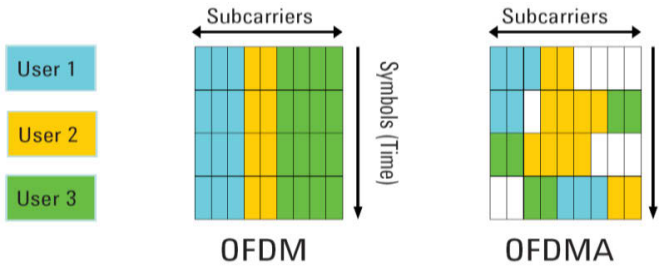

Figure 1.4. A Comparison of OFDM and OFDMA

use of a cyclic prefix of OFDM subcarriers. OFDMA can significantly simplify the equalization problem through changing the frequency-selective channel into a flat channel. Therefore, the sources of SINR degradation in an OFDMA system are the other-cell interference and the background noise [2].

1.2.2.2. Single-Carrier Frequency Division Multiple Access

One of the important characteristics for designing a cost-effective user power amplifier is Peak-to-Average Power Ratio (PAPR). However, due to PAPR properties of an OFDMA signal, using the OFDMA in uplink leads to worse uplink coverage. Therefore, SC-FDMA is deployed in the uplink which has more effective PAPR properties compared to an OFDMA (see Figure 1.5) [5]. Consequently, the objective of using of SC-FDMA is to decrease both PAPR and power consumption at the user side [8]. The SC-FDMA will not be discussed any further because the focus of this thesis is the downlink.

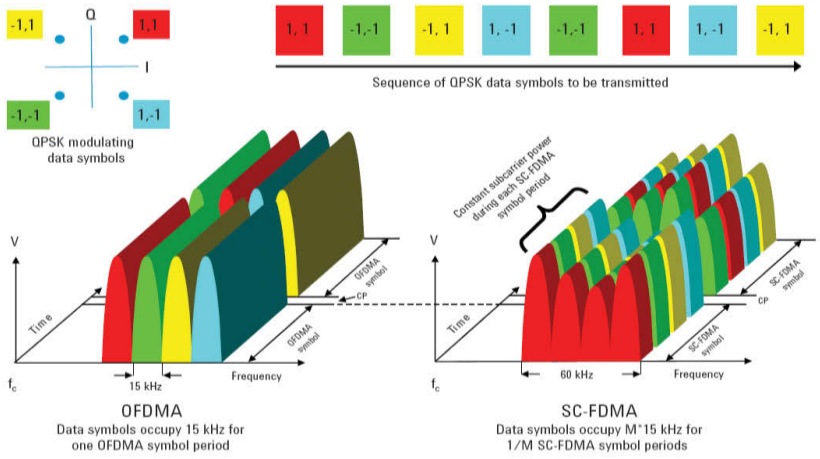

Figure 1.5. Difference between OFDMA and SC-FDMA for the transmission of a sequence of QPSK data symbols [10]

1.2.3. LTE Frame Structure

Since both FDD and TDD are supported by LTE system, two types of frame structures are defined for e-UTRA including frame structure type 1 for FDD mode, and frame structure type 2 for TDD mode.

1) **Frame structure type 1**: a 10 ms radio frame is divided into 20 equally-sized slots of 0.5 ms and each two consecutive slots is called subframe. Therefore, one radio frame consists of ten subframes. Figure 1.6 depicts the structure of frame in which T_s represents the basic time unit corresponding to 30.72 MHz.

2) **Frame structure type 2**: the 10 ms radio frame consists of two half frames with a length of 5 ms which every half-frame is split into five subframes; therefore each subframe equals to 1ms (see Figure 1.7). A non-special subframe is defined as two slots with a length of 0.5 ms. However, the special subframes include Downlink Pilot Timeslot (DwPTS), Guard Period (GP), and Uplink Pilot Timeslot (UpPTS) which are already known from TD-SCDMA and maintained in LTE TDD. The total length of these three fields equals to 1ms such that each of them has its individual lengths. This type supports seven uplink-downlink configurations with either 5 ms or 10 ms downlink to uplink switch point periodicity illustrated in Table 1.2. Note that in this table, "*D*", "*U*" and "*S*" represent a subframe reserved for downlink transmission, a subframe reserved for uplink transmission, and the special subframe, respectively.

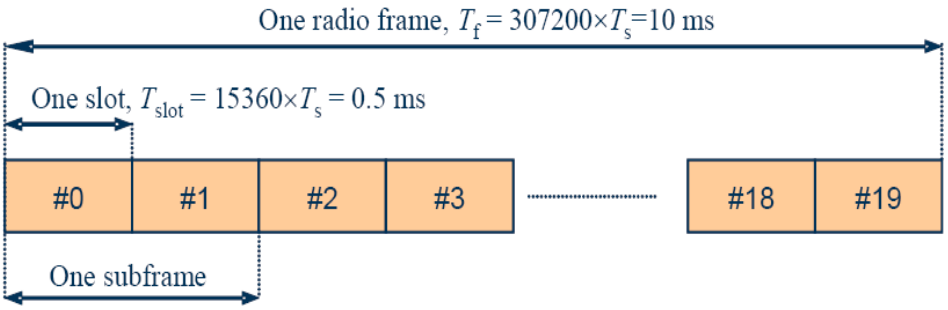

Figure 1.6. Frame structure type 1 [5]

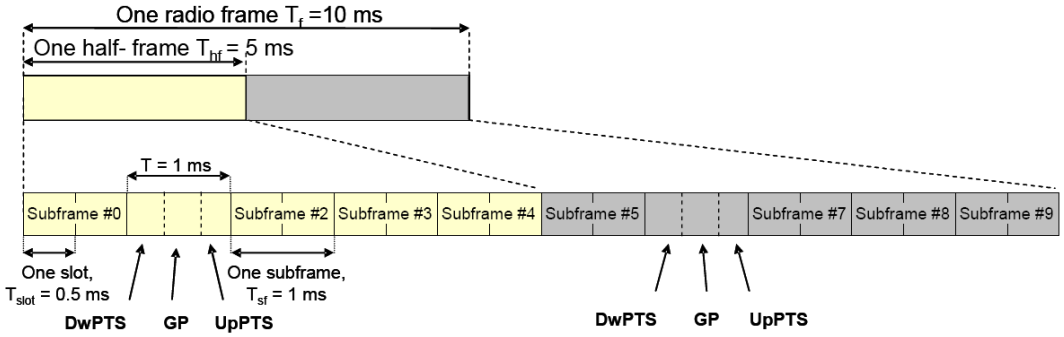

Figure 1.7. Frame structure type 2 (for 5 ms switch-point periodicity) [5]

Based on Table 1.2, in case of 5 ms switch point periodicity, the special subframe exists in both half-frames while in case of 10 ms switch point periodicity of the special subframe exists in the first half frame. Subframes 0 and 5 and DwPTS are always reserved for downlink transmission. UpPTS and the subframe which immediately follows the special subframe are always reserved for uplink transmission [5].

The structure of the resource grid used in both FDD and TDD is shown in Figure 1.8. LTE defines a Resource Block (RB) as the smallest resource allocation unit [11] consisting of 7 OFDM symbols in time domain (0.5 ms duration) and 12 consecutive subcarriers (180 kHz spectrum bandwidth) in the frequency domain for normal cyclic prefix configuration. In each TTI and for each sub-band, the packet scheduler assigns two consecutive RBs to one user in the time domain which is called Physical RB (PRB). Note that a constant spacing of Δf = 15 kHz is considered for subcarriers in LTE. The number of resource blocks is changed for different LTE bandwidths listed in Table 1.3 [5]. A Resource Element (RE) consists of one OFDM subcarrier during one OFDM symbol interval. Therefore, each RB comprises of 84 REs in case of normal cyclic prefix.

Table 1.2. Uplink-Downlink Configurations for LTE TDD [5]

Uplink-downlink configuration	Downlink-to-Uplink Switch-point periodicity	Subframe number									
		0	1	2	3	4	5	6	7	8	9
0	5 ms	D	S	U	U	U	D	S	U	U	U
1	5 ms	D	S	U	U	D	D	S	U	U	D
2	5 ms	D	S	U	D	D	D	S	U	D	D
3	10 ms	D	S	U	U	U	D	D	D	D	D
4	10 ms	D	S	U	U	D	D	D	D	D	D
5	10ms	D	S	U	D	D	D	D	D	D	D
6	5 ms	D	S	U	U	U	D	S	U	U	D

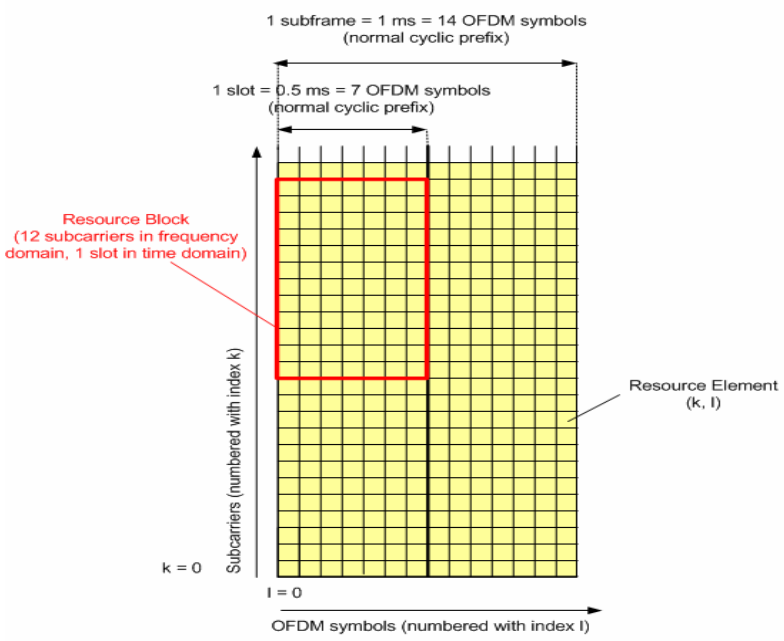

Figure 1.8. Downlink resource grid [11]

Table 1.3. Number of Resource Blocks for Different LTE Bandwidths (FDD and TDD)

Channel Bandwidth (MHz)	1.4	3	5	10	15	20
Number of Resource Blocks	6	15	25	50	75	100

1.2.4. Bandwidth

Spectrum flexibility is a key feature of the LTE system to operate in different geographical areas with the different frequency bands and different bandwidth. It can be implemented on either paired or unpaired frequency bands. In paired frequency bands, a separate frequency band is allocated for uplink and downlink transmissions, respectively, while uplink and downlink share the same frequency band in the unpaired frequency bands. As depicted in Figure1.9, the overall system bandwidth of LTE ranges from 1.4 MHz up to 20 MHz and the corresponding numbers of RBs are 6, 15, 25, 50, 75 and 100. Note that all users shall support the widest bandwidth [3].

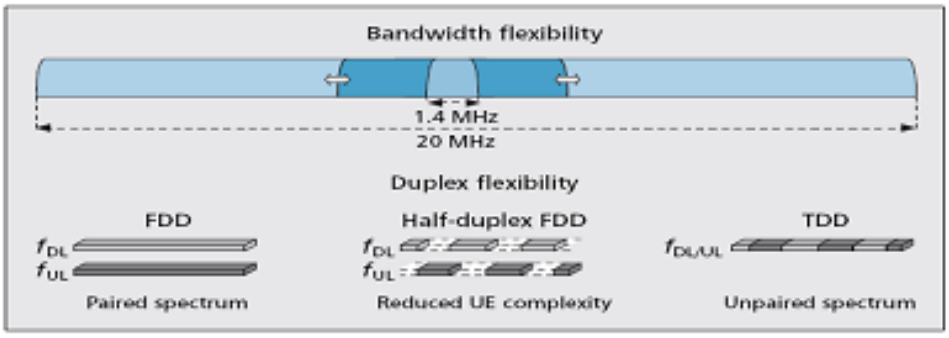

Figure 1.9. LTE spectrum flexibility

1.3. Heterogeneous Architecture

Although LTE Release 8 has many features required for 4G systems, the performance of LTE (Release 8) did not meet IMT-Advanced requirements defined by the International Telecommunications Union (ITU) for 4G, and hence other releases were introduced. The evolved versions (LTE Release 10 and beyond), called LTE-A, can satisfy the requirements defined by IMT-Advanced (see Table 1.4).

By growing the data traffic demand, more improvements are needed for spectral efficiency of LTE-A networks. Therefore, a cheaper, flexible and scalable deployment approach is needed to increase the coverage and capacity of LTE-A networks and improve the broadband user experience within a cell. One solution is the utilization of Heterogeneous Network (HetNet) in LTE-A system [12]. A HetNet consists of macrocells and low power nodes such as femto, pico and relay nodes which can be classified in terms of its transmission powers, antenna heights, the type of access mode provided for users, and the backhaul connection to other cells (see Figure 1.10) [13-14].

1) **Macrocells** are composed of conventional operator-installed eNBs which provide open access mode and covers wide area with few kilometres. In general, the open access mode means that each user in the network can automatically be connected to the eNBs. Macrocells are designed to guarantee the minimum data rate under maximum tolerable delay and outage restrictions. Macro eNBs emit transmission power up to 46 dBm and can serve thousands of customers.

Table 1.4. LTE-Advanced Requirements

Performance metrics	IMT-Advanced Requirements	LTE-Advanced Requirements
Peak data rate	DL 1 Gbps, UL 1 Gbps	DL 1 Gbps, UL 0.5 Gbps
Peak spectral efficiency	DL 15 bps/Hz, UL 6.75 bps/Hz	DL 30 bps/Hz, UL 15 bps/Hz
Bandwidth	Scalable bandwidth, minimum 40 MHz	Scalable bandwidth, 1.4/3/5/10/15/20 MHz per band, up to total 100 MHz
Latency User plane Control plane	 Maximum 10 ms Maximum 100 ms	 Maximum 10 ms Maximum 50 ms
Handover interrupt time Intra-frequency Inter-frequency	 27.5 ms 40 ms (within a band) 60 ms (between bands)	Better than LTE release 8
VoIP capacity Indoor Microcell Base coverage urban High speed	 50 users/sector/MHz 40 users/sector/MHz 40 users/sector/MHz 30 users/sector/MHz	Better than LTE release 8

2) **Picocells** are low power nodes which are deployed by the operator. Pico eNBs have lower transmission powers compared to macro eNB within a range from 23 to 30 dBm. Picocells can improve capacity as well as the coverage of outdoor or indoor regions for environments with inadequate macro penetration (e.g., office buildings). Since picocells work in open access mode, all users can access them.

3) **Femtocells** also called Home eNBs (HeNBs) are unplanned indoor low power nodes deployed by the consumer. Femtocells are equipped with omni-directional antennas and have a transmission power less than 100 mW.

4) **Relay Nodes** are operator-deployed access points to route data from the macro eNB to end users and vice versa. Relay nodes are able to improve coverage in new areas (e.g. Events, exhibitions etc.). In contrast to femtocells and picocells, relay nodes transmit traffic through a wireless link to an eNB. If relay nodes use backhaul communication in the same frequency as the communication to/from

UE on DL/UL, respectively, the relays are defined as in-band. If the backhaul communication is used a different frequency for UE in DL and UL, the relay node is dominated as out-of-band.

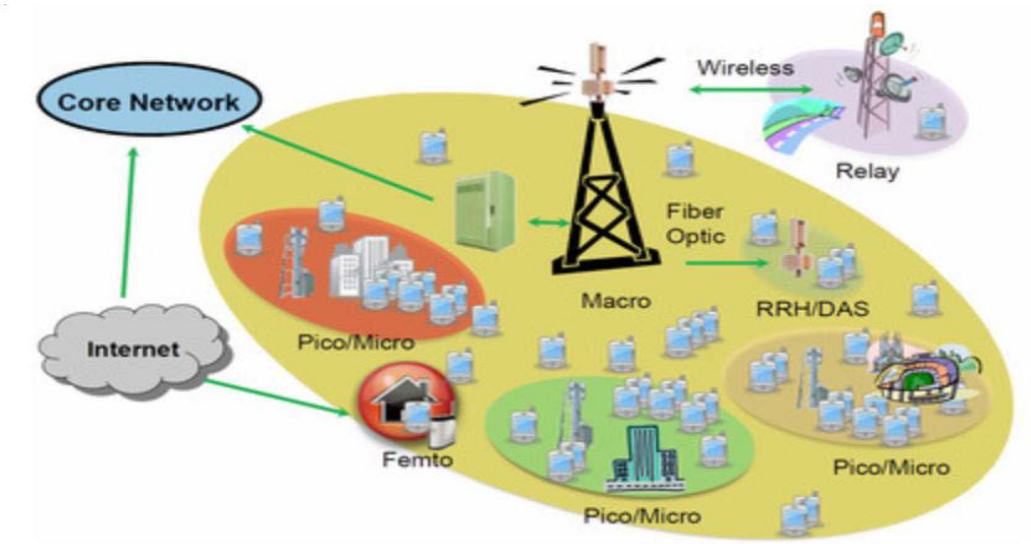

Figure 1.10. Heterogeneous network architecture [15]

Picocells are one of the important low power nodes because picocell can be efficiently deployed in local regions with high traffic volume to improve the overall system capacity and coverage. Therefore, the important role of macrocell and picocell in 4G network motivated us to study the macrocell-picocell scenario as the subsequent contribution of this thesis.

1.3.1. Backhaul

A picocell is connected to the core network via a wired or wireless backhaul. The wired backhaul connection (e.g., fiber) is generally more expensive when compared to wireless backhaul. Four categories can be specified for wireless backhaul spectrum including 1) unlicensed 2.4 and 5 GHz, 2) unlicensed 60 GHz, 3) licensed 6-42 GHz and 70-90 GHz, and 4) operator owned licensed spectrum. Macrocells and picocells can communicate using the standardized messages [16] over the X2 interface.

1.3.2. Frequency Deployment

One important factor considered in HetNet is how picocells and macrocell share the available bandwidth. Two important types of frequency deployments used in LTE-A are described as follows [17]:

1) *Carrier Aggregation* (*CA*): in CA technique, maximum five Component Carriers (CCs) up to 20 MHz are aggregated to obtain a total transmission bandwidth up to 100 MHz. Carriers can be contiguous or non-contiguous frequency in the same band or across multiple bands. In this way, a better utilization of the fragmented spectrum is achieved. Therefore, CA can increase the bitrate by increasing the bandwidth. Each eNB can deploy a CC for a downlink assignment while the data can be carried by other CCs. However, CA can increase complexity of transceiver on the user side such that the user can support the higher bandwidths and aggregate carriers in different frequency bands.

2) *Co-channel*: a subsequent option is co-channel deployment in which all network nodes use the same bandwidth to avoid bandwidth segmentation. Co-channel deployment in HetNets is important because it is applicable for any system bandwidth without high spectrum availability. Co-channel is the feasible deployment when spectrum is limited (20 MHz or less) because each cell can use the total available bandwidth, and hence the maximum peak data rates can be achieved. However, in co-channel deployment, both pico eNBs and macro eNB use the same bandwidth which can lead to severe interference problem. In this thesis, the co-channel was considered as the frequency deployment for HetNet.

1.4. Motivation and Objectives

In cellular mobile networks, the radio bandwidth is one of the limited resources and hence new resource allocation schemes are required to overcome this limitation particularly for high data rate applications. One common technique used in cellular network is frequency reuse where all cells use the same frequency band. Although the frequency reuse approach can increase the system capacity, the system performance is

dramatically degraded due to severe interference from neighbouring cells. As mention in Section 1.2, OFDMA is increasingly deployed in LTE networks to decrease interference and enhance overall system performance. However, similar to other frequency-time multiplexed systems, Intercell Interference (ICI) still leads to a real challenge that limits the system performance due to the interference on PRBs, particularly for users located at the cell edge. Consequently, interference mitigation techniques are crucial to improve the spectrum efficiency of cell edge users and cell centre users.

By increasing demand for ubiquitous coverage and higher data rates, HetNet has been introduced in the LTE-Advanced standardization. However, using low power nodes at the same frequency band as the macrocells presents severe interference problems for open access nodes such as picocells. Moreover, the coverage area of low power nodes may be overshadowed by the transmissions of macrocell. Consequently, the benefits of the introduction of low power nodes for the overall system capacity are limited if interference mitigation technique is not used.

1.4.1. Research Question

Based on the above mentioned challenges, the question that would be highlighted in this thesis is:

"How to design new ICI mitigation schemes to increase cell throughput, user throughput and cell-edge throughput in the macrocell-macrocell and macrocell-picocell configurations?"

The objective of this research is to develop new ICI mitigation techniques in LTE and LTE-A network under the following conditions:

- It shall enable the system to efficiently utilize the radio resources while providing high cell and cell edge throughput.

- It shall support users with full buffer and video streaming traffics while maintaining the individual QoS of users.

- It shall keep the granularity of time (1 TTI) for executing the proposed ICI mitigation technique.

There are several limitations which should be taken into account when a new approach would be proposed.

$$L_1 : \sum_{m,n} \rho_{m,n} \; P_{m,n} \le P_T$$

$$L_2 : \sum_{n=1}^{N} \rho_{m,n} \; C_{m,n} \ge r_m \quad \forall m$$

$$L_3 : if \;\; \rho_{m,n} = 1, \; then \; \rho_{m',n} = 0 \quad \forall m \ne m'$$

where $\rho_{m,n}$ is defined as an indicator to show whether PRB_n has been allocated to UE_m ($\rho_{m,n} = 1$) else ($\rho_{m,n} = 0$). The maximum transmission power of each eNB and transmission power on PRB_n for user m are represented by P_T and $P_{m,n}$, respectively. Moreover, $C_{m,n}$ is maximal bits supported by PRB_n for user m and r_m is the minimum required data rate.

L_1 represents the limitation of the total system transmission power and it means that the total transmission power allocated to PRBs must be smaller than or equal to the maximum transmission power of serving eNB. L_2 states that the data rate for each PRB should satisfy the minimum data rate required for users. Finally, L_3 ensures that each PRB must be only assigned to one user.

1.5. Research Method

This project will adopt a research methodology that combines the theory model with empirical evaluation and refinement of the proposed scheme on MATLAB simulation tool. MATLAB is a useful high-level development environment for systems which require mathematical modelling, numerical computations, data analysis, and optimization methods. This is because MATLAB consists of various toolboxes, specific components, and graphical design environment that help to model different applications and build custom models easier. Moreover, the visualization and debugging features of

MATLAB are simple. Since this thesis aims to mitigate the intercell interference problem using optimization approaches, MATLAB software is selected which covers a wide range of optimization algorithms. Therefore, the task of developing algorithms will be easier and it is not required to recreate the optimization methods. This research followed four steps:

Step1: Study the structure, background and previous proposed techniques related to the topic

The background study involved a comprehensive literature review on the existing work in relevant topic to deeply understand of the characteristic of LTE and LTE-A architecture and the ICI problem. The problems associated with the existing ICI mitigation schemes were investigated. This step consisted of identification of system requirements, limitations and suitable solutions to overcome the problems.

Step 2: Develop a theoretical model for a new ICI mitigation to solve the research problem

Based on requirements in Step 1, a theoretical model for the new ICI mitigation schemes was developed in the downlink LTE and LTE-A systems in step 2. The model ideally captured all the identified requirements for ICI mitigation such as QoS guarantee, system and cell edge throughputs.

Step 3: Model and validate the proposed ICIC scheme using a simulation tool

A computer simulation was developed to model the relevant system and then the new proposed schemes were implemented. Computer simulation was used to evaluate the performance of the proposed schemes and the current ICI mitigation schemes. Subsequently, numerous simulations were provided in different scenarios to validate the correctness of the simulation model. Further modifications were made when the simulation model was validated.

Step 4: Evaluate the performance of the proposed ICI mitigation schemes

Step 4 covered the performance evaluation of the proposed ICI mitigation schemes and the results were compared with the well-known ICI mitigation schemes developed for the LTE and LTE-A. Similar assumptions, simulation parameters, and mobility scenarios were used to evaluate and compare the performance of each scheme. The simulation results were analysed and then further improvements needed for the proposed schemes were applied. The new schemes could satisfy all requirements identified in Step 1 and outperformed well-known ICI mitigation schemes.

1.6. Thesis Overview

In this sub-section, the contribution and brief description of each chapter of this thesis are outlined.

Chapter 2: System Level Simulation of LTE and LTE-A Networks

This chapter describes a general downlink LTE system model, packet scheduling, traffic characteristics and performance metrics that were used to evaluate the performance of the proposed ICI mitigation schemes. Moreover, the relevant underlying assumptions used in this thesis are summarized in this chapter.

Chapter 3: Overview on Macrocell-Macrocell Downlink Intercell Interference Problem and Solutions

This chapter studies the ICI problem in LTE macrocell-macrocell downlink networks and then introduces the well-known ICI mitigation schemes and investigates its performances to find the advantages and disadvantages of each scheme and validates the simulation results provided in the next chapter. Thereafter, a review of intercell interference mitigation schemes in LTE macrocell-macrocell system is presented which focuses on schemes relevance with LTE downlink networks. Finally, a qualitative comparison is performed.

Chapter 4: An Intercell Interference Coordination Scheme in LTE Downlink Networks based on User Priority and Fuzzy Logic System

This chapter proposes a novel joint resource block and transmission power allocation scheme to overcome the ICI problem in macrocell-macrocell scenario. This scheme aims to improve cell throughput, cell edge user throughput and decrease the delay and interference level. The proposed scheme is executed in three phases including (1) calculation of users' priority, (2) scheduling users on the specified subbands based on the priority, and (3) transmission power allocation of PRBs using fuzzy logic system.

Chapter 5: Overview on Macrocell-Picocell Downlink Intercell Interference Challenges and Current Solutions

This chapter presents the concept of intercell interference in heterogeneous networks and describes major technical challenges of intercell interference coordination for picocells. The main focus of this chapter is the intercell interference in time, frequency and power domains when co-channel is used as the frequency deployment. Finally, the most of the current proposed ICI mitigation schemes for macrocell-picocell scenario is reviewed and a qualitative comparison is provided.

Chapter 6: Enhanced ICIC Scheme using Fuzzy Logic System in LTE-A HetNet

The main contribution of this chapter includes two important challenges of HetNet: selecting the optimum CRE offset value and ABS value when the macrocell and picocell share the bandwidth. A dynamic CRE scheme is proposed based on fuzzy logic system because the fixed CRE scheme cannot follow the changes of UE distribution and hence cannot proportionally offload the traffic between the macrocells and picocells. Thereafter, a dynamic almost blank subframe scheme is proposed using fuzzy logic system to mitigate interference occurred on both data and control channels for users located in range expanded. Subsequently, a novel enhanced intercell interference coordination (eICIC) is introduced which is a combination of dynamic CRE and dynamic ABS schemes for further improvement performance. The main goal of the proposed eICIC schemes in Chapters 6 and 7 is to maintain a good trade-off between users located in macrocell and picocells such that the increase of user throughput in picocell/ macrocell does not sacrifice the throughput of users in macrocell/ piocells.

Chapter 7: Enhanced ICIC Scheme in LTE-A HetNet for Video Streaming Traffic

In this chapter, a dynamic eICIC scheme is proposed based on fuzzy q-learning algorithm (FQL) in which a dynamic CRE scheme and a dynamic ABS scheme are combined to mitigate interference. The difference between the proposed scheme based on FQL and the proposed scheme in Chapter 6 is that in the new scheme, it is assumed that the operator has no prior acknowledge about the consequent part of the rules. Moreover, the eICIC scheme proposed in this chapter can support both full buffer and video streaming traffics. Thereafter, a Genetic Algorithm based eICIC scheme is suggested for video streaming traffic to determine the location of ABSs in each frame.

Chapter 8: Analytical Calculation of Optimum ABS and CRE Offset Values using a Stochastic Geometry Analysis

This chapter presents a mathematically tractable macrocell-picocell HetNet framework and then initially obtains the optimum offset value and its minimum and maximum values based on the acceptable outage probability. Thereafter, the required number of ABSs will be formulated based on the ergodic rate and minimum required data rate of users through stochastic geometry tools.

Chapter 9: Conclusions and Future Research Directions

This chapter summarises the thesis contributions and recommends some studies relevant for future research.

1.7. Related Publication

Ameneh Daeinabi, Kumbesan Sandrasegaran and Xinning Zhu, "An Intercell Interference Coordination Scheme in LTE Downlink Networks based on User Priority**,"** *International Journal of Wireless & Mobile Networks* (*IJWMN*), Vol. 5, No. 4, August 2013, pp.49-64.

Yongxin Wang, Kumbesan Sandrasegaran, Xinning Zhu, Cheng-Chung Lin, and **Ameneh. Daeinabi**, "Packet Scheduling in LTE with Imperfect CQI," *International Journal of Wireless & Mobile Networks* (*IJWMN*), V.3, No. 6, June 2013.

Ameneh Daeinabi, Kumbesan Sandrasegaran, and Pantha Ghosal, "A Dynamic Cell Range Expansion Scheme based on Fuzzy Logic System in LTE-Advanced Heterogeneous Networks", 11th *International Australasian Telecommunication Networks and Applications Conference* (*ATNAC*), Melbourne, Australia, November 2014, pp.6-11.

Pantha Ghosal , Kumbesan Sandrasegaran , **Ameneh Daeinabi**, Shouman Barua, and Farhana Afroz, "Interference Cancellation in OFDMA Femtocells: Issues and Approaches," 11th *International Australasian Telecommunication Networks and Applications Conference* (*ATNAC*), Melbourne, Australia, November 2014, pp. 87-92.

Pantha Ghosal , Shiqi Xing , Kumbesan Sandrasegaran, and **Ameneh Daeinabi**, "System Level Simulation for Femto cellular Networks," Accepted in 11th *International Australasian Telecommunication Networks and Applications Conference* (*ATNAC*), Melbourne, Australia, November 2014, pp. 180-185.

Ameneh Daeinabi, and Kumbesan Sandrasegaran, "A Fuzzy Q-Learning Approach for Enhanced Intercell Interference Coordination in LTE-A Heterogeneous Networks," 20th *Asia-Pacific Conference on Communications* (*APCC* 2014), Pattaya, Thailand, October 2014.

Ameneh Daeinabi, and Kumbesan Sandrasegaran, "An Enhanced Intercell Interference Coordination Scheme Using Fuzzy Logic Controller in LTE-Advanced Heterogeneous Networks," 17th *International Symposium on Wireless Personal Multimedia Communications* (*WPMC*), Sydney, Australia, September 2014, pp.1-6.

Ameneh Daeinabi, and Kumbesan Sandrasegaran, "Dynamic Almost Blank Subframe Scheme for Enhanced Intercell Interference Coordination in LTE-A Heterogeneous

Networks," *5th IEEE International Conference on Communications and Electronics* (*ICCE*), Da Nang, Vietnam, August 2014, pp.582-587.

Ameneh Daeinabi, Kumbesan Sandrasegaran and Xinning Zhu, "System Level Simulation to Evaluate the Interference in Macrocell-Picocell Downlink Systems," *16th ACM/IEEE International Conference on Modelling, Analysis and Simulation of Wireless and Mobile Systems* (*MSWIM*), Barcelona, Spain, November 2013, pp.125-131.

Ameneh Daeinabi, Kumbesan Sandrasegaran and Xinning Zhu, "Performance Evaluation of Cell Selection Techniques for Picocell in LTE-Advanced Networks," *Electrical Engineering/Electronics, Computer, Telecommunications and Information Technology Conference* (*ECTI-CON*), Krabi, Thailand, May 2013, pp.1-6.

Ameneh Daeinabi, and Kumbesan Sandrasegaran, "An Enhanced Intercell Interference Coordination Scheme with Cell Range Expansion in LTE-A Heterogeneous Networks," *1st workshop of CRIN*, UTS, Sydney, Australia, July 2013.

Ameneh Daeinabi, Kumbesan Sandrasegaran and Xinning Zhu, "Survey of Intercell Interference Mitigation Techniques in LTE Downlink Networks," 9*th International Australasian Telecommunication Networks and Applications Conference* (*ATNAC*), Brisbane, Australia, November 2012, pp.1-6**.**

Chapter 2

SYSTEM LEVEL SIMULATION OF LTE AND LTE-A NETWORKS

Computer simulation allows a researcher to create a model for large scale and complex mobile cellular system and then investigates system performance under particular parameters and assumptions. For this purpose, a MATLAB system level simulator was developed to model LTE and LTE-A downlink systems. System level simulations are required to reflect the influences of some problems such as cell planning, scheduling, or interference on the performance of the new mobile network technologies.

The development of the system level simulator results in a deeper understanding on the LTE system performance when a new interference management technique is developed. Note that, it is impractical to simulate the whole radio links between the users and eNBs in system level simulations because of the massive power computations. Therefore, the physical layer is represented in system-level simulations by the simplified models give in [18]. This chapter introduces the system model and characteristics considered for the downlink LTE and LTE-Advanced system.

This chapter is organized as follows: Section 2.1 demonstrates the implemented downlink LTE system model. Link performance model and packet scheduling are described in Section 2.2 and Section 2.3, respectively. The descriptions of traffic model characteristics are provided in Section 2.4. The performance metrics to evaluate the system performance are defined in Section 2.5. Section 2.6 represents the pseudo code and block diagram developed for interference simulation. Finally, Section 2.7 summarises this chapter.

2.1 Downlink LTE System Model

The network consists of macro eNBs for LTE and macro and pico eNBs for LTE-A classified in terms of its transmission powers, antenna heights, and the type of access mode provided for a User Equipment (UE). Macro eNBs emit transmission power up to 46 dBm while pico eNBs use lower transmission power than macro eNBs in a range of [23 30] dBm [19]. Since picocells and macrocells work in open access mode, each UE in the overlapped coverage area can automatically be connected to either eNBs.

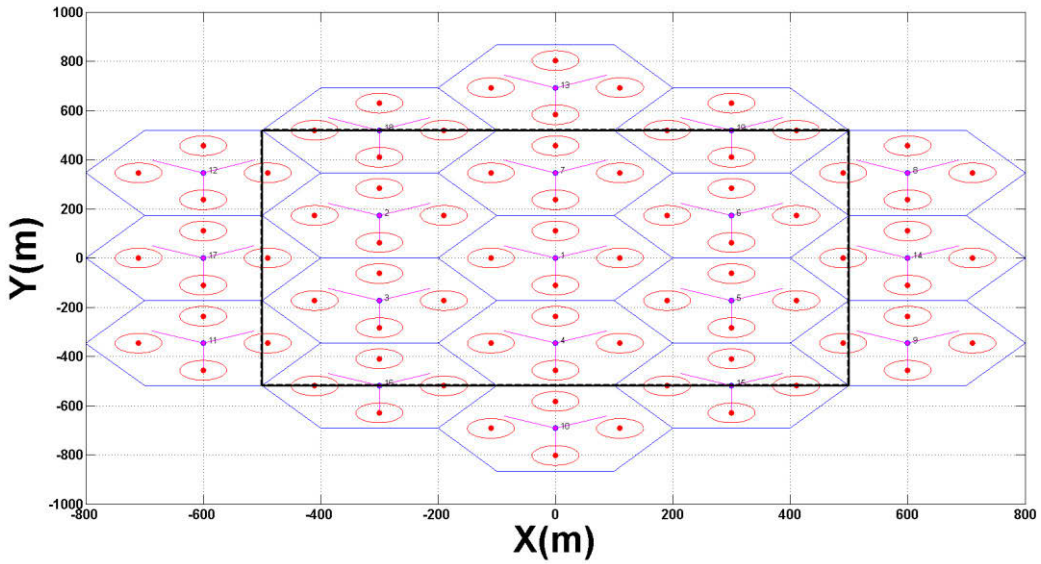

Figure 2.1.Topology network for macrocell- picocell scenario

2.1.1 Mobility Modelling

Each UE moves within the cell at a constant speed and in a constant direction. In this thesis, each UE was assigned a random direction at the beginning of its data session. In addition, an equal speed was assumed for all UEs. The location of UE i at time t is calculated by a complex number in Equation (2.1).

$$loc_i(t) = loc_i(t-1) + v_i(t-1) \times dir_i(t-1) \quad (2.1)$$

where $loc_i(t)$ is the location (complex number) of UE_i at time t, $v_i(t\text{-}1)$ is the speed of UE_i at time t-1 and $dir_i(t\text{-}1)$ is the direction of UE_i at time t-1.

A wraparound function was used to ensure that UEs do not exit from the simulation area during its data session [20]. Figure 2.2 illustrates a wrapped around process where a UE reaches the cell boundary (a), the UE will enter from the opposite side of the cell (b).

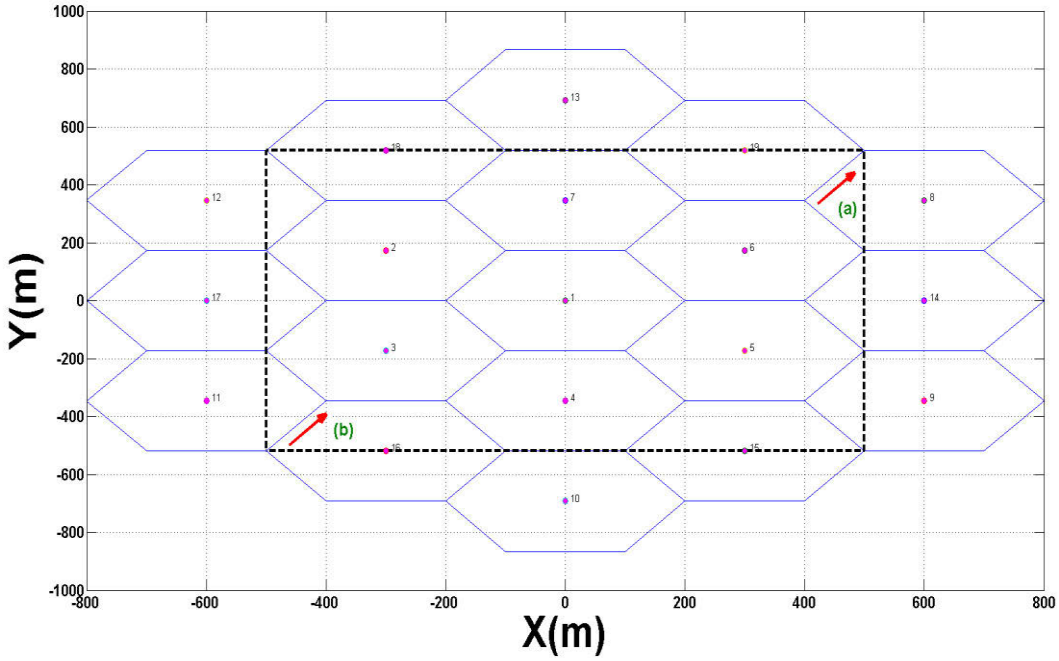

Figure 2.2.An example of a wrapped-around process

2.1.2 Radio Propagation Modelling

When a signal is transmitted through a wireless channel from a transmitter to a receiver, the quality of signal can be affected by different physical factors and leads to change the signal strength experienced at a receiver. In order to show how radio signals are propagated/ transmitted, the radio propagation is modelled in this subsection.

2.1.2.1 Propagation Environment

Different propagation models are considered to model the channel such as indoor office, outdoor- to- indoor, pedestrian and vehicular radio environments. The key parameters to describe each propagation model are time delay, speed and its statistical variability, path loss, operating radio frequency, shadow fading and multipath fading features [4]. In this thesis, the ITU pedestrian *B* was considered as the channel model as shown in Table 2.1.

Table 2.1. International Telecommunication Union (ITU) Channel Models [4]

ITU Pedestrian A		**ITU Pedestrian B**		**ITU Vehicular A**	
Relative Delays (ns)	Relative Mean Power (dB)	Relative Delays (ns)	Relative Mean Power (dB)	Relative Delays (ns)	Relative Mean Power (dB)
0	0	0	0	0	0
110	-9.7	200	-0.9	310	-1.0
190	-19.2	800	-4.9	710	-9.0
410	-22.8	1200	-8.0	1090	-10.0
		2300	-7.8	1730	-15.0
		3700	-23.9	2510	-20.0

Extended Pedestrian A		**Extended Vehicular A**		**Extended Typical Urban**	
Excess Tap Delays (ns)	Relative Mean Power (dB)	Excess Tap Delays (ns)	Relative Mean Power (dB)	Excess Tap Delays (ns)	Relative Mean Power (dB)
0	0.0	0	0.0	0	-1.0
30	-1.0	30	-1.5	50	-1.0
70	-2.6	150	-1.4	120	-1.0
80	-3.0	310	-3.6	200	-0.0
110	-8.0	370	-0.6	230	0.0
190	-17.2	710	-9.1	500	0.0
410	-20.8	1090	-7.0	1600	-3.0
		1730	-12.0	2300	-5.0
		2510	-16.9	5000	-7.0

2.1.2.2 Pathloss

In general, the path loss between a transmitter and receiver can be defined as the ratio of the transmitted power to the received power [21]. However, most mobile networks operate in complex propagation environments that cannot be precisely modelled by free-space pathloss. Therefore, the pathloss model has been developed to predict path loss in wireless environments. In the area of wireless communications, pathloss is a function of distance, frequency and antenna height. In this thesis, the pathloss between a macro eNB and UE (L_m) and a pico eNB and UE (L_p) with distance R in urban area were modelled as follows when carrier frequency was set to 2 GHz [21]:

$$L_m = 128.1+37.6 \log_{10}(R), \quad R \text{ in [Km]} \tag{2.2}$$

$$L_p = 38+30 \log_{10}(R), \quad R \text{ in [m]} \tag{2.3}$$

2.1.2.3 Signal Fading

In general, the fading term depicts the fluctuations in the envelope of a transmitted radio signal. In the wireless channel, large-scale fading is referred to as the slow varying envelop of signal over a long time duration while small scale fading characterizes the rapid fluctuation of the received signal strength over a very short time duration.

2.1.2.3.1 Shadow Fading

Large scale fading can be statistically represented in terms of path loss which is a function of distance and a log-normal distributed variation about the mean pathloss which is called shadow fading. Shadow fading is caused by shielding phenomenon from obstacles in the propagation path between the UE and the serving eNB. It arises due to irregularities of the geographical features of the territory. A one-dimensional random function of time cannot sufficiently model the effects of shadow fading due to the high waveform variations even for small amounts of movement. Therefore, a two-dimensional Gaussian process has been defined to find the dynamics influence of macrocell diversity in a realistic [18]. The experimental result has shown that the autocorrelation function for the fluctuation of the shadow fading component is a reducing function over distance. The equations below are used to determine the shadow fading, φ, for UE_i at time t:

$$\varphi_i(t+1) = \psi_i(t) \times \varphi_i(t) + \omega \times \sqrt{1-\psi_i(t)^2} \times G(t) \tag{2.4}$$

$$\psi(t) = \exp\left(\frac{-v(t)}{d_0}\right) \tag{2.5}$$

where ψ_i (t) is the shadow fading autocorrelation function and $G(t)$ is a Gaussian of UE_i at time t with zero mean. Moreover, $v_i(t)$ represent the speed of UE_i at time t and ω is the shadow fading standard deviation and d_0 is the shadow fading correlation distance.

2.1.2.3.2 Multipath Fading

The signal may arrive at receiver from multiple paths because of reflection and scattering of a radio signal. This effect is called multipath fading. The multipath fading gain in wireless channels with relatively small bandwidth can be characterized as the

Rayleigh-fading channel. The Rayleigh fading is based on a statistical model and is considered as a reasonable model for signal propagation. It is representative of a case with a very large number of multipaths modelled as a time-dependent process [22]. In this thesis, the flat Rayleigh fading is approximated by a complex Gaussian random process [23-24] as follows:

$$\mu\_ap_i(t) = \sum_{n=1}^{N} c_{i,n} \cos(2\pi f_{i,n} t + \theta_{i,n}) \qquad i=1, 2, 3 \tag{2.6}$$

$$c_{i,n} = o_{\kappa_0} \sqrt{\frac{2}{N_i}} \tag{2.7}$$

$$f_{i,n} = f_{\max} \sin(\frac{\pi}{2} \kappa_n) \tag{2.8}$$

where $\mu\_ap_i(t)$ represents the approximated uncorrelated filtered white Gaussian noise with zero mean of process i at time t. Moreover, $c_{i,n}$ and $f_{i,n}$ are the Doppler coefficient and discrete Doppler frequency of process i of the n^{th} sinusoid, respectively. $\theta_{i,n}$ is the Doppler phase of process i of the n^{th} sinusoid and N_i is the number of sinusoids of process i. In addition, κ_n shows the uncorrelated filtered white Gaussian noise with zero mean of the n^{th} sinusoid, o_{κ_0} is the variance (mean power) and f_{max} is the maximum Doppler frequency. Figures (2.3) and (2.4) illustrate the shadow fading and multipath propagation of a UE during the simulation time at a user speed of 3 km/h speed.

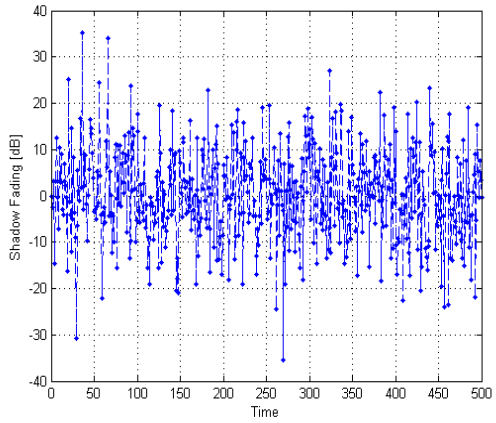

Figure 2.3. Shadow fading of a UE during simulation time at speed 3 Km/h

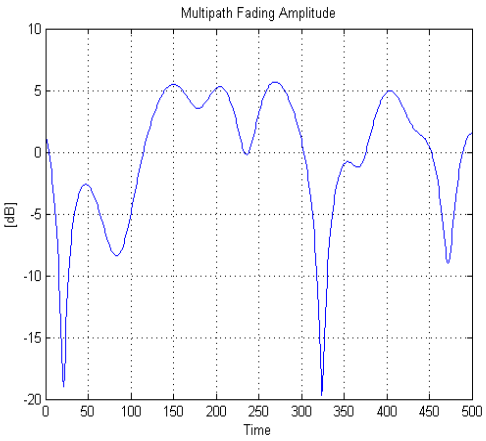

Figure 2.4. Multi path propagation of a UE during simulation time at speed 3 Km/h

2.1.2.4 Signal to Interference plus Noise Ratio

The Signal to Interference plus Noise Ratio (SINR) is an important metric in wireless cellular networks. In order to consider the spatial and time correlation of the channel, the channel gain is modelled by three terms to achieve SINR including: 1) pathloss, 2) shadow fading and 3) multipath fading. In this thesis, The SINRs at UE_m on RB_n in macrocell-macrocell and macrocell-picocell configurations are given by (2.9) and (2.10), respectively:

$$SINR_{n,m}^{macro-macro} = \frac{P_n^i H^i_{n,m}}{\sum_k^{mc} P_n^k H_{n,m}^k \rho_{n,m}^k + P_N} \tag{2.9}$$

$$SINR_{n,m}^{macro-pico} = \frac{P_n^i H^i_{n,m}}{\sum_k^{mc} P_n^k H_{n,m}^k \rho_{n,m}^k + \sum_{j,j\neq i}^{pc} P_n^j H_{n,m}^j \rho_{n,m}^j + P_N} \tag{2.10}$$

where P_n^i, P_n^j and P_n^k are the transmission powers from the serving eNB_i, interfering picocell j and macrocell k on PRB_n, respectively. Moreover, $H_{n,m}^i$, $H_{n,m}^j$ and $H_{n,m}^k$ represent the channel gains from the serving eNB i, interfering picocell j and macrocell k to UE_m on PRB_n. The number of interfering picocells and macrocells are denoted by pc and mc, respectively. $\rho_{n,m}^k$ and $\rho_{n,m}^j$ are set to 1 or 0 to indicate whether the neighbouring cell k or j allocates RB_n to its UEs. P_N is the noise power.

2.2. Link Performance Model

In LTE, the UE sends a Channel Quality Indicator (CQI) report to its serving eNB to help eNB select an appropriate Modulation and Coding Scheme (MCS). The CQI reports are obtained from the downlink received signal quality, typically based on measurement of downlink reference signal. In order to enable the UE to measure the channel quality on a PRB, the reference signals are transmitted in each PRB. In each PRB, four RE, out of the 84 REs, are deployed to transmit reference symbols (in case of single antenna transmission).

In LTE, 15 different MCSs are defined by 15 CQI values. The CQIs use Quadrature Phase Shift Keying (QPSK), 16- Quadrature Amplitude Modulation (QAM), and 64-QAM modulations as shown in Table 2.2. Although a lower order modulation (e.g. QPSK) is more robust against noise and can tolerate higher levels of interference, it provides a lower transmission bit rate. A higher order modulation (e.g. 64 QAM) offers a higher bit rate. However, it is more susceptible to errors because it is more sensitive to interference, noise and channel estimation errors and hence this case can be suitable for the high SINR [4].

Table 2.2. CQI Parameters [4]

CQI index	Modulation	Approximate Code Rate	Efficiency (Information Bit per Symbol)
0	Out of range	0	0
1	QPSK	0.076	0.1523
2	QPSK	0.12	0.2344
3	QPSK	0.19	0.3770
4	QPSK	0.3	0.6016
5	QPSK	0.44	0.8770
6	QPSK	0.59	0.1758
7	16 QAM	0.37	1.4766
8	16 QAM	0.48	1.9141
9	16 QAM	0.6	2.4063
10	64 QAM	0.45	2.7305
11	64 QAM	0.55	3.3223
12	64 QAM	0.65	3.9023
13	64 QAM	0.75	4.5234
14	64 QAM	0.85	5.1152
15	64 QAM	0.93	5.5547

A set of Additive White Gaussian Noise (AWGN) link-level performance curves are deployed to assess the Block Error Rate (BLER) of the received Transport Blocks (TBs). Note that a TB refers to a group of RBs with a common MCS. Then to a SINR-to-BLER mapping function is required to obtain an effective SINR value. It is achieved by mapping a set of sub-carrier-SINRs assigned to the TB to an AWGN-equivalent SINR [18].

The Exponential Effective Signal to Interference and Noise Ratio Mapping (EESM) is the technique which is used to achieve an effective $SINR_{eff}$ of TB. Its result can be mapped to the BLER obtained from AWGN link-level simulations. The EESM model maps the instantaneous channel state experienced by the OFDM subcarriers into a

single scalar value (i.e., an effective SINR) which is used to estimate the BLER for this specific channel state [25]. The effective SINR is achieved by executing the following non-linear averaging of the several PRB SINRs:

$$\varsigma_{eff} = EESM(\varsigma, \Lambda) = -\Lambda \times \ln\left(\frac{1}{N_{PRB}} \sum_{i=1}^{N_{PRB}} e^{\frac{-\varsigma_i}{\Lambda}}\right) \quad (2.11)$$

where N_{PRB} represents the total number of PRBs to be averaged and Λ indicates the calibration by means of link level simulations to fit the compression function to the AWGN BLER results. Moreover, ς is a vector $[\varsigma_1, \varsigma_2, ..., \varsigma_{N_{PRB}}]$ of the PRB SINR values [26].

BLER threshold approach is the simple method to select an appropriate CQI value by UE. The UE would report the CQI value corresponding to MSC that ensures BLER$\leq 10^{-1}$. Therefore, the CQI can be used to adapt MSC to the channel conditions and optimize the time/frequency selective scheduling [18].

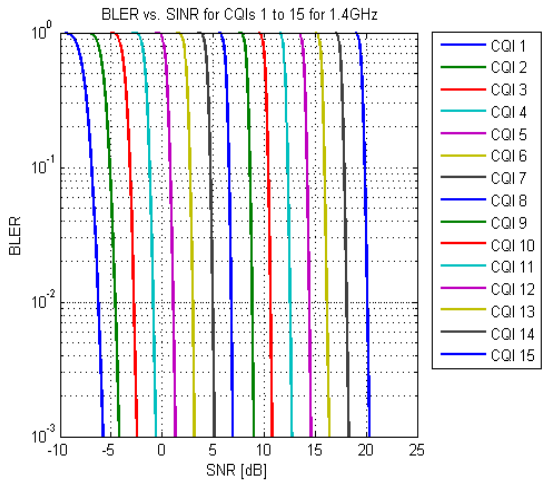

Figure 2.5. SNR–BLER curves for CQI from 1 to 15

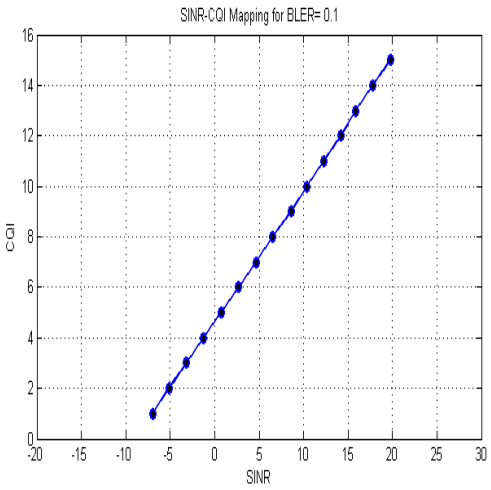

Figure 2.6. SINR to CQI mapping for BLER smaller than 10%

2.3. Packet Scheduling

The aim of packet scheduling is to allocate PRBs to UEs such that the system throughput is maximized while the fairness is maintained. In the downlink, the decision about PRB allocation is performed every TTI through the eNB and then sent to the UE

using the Physical Downlink Control Channel (PDCCH). A PRB is allocated to a UE for each TTI but a UE can be assigned several numbers of PRBs in each TTI. This thesis assumed that the buffer capacity of each UE at the eNB is infinite.

The packet scheduler used in this thesis was round robin (RR) because RR is simple for using in a theoretical model to ensure that all UEs have the same chance to being scheduled. In this algorithm, all UEs are placed in a queue and if a UE has data for transmission, the PRB are allocated to it otherwise the next UE is served. This thesis used RR scheduling to minimize the effect of scheduling on system performance and then investigate the impact of interference management technique in more detail.

2.4. Traffic Models

Two types of traffic models were used in this thesis where a UE was running for both full buffer (FB) and video streaming (VS) traffics. In FB traffic, it is assumed the traffic buffers at eNB are always full of packets awaiting downlink transmission. Hence data payloads are continuously transmitted throughout the simulation interval.

Another type of traffic used in this thesis was VS with average data rates of 256 kbps including a sequence of frames containing a fixed number of packets (N_{packet}) which arrive at a regular time interval (T). The size of a packet (S_p) and the inter-arrival time between two consecutive packets in each frame were assumed to be based on Truncated Pareto distribution [27]. D_c is the encoding delay at the video encoder which represents delay intervals between the packets of a frame. The video streaming generates an average data rate of 256 kbps as shown in Table 2.3.This Table is used to create the VS for simulation.

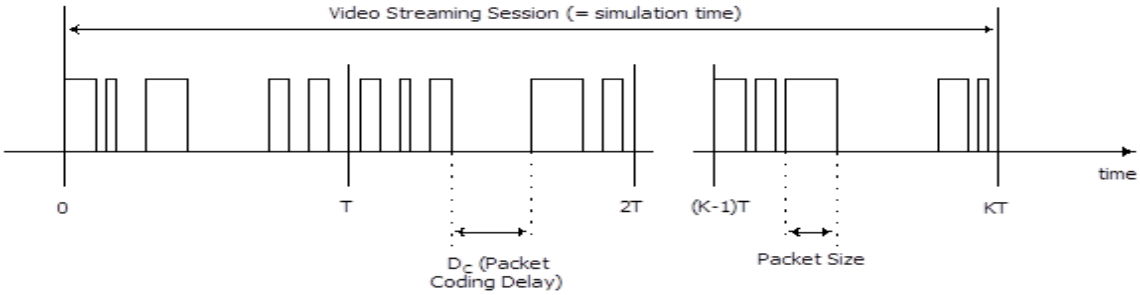

Figure 2.7. Video streaming traffic

When the resided time in the eNB buffer becomes greater than the buffer delay threshold, the packet is discarded. The buffer delay threshold is the maximum allowable time that a packet can wait at the eNB buffer. The defined threshold can be changed based on the traffic models.

Table 2.3. Video Streaming Traffic Parameters with 256 kbps Average Data Rate

Information Types	**Distribution Parameters**	**Distribution Parameters**	**PDF**
Number of packets in a frame (N_{packet})	Deterministic	8 packets	--
Packet size (S_p)	Truncated Pareto Mean = 200 bytes Maximum = 350bytes Minimum = 125 bytes	K=110 bytes α=1.2	$f_x = [\frac{\alpha.k^{\alpha}}{x^{\alpha+1}}]$
Inter-arrival time between the beginning of each frame (T)	Deterministic (Based on 20 fps)	50 ms	--
Inter-arrival time between packets in a frame (D_c)	Truncated Pareto Mean = 3.65 ms Maximum = 6.25 ms	K=2.5ms, α=1.2	$f_x = [\frac{\alpha.k^{\alpha}}{x^{\alpha+1}}]$

2.5. Performance Metrics

Since the ICI problem can restrict the 4G system performance in terms of throughput, the main purpose of ICI mitigation schemes is to improve throughput. Moreover, the implementation requirements for real environment should be taken into account. Here, the most common metrics which were used to evaluate the performance of ICI management techniques are described.

1) *User throughput*: the user throughput is defined as the amount of data sent successfully to a UE in the downlink divided by the simulation time. It is calculated as follows:

- Find number of PRB allocated to each UE (N_{PRB}).
- Obtain the efficiency rate based on the allocated MCS.
- Calculate the number of REs for normal cyclic prefix :

  N_{RE} = 12 (subcarriers) × 7 (OFDMA Symbols) × N_{PRB} × 2 (slots)

  = 168 N_{PRB}
- Compute the Throughput :

  Thr=N_{RE} ×Efficiency rate
- Consider the total approximated overhead

  The overhead is estimated approximately 22.5% for control signalling such as PDCCH and physical Broadcast Channel (PBCH), reference signals, synchronization signals, and coding.

  Thr_{UE}=77.5%×Thr

2) *Cell edge throughput*: it equals as the 5^{th} percentile point of the Cumulative Distribution Function (CDF) of the user throughput which indicates the minimum throughput achieved by 95% of UEs (i.e., only 5% of the UEs experience a lower average throughput than the required data rate) [28].

3) *Average macrocell throughput*: it is defined as the throughput of macrocell without considering picocells.

4) *Average picocell throughput*: it equals the sum of throughputs of picocells distributed in each macrocell.

5) *Average cell throughput*: it is achieved by dividing the total bits correctly delivered over all the active sessions in the system to simulation time. For HetNet, cell throughput is defined as the cell throughput for one macrocell and equals the sum of one macrocell and related picocells.

6) *RE UE throughput*: it equals the 5% of CDF of the user throughput of pico UEs.

7) *Average macro UE throughput:* it equals the average user throughput of UEs connected to macro eNB.

8) *Average UE throughput*: it represents the average user throughput of all UEs in the network.

9) *Percentage of the offloaded UEs*: it indicates the ratio of UEs which are offloaded to picocells to total number of UEs. It was also called user ratio in this thesis.

10) *Outage probability*: it indicates the number of UEs with average SINR smaller than a SINR threshold [29-30]. It means the rate supported by the random fading channel is less than the target value for the UEs to function appropriately

11) *Delay*: it is the average delay of Head-of-Line (HOL) packets of all UEs during simulation time. The HOL packet of a UE is defined as the packet that has the longest resided time in the buffer of eNB.

2.6 Simulation Algorithm

The pseudo code of MATLAB-based simulation and the block diagram proposed to evaluate interference management techniques are illustrated in Figure 2.8. Based on this block diagram, for each TTI, a UE calculates the SINR using transmission power, shadowing, path loss, channel gain, interference value, noise and the interference management technique because the interference management technique specifies the neighbouring eNBs using the same PRBs. By using the obtained SINR and target BLER, UE selects a CQI through link level and then sends CQI to its serving eNB. All assumptions that were used in simulations are summarized in Table 2.4.

2.7. Summary

In this chapter, the system level simulation for LTE and LTE-A downlink system was explained. Moreover, the link level parameters, packet scheduler and traffic models implemented in this thesis were described. The performance metrics used to evaluate the performance of the interference management techniques were defined and the MATLAB-based pseudo code and block diagram used for simulation were developed.

Pseudo code

Initialize (channel, users, BSs…)
For each simulated TTI do
move UEs
For each eNodeB do
- receive UE feedback after a given feedback delay
- schedule users

For each UE do
- Calculate SINR
- MCS allocation
- BLER
- Send feedback

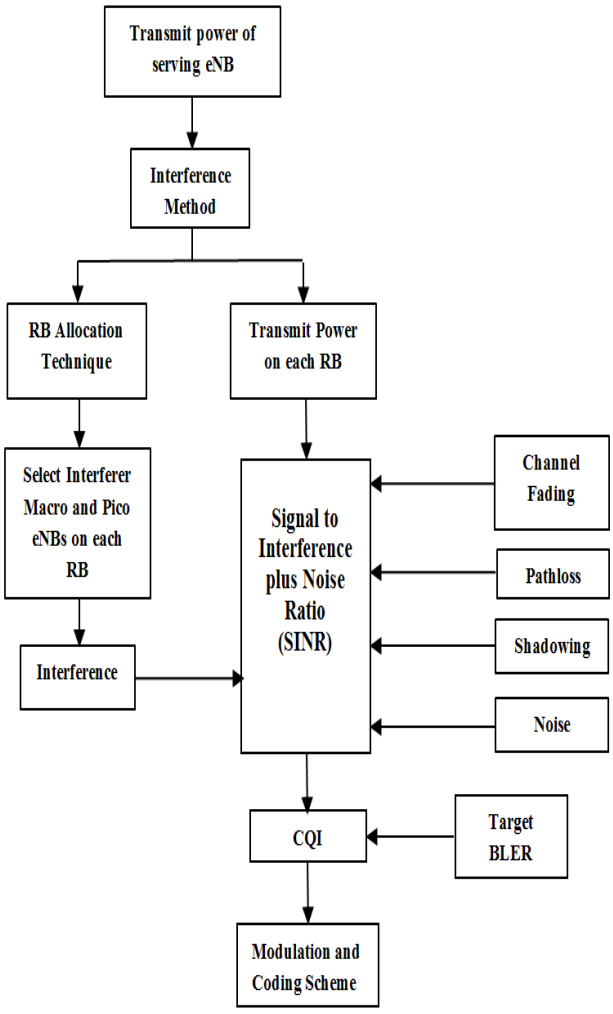

Figure 2.8. Pseudo code and the block diagram used to evaluate the interference management schemes

Table 2.4. Summary of Simulation Parameters and Values

Parameter	**Value**
Network Configuration Parameters	
Layout	7, Hexagonal, wrap around
Inter-site distance	500 m
Carrier frequency	2000 MHz
Traffic model	Full buffer, Video streaming
Number of user	150
L2S interface	EESM
eNodeBs Configuration	
Macro available transmission power	43 dBm For 1.25 MHz, 3 MHz, 5 MHz 46 dBm For 10MHz, 15MHz ,20 MHz
Macro power assigned to pilots/data	2 W/ up to 18 W
Macro noise figure	5 dB
Macro and pico antenna patterns	$A(\theta) = -\min\{12(\frac{\theta}{\theta_{3dB}})^2, 20dB\}$ $-180 \le \theta \le 180, \quad \theta_{3dB} = 65$
Pico transmission power	30 dBm
Pico noise figure	6 dB
Propagation Model	
Macro cell propagation model	$128.1+37.6 \log_{10}(R_{macro}[km])$
Pico cell propagation model	$38+30 \log_{10}(R_{pico}[m])$
Macro shadowing standard deviation	10 dB
Pico shadowing standard deviation	6 dB
Correlated between sites	0.5
Fast fading	ITU Rayleigh
User Configuration	
Noise power density	-174 dBm/HZ
Antenna gain	0 dBi
Antenna pattern	Omni-directional
CQI reporting	1 ms
User speed	3 km/h
Minimum distance between eNB & UE	35 m

Chapter 3

OVERVIEW ON MACROCELL-MACROCELL INTERCELL INTERFERENCE PROBLEM AND SOLUTIONS

Two major categories of interference in cellular mobile system are called intracell interference and intercell interference. Since the 4G systems use OFDMA as the downlink access technology, the orthogonality among subcarriers inherently results in mitigating the intracell interference. However, intercell interference (ICI) caused by using the same frequency in neighbouring cells can restrict the 4G performance. Therefore, the interference management is a critical point to improve the performance of LTE and LTE-A systems.

In this chapter, the ICI problem in LTE downlink network is studied initially and then the well-known ICI mitigation schemes are described. The performances of different ICI mitigation schemes are studied to find the advantages and disadvantages of each scheme and to validate the simulation results provided in next chapter. Thereafter, the most of the proposed ICI mitigation schemes will be classified and reviewed. Finally, a qualitative comparison is provided in terms of cell throughput and cell edge throughput. This comparison can be useful to select the most appreciate scheme for each particular goal.

This chapter is organised as follows: Section 3.1 formulates the intercell interference problem in downlink. Section 3.2 classifies and summarizes the intercell interference mitigation schemes proposed for macrocell-macrocell scenario. A qualitative comparison is provided in Section 3.3. Finally, a summary of the chapter is given in Section 3.4.

3.1. Intercell Interference Formulation

Figure 3.1 shows that the strength of the desired received signal decreases when a UE moves away from the serving eNB and becomes closer to the neighbouring eNB. In this case, the received interference from the neighbouring cell significantly increases. The SINR of UE_m on PRB_n (defined in Section 2.1.2.4) is studied to analyse the influence of ICI on downlink system performance.

$$SINR_{n,m} = \frac{P_n^i H_{n,m}^i}{\sum_{k}^{mc} P_n^k H_{n,m}^k \delta_n^k + P_N} \tag{3.1}$$

Equation (3.1) demonstrates that three important factors have a significant influence on the SINR of each UE including: (1) channel gain from eNB to UE, (2) transmission power of each PRB, and (3) PRB allocation scheme as shown in Figure 3.2. It can be observed that the SINR of UEs close to its serving eNB is higher compared to the UEs which are further away from its serving eNB. Furthermore, UEs at the cell boundary would experience higher interference (denominator term in Equation (3.1)) while the desired signal (numerator term) is low particularly for UEs located in cell edge area. As a result, in this chapter, UEs are classified into Cell Edge UE (CEU) and Cell Centre UE (CCU) to study the interference effect on UEs located in different regions of a cell. For different UE classifications (i.e., either CEU or CCU), alternative power and frequency allocation schemes can be adopted. This allows each UE (particularly CEU) increasing the transmission power which leads to a conflict over the system performance. More specifically, transmitting at higher power for CEU may marginally improve the SINR but results in a significant increase of overall interference in the

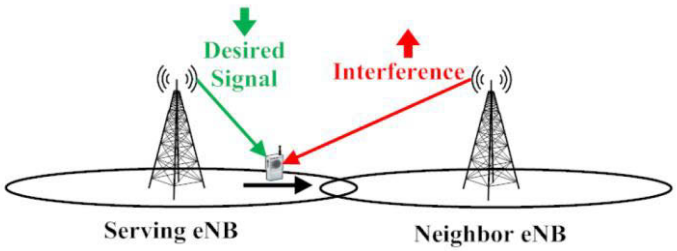

Figure 3.1. Illustration of UE moving far away from its serving eNB

system. Consequently, the higher transmission power has an impact on the overall system performance of all UEs. Therefore, a number of power allocation schemes are proposed to achieve an optimal compromise between the SINR and the interference to improve the system performance. The third factor turns the ICI mitigation scheme into a frequency or PRB allocation schemes. The objective of this optimization is to reduce the ICI and achieve higher spectral efficiency simultaneously, especially for the CEUs. From Equation (3.1), it can be seen that the interference can significantly decrease when the serving cell transmits data on PRB_n that the neighbouring cells do not allocate that PRB_n to its UEs. The granularity of the allocation can be a PRB or a portion of the available bandwidth.

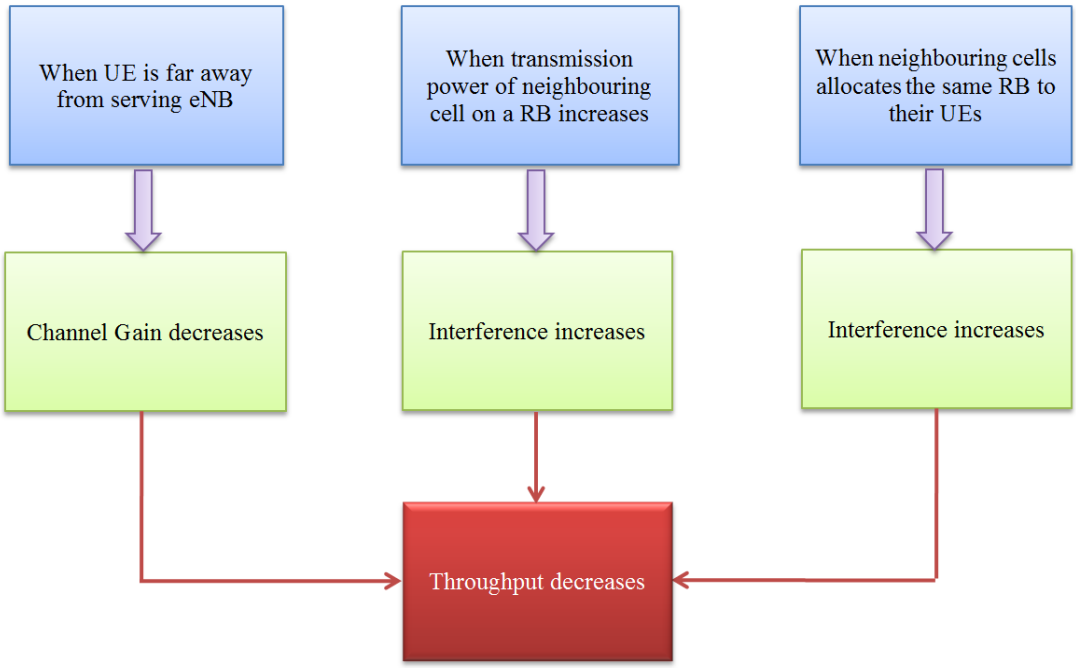

Figure 3.2. Effect of SINR on throughput

3.2. Intercell Interference Mitigation Techniques in Macrocell-Macrocell Scenario

The most of ICI mitigation schemes divide UEs into CEUs or CCUs groups based on static thresholds such as path loss, SINR and geometry factors. However, in a realistic communication environment, the UE distribution and the coverage of a cell may vary from time to time. Therefore the selection of the cell edge bands is difficult and can be

optimized based on the time variation. Reference [31] proposed an ICI mitigation algorithm that can dynamically change cell edge bands based on a threshold value. Then, for each active UE and every time gap (i.e., the update duration of CEU/CCU), the threshold is updated based on the measured SINR and ratio of CEU.

In order to mitigate ICI and enhance the throughput of the CEUs, a wide range of techniques has been presented which are reviewed in this section.

3.2.1. General Classification

ICI mitigation schemes can be divided into three major techniques including averaging, cancellation, and avoidance as shown in Figure 3.3.

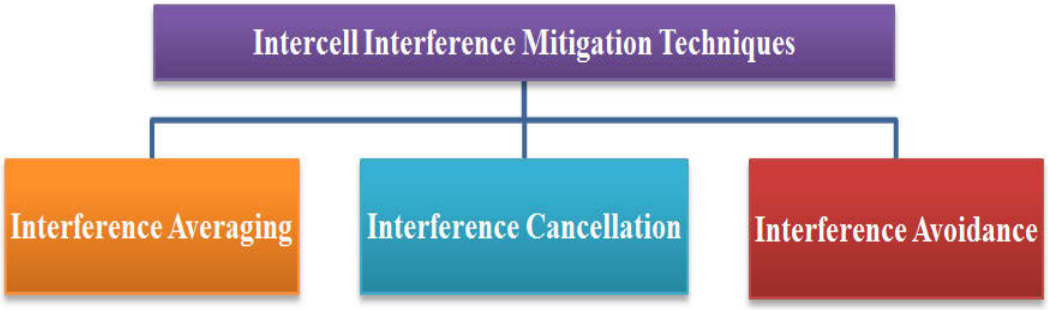

Figure 3.3. Classification of ICI mitigation techniques

1) *Interference Averaging* [32]

This technique attempts to randomize the interfering signals and hence distribute the interference among all UEs such that the CEUs do not always suffer strong ICI during all the transmission period. Moreover, no additional measurements and signalling are needed. However, ICI averaging is unlikely to meet the e-UTRA requirements regarding cell edge throughput because there is no SINR gain for CEUs. Therefore, this approach cannot improve the performance of CEUs. It will leads to impact interference on some UEs which may be initially in higher signal quality conditions. Furthermore, it is mainly beneficial for narrow band services with small packet size and even then, the overall performance benefit is still quite trivial.

2) *Interference Cancellation* [32]

This technique is based on receiver processing and it uses an extra signal processing at the receiver to suppress the interference. In order to perform an interference cancellation, the receiver carries out the channel estimation of the interference signals (using approaches such as minimum mean squared estimation or maximum likelihood sequence estimation on the reference signals) and then subtracts the estimation value from the received signal to obtain the interference signal. Since the data detection is performed on the interference, the cancelled signal is the interference instead of the original received signal, and hence the signal quality can be improved. However, it will impose additional complexity on UE side and additional processing latency. Furthermore, the network needs to be synchronized well in the time domain for the accuracy of the channel estimation. In addition, it may require some extra control signalling for parameters of the interfering signals.

3) *Interference Avoidance* [32]

ICI avoidance technique aims to deploy certain restrictions on the resources used in different cells through a coordinated method. It can provide a higher quality of services to CEUs without sacrificing cell centre throughput. These restrictions can be performed on available time–frequency resources and also on the transmission power assigned to certain time–frequency resources.

Based on the advantages and disadvantages of three ICI mitigation techniques mentioned above, this thesis suggests that the interference avoidance schemes are the most suitable for LTE among the three schemes because it provides higher quality of services to CEUs without sacrificing cell centre throughput with lower complexity. Hence, the interference avoidance will be the focus of this thesis in the next chapters. Interference avoidance schemes can be classified into three time scales (see Figure 3.4) described as follows.

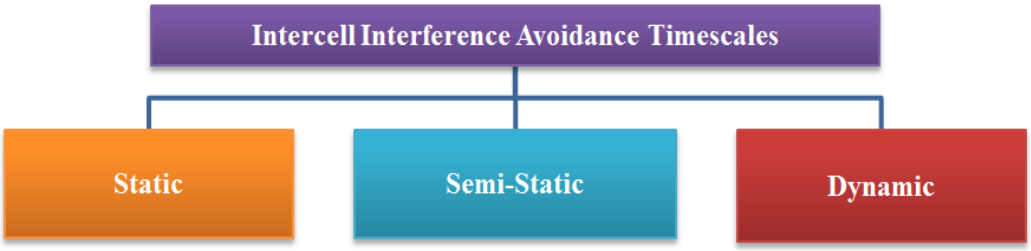

Figure 3.4. Time scales of ICI avoidance techniques

1) *Static*

In the static time scale, the total available resources are divided into several sub-resources and then allocated to each cell for total time [33]. The sub-resources and their power levels are computed during radio planning process. Long-term re-adjustments are performed during the network operation.

2) *Semi Static*

Semi-static schemes usually deploy approaches similar to static time scale but their parameters are varied on demand or infrequently. In the semi static, some resources are constantly allocated while some of the allocated resources are changed based on the load distribution in cell edge and cell centre. The time of reallocation in this time scale technique is set to seconds or several hundred milliseconds [34].

3) *Dynamic*

In the dynamic time scale, when the network condition changes (e.g., traffic variation or load distributions), the system parameters are instantaneously adapted to avoid interference [35]. In contrast to static and semi static, the resources are frequently reallocated to each cell in a very short time period. Based on Table 3.1, dynamic time scale can be an effective approach to avoid interference in the macrocell - macrocell scenario while it is capable to handle the interference from macrocells on low power nodes.

Table 3.1. Comparison among Static, Semi-static and Dynamic Schemes

Schemes	Advantages	Disadvantages
Static	1.Low complexity 2.Low improvement of performance 3.Easy implementation 4.Low overhead 5.No signalling	1.Fit to light load 2.Low spectral efficiency 3.Not fit to varying load 4.Need to pre-planning for frequency
Semi - static	1.Middle overhead 2.Suitable for moderate load 3.Better performance than static scheme	1.High complexity 2.Not easy implementation 3.Fit to slowly varying load 4.Need to pre-planning for frequency
Dynamic	1.Fit to high load 2.Most improvement in performance 3.Fit to varying load 4.Adapt instantly to network changes	1.High complexity 2.Hard implementation 3.High overhead

3.2.2. Classification of Current ICI Avoidance Schemes in Macrocell-Macrocell Scenario

In this section, the different proposed ICI avoidance schemes are classified into two major classes called non-intercell coordination and intercell coordination schemes. Each of classes can include different time scale and different approaches which will be summarized in the next sub-sections. A tree diagram of the current intercell interference avoidance schemes is shown in Figure 3.5.

3.2.2.1. Non- intercell Coordinated Schemes

In non-intercell coordinated schemes, the intercell communication is not needed or is performed at very limited times. This class is further divided into three subclasses: conventional frequency reuse, fractional frequency reuse and autonomous schemes.

3.2.2.1.1. Conventional Frequency Planning

Conventional frequency planning, called Reuse-n, reuses the same band among every *n* cells. Two types of Reuse-n used in LTE are named Reuse Factor 1 and Reuse Factor 3 [2].

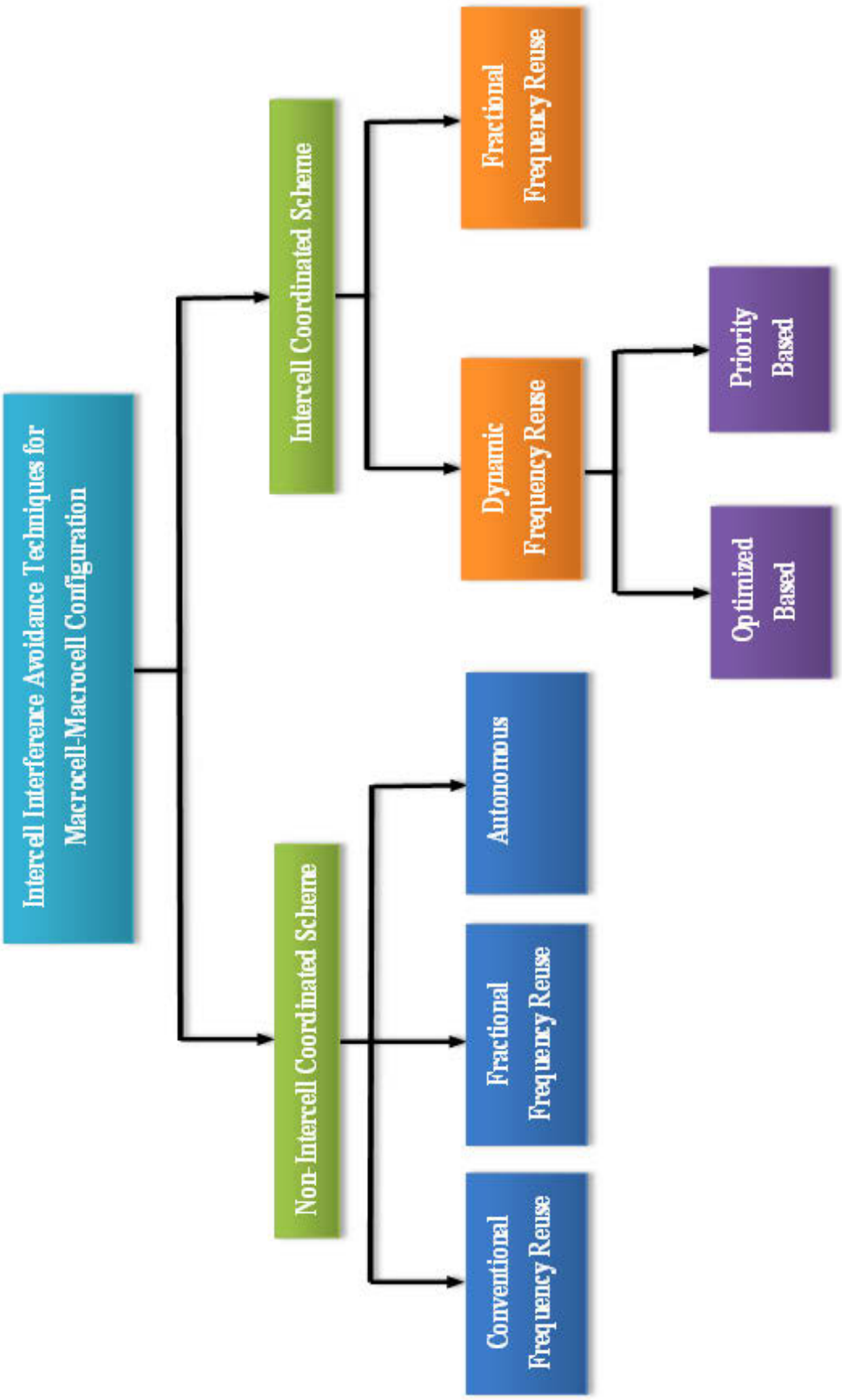

Figure 3.5. Classification of intercell interference avoidance schemes for macrocell-macrocell configuration

3.2.2.1.1.1. Reuse factor one

Reuse Factor 1 (RF1) is the simplest scheme to allocate frequency in a cellular network in which the available bandwidth is reused in each cell without any restriction on frequency or power allocations as shown in Figure 3.6 (a). Although RF1 scheme can obtain the high peak data rate, the interference between neighbouring cells is too high particularly for CEUs [2].

3.2.2.1.1.2. Reuse factor 3

In Reuse Factor 3 (RF3), the total bandwidth is divided into three equal and orthogonal sub-bands, and then each sub-band is assigned to each cell such that neighbouring cells use orthogonal sub-bands (see Figure 3.6 (b)). In this way, the intercell interference between neighbouring cells can be mitigated at the cost of losing large capacity because each cell can only use 1/3 of the available bandwidth [36]. Therefore, the worst cell throughput is achieved by RF3.

3.2.2.1.1.3. Softer frequency reuse

Softer Frequency Reuse (SerFR) is similar to RF1 [37] but the main difference is that SerFR schedules PRBs with more flexibility among CEUs and CCUs. It means that frequency band with a higher power are assigned to CEUs and CCUs use frequency band with lower power as shown in Figure 3.6 (c)**.**

3.2.2.1.2 Fractional Frequency Reuse

The Fractional Frequency Reuse (FFR) techniques have been introduced to enhance the performance of RF1 and RF3 schemes. In FFR based schemes, UEs which experience higher signal quality can use a lower RF schemes (e.g. RF1) while UEs with lower signal quality use higher RF schemes (e.g. RF3) [2]. In FFR approach, frequency and power allocations are combined with different methods. In this sub-class, the FFR schemes where the power is allocated without any coordination are discussed.

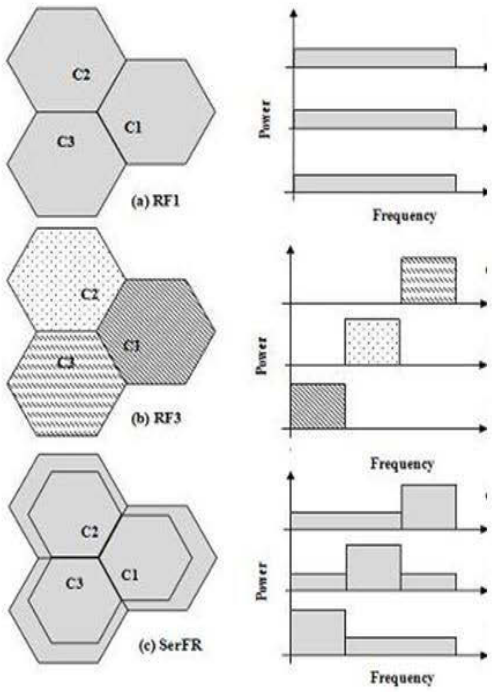

Figure 3.6. Power and frequency allocation for (a) RF1, (b) RF3 and (c) SerFR

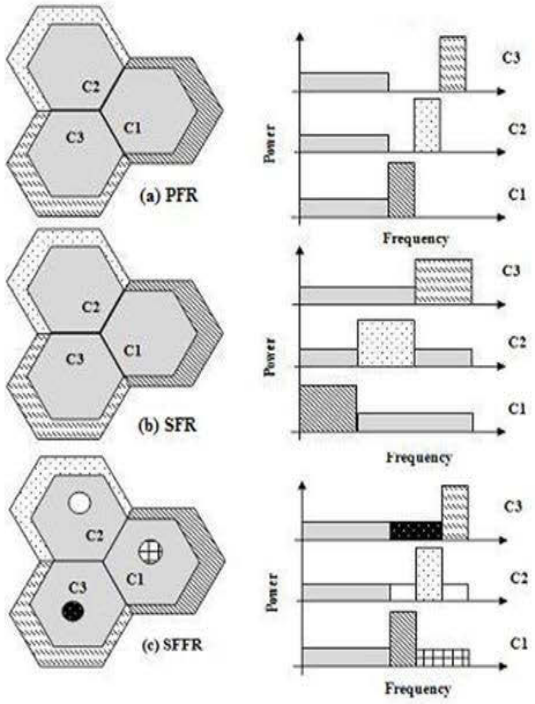

Figure 3.7. Power and frequency allocation for (a) PFR, (b) SFR and (c) SFFR

3.2.2.1.2.1. Partial frequency reuse

Partial Frequency Reuse (PFR) is one type of FFR schemes in which a portion of the resources are restricted such that other neighbouring cells are not allowed to use them. The effective reuse factor of PFR depends on the fraction of the unused frequency band. For instance, for a system with available bandwidth BW, the bandwidth is divided into BW_c and BW_e for cell centre and cell edge region, respectively, as shown in Figure 3.7. (a). The cell centre regions use RF1 while RF3 is deployed in the cell edge region. In this case, the effective frequency reuse factor is given by $\frac{BW}{BW_c + BW_e/3}$.

As a result, the effective reuse factor of PFR scheme is more than one [38]. Although the ICI is completely eliminated for CEUs, available frequency resources may become under-utilization because of using no-sharing bandwidth.

3.2.2.1.2.2. Soft frequency reuse

The idea of Soft Frequency Reuse (SFR) [39] is to present a balance between the RF1 and the PFR schemes. The SFR scheme avoids the high ICI levels related to the RF1

configurations and provides more flexibility to the PFR scheme. The term of "soft reuse" is due to the fact that effective reuse of the scheme can be adjusted by the division of powers between the frequencies used in the centre and edge regions [40].

In SFR, The available bandwidth is divided into orthogonal sub-bands for cell edge regions while the rest of bandwidth is allocated to cell centre regions as depicted in Figure 3.7.(b). In this configuration, CEUs have higher transmission power on cell edge bands whereas CCUs of neighbouring cells have access to this cell edge band only with lower transmission power. Therefore, UEs experience the higher spectral efficiency at the cost of receiving higher ICI. This is because the orthogonality between the cell edge sub-band of one cell and cell centre sub-bands of its neighbouring cells is not guaranteed. Also, different types of SFR schemes have been proposed to improve the system performance in [41-43]. Note that it was assumed that the traffic load is homogeneous in each cell for FFR and SFR schemes.

3.2.2.1.2.3. Soft fractional frequency reuse

SFFR proposed in [44] aims to improve the total cell throughput using FFR schemes. In this scheme, the sub-bands assigned to the cell edge region are reused for the CCUs of adjacent cells with low transmission power levels. The main difference between SFFR and SFR is that the SFFR deploys the common sub-band to improve the throughput of the CCUs.

There are some analyses on FFR schemes [45-47] but [36] provided a stronger analytical comparison among RF1, RF3, PFR and SFR. It demonstrates these schemes can enhance the cell edge throughput while the overall cell throughput decreases dramatically. Therefore, subsequent schemes have been proposed to improve the downlink performance systems. The cell throughput and cell edge throughput of well-known RF schemes are shown in Figures 3.8 and 3.9.

3.2.2.1.3. Autonomous

The autonomous scheme aims to optimize the resource allocation independently for each cell through a selfish optimization manner. Reference [48] proposed four

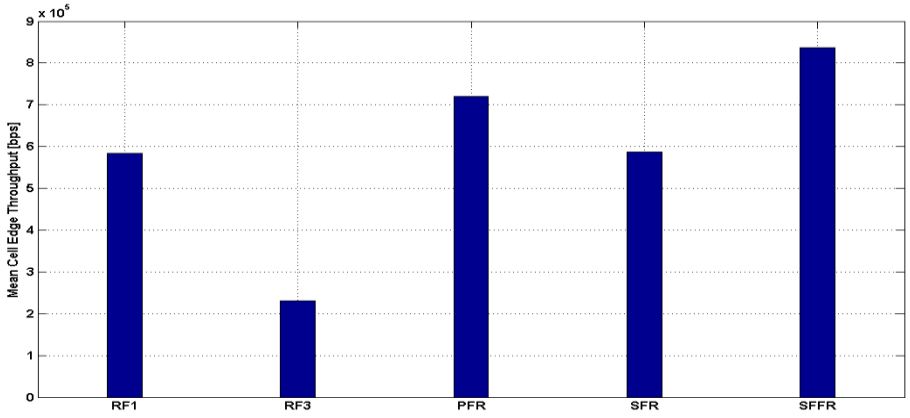

Figure 3.8. Average cell edge throughput of well-known ICI avoidance schemes

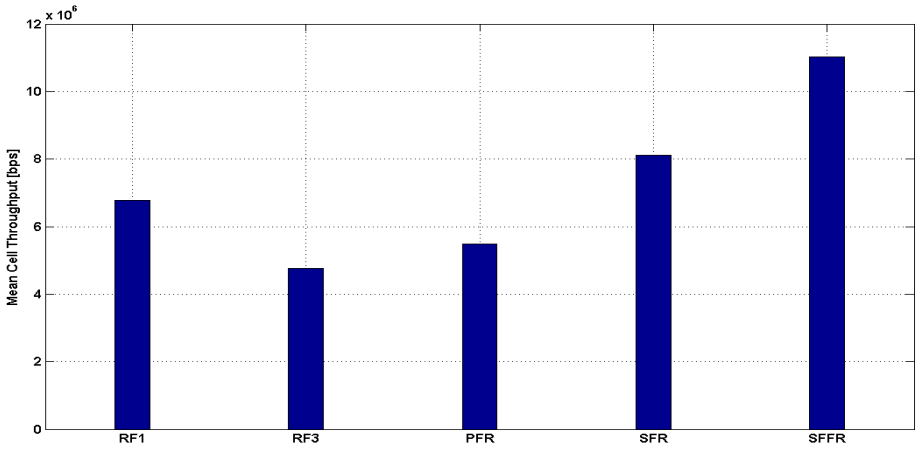

Figure 3.9. Average cell throughput of well-known ICI avoidance schemes

algorithms to optimize the resource allocation using available information in each cell. These algorithms used different parameters including orthogonal RB allocation, weighting factor, TTI or quality estimation of PRBs without intercell coordination.

3.2.2.2. Cell Coordination-based Schemes

Although the schemes discussed in previous sub-sections are suitable for homogeneous networks with the same load in all cells, those schemes are not designed for non-homogeneous networks. Cell coordination schemes have emerged as an efficient solution to cope with the dynamic nature of cellular systems. With cell coordination, interference reduction is realized by real time coordination among all involved cells to avoid that two CUEs located in neighbouring cells using the same resources. Therefore, an interface is needed among different eNBs to achieve the required coordination. The coordination between eNBs takes place on the X2 interfaces through three major load information messages [16]:

- *Uplink Interference Overhead Indication* (*OI*): this is a backhaul message used by a cell to inform its neighbours that it will be causing high uplink interference on a given PRB because it is scheduling its CEU on these PRBs.

- *Uplink High Interference Indication* (*HII*): it is defined as an indicator for the uplink used by a cell to notify its neighbours which PRBs are allocated to its CEU. Therefore, neighbour cells can avoid using the same PRBs for CEUs.

- *Relative Narrowband Transmission Power* (*RNTP*): it is a downlink bitmap consisting of a binary vector where each element of bitmap is used for each PRB in the frequency domain. It indicates the transmission power of each PRB to the average transmission power of all PRBs. This indicator demonstrates whether a cell would like to set the transmission power of a PRB to a value lower than a threshold.

There is a trade-off between the performance and the complexity, overhead and/or delay. Therefore, the amount of messages sent in load indication phase must be limited.

The coordination schemes can be divided into two subclasses: fractional frequency reuse and dynamic frequency reuse schemes as described as follows.

3.2.2.2.1. Fractional Frequency Reuse Schemes

The FFR schemes based on dynamic PRB or power allocations are summarized in this sub-section. A Novel Enhanced Fractional Frequency Reuse (NEFFR) [49] has been introduced where the total available bandwidth is divided into three sub-bands. One sub-band is allocated to the cell edge region with a higher transmission power while two sub-bands are assigned to cell centre region with lower transmission power. An Interference Avoidance Factor (IAF) is defined based on fairness to keep the balance between the number of UEs and PRB allocation. IAF determines the number of PRBs which cannot use them. Hence, the number of PRBs used by CCU is dynamically determined.

In Dynamic Fractional Frequency Reuse (DFFR) [50], the available bandwidth is divided into three sub-bands including 1) Common Sub-band (CSB) which is same for all cells and is used to measure SINR, 2) Priority Sub-band (PSB) which is not used in neighbouring cells, and 3) Interference Avoidance Sub-band (IASB). CSB and PSB have the maximum transmission power while the power of IASB is dynamically changed through an Interference Avoidance Request (IAR) message and proportional fairness scheduling algorithm. Each UE calculates number of its required IAR based on its average measurement of SINR over all CSBs during a certain period of time. Then, UE sends IAR to eNB and then the list of IARs are exchanged via eNBs to control the transmission power of IASB. When an eNB receives the IAR message, it adjusts its transmission power based on the context of the received message.

A modified version of enhanced fractional frequency reuse scheme has been suggested in [51] where cells are categorized into three groups (*A*, *B*, and *C*) based on RF3 to overcome the limitations of the FFR and the SFR schemes (see Figure 3.10). A part of the available entire bandwidth is reserved for each cell, called Primary Segment, which is orthogonal for each group. The rest of subchannels are defined as Secondary Segment. The Primary Segment of each cell is divided into RF1 part and RF3 parts. All groups can reuse the RF1 part while RF3 part can only exclusively be reused by the same groups (e.g., groups *A*). Note that the dominant neighbouring cells cannot reuse subchannels of RF3 to reduce the co-channel interferences among them. As a result, the CEUs have higher priority to use these subchannels than CCUs. Note that the Primary Segment of a group can simultaneously be a part of the Secondary Segments of other groups.

Several dynamic schemes with semi static time scale have been proposed in the literature [52-54]. For instance, [52] combined the advantages of static and dynamic schemes. For this purpose, UEs are classified as CCUs and CEUs based on the geometry factor. Thereafter, several non-overlapping handover regions are defined in order to divide CEUs of each cell into several cell edge groups. Identical ICI Correlative Groups (CGs) are allocated to CEUs located in a handover region because these CEUs can see the same group of adjacent eNBs. Therefore, it is a practical way to cluster UEs into different groups. Figure 3.11 illustrates UEs grouping and ICI correlative groups. A dedicated PRB list is assigned to each group consisting of the indexes of available PRBs

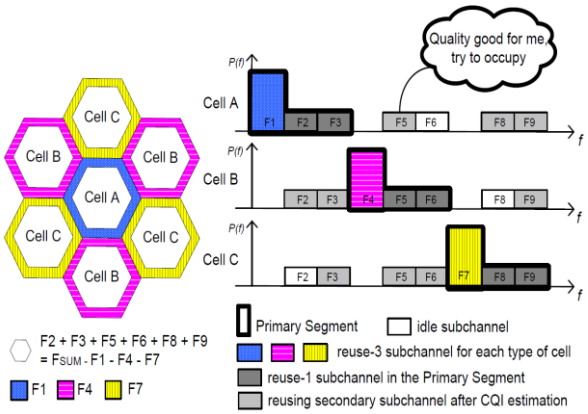

Figure 3.10. Enhanced Fractional Frequency Reuse [51]

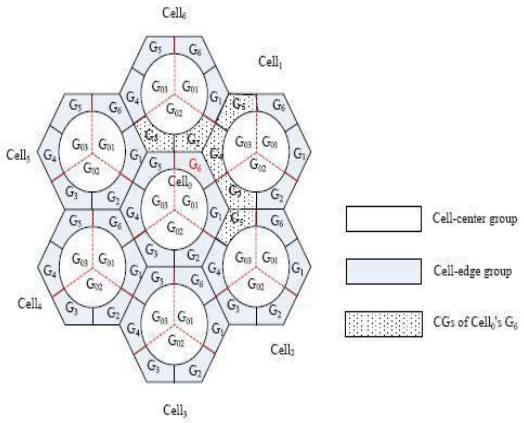

Figure 3.11. An illustration for UE grouping and ICI correlative groups [52]

in a descending priority order. For cell edge group two steps are executed to achieve the list of PRBs called the static resource pre-allocation and dynamic borrowing or leasing. In the static resource pre-allocation, overall subchannels are divided into six parts, and then each part is assigned to a cell edge group. Cell centre groups are allowed having access to the entire available bandwidth. In dynamic resource borrowing/leasing, an overloaded cell edge group can borrow parts of the idle resource or non-idle resources from other cell edge groups if it has used its pre-allocated bandwidth during a resource allocation. The resource allocation procedure for the CCUs starts from the top of the PRB list while different allocation strategies are used for cell edge groups based on the rank of PRBs. Moreover, some intercell negotiation may be required for power allocation based on the rank of PRBs. In [54], the total available bandwidth is divided into three non-overlapping sub-bands and each sub-band is allocated to a cell. However, if a cell requires more resources to satisfy the minimum data rate of its UEs, it can borrow PRBs from its neighbours. For this purpose, the borrower cell communicates with its neighbouring cell on X2 interface using HII and OI messages. This communication is necessary as borrower cell and owner cell of PRB make sure the borrowing of PRB does not lead to a serious interference on the owner cell. In order to find the state of each PRB, several weights are assigned to the preferred PRB based on its interference level in neighbouring cell. Then the summation of these weights is multiplied by the interference level of PRB in its owner cell. If the obtained value is smaller than a threshold, the borrower cell can use that PRB. The transmission power of PRB is determined based on its interference level and HII indicator.

In [55], ICI is mitigated using a region based technique where each cell is divided into different regions based on the received interferences, UEs thresholds and UE measurements. Based on the information sent by UEs, each eNB labels its assigned frequency band as the preferred or un-preferred sub-bands. CEU cannot use the un-preferred sub-band while CCUs are allowed to use the entire available bandwidth assigned to each cell. However, CEU can use the total available bandwidth under special condition. For this purpose, a Monopoly Indication is sent to the interfering cell over the X2 interface to indicate CUEs intend to use un– preferred sub-band. Moreover, this scheme categorizes the interference region into three parts including interference free, low interference, and interference parts.

A decentralized ICI mitigation scheme has been proposed in [56] which resources are allocated based on the SFR scheme and an iterative method. In this approach, each cell is divided into two areas called inner cell and outer cell areas. Moreover, the total available bandwidth is split into a number of non-overlapping sub-bands. Some sub-bands belong to the major subcarrier group and the rest sub-bands are allocated to the minor subcarrier group. Note that major subcarriers group refers to subcarriers which are orthogonal with each other in neighbouring cells and can be used by UEs of inner and outer cell areas while the minor subcarriers can only be deployed by UEs of the inner cell area at lower transmission power. The aim of the proposed scheme is to find the minor and major subcarrier groups and the transmission powers such that the throughput can be maximized. For the single cell SFR optimization algorithm, the algorithm first finds the number of major and minor subcarriers and the minimum transmission power that is able to satisfy the required data rate of inner and outer areas. This step is executed through an exhaustive search. If the minimum transmission power is less than the maximum available power, then the subcarriers and remaining amount of power will be reallocated to increase the system throughput. For this purpose, the number of major subcarriers is reduced while the transmission powers increase. Note that during this step the satisfaction of the required data rate of outer area must be considered. The decrease of major subcarriers will be executed until the entire transmission power deployed in the cell reaches to the maximum available power. After doing these two steps, the inner area's rates are reallocated by the new resource allocation values. The algorithm is repeated by new inner cell target data rate until the variation of the cell throughput becomes small. For multi cell scenario, a rate indicator

is used such that each cell can check the rate information of its neighbouring cells. After updating of the resource allocation in all cells, if there is a cell such as cell *l* that its required data rate has not been satisfied, the ICI of neighbouring cell must be reduced. For this purpose, the target data rate of cell *l* can decrease by a small predefined value for the next iteration. Note that the new target value cannot be smaller than the minimum required data rate.

3.2.2.2.2. Dynamic Frequency Reuse Schemes

ICI mitigation based on power control cannot effectively improve the throughput especially for those UEs that are close to each other in the system [57]. Therefore, some schemes have been developed to jointly perform on both resource allocation and power allocation to maximize the throughput. In this subclass, the available bandwidth is not initially divided to different sub-bands such as FFR schemes. The resource allocation is based on the optimization approaches or the priority of UEs.

3.2.2.2.2.1. Optimization based schemes

One of the popular approaches to mitigate the ICI is to optimize different functions such as utility functions. In [58-61], the ICI is mitigated using non-cooperation Game theory [58]. A subsequent Game theory approach proposed in [59] for real time systems using the combination of the virtual token approach and the exponential rule. In [60], the utility function is defined based on the resources receiving the least interferences from neighbouring cells. Moreover, a fairness scheduling algorithms (e.g., round robin or proportional fairness) is used to sort the active UEs. Thereafter, a PRB usage function is computed for UE_m in the ordered list. Finally, the PRB with the least usage function is chosen. If the selected PRB has not been allocated before, it can be allocated to UE_m with probability $1/p$ (where p=10 in [60]) and keeps the same PRB same as the last TTI with probability $1-1/p$; otherwise the next least PRB usage function is required to check. All UEs in the ordered list run this approach until all available PRBs are finished.

In [62] and [63], a utility matrix is used for each eNB with three sectors. For this purpose, different utility matrices are defined for sectors based on the possible simultaneous ICI when sectors use PRBs at the same time. It equals the multiple of the

achievable rate on RB_n when it is allocated to UE_m and the current demand factor of UE_m, when both other interferers are active. The demand factor is defined for UEs as the ratio of the received throughput to the average sector throughput and it is greater for CEUs than CCUs. Thereafter, the Hungarian algorithm [64] is used in the utility matrix. Finally, in order to maximize the utility matrix, a threshold-based approach is applied to find which interferers have to be restricted.

Reference [65] suggested an autonomic ICI scheme based on RNTP indicator. The goal of using RNTP indicator is to retrieve information about PRBs used in the neighbouring cells. This is because neighbouring cells are the main sources of interference on the target cell. The proposed algorithm aims to optimize the RNTP threshold and its reporting period such that the system throughput and spectral efficiency can be improved. For this purpose, a fuzzy logic system and a Genetic algorithm are used to minimize the ICI problem. For example, when a PRB used by a neighbour cell causes a high interference on the target cell, the RNTP threshold will be exceeded or when the spectral efficiency is low the RNTP threshold decreases.

The Lagrange decomposition [66] is a subsequent optimization method used in [57] and [67]. In [67], the proposed resource allocation algorithm is executed in two steps. In the first step, an equal transmission power is assumed for all PRBs and then a Channel to Interference and Noise Ratio (CINR) is computed. PRBs are allocated to CEUs or CCUs based on the obtained CINR and a greedy algorithm. At the second step, the transmission power is allocated to each PRB used by CCUs and CEUs. For PRBs used by CCU, optimization approach is not required and the transmission power of each PRB is allocated using power distribution over PRBs. However, for PRBs used by CEU, the power allocation is performed through the Lagrange decomposition method.

A subsequent optimization approach is based on graph and colouring based methods [68-72] to mitigate ICI in macrocell-macrocell scenario. In [68], interference estimation is used to create a graph. The estimated interference indicates the effect of transmission of one UE on other UEs. In the defined interference graph, all UEs must use the different set of PRBs. For this purpose, the minimum set of disjoint resources is found based on the colouring approach. In this method, colours are allocated to the interference graph such that the same colour is not assigned to two connected vertices.

Heuristic Dsatur [73] and a Tabu [74] search techniques are used to solve graph colouring problem as this is a Nondeterministic Polynomial (NP) hard problem. Reference [71] proposed a subsequent colour based algorithm executed for each eNB. Each new cell collects the received information about its neighbouring cells and then stores in a Neighbour Relation Tables (NRT). The NRT contains information about its neighbouring cells and the allocated colours. Therefore, the proposed algorithm makes a decision about the colour allocation based on NRT. After a random time, the cell attempts to select a colour for itself which has not been used by the neighbouring cells. If the cell cannot find a proper colour, it continues searching without considering ICI mitigation. At the next step, the algorithm finds the best colour allocation for all cells within a local region optimization. This step can lead to change or reallocate of colour assigned to other cells.

3.2.2.2.2.2. Priority based schemes

A subsequent technique uses the priority of UEs which is calculated based on different metrics such as UEs' location or traffic models. Reference [75] suggested a dynamic resource allocation scheme in time domain. In this scheme, the interference level is labelled as 0, 1 and 2 for different frame structures used in the target cell and neighbouring cells. For this purpose, the interference power from neighbouring cells is calculated for all UEs and then interference powers of all UEs are compared with a threshold value to determine the interference level of UEs. For the downlink service of target cells, the interference levels of all UEs are sorted from high to low (i.e., level 2 to level 0). At first, UEs labelled level 2 are scheduled using maximum carrier to interference and then UEs with interference level 1 are scheduled. Note that the PRB assigned to levels 2 and 1 are excluded from the list of the available PRBs. At the end, the rest of UEs are scheduled.

In [76], a QoS approach has been introduced for multiclass services in which resources are allocated based on QoS for different traffic models. In this scheme, UEs are prioritizes based on traffic models and delay. For this purpose, two different variances are defined including 1) variance of channel quality for one UE on different PRBs and 2) variance of QoS for different UEs on a same PRB. Moreover, a remaining time parameter is defined to indicate the real priority of a data packet. It equals the difference

between the maximum legal packet delay of UE_m and the waiting time for the first data packet of UE_m in the buffer.

For latency-sensitive service, the [77] proposed a scheme in which the QoS of a UE is converted to the required number of RBs using size of the packet (in bit), the remaining scheduling time and channel capacity. In this scheme, the available spectrum of each cell is divided into three sub-bands based on the priority of UEs. The PRBs in high priority sub-band have the maximum transmission power while the transmission powers of other PRBs are lower. In addition, the effects of SINR and PRBs on throughput are measured. Note that the allocated PRB_n is excluded for later resource allocations.

3.3. Qualitative Comparison

ICI problem in wireless networks has been reviewed in several survey papers [5], [40], [78], [79], and [80]. The schemes reviewed in this thesis are compared qualitatively in Table 3.2 based on results obtained from references and compared to RF1. The terms of high, medium and low express the qualitative amount of throughput improvement resulting from the proposed techniques in compared with the throughput of RF1.As can be seen in Table 3.2, the fractional frequency reuse scheme without using intercell coordination can improve the cell edge throughput because the cell edge and the cell centre regions have lower conflicted (such as SFR) or no conflicts (such as PFR). However, the overall cell throughput is not good because the sub-bands used in each region are limited. Moreover, the allocated sub-bands and transmission powers cannot be changed because sub-band and transmission power allocations are determined during the pre-planning procedure. In cell coordination, the interference avoidance is realized by real time coordination among all involved cells for those CUEs using the same resources in neighbouring cells.

Based on Table 3.2, the schemes with intercell coordination obtain higher throughput than schemes without intercell coordination. Moreover, among intercell coordinated based schemes, dynamic frequency reuse schemes achieved better performance in term of cell throughput and cell edge throughput. This is because the dynamic scheme are instantaneously adapted to the network condition changing such as traffic variation or load distributions without a priori resource partitioning at the cost of imposing a high

amount of overhead to the system. On the other hand, the optimal solutions may significantly increase system performance in theory at the expense of arising new challenges for capability of real system networks. For example, a scheme with high required computations, overhead and time causes the system cannot follow the network changes and therefore cannot rapidly adapt. Consequently, the better theoretical algorithm may not be suitable for real world and therefore complexity, time and overhead should be taken into account before selecting a technique to use in real environment.

3.4. Summary

This chapter initially studied the ICI problem and then the well-known ICI mitigation algorithms were introduced. Thereafter, different useful ICI avoidance schemes proposed for downlink macrocell-macrocell scenario were reviewed and classified in two main classes including non-intercell coordinated and intercell coordinated schemes. Afterwards, a qualitative comparison was provided in terms of throughputs when compared to RF1. Advantages and disadvantages were discussed to help select the schemes which are more suitable for each specific goal.

Table 3.2. Comparison among ICI Avoidance Schemes for LTE Downlink Systems

Class	Subclass	Scheme	Time Scale	Metric to Divide CCU/CEU	Cell edge Throughput	Cell Throughput
Non-Intercell Coordinated based Schemes	Conventional Frequency Reuse	RF1	Static	N/A	Low	Medium
		RF3	Static	Path loss	High	Low
		SerFR	Static	SINR	High	Medium
	Fractional Frequency Reuse	PFR	Static	SINR	High	Low
		SFR	Static	SINR	Medium	Medium
		SFFR	Static	SINR	Medium	Medium
Intercell - Coordinated based Schemes	Dynamic Frequency Reuse	DFFR	Static	SINR	Medium	High
		NEFFR	Static	SINR	Medium	High
		Ref.[52]	Semi Static	Geometry factor	Medium	Medium
		Ref.[54]	Semi Static	N/A	N/A	Medium
		Ref.[55]	Static	Interference over Thermal	Medium	High
		Ref.[56]	Using SFR	SINR	Medium	Medium
	Fractional Frequency Reuse	Ref.[53]	Dynamic	SINR &UE location	High	High
		Ref.[62]	Dynamic	Demand factor	High	High
		Ref.[63]	Dynamic	N/A	N/A	High
		Ref.[64]	Dynamic	Scheduler decision	Medium	High
		Ref.[70]	Dynamic	Geographic Location	High	High
		Ref.[71]	Dynamic	N/A	Medium	Medium
		Ref.[75]	Dynamic	Power	High	High
		Ref.[76]	Dynamic	N/A	N/A	High

Chapter 4

AN INTERCELL INTERFERENCE COORDINATION SCHEME IN LTE DOWNLINK NETWORKS BASED ON USER PRIORITY AND FUZZY LOGIC SYSTEM

As discussed in chapter 3, the intercell interference problem is one of the main challenges in LTE downlink system particularly for UEs located in cell edge areas. The qualitative comparison in Table 3.2 showed that dynamic scheme can instantaneously adapt to the network condition changing. As a result, this chapter introduces a novel dynamic ICI coordination scheme using the user priority and fuzzy logic systems to overcome the ICI problem in downlink macrocell-macrocell scenario.

The proposed scheme divides the total available bandwidths into three sub-bands and then allocates sub-bands based on the user priority. Moreover, the power allocation is dynamically performed through a fuzzy logic system. In order to follow the network conditions, the proposed scheme considers the system traffic loads and system changes when the PRBs and transmission powers are assigned to different UEs. Consequently, this scheme can jointly optimize PRB and power allocations for each cell in contrast to traditional methods where the spectrum allocation or the power allocation is fixed for each cell (see Section 3.2.2.1). The proposed scheme is a decentralized scheme in which each eNB can determine its PRB and power allocations through exchanging messages with neighbouring eNBs over X2 interface.

The chapter is organized as follows. Section 4.1 presents the proposed ICIC scheme. Section 4.2 contains the simulation results and a discussion. The conclusion is given in the final section.

4.1. The Proposed Intercell Interference Coordination Scheme

The proposed ICIC scheme aims to allocate PRB to different UEs and determine the transmission power of PRBs in each cell such that the system performance can be improved. The main focus of this scheme is the downlink system because the related broadband services pose higher rate requirements than those in uplink. In the proposed scheme, three steps are defined (as shown in Figure. 4.1) which are performed by each macro eNB. Phase *A* focuses on how to prioritize UEs and sort the UEs. The sub-band for each priority is determined in phase *B*. After sub-band division, the transmission power is allocated to each PRB in phase *C* using a fuzzy logic system. In the next subsections, each step is described in more details.

Figure 4.1. Overview of the proposed scheme

4.1.1. Phase A: Priority of UEs

In this phase, the priority of UEs is specified both in cell *l* and its neighbouring cells that are going to schedule its UEs on the same PRB at the next TTI. For this purpose, three different parameters are taken into account including interference level, QoS and Head of Line (*HoL*).

When a UE comes away from the serving eNB and becomes closer to a neighbouring eNB, the interference level receiving from the neighbouring eNB increases. In order to reduce interference for that UE, the serving eNB schedules UE on a PRB that has higher transmission power in the serving cell and lower transmission power in the neighbouring cells. Moreover, when the system supports different types of services (e.g., real time and non-real time services), QoS requirements and HoL must be considered to allocate PRBs to different UEs.

4.1.1.1. Interference Level

The interference level of UE_m on PRB_n (I_m) from neighbouring eNBs is calculated using the transmission powers and channel gains of neighbouring cells. Note that, the same transmission power is considered for all eNBs on all PRBs to calculate the interference level [67]. This assumption allows to calculate I_m when all eNB are in the same situation.

$$I_m = \sum_{k=1}^{K} p_{m,n}^{k} H_{m.n}^{k} \tag{4.1}$$

where $p_{m,n}^{k}$ and $H_{m.n}^{k}$ are transmission powers and channel gains of interfering eNB_k on PRB_n. Note that, it is assumed that each eNB can calculate the interference level. Moreover, I_{max} can be calculated for a typical UE located at a point where it receives the minimum shadowing, the minimum fading, the minimum pathloss and the maximum transmission power on the RB_n. The minimum pathloss can be obtained where a UE is located on the boundary of a cell. In this case, UE has the maximum distance from the serving eNB and minimum distance from the neighbouring cell which is represented by *Pos* in this thesis.

$$Pos = \frac{|Pos_l - Pos_k|}{2} \tag{4.2}$$

where Pos_l and Pos_k are locations of serving eNB_l and neighbouring eNB_k. This assumption is used to find minimum path loss from each neighbouring eNB. I_{max} is obtained by replacing these values into (4.1).

4.1.1.2. Head of Line (*HoL*)

HoL is defined as the difference between the current time and the arrival time of a packet in the eNBs' buffer. $T_{arrival}$ is the time that the packet arrives to the buffer while T_{max} represents the maximum allowable packet delay.

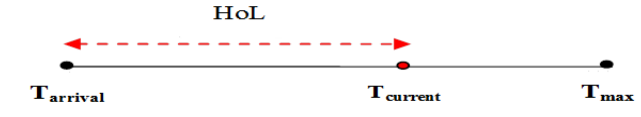

4.1.1.3. Quality of Service (QoS)

QoS Class Identifier (QCI) is used as the third parameter to consider QoS in priority calculation. QCI is a scalar value used as a reference to particular parameters that controls packet forwarding behaviours such as scheduling weights, admission thresholds, and queue management thresholds [81]. QCI is pre-configured by the operator owning the node (e.g., eNB). Note that the QCI is unique for each Service Data Flow (SDF) as shown in Table 4.1. In this table, the Guaranteed Bit Rate (GBR) is defined as the minimum bit rate which applications request and usually deployed for applications such as Voice over Internet Protocol (VoIP). Moreover, Non-GBR bearers cannot guarantee a specific bit rate, and are usually deployed for applications such as web browsing. As shown in Table 4.1, each QCI has a priority level where the Priority Level 1 is the highest priority level [81]. The proposed scheme uses the QCI priority as the third parameter, represented by Q_m, to find the UE priority.

A simple weighting algorithm is used to combine the required parameters as follows:

$$W = w_1 \times I_m^{'} + w_2 \times HoL_m^{'} + w_3 \times Q_m^{'} \tag{4.3}$$

$$\sum_{i=1}^{3} w_i = 1$$

where w_i is a weighting of each parameter. Parameters $I_m^{'}$, $Hol_m^{'}$, and $Q_m^{'}$ represent the normalized values of the interference level, *HoL* and *QCI* priority of UE$_m$, respectively. These normalized values are calculated as follows:

$$I_m^{'} = \frac{I_m}{I_{\max}} \ , \ HoL_m^{'} = \frac{HoL_m}{T_{\max}} \ , \ Q_m^{'} = \frac{1}{Q_m} \tag{4.4}$$

4.1.2. Phase B: PRB Allocation

In the proposed scheme, the total available bandwidth *BW* is divided into three non-overlapping sub-bands based on the UE priority (calculated in Section 4.1.1) including 1) High Sub-band (*HS*) which is allocated to UEs with higher priority; 2) Low Sub-band (*LS*) used for UEs with lower priority, and 3) Common Sub-band (*CS*) which is

allocated to all UEs with different types of priority. At first, the UEs with highest priorities should be allocated to *HS*, then the UEs with lowest priorities are allocated to *LS* and finally the rest of UEs are allocated to *CS*. PRB allocation for UE with lower priority in *LS* cannot affect the number of PRBs allocated to UEs with highest priority in *HS*. Figure (4.2) illustrates the bandwidth division.

Table 4.1. Standardized QCI Characteristics [81]

QCI	Resource Type	Priority	Packet Delay Budget	Packet Error Loss Rate	Example Services
1	GBR	2	100 ms	10^{-2}	Conversational Voice
2		4	150 ms	10^{-3}	Conversational Video (Live Streaming)
3		3	50 ms	10^{-3}	Real Time Gaming
4		5	300 ms	10^{-6}	Non-Conversational Video (Buffered Streaming)
5	Non-GBR	1	100 ms	10^{-6}	IMS Signalling
6		6	300 ms	10^{-6}	Video (Buffered Streaming) TCP-based
7		7	100 ms	10^{-3}	Voice, Video (Live Streaming), Interactive Gaming
8		8	300 ms	10^{-6}	Video (Buffered Streaming) TCP-based
9		9			

At this step, UEs located in serving and neighbouring cells which use the same PRB are sorted based on UEs' priorities. For this purpose, UEs placed in each cell are sorted such that a UE with the highest priority is located at the beginning of the queue as shown in Figure 4.2 (b). Then, the proper PRB from the relevant sub-band is assigned to that UE. In *HS*, the PRB allocation starts from the UE with the highest priority while in *LS* the UE with the lowest priority is selected at first. Based on Figure 4.2, the *LS* of the neighbour cell can be *HS* of serving cell, hence for *HS*, the serving cell can ask the neighbouring eNB to reduce the transmission power on PRB of *HS* to decrease the interference. Moreover, this approach allows using the remaining transmission power from *LS* for *HS* under the specified conditions to enhance the throughput while the total transmission power is still smaller than or equal to the maximum transmission power of eNB. More details about transmission power are demonstrated in Phase *C*.

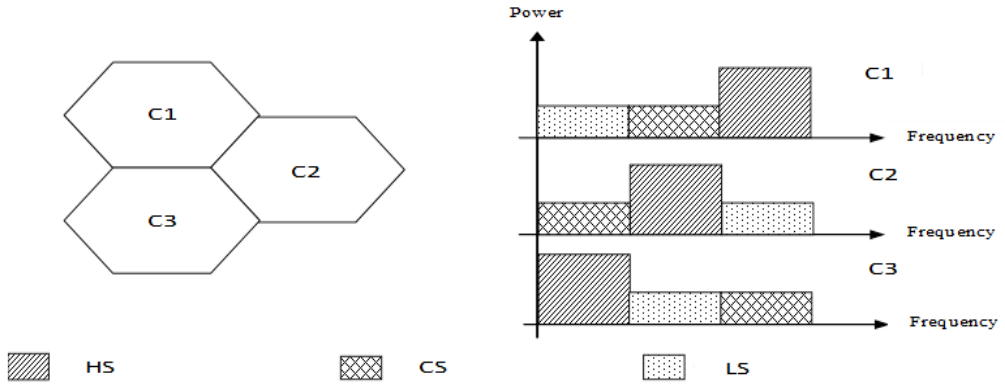

(a)

		Priority					
		Highest ----------->Lowest					
Queue	Cell 3	UE1	UE2	UE3	...	UE14	UE15
	Cell 2	UE16	UE17	UE18	...	UE29	UE30
	Cell1	UE31	UE32	UE33		UE43	UE44

(b)

Figure 4.2. (a) Bandwidth division, (b) Locations of UEs in queues of different cells based on UE's priority

4.1.3. Phase C: Transmission Power Allocation

The increase or decrease of transmission power on the PRBs reused in neighbouring cell can directly affect a UE's received signal quality. This is because it changes the interference level on the UE from neighbouring eNB. In the proposed scheme, the power allocation is dynamically performed using Fuzzy Logic System (FLS) [82] and exchanging messages among eNBs. This algorithm is executed for several TTIs and then it is stopped whenever the transmission power changes in a small range. Thereafter, the transmission power allocation is executed periodically or by a trigger.

Transmission power allocation is performed by each eNB when UEs located in neighbouring cells are scheduled on the same PRBs. For example, as shown in Table 4.2, UE44 belongs to *LS* of cell 1while UE1 is in *HS* of cell 3. If UE1 experiences a very low SINR because of highest interference from Cell 1, serving eNB of UE1 (eNB3) requests eNB1 to reduce its transmission power on that PRB. In other words, the strongest interferer has to reduce transmission power on the requested PRB if its UE has lower priority on that PRB while the minimum achievable data rate is satisfied. If an eNB receives requests from different neighbouring to reduce its transmission power on

Table 4.2. Allocating UEs to Subbands for Different Cells based on UE's Priority

Cell	RB1	RB2	...	$RB_{n/3}$	$RB_{(n/3)+1}$	$RB_{(n/3)+2}$	...	$RB_{(2n/3)}$	$RB_{(2n/3)+1}$	$RB_{(2n/3)+2}$	...	RB_n
3	UE1	UE2	...	...	U15	U14	...	...	...	...	...	...
2	...	...	...	...	UE16	UE17	...	...	UE30	UE29	...	...
1	UE44	UE43	...	...	...	...	...	...	UE31	UE32	...	...
...	...	...	...	...	...	...	...	...	...	...	...	...

a PRB when its UE has the lowest priority on that PRB, the eNB has to decrease its transmission power to the minimum requested transmission power. The amount of power decreasing or increasing is calculated by FLS [82].

FLS is an expert controller system which can be simply designed and works on real time systems [83] based on a set of "IF... THEN" rules. In general, FLS is a simple and flexible controller with a few calculations. In addition, it can handle problems with imprecise and incomplete data. One of the important features of FLS is that it can simultaneously work with numerical data and linguistic information through a mapping between input data and output data. By using linguistic terms, the prior knowledge can be collected easier based on the experience of an operator. The main difference between FLS and conventional rule based controllers is that FLS simultaneously triggers several rules to do a smoother control. In general, FLS consists of three steps shown in Figure 4.3:

1. *Fuzzification step*: in this step, inputs are fuzzified using membership functions and then mapped to truth values. A membership function is a curve which defines the mapping from a given point in the input or output space with a membership degree within the real interval [0, 1].

2. *Processing step*: this step selects the best rules from the fuzzy rule set and then aggregates its results based on an aggregation method.

3. *Defuzzification step*: in this step, the result obtained from the processing step is converted to a scalar output value.

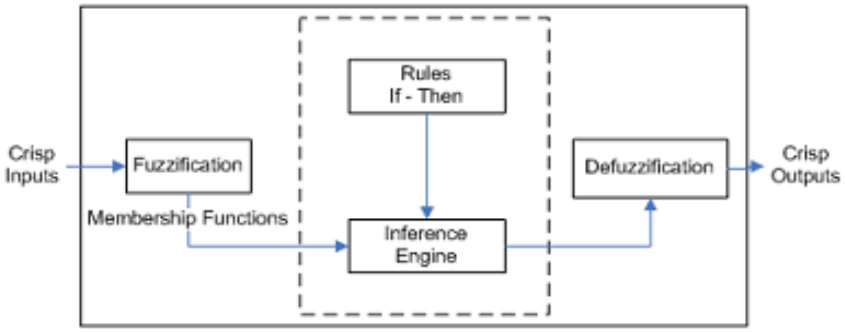

Figure 4.3. Overview of fuzzy logic system

Several important downlink parameters are considered as inputs of FLS to control the transmission power allocation including the SINR, historical throughput and achievable data rate. Using these parameters, each eNB can monitor the link quality of its UEs and system performances. Consequently, the following parameters are defined as inputs:

1) SINR of UEs with higher priority.

2) Historical throughput of UEs with lower priority.

3) The current achievable data rate that UE with lower priority can achieved on a PRB. Each cell checks the achievable data rate from its neighbouring cells using a data rate indicator. This indicator is set to 2 if the achieved data rate is more than minimum achievable data rate while 1 represents that the minimum achievable data rate is satisfied, otherwise it is set to 0.

The output of FLS is the transmission power of PRBs which can be changed as follows:

1) Transmission power of PRB allocated to UE with lower priority (i.e., *LS* or *CS*) can decrease or be fixed.

2) Transmission power of PRB assigned to UE with higher priority (i.e., *HS*) can increase or be fixed.

The flow chart of the proposed ICIC scheme is shown in Figure 4.4. Each dash box shows one step of the proposed algorithm.

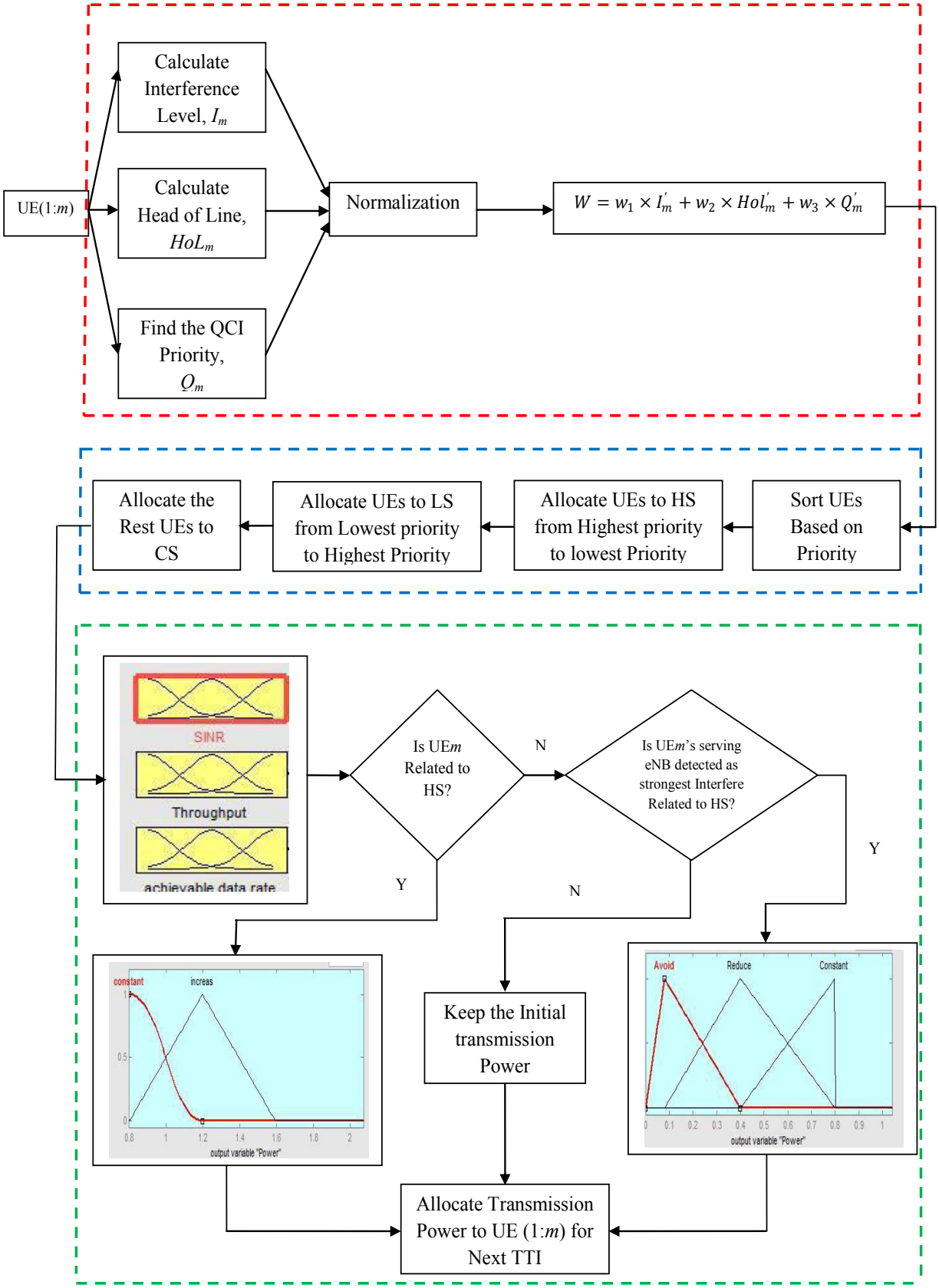

Figure 4.4. Flow-chart of the proposed priority based ICIC scheme

4.2. Simulation Results and Discussion

In this section, the simulation results of the proposed ICIC scheme are illustrated to evaluate its performance for video streaming traffic. The parameters described in Section 2 were considered and then delay, cell edge throughput, total cell throughput (as described in Section 2.5) were used to evaluate the performance of the proposed scheme. Simulation results of the proposed scheme were compared with the RF1 and SFR schemes explained in Section 3.2.2.1.

4.2.1. Simulation Setup

The transmission power is initialized based on SFR scheme to consider power spectral density mask limitations. Therefore, the transmission power of *HS*, *LS*, *CS* (represented by P_H, P_L, and P_C, respectively) are initially set to $z\frac{P_T}{N}$, $\frac{(3-z)}{2}\frac{P_T}{N}$ and $\frac{(3-z)}{2}\frac{P_T}{N}$ (z>1), respectively. P_T indicates the total transmission power of each macro eNB and N is number of PRBs.

In the proposed scheme, inputs and outputs are fuzzified using the specified fuzzy label sets called T_{x1}, T_{x2}, T_{x3}, T_{o1} and T_{o2}, respectively:

$$T_{x1} = \{Low, Medium, High\}$$
$$T_{x2} = \{Low, Medium, High\}$$
$$T_{x3} = \{Low, Medium, High\}$$
$$T_{o1} = \{Constant, Increase\}$$
$$T_{o2} = \{Avoid, Reduce, Constant\}$$

An input value x_i is mapped to the fuzzy set T_{xi} with a membership degree μ_i. In addition, the output value o_j is mapped to the fuzzy set T_{oj} with the membership degree of μ_j. The linguistic terms of each component are mapped to a mathematical expression as follows:

$$F_{x1} = \{Z\text{-}shape, Triangular, S\text{-}shape\}$$
$$F_{x2} = \{Z\text{-}shape, Triangular, S\text{-}shape\}$$

F_{x3}= {*Z-shape, Triangular, S-shape*}

F_{o1}= {*Z-shape, Triangular*}

F_{o2}= {*Triangular, Triangular, Triangular*}

where the Triangular, *S*-shape and *Z*-shape functions are given by (4.5), (4.6) and (4.7), respectively. In general, these shapes are functions of a vector, *X*, and depends on scalar parameters *a*, *b*, and *c*.

$$f(X;a,b,c)=\begin{cases}0, & X\le a\\ \dfrac{X-a}{b-a}, & a\le X\le b\\ \dfrac{c-X}{c-b}, & b\le X\le c\\ 0, & X\ge c\end{cases} \tag{4.5}$$

$$f(X;a,b)=\begin{cases}0, & X\le a\\ 2\left(\dfrac{X-a}{b-a}\right)^2, & a\le X\le \dfrac{a+b}{2}\\ 1-2\left(\dfrac{X-b}{b-a}\right)^2, & \dfrac{a+b}{2}\le X\le b\\ 1, & X\ge b\end{cases} \tag{4.6}$$

$$f(X;a,b)=\begin{cases}1, & X\le a\\ 1-2\left(\dfrac{X-a}{b-a}\right)^2, & a\le X\le \dfrac{a+b}{2}\\ 2\left(\dfrac{X-b}{b-a}\right)^2, & \dfrac{a+b}{2}\le X\le b\\ 0, & X\ge b\end{cases} \tag{4.7}$$

The range of membership functions for each input and output are selected based on the system requirements as follows:

- The range of membership functions of SINR is based on SINR range obtained from SINR–BLER curves [84] as shown in Section 2.2.

- The range of membership functions of achievable data rate is based on CQI efficiency [84] as shown in Section 2.2.

- The range of membership function is changed for throughput based on the average number of PRBs allocated to each UE in each cell.

- For the transmission power of PRB belonging to *LS* and *CS*, the range of membership functions is varied from zero to maximum transmission power per PRB.

- For transmission power of PRB in *HS*, the range of membership functions are changed from initial transmission power to maximum transmission power plus to ΔP. ΔP represents the additional transmission power achieved from decreasing of transmission power on other PRBs in each cell.

Based on the number of inputs and its membership functions, 27 rules are defined for FLS to control the outputs. For example "IF SINR is low and the historical throughput is high and the achievable data rate is high THEN the transmission power of *LS* reduces". Or "IF SINR is low and historical throughput is high and achievable data rate is high THEN the transmission power of *HS* increases".

4.2.2. Results and Discussion

As mentioned in Section 4.1.1, the priority is calculated using a weighing algorithm with three coefficients named w_1, w_2 and w_3. Different coefficient values can lead to different results as represented in Table 4.3. For instance, when the coefficient value of interference level, w_1, is higher than w_2 and w_3, the interference level has a higher priority than delay and type of service. Therefore, the interference on UEs decreases which leads to increase the SINR and hence enhance the throughput. However, the delay increases because the UEs having the higher interference level (i.e., CEUs) are selected as highest priority instead of UEs with larger delay. On the other hands, when the highest coefficient value is assigned to delay, the delay of system is reduced at the cost of throughput degradation. As a result, the coefficient values affect the system performance and must be specified precisely. Since the packets arrive at a regular interval with fixed source video rate, all of PRBs may be not used for UEs. Therefore, results do not show much variation when the w_i's are varied.

Table 4.3. System Performance Comparison for Different Coefficient Values

W_1	W_2	W_3	Cell Edge Throughput [Kbps]	Mean Cell Throughput [Mbps]	Delay [ms]	Interference [dB]
0.33	0.33	0.33	233.92	8.64	10.13	-89.06
0.2	0.6	0.2	230.84	8.48	11.35	-88.94
0.2	0.2	0.6	209.07	8.40	9.88	-89.08
0.6	0.2	0.2	274.55	9.14	11.24	-87.83

In order to evaluate the performance of system in terms of delay and interference level, these two parameters are shown in Figures 4.5 and 4.6 for w_1=0.6, w_2=0.2 and w_3=0.2. The simulation results illustrate the proposed scheme (called priority) decreases the delay more than RF1 and SFR because the proposed scheme considered the delay as a factor in the weighting algorithm. Based on the weighing algorithm, increasing of *HoL* of a UE leads to increase of its priority, and then UE will be scheduled on *HS*. Moreover, Figure 4.6 shows that the interference level of the proposed scheme is less than RF1 and SFR schemes because the power allocation is performed dynamically using FLS and exchanging messages among neighbouring eNBs. As a result, the interference level on PRBs in each cell can decrease.

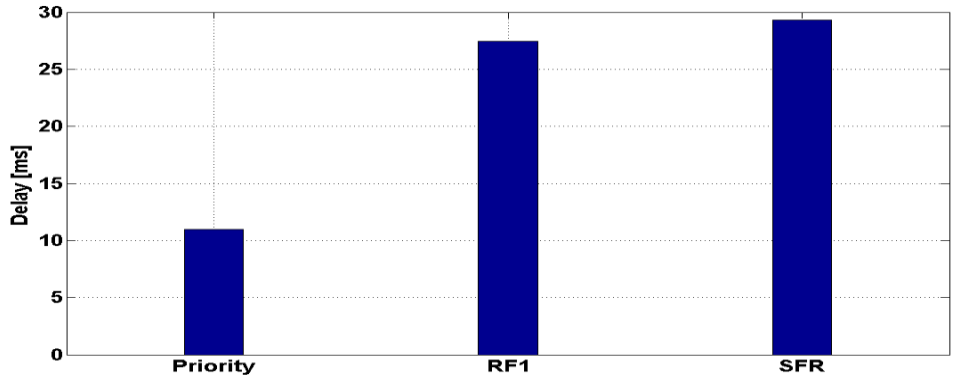

Figure 4.5. Delay comparison among priority, RF1 and SFR schemes

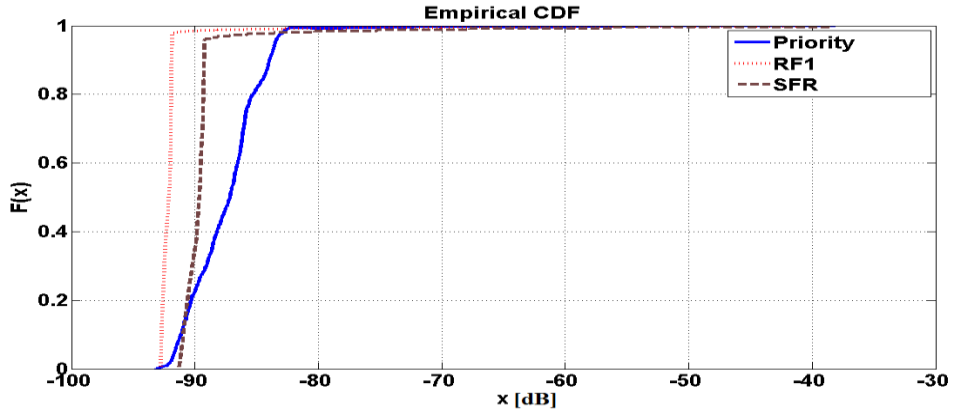

Figure 4.6. Interference level comparison among priority, RF1 and SFR schemes

Figure 4.7 depicted that the proposed priority based scheme can significantly improve the cell edge throughput due to considering interference level, approximately 68% and 96% more than SFR and RF1, respectively. Figure 4.8 compares the average cell throughput of the proposed scheme, RF1 and SFR. The proposed scheme can achieve a higher average system performance than SFR and RF1 schemes around 12% and 28.7%, respectively. This is because the proposed scheme dynamically allocates the transmission power of each PRB based on the SINR, throughput and achievable data rate through the FLS. Moreover, it considers the system traffic loads and system changes when the PRBs are allocated to different UEs.

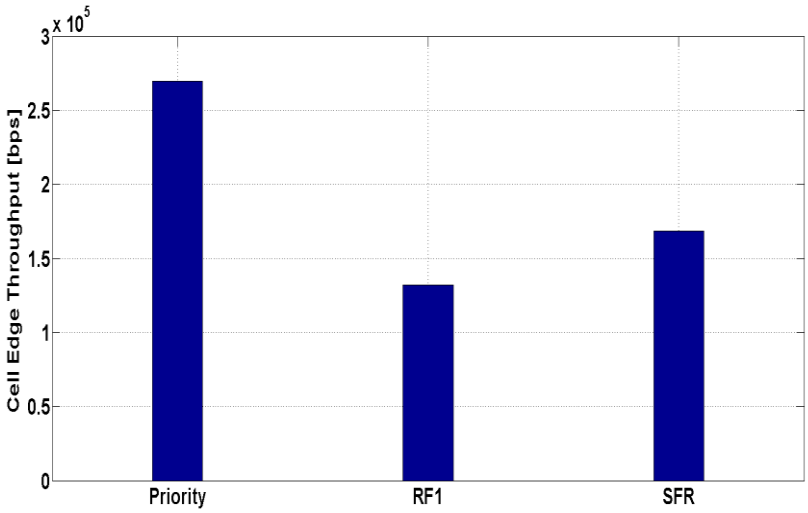

Figure 4.7. Average cell edge user throughput comparison

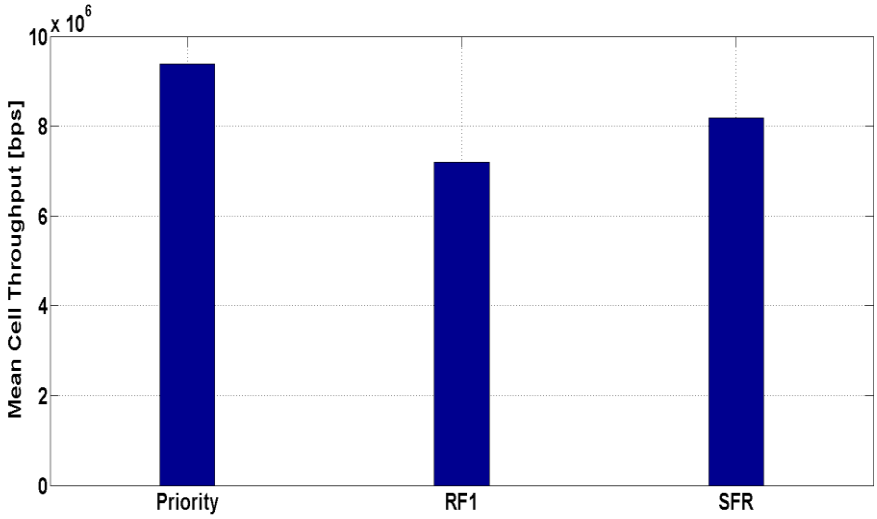

Figure 4.8. Average cell throughput comparison

4.3. Summary

In this chapter, a dynamic ICIC scheme for downlink LTE system was introduced based on the user priority and fuzzy logic system. The proposed scheme specified the priority of each UE based on three parameters including interference level, *QoS* and *HoL*. UEs were scheduled based on priorities on the defined subbands. Moreover, real time coordination was performed among all involved cells to avoid using same PRB for CEU located in neighbouring cells. The transmission power was allocated adaptively using a fuzzy logic system. Simulation results demonstrated that the proposed scheme outperformed the RF1 and SFR schemes in terms of delay, interference level, cell edge user throughput, and system throughput.

Chapter 5

OVERVIEW ON MACROCELL-PICOCELL DOWNLINK INTERCELL INTERFERENCE CHALLENGES AND CURRENT SOLUTIONS

Since the data traffic demand is exponentially growing, more improvements are needed for spectral efficiency in 4G system. Cell splitting is a simple solution to improve the spectral efficiency but it is prohibitively expensive because more macro eNBs are required in the network. In addition, site acquisition for macro eNBs is difficult for operators particularly in a space limited dense urban region [85]. Consequently, a cheaper, flexible and scalable deployment technique is required to improve the coverage, capacity and the broadband user experience within a cell. One solution is to utilize HetNets [2] consisting of macrocells and low power nodes (i.e., femto, pico and relay nodes). Low power nodes aim to offload the traffic from the macrocells, increase the coverage, and improve the spectral efficiency by spatial reuse of spectrum.

Picocell is one of the important low power nodes because it can be used efficiently in regions with high volume of traffic to enhance the overall system capacity. However, the transmission power difference between macro eNB and pico eNB can lead to new challenges for network management such as intercell interference.

This chapter initially presents the challenges in HetNets and then studies the concept of intercell interference in macrocell-picocell scenario. Thereafter, major technical challenges of intercell interference coordination for picocells are described. Finally, the proposed ICI mitigation schemes for macrocell-picocell scenario are reviewed and a qualitative comparison will be provided.

This chapter is structured as follows. Challenges of macrocell-picocell scenario are discussed in Section 5.1. The intercell interference management issues are outlined in Section 5.2. Section 5.3 reviews current proposed ICI mitigation schemes for macrocell-

picocell scenario and then provides a qualitative comparison. Section 5.4 summarises the chapter.

5.1. Challenges of Macrocell-Picocell Scenario

Using nodes with different transmission powers causes new challenges in HetNets which will be explained in this section.

5.1.1. Unbalanced Coverage

Nodes with different transmission powers can result in the imbalanced coverage between uplink and downlink. The downlink coverage of the macro eNB is much larger than the coverage of the pico eNBs because of larger transmission power. However, the transmission power difference of macrocell and picocells does not affect the coverage in the uplink because the UE is the transmitter and the transmission powers of all UEs are approximately same. Thus, the eNB that provides the best downlink coverage may be different from the eNB providing the best uplink coverage. Therefore, it is important for a UE to select the best eNB as its serving cell. Reference [86] suggests that one solution for the unbalanced coverage is using different serving eNBs for uplink and downlink independently.

5.1.2. Cell Selection

In the traditional cell selection method, called maximum Reference Signal Received Power (RSRP), UEs can select the serving cell by comparing the RSRP of macro eNBs and pico eNBs. In this thesis, RSRP is defined as the average received power of all downlink reference signals measured by a UE across the entire bandwidth used by a eNB. The cell with higher RSRP is selected as a serving cell.

$$Serving\ cell = \arg\max_{j \in J}(RSRP_j) \tag{5.1}$$

where j represents the eNB and J is a set of macro eNBs and pico eNBs.

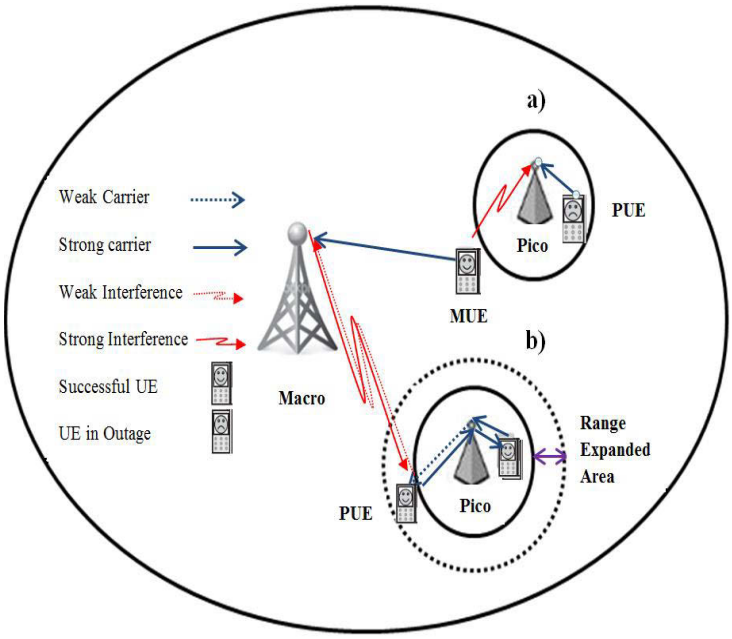

Figure 5.1. (a) Macro UE (MUE) interferes on the uplink of a nearby picocell; (b) Using the cell range expansion scheme to mitigate pico uplink interference.

However, in HetNets, cell selection based on the strongest downlink RSRP is not the best strategy because UEs will be connected to a higher power node instead of the lower power nodes at the shortest pathloss distance. Therefore, traffic load is distributed unequally which can lead to macrocell overloading. Moreover, the maximum RSRP method causes severe uplink interference between macro UEs and pico UEs as shown in Figure 5.1 (a). Consequently, new cell selection techniques are required to address the problems caused by nodes with different transmission power. One technique is to add an offset value to the RSRP received from pico eNB_j such that the UE preferentially selects a pico eNB as the serving cell even when it is not the strongest cell. This technique is known as Cell Range Expansion (CRE) and the resulting range expanded area is depicted in Figure 5.1 (b). Note that the range expanded area is an area around picocells where UEs are connected to pico eNBs because of receiving RSRP plus an offset value.

$$Serving\ cell = \arg\max_{j \in J}(RSRP_j + offset\_value) \tag{5.2}$$

CRE offset values in the range (0 20] dB can be added by a UE to the RSRP received from pico eNBs. If the offset value is not selected correctly for CRE, the enhancement

of network performance cannot compensate the cost of using picocells. For example, if a small offset value is used, a fewer number of UEs are offloaded to picocell because the RSRP received from the macro eNB is still stronger than RSRP received from the pico eNB plus the offset value. Therefore, the performance of macro UEs will decrease because more UEs are served by macro eNB. On the other hand, if a large offset value is used, more UEs are offloaded to the picocell while these UEs are far away from the pico eNBs. Hence, these UEs will suffer severe interference from macro eNB. As a result, although the CRE can mitigate the interference on uplink, the downlink signal quality of UEs located in the range expanded area decreases due to high interference from macro eNB.

5.1.3. Intercell Interference

As described in Section 3.1, the effect of downlink interference can be analysed using the received SINR of UE$_m$ on RB$_n$. The SINR at pico UE on RB$_n$ is given by (5.3):

$$SINR_{n,m}^{macro-pico} = \frac{P_n^i H_{n,m}^i}{\sum_{k}^{mc} P_n^k H_{n,m}^k \rho_n^k + \sum_{j,j\neq i}^{pc} P_n^j H_{n,m}^j \rho_n^j + P_N} \tag{5.3}$$

where P_n^i and $H_{n,m}^i$ are the transmission powers from the serving pico eNB$_i$ on RB$_n$, and the channel gains from the serving pico eNB$_i$ to UE$_m$ on RB$_n$, respectively. The number of interfering picocells and macrocells are represented by *pc* and *mc,* respectively. Parameters P_n^j and P_n^k are the transmission powers of the interfering picocell and macrocell. Moreover, $H_{n,m}^k$ and $H_{n,m}^j$ represent the channel gains from the interfering macrocell *k* and picocell *j* to UE*m* on RB*n*. ρ_n^k and ρ_n^j are set to 1 or 0 to indicate whether the neighbouring cell *k* or *j* allocates RB$_n$ to its UEs. P_N is the noise power. Equation (5.3) represents that the UEs located in range expanded areas suffer strong downlink interference because the transmission power of macro eNB is higher than pico eNB.

5.2. Challenges of Intercell Interference Management

Since picocells may become underutilized due to severe interference, one of the important aspects of HetNets is interference management. The interference management must be able to support the co-channel deployment for various traffic loads and using different number of picocells at various geographical regions.

In general, several techniques have been suggested to increase capacity and mitigate ICI in LTE-A including 1) Randomization, 2) Cancellation, 3) Coordinated Multi-Point transmission (CoMP) [87], 4) Multiple –Input Multiple-Output (MIMO) [88], and 5) ICI Coordination (ICIC) [89]. The randomization technique attempts to randomize the interfering signals and distribute the interference among all UEs as described in Section 3.2.1. In the cancellation technique, the data detection is performed on the interference, and the cancelled signal is the interference instead of the original received signal (see Section 3.2.1). Hence the signal quality can be improved. Although these two techniques are useful to mitigate interference, the complexity at receiver side is an issue specially when there are multiple dominant interferers. MIMO is another technique used to increase the coverage and system performance and CoMP can be considered as an extension of multi user MIMO in downlink [90]. CoMP can improve the performance and coverage via joint processing and decoding signals from multiple transmissions. However, these two techniques cannot significantly enhance the indoor coverage because of requiring the processing and implementation complexity. Moreover, it is assumed that the picocells are low cost cell while using antenna arrays for picocells can lead to increase of costs. The ICIC technique deploys certain restrictions on the resources used in different cells in a coordinated way to provide higher quality of services to UEs with lower SINR without sacrificing throughput of other UEs. Consequently, ICIC technique can be useful for picocells and it is classified into three major categories: 1) time-domain, 2) frequency-domain, and 3) power-domain. In this section, issues of the two important ICIC categories are explained including time domain and frequency domain.

5.2.1. Time Domain

The interference problem can be mitigated in time domain through subframe utilization. This utilization is performed across different cells through the Almost Blank Subframes (ABSs) [91]. In macrocell-picocell scenario, the macro eNB can either stop data transmission on the ABSs or reduce the transmission power. There are two types of ABS which are called Zero Power ABS (ZP-ABS) and Low Power ABS (LP-ABS). Z-ABSs are subframes without any transmission or only transmitting the reference signals from macro eNB whereas in LP-ABS the macro eNB only reduces the transmission power of data channels as shown in Figure 5.2 (a). Macrocell-picocell configuration uses the ABSs at the macrocell and schedules UEs located in the range expanded area within subframes that overlap with the ABSs of the macrocell as shown in Figure 5.2 (b). Moreover, pico eNB can also transmit to its UEs on the non-ABSs. In other words, ABS configurations show how pico eNBs are informed about the interference pattern from the macro eNB and then schedule its UEs on subframes to avoid from high interference. Note that, in the case of LP-ABS, only the UEs close to macro eNB can be scheduled on the ABSs. Although LP-ABS would improve the throughput of macro UEs, the throughput of pico UEs decreases due to increase of interference on UEs in range expanded area. Consequently, a trade-off between both macro and pico UE throughput is needed to optimize the performances of macrocell and picocell [92]. In Release 10, only the ZP-ABS configuration was supported and LP-ABS was investigated for Release 11 LTE-Advanced [93]. In this thesis, ZP-ABS was investigated.

In time domain, the power reduction is applied on data channels while the Common Reference Signal (CRS), synchronizations and paging channels are transmitted at full power. These signals are used for measurements and are required for cell selection and handover for all UEs. For this reason, [94] recommends that the interference cancellation approach is applied for CRS on pico UEs during ABSs [92]. In addition, a strict synchronization is needed between macro and pico eNB to set the optimum ABS pattern. The macro UE should be informed by eNB when a new ZP-ABS or LP-ABS pattern is applied. Release 10 supports the information exchange between macro eNB and pico eNB over X2 interface including ZP-ABS information and ZP-ABS status. By

introducing the LP-ABS, it would be advantageous to exchange information about the amount of the LP-ABS power reduction.

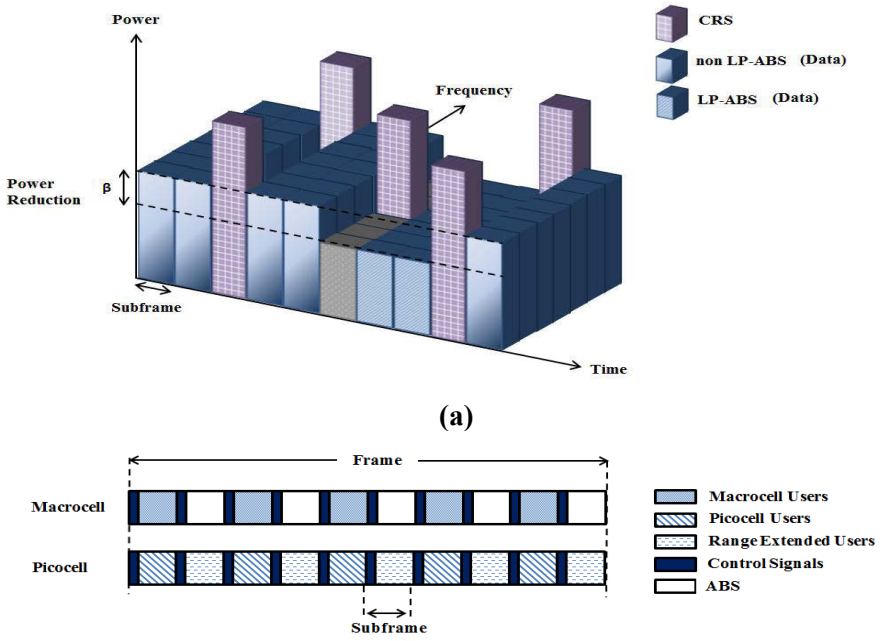

Figure 5.2. (a) A simplified scheme for LP-ABS, (b) Scheduling of UE located in range expanded area on the ABSs

5.2.1.1. Constraints on Transmission Power Reduction

When power reduction is applied on ABSs, several parameters must be considered such as level of transmission power reduction, CRE offset value, and ABS value. On the other hand, the power reduction has a direct effect on modulation scheme which will be described in more detail in this subsection. Consequently, the challenges of designing a LP-ABS scheme can be divided into four aspects: the ABS value, CRE offset value, level of transmission power reduction and modulation scheme.

1) *ABS value*: LP-ABS can decrease the influence of ABSs on the throughput of macro UEs because the macro UE can transmit data on both ABS and non-ABS. On the other hand, using ABS and non-ABS by macro UEs causes the throughput of UEs located in range expanded area to decrease because of interference from macro eNB on the ABSs. Therefore, numbers of the ABS and the non-ABS affect the system performance.

2) *Level of transmission power reduction*: the important parameter which is taken into account in LP-ABS scheme is the level of transmission power reduction. When the transmission power is considerably reduced the macro UE's throughput is not improved significantly because the received signal quality of macro UE on ABSs is poor. On the other hand, if the reduction in the power level is very low, the throughput of UEs located in range expanded area decreases compared to ZP-ABS because these UEs still suffer the interference from the macro eNBs on ABSs.

3) *CRE offset value*: in order to investigate the relationship between the transmission power reduction and the CRE offset value, the SINR experienced by pico UEs on the non-ABSs and the ABSs are simplified to the received RSRP from pico eNB and macro eNB. For the UEs located in the basic coverage of picocell, the difference in signal level received from the strongest interfering macro eNB and the serving pico eNB on non-ABSs can be approximated as follows [92]:

$$SINR\ (\text{dB}) \approx RSRP_{\text{pico}} - RSRP_{\text{macro}} \geq 0 \tag{5.4}$$

For UEs located in range expanded area with a CRE offset value of L dB, the RSRP received from macro eNB is M dB greater than RSRP received from pico eNB. In this case, if the transmission power decreases by M dB due to applying LP-ABS scheme, the SINR of these UEs on ABSs can be approximated by:

$$\begin{aligned} SINR\ (\text{dB}) &\approx RSRP_{\text{pico}} - RSRP_{\text{macro LP-ABS}} \\ &= M - L \end{aligned} \tag{5.5}$$

Thus when the offset value is larger than the transmission power reduction, the UEs located in range expanded area may suffer ($L - M$) dB interference from the macro eNB. The macro UEs close to the cell border must be scheduled on the non-ABSs.

4) *Modulation*: for the ABSs in LP-ABS scheme, the transmission power of data transmitted by macro eNB is reduced while the transmission power of CRSs is

same as the non-ABSs. This difference between the transmission powers of data signal and CRS can lead to the leakage power and hence impacts the interference on the data signals. The effect of this interference becomes more significant when a higher order modulation is deployed. Therefore, the modulation scheme must be restricted based on the transmission power reduction for data transmitted by macro eNB on the ABS. Based on 3GPP standardization [95], the RE power control dynamic range in LTE is defined as the difference between the power of a RE and the average RE power for an eNB at the maximum output power as shown in Table 5.1 [95]. Based on this table, the maximum reduction in power of PDSCH for 16QAM (64QAM) is -3 (0) dB while it equals -6 dB for PDSCH for QPSK. Consequently, a lower order modulation (e.g., QPSK) must be used when the level of transmission power reduction is high. Using power reduction more than 6 dB can lead to a significant increase in the dynamic range of RE power within an OFDM symbol. Note that restriction on modulation schemes has no effect on the throughput of pico UEs because pico eNB does not decrease the transmission power of ABS and non-ABS.

Table 5.1. RE Power Control Dynamic Range [95]

Modulation scheme used on the RE	**RE power control dynamic range (dB)**	
	Down	**Up**
QPSK (PDCCH)	-6	+4
QPSK (PDSCH)	-6	+3
16 QAM (PDSCH)	-3	+3
64 QAM (PDSCH)	0	0

5.2.2. Frequency Domain

Although the CRE significantly mitigates interference in uplink, the downlink signal quality of UEs located in the range expanded area decreases. Such UEs may experience a downlink SINRs below 0 dB because these UEs are connected to eNBs that do not provide the maximum downlink RSRP. Therefore, in the range expanded area both data and control channels will suffer from ICI because these channels are not planned for very low SINR. For this reason, the frequency ICIC schemes may not work longer in

macrocell-picocell scenario. In order to explain why the exiting frequency ICIC scheme cannot be used, the control channels will be described in more details in this subsection.

5.2.2.1.Constraints on Control Channel

In LTE and LTE-A, a downlink PRB consists of REs defined for data, control, broadcast, synchronization and antenna reference signals. The control region comprises the Physical Control Format Indicator Channel (PCFICH), PDCCH, Physical Indicator Channel (PHICH) and the Hybrid Automatic Repeat request (HARQ) as shown in Figure 5.3. The control region spans between one and three first OFDM symbols of every subframe.

The PCFICH consists of the Control Format Indicator (CFI) to carry information about the number of OFDM symbols used to transmit the PDCCHs in the corresponding subframe. The PCFICH is transmitted on four RE Groups (REGs) which are spread in the first OFDM symbol of a corresponding subframe over the total bandwidth. Each REG includes four REs.

The PDCCH region can occupy up to three OFDM symbols in a normal subframes when the system bandwidth is greater than 1.5 MHz. The Physical Downlink Shared Channel (PDSCH) and Physical Uplink Shared Channel (PUSCH) scheduling grant information are carried on PDCCH transmitted by serving eNB to UEs. Each PDCCH contains 1, 2, 4 or 8 Control Channel Elements (CCE) and each CCE is formed from 9 REGs. The REGs are interleaved across the system bandwidth and across the considered OFDM symbols. A cyclic shift is used for the interleaved REGs based on the cell IDs. In LTE, there are a limited set of CCEs for each UE including its PDCCH. It can help that the UE does not perform a blindly search over the whole control channel in the frequency domain to find its allocated PDCCH. A unique Cell Radio Network Temporary Identifier (C-RNTI) is allocated to each UE by the eNB. C-RNTI is deployed to specify the location of PDCCH of each UE.

The downlink HARQ Acknowledgements (ACK)/ Non-Acknowledgements (NACK) information is transmitted on PHICH to response to an uplink PUSCH transmission. For this purpose, some REGs in PDCCH region can be occupied by PHICH where the

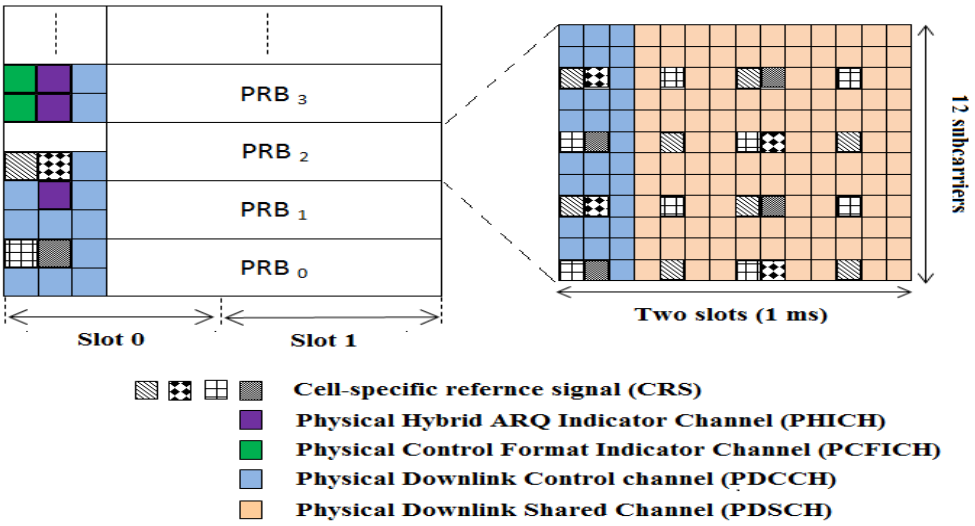

Figure 5.3. Locations of control and data regions defined in PRBs

PHICH duration is carried on the Master Information Block (MIB) to specify the number of OFDM symbols assigned to PHICH. Note that the MIB is transmitted on the Physical Broadcast Channel (PBCH). The REGs used for the PHICH are spread across the system bandwidth and the OFDM symbols defined for PHICH.

Consequently, REs of PCFICH are spread across the system bandwidth while the REs occupied by PDCCH and PHICH are spread across both the system bandwidth and the OFDM symbols. As a result, although ICIC can be performed on the PDSCH region by reserving different PRBs and/or controlling power for the macrocell and the picocell, ICIC schemes based on the frequency division cannot work longer in HetNets because different REs or PRBs cannot be reserved for control channel transmission in different cells. Moreover, the capability of changing the reference signal powers in different sub-bands in frequency domain has been not included in the standard. On the other hand, receiving the correct PDCCH and PCFICH is important because for a UE, the PDCCH specifies the number of REs allocated to PDSCH. Moreover, a UE is expected to decode the PCFICH correctly and thereafter decode the PDCCH. By identifying the PDCCH region boundary, a UE can find the starting symbol of PDSCH. Therefore, if the PCFICH or PDCCH cannot be correctly decoded, the data region will be lost. Finally, HARQ retransmission cannot be used on PDCCH in contrast to PDSCH.

Furthermore, since the transmission power of the interferer macro eNB is higher than the serving pico eNB in CRE scheme, channel conditions between the macro eNB and macro UEs are better than the pico eNB and UEs located in the range expanded area. Therefore, different aggregation levels are assigned to macro UEs and UE located in the range expanded area. The aggregation level is defined as the number of control channel elements used to transmit the PDCCH and takes values in {1, 2, 4, 8}. The aggregation levels allocated to UEs in range expanded area is usually large while for macro UE the aggregation level is small. Consequently, for the macro UE, the low number of physical control channels is needed to transmit. That is one OFDM is assigned for control region and the rest of subframes are used for data transmission. While for UEs located in the range expanded area, more than one OFDM symbol are allocated to control region. It can lead to interference on control region of UEs located in the range expanded area.

5.2.2.2. Solution: Enhanced-PDCCH

Enhanced-PDCCH (EPDCCH) [96] has been proposed to support frequency domain ICIC. EPDCCH can support the increased downlink control channel capacity, beam forming and the enhanced spatial reuse which are outside the scope of this thesis. An EPDCCH cannot deploy the resources within the downlink control region to avoid interference with the control channels. The EPDCCH should not affect the data transmitted to a UE on the PDSCH. For this purpose, an EPDCCH does not span the whole bandwidth such that the PRB not used by EPDCCH can be assigned to UEs. Moreover, if the EPDCCH spans in the total subframes, the available time to decode the PDSCH is reduced. Consequently, the EPDCCH can be frequency division multiplexing (FDM) with the PDSCH to occupy a subset of the PRB of the system bandwidth.

Since a maximum of three OFDM symbols are used by PDCCH, a UE is able to decode the PDCCH and then start decoding the PDSCH before the end of a subframe. However, for EPDCCH spanning the total subframes, a UE has to wait for several hundreds of microseconds after the end of the subframe to decode the EPDCCH. Thus, the time available to decode PDSCH and generate the HARQ-ACK feedback is reduced. For these reasons, some alternative multiplexing approaches have been considered between PDSCH and EPDCCH as shown in Figure 5.4. For example, DL grants are transmitted in the first slot of the subframe with some forms of Time Division

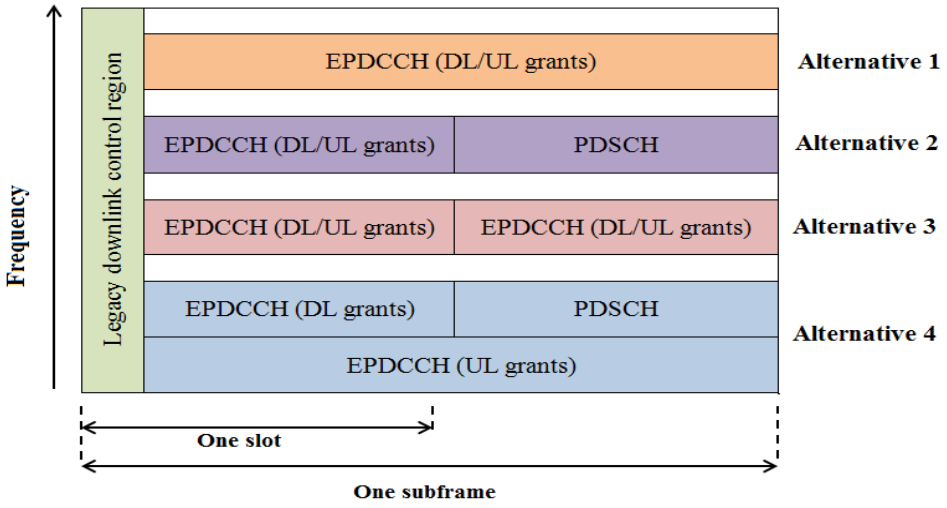

Figure 5.4. Alternatives for multiplexing of EPDCCH and PDSCH [96]

Multiplexing (TDM). For simplicity, EPDCCH and PDSCH cannot be multiplexed within one PRB. In this case, in order to improve the resource utilization, PDSCH can transmit on a PRB assigned to EPDCCH but EPDCCH does not use it in a subframe. Radio Resource Control (RRC) signalling is used to configure the location of PRB for EPDCCH in the frequency domain. It enables the system to coordinate EPDCCH interference in the frequency domain between macrocells and picocells when macrocell and picocells share the same carrier. The improved version of the EPDCCH is currently planned for Release 12 [96].

5.3. Enhanced Intercell Interference Coordination Techniques in Macrocell-Picocell Scenario

In HetNet, the interference situations may change in different locations because of different powers and traffic loads. As discussed in Section 5.1, the ICI problem can occur for both data and control channels in the range expanded areas. Although in 3GPP, the interference of data channel can be mitigated through ICI mitigation techniques proposed for LTE Release 8, the suggested ICI mitigation methods did not consider the problem of control channel interference. Therefore, in order to keep the cell coverage and improve the system performance, ICI mitigation must be deployed for control and data channel when CRE is used. Moreover, due to small radius of picocells, the LTE ICI mitigation schemes such as the FFR schemes cannot be used. A number of ICIC schemes have been proposed to overcome the ICI problem in LTE-A. The ICIC

schemes are divided into three major categories [97] including time domain, frequency domain and power domain which are reviewed below.

5.3.1. Time Domain Schemes

Several papers have been proposed to mitigate interference in time domain. Reference [98] investigated the performance of eICIC and CRE in picocell downlink system. Two types of subframes have been considered for eICIC scheme: ABS and non- ABS. In this scheme, the macrocell does not transmit on some ABS to protect UEs connected to the pico eNB because the interference caused by the picocells is not important in a HetNet. Then macrocell uses other resources (non- ABS) to send data to its UEs. The ratio of the ABS is obtained based on the number of the UEs connected to the pico eNBs without CRE, and the number of the UEs connected to the pico eNBs with CRE. Note that, the location of the ABS and non- ABS and number of ABSs are set by ABS pattern. Reference [99] computed the number of ABSs based on the macro load, pico load and pico CRE load and using a minimization approach.

Reference [100] has considered a non-static eICIC scheme using Lightly Loaded Control Channel Transmission Subframe (LLCS) to mitigate the downlink control channel interference problem caused by CRE. Based on Figure 5.5, the first symbols in every subframe are reserved for control channels involving multiple PDCCHs to inform the downlink resource allocation and carry uplink scheduling granted to UEs or some other kinds of the control channels. Each PDCCH is one or several consecutive control channel elements consisting of multiple RBs. However, PDCCH is the least robust for the interference in the control channels [100]. The proposed scheme deploys both LLCS and ABS in the macrocells to mitigate the PDCCH interference from the macrocell. Since PDCCH is distributed based on a predetermined hopping pattern over the control channel region, the interference of PDCCH in neighbour cells can be mitigated by the LLCS. Note that the macrocell has to inform its neighbouring picocells via interface about the subframes used for LLCS/ABS. By restricting the resource allocation of pico UEs to those subframes, the PDCCH interference problem will be eliminated. The interference of PDCCH in neighbouring cells can be mitigated most considerably in ABS because a cell transmits only CRS in ABS. Note that the CRS is usually used to measure the channel condition. Although LLCS is weaker than ABS when a large offset

value is not applied for CRE, LLCS can mitigate the PDCCH interference and allow the PDSCH transmission for some UEs in contrast to ABS. Moreover, the large CRE offset value leads to significant interference therefore the UE needs to use interference cancellation. Since using both LLCS and ABS in macrocells leads to reduce the user throughput, the ratio of these subframes to normal subframes should be appropriately determined.

Some schemes are proposed based on a utility function to mitigate the interference in time domain. Reference [101] proposed a method to find the optimal amount of ABS in ABS configuration. This scheme has assumed that pico UEs are categorized into victim UEs and normal UEs. Moreover, the macro eNB works only on non-ABS but the pico eNB operates on all subframes and victim UEs are scheduled on ABSs (see Figure 5.6). The optimal selection for victim UEs and normal UEs is performed through the utility function. The utility function is obtained based on ABS density, initial numbers of victim and normal UEs and the achievable data rate. The initial values for victim and normal UEs are selected based on the criteria such as a SINR threshold. Then each eNB deploys the Dynamic Programming [102] solution to maximize the utility function for each ABS density and records the UE selection results. Macro eNBs and pico eNBs inform each other about the result of utility functions through X2 interface. After receiving the information, each eNB calculates the sum of all received sub-utilities to obtain the overall system utility and then find the optimal value of ABS density corresponding to maximum overall system utility. Finally, all eNBs use the updated ABS density. In [103], two interacting factors have been considered to improve the performance of macrocells and picocells: UE partition and the number of ABSs. The

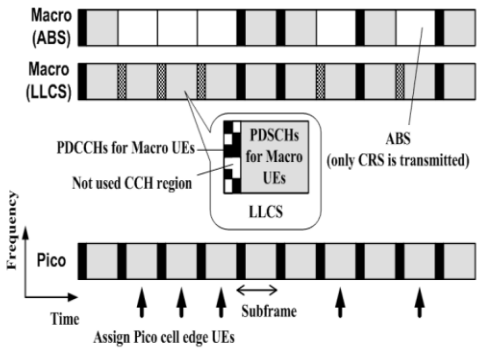

Figure 5.5. eICIC using LLCS/ABS [100]

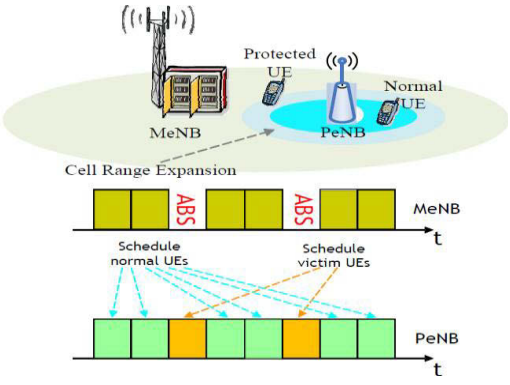

Figure 5.6. Normal and victim UEs defined in [101]

algorithm starts by some initial values. Then for each iteration procedure, both UE partition and subframe ratio selection are executed. Subframe ratio specifies the number of ABSs to the number of total available subframes. A Nash Bargaining Solution [104-105] has been used to model the UE partition problem. That is, the UE partition problem of picocell is such as a game with two players where UEs compete with each other to obtain one kind of following subframes: non-ABSs or ABSs. For simplicity, the number of ABS is fixed during UE partition iterations. After the UE partition procedure, the subframe ratio selection is executed by a centre controller to select the proper value and maximize the utility function defined for all eNBs. The centre controller knows the transmitted data of each eNB for each type of subframes which is reported frequently by eNBs. The ABS pattern will be generated based on the subframe ratio and then broadcasted to all eNBs. The UE partition is performed periodically but the subframe ratio reselection can be executed by a trigger. The trigger can be set when the UE partition is significantly different as before or when an event occurs such as UE handover. Reference [106] suggested a scheme to find the optimal ABS value based on optimizing a system utility function which is defined as a function of the all UEs' throughputs. Since the ABS optimization is NP-hard problem, a dual-based approach [107] has been used to solve the problem. In addition, [108] introduced a utility function using the throughput of macrocell, edge and centre throughput of picocells, number of picocell and macrocells, and the number of UEs. By derivative from the utility function, the required number of ABS is obtained.

Reference [109] investigated the effect of static and dynamic Protected Subframes (PSF) configuration on the system performance. Since only the static PSF configuration has been taken into account by 3GPP, the author proposed a dynamic scheme to determine the PSF density (i.e., number of PSF). Therefore, a new metric has been deployed (based on the average logarithmic throughput of the macro and pico UEs) to find the suitable PSF density because the low PSF density decreases the performance of pico UEs. For this purpose, this scheme compares the utility of macrocell and picocells UEs and then finds the probability of changing the PSF density (P_d). Thereafter, the PSF density is changed corresponding to the obtained probability. If the probability is greater than or equals zero, the PSF density increases with probability equal to P_d; otherwise PSF density decreases with probability equal to one. The results [109] show that static configuration is only useful for small CRE offset value with full buffer traffic

while dynamic configuration is better for other situations (i.e. the large CRE offset value with full buffer and non-full buffer traffics and small pico CRE with non-full buffer traffics).

CQI adjustment is another problem which has been considered when ABSs are used. Due to the time delay in CQI reporting, it is possible the CQI measured for one type of subframes is deployed for another type of subframes. Therefore, the channel cannot be appropriately estimated and then a wrong MCS will be selected. Consequently, using incorrect CQI leads to transmission failure or transmission inefficiency. References [110-112] worked on CQI adjustment to improve the UE performance. For instance, in [110] multiple CQI feedbacks have been used along with the joint decision method. For this purpose, a set of K neighbouring macro and pico eNBs cooperate to select the status of each eNB. In general, two types of status are considered: normal and muted. The muted status means the macro eNB is partially muted on subframes (i.e., ABSs) to decrease interference on the pico UE. Each macro UE feeds back K number of CQIs and each pico UE feeds back (K+1) CQIs containing the signal strength and the interference strength of all macro eNBs located in the neighbouring set. When each eNB receives the CQIs, it updates the status of each member of the neighbouring set. After updating the status, each eNB can use them to estimate system performances. The estimated values are reported to the macro eNB to compare the performances of the mentioned set and then the status with the highest performance will be selected. Finally, each eNB can deploy updated CQI corresponding to the selected status for its scheduling.

5.3.2. Power Domain Schemes

This part reviews the power domain scheme which is a method deployed at macrocells to manage the dominant interference. Two major problems must be considered in the real action to decrease the transmission power. On one hand, eNB does not know the transmission power of which UE should decrease. That is the transmission power of its UE should reduce or the transmission power of UE which belongs to neighbouring cell. On the other hand, eNB does not know how much power should be reduced for its UE if its priority is lower.

A cooperative macrocell-picocell scheduling approach has been proposed in [113] to mitigate downlink ICI. UEs continuously measure the downlink Received Signal Strength (RSS) of the pilot signals of neighbouring cells to choose the best serving cell. Note that, the pilot signal indicates physical cell identities and it is usually transmitted at a constant power. Moreover, a list of cells and pilot signals is periodically broadcasted by the serving cell called Neighbouring Cell List (NCL). By receiving the NCL, a UE regularly performs the channel measurement and then reports the results to its serving cell in order to make a decision to trigger a handover procedure. The proposed ICIC scheme can be implemented in two steps: at first, the algorithm makes a decision about the maximum power which the macro eNB can apply on each PRB used by UEs located in the range expanded area. The aim of this decision is to provide the desired downlink SINR for UEs located in range expanded area. Some messages are required to establish coordination/ communication between macro eNBs and pico eNBs. Intercell communication among macro eNBs and pico eNBs can be periodically performed or event triggered through the interface. In the first step, a UE located in the range expanded area calculates the largest ICI which it can tolerate based on the measured downlink RSS, a target SINR and noise power. Then it obtains the maximum power that the interfering macrocell can allocate to PRBs to avoid the outage of UE located in range expanded area. Thereafter, both the obtained maximum power and index of PRB to macrocell are sent to neighbours. At the second step, the macro eNB must allocate PRBs and its transmission powers to its UEs. For this purpose, the macro eNB considers the power constraints derived from previous steps to support UEs located in range expanded area. For scheduling procedure, macro eNB independently allocates PRBs to its UEs such that the transmission powers are minimized while the required data rates of its attached UEs are met. For this purpose, the macrocell estimates the number of the required PRBs for macro UEs based on the target throughput and efficiency. The macrocell uses a network flow approach to solve the linear problem of cooperation of the PRB and power allocation. Through the proposed scheme, PRBs used by UEs located in range expanded area are allocated to macro UEs which have lower data rate demands and lower transmission powers or UEs which are closer to the macro eNBs. Therefore, macro UEs and UEs located in the range expanded area can reuse the same PRB, while their SINR requirements are satisfied.

Reference [114] proposed an eICIC method based on region splitting where the borders of cells are divided into several segments based on the channel fading or geometry, and then marked by identities as shown in Figure 5.7. The cell informs all neighbouring cells about its division and identities of each segment. During a severe interference, the cell sends an indication including the index of the interfered PRB and the index of the area where this PRB is used. Finally, each neighbouring cell uses based on the scheduling table and region information to find whether it has caused interference, and then deploys the accurate ICIC action such as avoiding the high interfering PRB or reducing the power on this PRB.

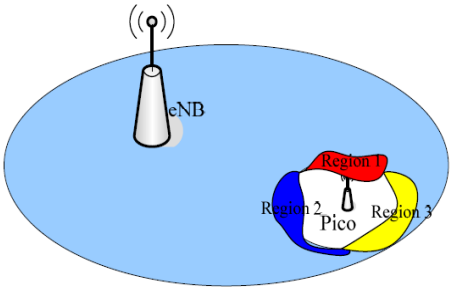

Figure 5.7: Region division [114]

An ICIC technique based on the priority has been suggested in [115] to specify the correct amount of power reduction on the selected PRBs. The goal of this scheme is to find a coefficient value for reducing the transmission power. For this purpose, two users, UE_1 (UE with lower priority) and UE_2 (UE with higher priority), are considered in an interfered region of macro cell and picocell. If there is no free PRBs to assign to UE_2, macro eNB decreases the transmission power of PRB used by UE_2. Then the channel capacity of each UE is calculated through Shannon theorem. From this theorem, the transmission powers of two UEs are obtained as a function of capacity. On the other hand, the capacity corresponding to the new value of transmission powers must be higher than the old capacity to improve the system spectral efficiency. By replacing of these parameters and considering the minimum required data rate of UE_2, the amount of the transmission power reduction is achieved.

A scheme has been introduced in [116] to mitigate interference through setting the cognitive critical ratio and a power reward factor. The interference management problem is modelled as a multiple objective optimal problem of saving power for the macro eNB and pico eNB. In this scheme, the cognitive sensing is executed by the pico

eNB to sense its surrounding wireless environments and gather the subcarrier usage knowledge from the dominant interferers. Pico eNBs are randomly placed in macro coverage and have overlay with the macrocell. It is assumed that interference happens only inside and around the overlapping region called Interference Zone (IZ). A probe signal is sent by a pico eNB to start the cognitive sensing and gather the subcarrier usage information about the current macro UEs. When a macro UE receives this probing signal, it will reply and report its existence as well as the PRB which has presently deployed in the circular sensing region. The macro eNB can provide a certain amount of 'reward' power for cognitive sensing of pico eNB. The reward power allocates additional power to a pico eNB that executes cognitive sensing in a circle. Then, for picocell and macrocell, the utility function of power reward factor and cognitive critical ratio is obtained using the following parameters: the number of picocells, critical radius, power reward factor, the consumed power, power exchange rate, the wasted power, downlink power and traffic load in macro coverage. Genetic Algorithm is used to get the global optimal solution for saving power strategy. The practical implementation of the proposed scheme can be summarized as follows: at first the channel path loss from the macro eNB to macro UEs is measured then reported to the macro eNB. The macro eNB computes the maximum saving power using the interactive multiple objectives nonlinear programming Genetic algorithm and informs the pico eNB about the optimal strategy. Then the optimal reward power is allocated to the pico eNB. The cognitive sensing is performed based on the sensing radius and the interference information about the PRBs used by macro UEs is reported to the pico eNB. Finally the independent PRBs are allocated to the pico UEs located in IZ to mitigate the interference.

5.3.3. Frequency Domain Schemes

The aim of [117] is to formulate the spectrum sharing problem such that the maximum overall throughput and fairness are achieved and also the variable traffic demand of UE can be satisfied. In this work, the available bandwidth is divided into a set of contiguous PRBs, called B-Bands which are the smallest radio resource allocated to a picocell. The proposed approach consists of two algorithms: 1) the non-cooperative algorithm in which each picocell selects its resources independently and updates the resources allocation using the local measurements; it considers a back off period to determine the

upcoming updating instant, and 2) the cooperative algorithm which considers a common time based on the resource updating for picocells. In this scheme information is exchanged on X2 interface. Both algorithms start by a random selection of B-bands. The objective function is calculated for each B-band by picocells through measurement reported by the attached UEs. Based on the calculated cost function, the B-bands are ranked by picocells and the best numbers of B-bands are selected. Finally, the pico eNB compares a threshold value of SINR with the average received SINR on the selected B-bands from its UEs; if it is greater than a threshold, the number of B-bands allocated to picocell increases otherwise it will decrease. In order to support the load, the amount of B-bands is determined by dividing the number of pico UEs by the total number of UEs.

A combination of power and frequency inter-layer interference coordination technique has been introduced in [118]. In this technique, the total available bandwidth is divided into two sub-bands: normal and protected sub-bands. The protected subband is reserved for pico CEUs in which the macro eNB decreases its transmission power on them using a power reduction factor (P_{rf}) while pico eNB transmits with maximum power. P_{rf} is the ratio of the transmission power of normal sub-band to the transmission power of the protected subband and was set to 10 dB. In normal sub-band, both pico and macro eNBs use its maximum transmission powers. Note that UEs were divided to CEUs and CCUs based on average SINR and the threshold value for SINR was set to 0 dB. It is assumed that both pico CEUs and macro CCUs can be scheduled on the protected sub-bands while pico CCUs, macro CCUs and macro CEUs can schedule on normal sub-band. The ratio of the protected sub-bands to the normal sub-band can be determined adaptively based on user distribution. For this purpose, a bandwidth partition ratio is defined as the ratio of the number of pico CEUs to the total number of UEs located in both macrocell and picocells. The protected sub-band equals the product of the bandwidth partition ratio and the total available bandwidth.

5.3.4. Qualitative Comparison

When macrocell and picocells share the bandwidth, each cell can use the total available bandwidth based on RF1 scheme. In this case a transmitter transmits on sub-bands which are randomly selected using the amount of traffic in the buffer. Therefore, using

RF1 especially in cell expanded area causes a large number of UEs experience low SINR because of receiving sever interference from the macro eNB.

Although in 3GPP the interference of data channel can be mitigated through ICI mitigation techniques proposed for LTE Release 8, the suggested methods did not consider the problem of the control channel interference. Moreover, the FFR schemes are not applicable for picocells because the radius of picocells is small. Therefore, the eICIC techniques proposed for picocells are compared with RF1. Table IV provides a qualitative comparison between macrocell-picocell ICIC techniques and RF1 scheme. Note that the results were obtained from their references. The terms of high, medium and low express the qualitative amount of throughput improvement resulting from the proposed schemes are compared with the throughput of RF1. Most of the proposed schemes could improve both cell throughput and throughput of UEs located in the range expanded area.

In the time domain scheme, the interference is mitigated when UEs located in range expanded area are scheduled on the ABSs. When the CRE offset value is low, a small number of UEs are connected to the picocells. Consequently, throughput of UEs located in range expanded area is still high when the ratio of the subframes allocated to picocell is low and UEs connected to the macrocell can use more resources too. However, when the high CRE offset value is used, a large number of UEs are offloaded to the picocells. Therefore, the high ratio of the picocells' subframes is required to improve the throughput of UEs located in range expanded area. On the other hand, the cell throughput decreases by increasing the CRE offset value because the picocell throughput decreases when the UEs far away from the picocells are connected to the picocells. Consequently, in time domain eICIC techniques, the ratio of subframes selected for the macrocell-picocell configuration is a crucial factor and an inappropriate ratio can degrade the throughput of UEs located in the range expanded area or cell throughput. Table 5.2 demonstrates that approaches with a dynamic ABS ratio selection have better performance among proposed time domain eICIC schemes.

Power control is a method used at macrocells to manage dominant interference. For this purpose, picocells and macrocell cooperate with each other to reduce the interference on the same PRBs. Based on information exchanged among all picocells and the macrocell,

the macrocell can find lower downlink transmission power value to deploy in the same PRBs used by UEs located in the range expanded area. Note that the downlink interference from picocell to macrocell is not important because the transmission power of picocell is much lower than macrocell. Based on Table 5.2, the schemes using utility or cost functions (such as [113] and [116]) have higher performance because these schemes find optimal solutions for cooperative PRB and power allocation problems.

The proposed frequency domain ICIC technique updates the number of the allocated resources periodically based on the number of users attached to picocells and the averaged value of SINR over all UEs. Therefore, it can allocate the picocell's resources based on loads and then significantly improve the throughput when compared with RF1. However, the signalling between picocells leads to increase of the system overhead. Moreover, these schemes did not consider the constraints of control channel.

5.4. Summary

The HetNet architecture introduced new ICI problems because of the transmission power difference between macro eNB and pico eNB. In this case, the ICI can occur on both data and control channel for UEs located in the range expanded area when macrocell and picocells share the bandwidth. This chapter has identified the technical challenges and research problems in terms of intercell interference in both time domain and frequency domain. Particular attention has been given to the ICIC between macrocell and picocell. Thereafter, the proposed schemes to mitigate ICI in time, power and frequency domains were reviewed and a qualitative comparison was provided.

Table 5.2. Comparison among ICIC Algorithms in Macrocell-Picocell Downlink Systems

Domain	Scheme	Method	Number of Picocell in each Microcell	Throughput of UEs Located in Range Expanded Area	Cell Throughput
Time	Ref. [98]	ABS/non-ABS	4	Medium	High
	Ref. [99]	Minimization of ABS/non-ABS	1	Medium	Medium
	Ref. [100]	Loaded CCH transmission subframe	2	Medium	Medium
	Ref. [101]	Synchronous ABS	2	Medium	High
	Ref. [106]	Utility function	-	High	High
	Ref. [108]	Utility function	2	Medium	Medium
	Ref. [109]	Dynamic PSF	2	High	Medium
	Ref. [110]	CQI adjustment	4	Medium	Medium
Power	Ref. [113]	Minimal cost function of macro transmit power using network simplex algorithm	4	Medium	High
	Ref. [114]	Border region division based on channel fading or geometry	4	Medium	Medium
	Ref. [115]	Transmission power reduction based on user priority	4	Medium	Low
	Ref. [116]	Cognitive sensing and maximum net saving power strategy	4	High	Medium
Frequency	Ref. [117]	Updating the number of B-Bands based on objective function	4	High	Medium
	Ref. [118]	Adaptive frequency partition	6	High	Medium

Chapter 6

ENHANCED ICIC SCHEME USING FUZZY LOGIC SYSTEM IN LTE-A HETEROGENEOUS NETWORKS

As discussed in Chapter 5, although the picocell is one of the important low power nodes in HetNet, its coverage may be limited because of transmission power difference between macro eNB and pico eNB. In order to overcome this issue, CRE was introduced where an offset value is added to the received RSRP from pico eNB. However, using CRE scheme can lead to severe interference on both data and control channels in downlink for UEs located in the range expanded area (RE UE). In order to mitigate the interference in co-channel HetNets, the time domain eICIC was introduced as described in Section 5.3.1.

However, if the CRE offset value is fixed at a constant value, the CRE scheme cannot consider the UE distribution and satisfy the system requirements. Therefore, the number of offloading UEs cannot be suitably controlled by the static CRE offset value. Moreover, the static ABS value cannot support the dynamically changing network conditions.

This chapter answers two important questions (1) how to determine which UE should be connected to the pico eNB, and (2) how the radio resources should be shared in time domain to mitigate the interference in macrocell- picocell scenario. In the proposed scheme, the offset value is dynamically calculated such that UEs are connected to the appropriate eNB. Moreover, it is combined with the proposed dynamic ABS value scheme to mitigate the downlink interference in time domain. In contrast to eICIC schemes proposed in literature, this thesis aims to maintain a trade-off between macro UE and RE UE throughputs while other schemes focus only on RE UE throughputs.

This chapter is organised as follows. Section 6.1 introduces a dynamic CRE scheme and Section 6.2 proposes a dynamic ABS scheme. A new dynamic and effective eICIC is provided in Section 6.3. The performance results of the proposed schemes are given in Section 6.4. Finally, Section 6.5 summarizes the chapter.

6.1. A Dynamic CRE Scheme based on Fuzzy Logic System

In the CRE scheme (see Equation (5.2)), an offset value is added to the received RSRP from pico eNB to overcome the coverage issue. This scheme helps a UE select the pico eNB as its serving eNB even if it is not the strongest cell.

As described in Section 5.1.2, if the CRE offset value is not correctly chosen, the picocell cannot significantly enhance the system performance. For instance, when a large number of UEs are located in a macrocell and if a small CRE offset value is applied, only a few UEs are offloaded to the picocell due to a stronger RSRP received from the macro eNB. Consequently, the use of picocell cannot improve the performance of macrocell because more UEs continue to be served by the macrocell. In contrast, for a large offset value, more UEs are offloaded to the picocell and some of the offloaded UEs are far away from the pico eNBs. In this case, UEs suffer severe interference from macro eNB which leads to an increase of outage probability. Consequently, the fixed CRE offset value cannot offload the traffic appropriately between the macrocell and picocells. In this section, a dynamic and decentralized CRE scheme is introduced in which the CRE offset value is determined based on the historical system performance using a fuzzy logic system (FLS) to satisfy the system requirements.

6.1.1. CRE Offset Value Module Description

In the proposed scheme, the CRE offset value is calculated based on the most important performance metrics in downlink such as the throughput, SINR and number of UEs connected to pico and macro eNBs. Each macro eNB monitors these metrics in the specified time windows and then determines the next offset value. The offset value is broadcast to help UEs select the correct eNB as its serving eNB. The proposed scheme is repeated till the system performance reaches a desired value.

As shown in Figure 6.1, the proposed dynamic CRE scheme consists of five steps including inputs and output monitoring, fuzzification, fuzzy rules selection, aggregation, and defuzzification and is described below.

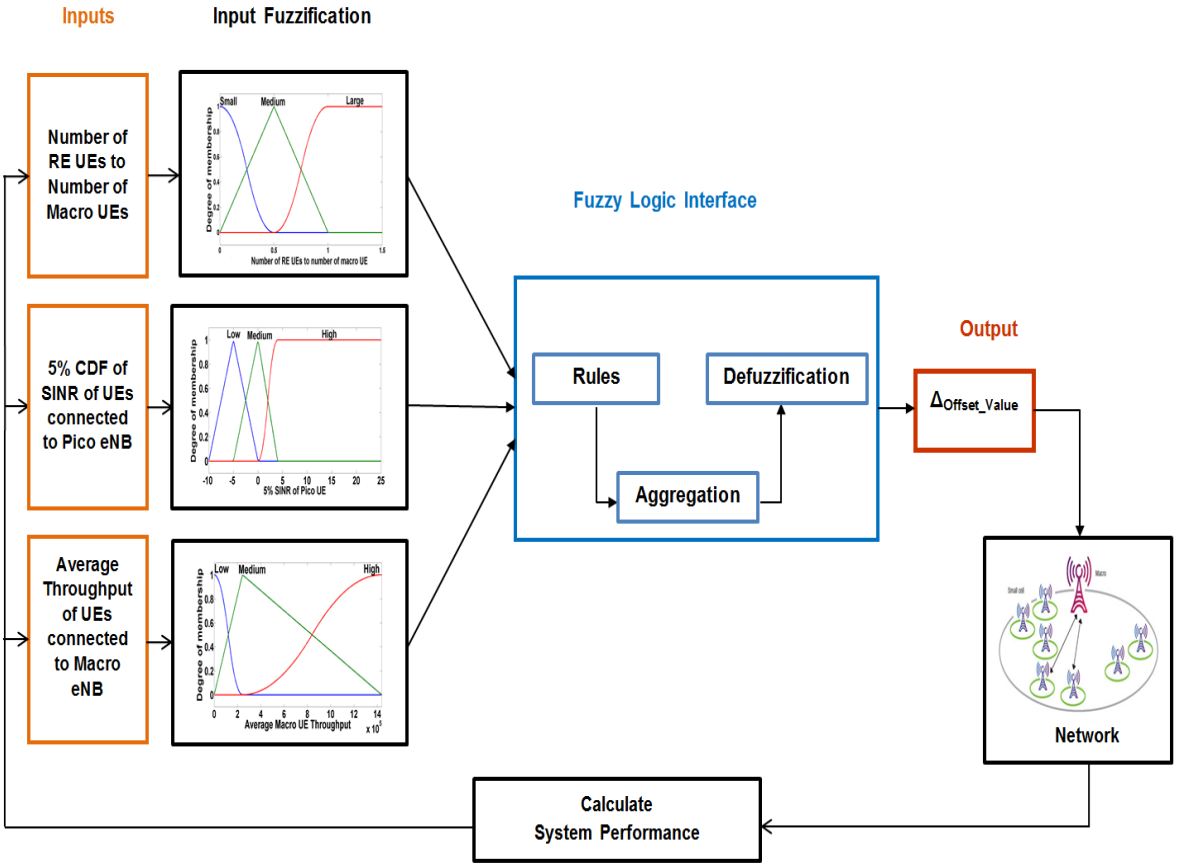

Figure 6.1. Graphical representation of the proposed dynamic CRE scheme based on FL

Step 1: Inputs and output

Since the CRE offset value can directly affect performance of macro UEs and UEs connected to pico eNBs, particularly RE UEs, a vector $x=[x_1, x_2, x_3]$ is introduced as the input where:

1) x_1 indicates number of RE UEs to number of macro UE.
2) x_2 is the 5% of CDF of SINR of pico UEs.
3) x_3 represents the average throughput of macro UEs.

5% of CDF of SINR represents the minimum SINR achieved by 95% of pico UEs. The SINR and average throughput of macro UEs can guarantee the throughputs of UEs with the lower SINR are enhanced while the required throughputs of macro UEs are satisfied.

Δ_{offset_value} is defined as the output of the system and represented by o_1 in this scheme. After each iteration, the Δ_{offset_value} is added to the last offset value. As shown in Figure 7.1, each input is directly fed back from the system. This feedback helps the FLS monitor the system performance and then change the offset value to improve the system performance.

Step 2: Fuzzification

In this step, each input or output is fuzzified through different membership functions. Moreover, the range of each membership function is determined based on the required system performance and operator's knowledge to achieve the desired results. Sets of fuzzy labels are defined using linguistic terms to fuzzify the variable. The fuzzy label sets of inputs and output are shown by T_{x1}, T_{x2}, T_{x3}, and T_{o1} as follows.

$$T_{x1} = \{Small, Medium, Large\}$$
$$T_{x2} = \{Low, Medium, High\}$$
$$T_{x3} = \{Low, Medium, High\}$$
$$T_{o1} = \{Decrease, Constant, Increase\}$$

Each input value x_i can be mapped to its corresponding fuzzy set T_{xi} with a membership degree μ_i. In addition, the output value o is mapped to the fuzzy set T_o with the membership degree of μ. The mathematical expressions of each linguistic term are given by:

$$F_{x1} = \{Z\text{-}shape, Triangular, S\text{-}shape\}$$
$$F_{x2} = \{Triangular, Triangular, S\text{-}shape\}$$
$$F_{x3} = \{Z\text{-}shape, Triangular, S\text{-}shape\}$$
$$F_{o1} = \{Triangular, Triangular, Triangular\}$$

The Triangular, S-shape and Z-shape functions are calculated by (4.5), (4.6) and (4.7), respectively.

Step 3: Definition of Fuzzy Rules

A set of fuzzy rules, represented by *s*, is defined to provide mapping between inputs and output. Based on the number of inputs and its membership functions, 27 rules are defined. This step can choose appropriate rules to map inputs to output correctly. One example of rule set is described below:

IF (x_1 is *Medium*) AND (x_2 is *Low*) AND (x_3 is *Medium*) THEN (o_1 is *Decrease*)

Step 4: Aggregation

As mentioned in Step 3, 27 rules were defined to map inputs to output. All rules in *s* have to be evaluated and then results will be combined using an aggregation method to make a best decision. In this scheme, the maximum method [84] was used as the aggregation method as shown in Figure 6.2. In this method, the overall fuzzy output is computed from the set of individual outputs taking the maximum membership degree where one or more membership functions overlap.

Step 5: Defuzzification

In the defuzzification step, the output value is given by the centre of gravity approach:

$$\Delta_{offset\_value} = \frac{\int_s \mu_j(y)\, y\, dy}{\int_s \mu_j(y)\, dy} \tag{6.1}$$

6.2. A Dynamic ABS Scheme based on Fuzzy Logic System

A new dynamic ABS scheme aims to share the radio resources in time domain between macrocell and picocells such that the interference is mitigated without sacrificing the throughput of macro UEs. Similar to the proposed CRE scheme, FLS is deployed to obtain the required ABS value to enhance the system performance of co-channel deployment where all network nodes use the same bandwidth.

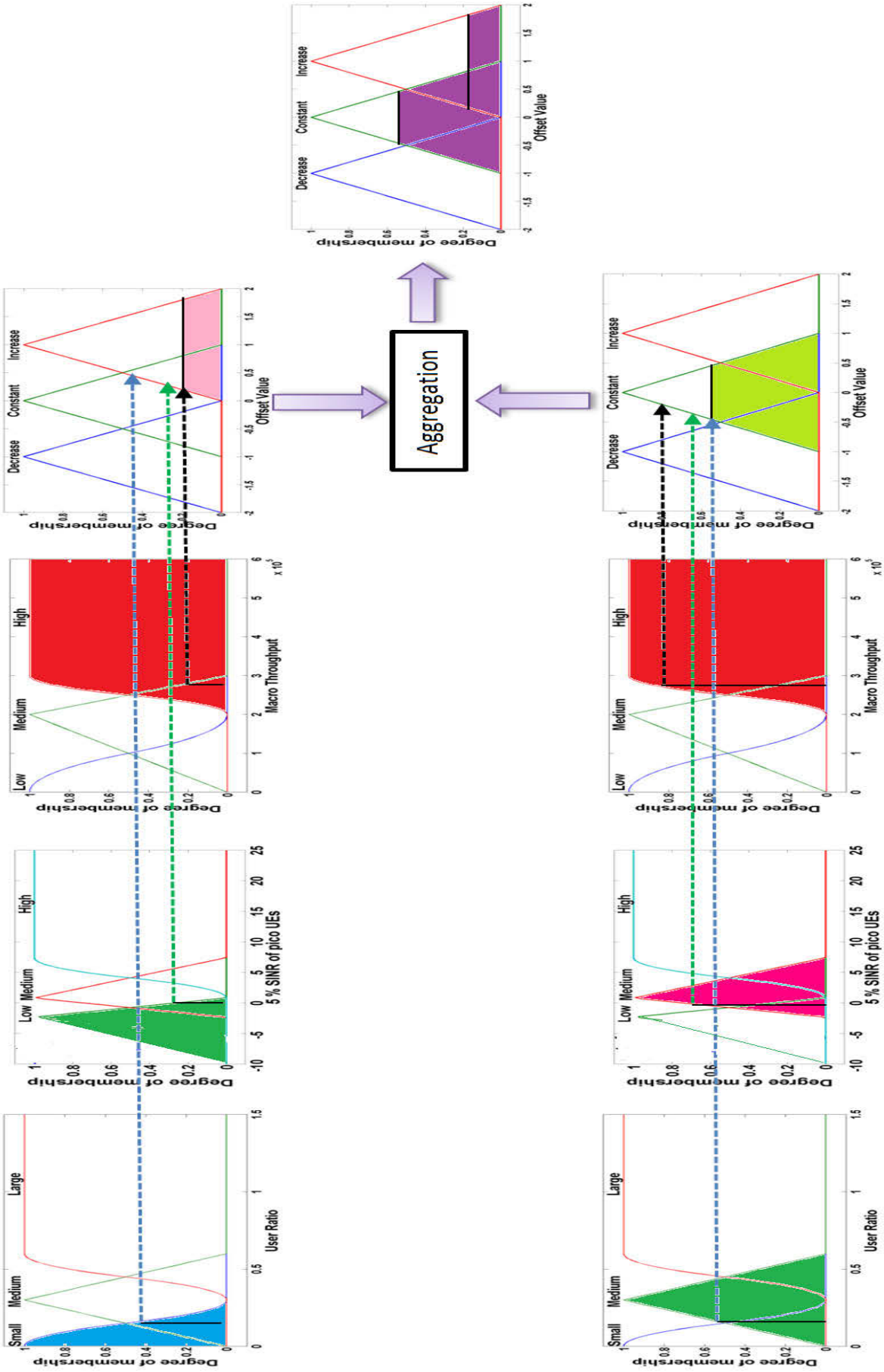

Figure 6.2. An example of the maximum aggregation method

6.2.1. ABS Value Module Description

Since the concept of FLS is same as scheme described in Section 6.1.1, the required steps are explained briefly in this section.

Step 1: Inputs and Output

When the ABS scheme is used, if the number of ABSs and non-ABSs are not corresponding to number of RE UEs and macro UEs, ABS scheme cannot adequately enhance the system throughput. This is because there is not enough subframes to schedule macro UEs and RE UEs. This can be worse for RE UE because these UEs are scheduled on non-ABSs and then experience severe downlink interference from macro eNB. As a result, the SINR, throughputs and number of macro and RE UEs can be used to determine the ABS value such that the total system performance is improved. The following vectors $x=[x_1, x_2, x_3]$ and o_2 are considered as inputs and output of ABS value algorithm:

1) x_1 represents number of RE UEs to number of macro UE.
2) x_2 is the 5% of CDF of SINR of pico UEs.
3) x_3 represents the average throughput of macro UEs.
4) o_2 is Δ_{ABS_value} that is added to the last ABS value.

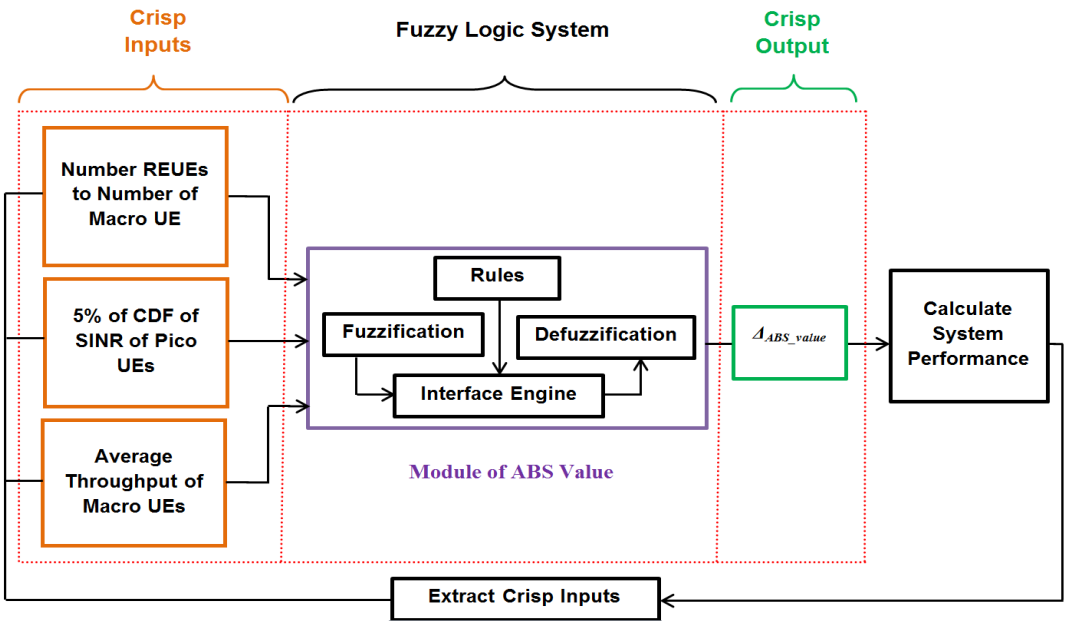

Figure 6.3. Block diagram of the proposed dynamic ABS scheme based on FL

Figure 6.3 shows that the inputs are directly fed back from the system after using the obtained ABS to precisely monitor the system performance and then change the ABS value to reach the desired system performance.

Step 2: Fuzzification

In FLS, each input and output is fuzzified using different membership functions and the range of membership functions are specified based on the system requirements. Moreover, the selected ranges and shapes must ensure that the ABS changes are not changed abruptly. In the proposed scheme, inputs and output are fuzzified as follows:

- x_1 is fuzzified using three membership functions labelled "Small", "Medium" and "Large" with Z-shaped, Triangular-shaped and S-shaped membership functions as shown in Figure 6.4 (a).

- x_2 is fuzzified through three membership functions "Low", "Medium" and "High" with Triangular-shaped, Triangular-shaped and S-shaped membership functions, respectively as shown in Figure 6. 4 (b).

- x_3 is fuzzified via three membership functions labelled "Low", "Medium" and "High" with Z-shaped, Triangular-shaped and S-shaped membership functions, respectively (see Figure 6. 4 (3)).

- o_2 is fuzzified by "Decrease", "Constant", and "Increase" membership functions with Triangular-shaped membership functions, respectively as depicted in Figure 6.4 (d).

Step 3: Definition of Fuzzy Rules

Based on the number of inputs and membership functions, 27 rules are defined. An example of a fuzzy rule set is as follows:

IF (x_1 is *Medium*) AND (x_2 is *Low*) AND (x_3 is *Medium*) THEN (o_2 is *Increase*)

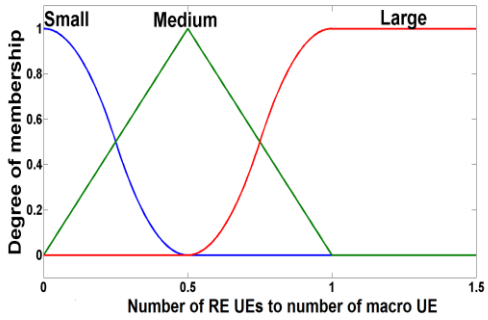

(a) Membership functions of number of RE UEs to number of macro UE

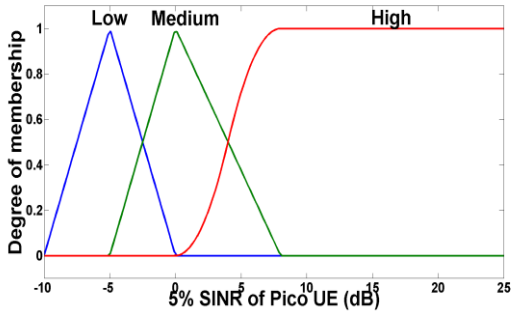

(b) Membership functions of 5% SINR

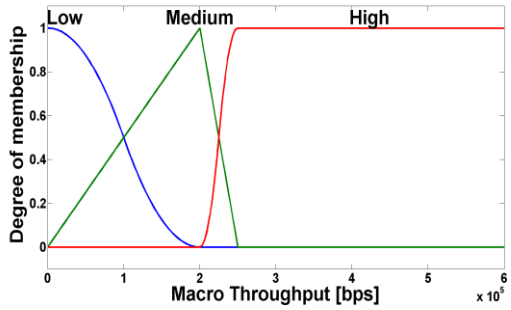

(c) Membership functions of macro UE throughputs

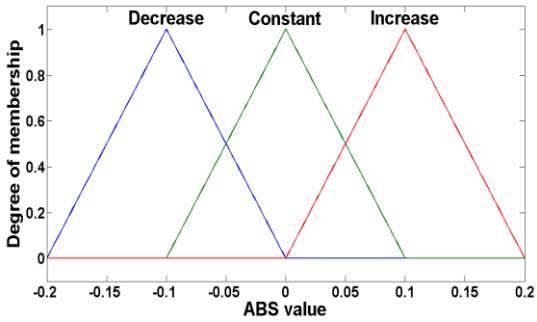

(d) Membership functions of Δ_{ABS_value}

Figure 6.4. Membership functions of inputs and output

Step 4: Aggregation

In this scheme, the maximum method was used as the aggregation method [84] to aggregate the results of fuzzy rules similar to Figure 6.2.

Step 5: Defuzzification

In the defuzzification step, the output value is calculated through the centre of gravity approach given in (6.1). The Δ_{ABS_value} is added to the last ABS value. The new ABS value indicates the number of subframes where macro eNB is muted and hence pico eNB can schedule RE UEs on those subframes to mitigate the interference.

6.3. A Dynamic Enhanced ICIC Scheme with CRE

As explained in Sections 6.1 and 6.2, if the number of ABSs is not precisely chosen, the throughputs of macro UEs and pico UEs are significantly degraded. In addition, if the CRE offset value cannot follow the user distribution, the interference on RE UE increases which leads to a reduction of throughput. As a result, both the ABS and CRE offset values simultaneously affect the system performance.

This subsection proposes a dynamic scheme for joint interference management and cell selection technique to improve system performance. For this purpose, the proposed dynamic ABS value and dynamic CRE schemes are combined (see Figure 6.5) for further improvements of system performance. In this scheme, each macrocell can simultaneously change the ABS configuration and CRE offset value to reach the expected system performance.

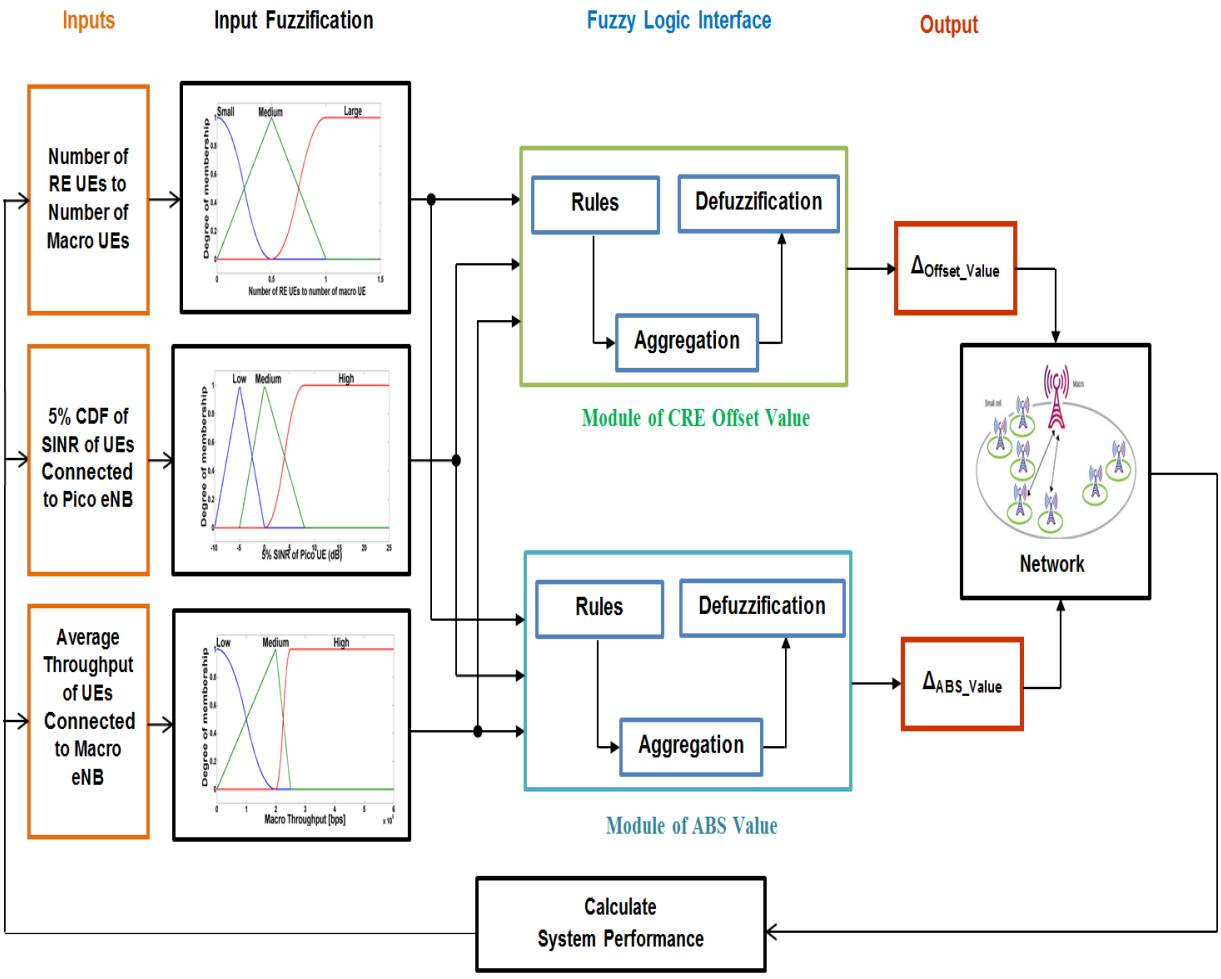

Figure 6.5. Block diagram of the proposed eICIC scheme based on FL

6.4. Performance Evaluation

This subsection evaluated the proposed schemes using a system level simulation introduced in Section 2.4 for full buffer traffic. In addition, the assumptions discussed in Chapter 2, are relevant to this chapter. The performance of the proposed schemes were evaluated in terms of number of the offloaded UEs, RE UE throughput , average macro UE throughput, and outage probability (as described in Section 2.5). The proposed dynamic CRE scheme (FL) was compared with the static CRE, the maximum RSRP (offset value=0) and Adaptive Offset Configuration Strategy (ABCS) [119] which is a CRE scheme with an adaptive offset value based on throughput and number of UEs using a logarithmic approach. Moreover, the performance of the proposed eICIC scheme was compared with the static CRE scheme, ABS schemes, schemes [99] and [108] in the literature.

6.4.1. Performance Analysis of Dynamic CRE Scheme

6.4.1.1. Number of the Offloaded UEs

Figure 6.6 shows the offset value achieved by the proposed dynamic CRE and ABCS schemes where initial offset value was set to 18 dB. As shown in Figure 6.6, the proposed scheme converged to the optimum value faster than ABCS.

Based on Figure 6.7, a small number of UEs are offloaded to picocells for small offset value because of receiving higher RSRP from the macro eNB while most UEs are connected to the picocells for larger offset values. The reason is that the received RSRP from pico eNB plus offset value is greater than the received RSRP from macro eNB. Using the proposed scheme, 43% of UEs are offloaded to picocell.

6.4.1.2. Throughput Performance

As described earlier, when the small offset value is used more UEs are connected to macrocell which leads to decrease of macro UEs throughput as shown in Figure 6.8. A large offset value is added to enhance the macro UE throughput which leads to extend the range expanded area and hence more UEs will be offloaded to picocells. However, increasing the range expanded area results in the degradation of RE UE throughput

because UEs far away from the picocells are connected to the pico eNB while these UEs suffer a high interference from macro eNB (see Figure 6.9). It can be concluded that if the offset value is not accurately set, the increase of macro (/RE) UE throughput can sacrifice the throughput of RE (/macro) UEs. Since the proposed CRE and ABCS schemes determine the offset value based on the throughputs of macro UEs and pico UEs, these two schemes maintain a good trade-off between macro UEs and pico UEs throughputs.

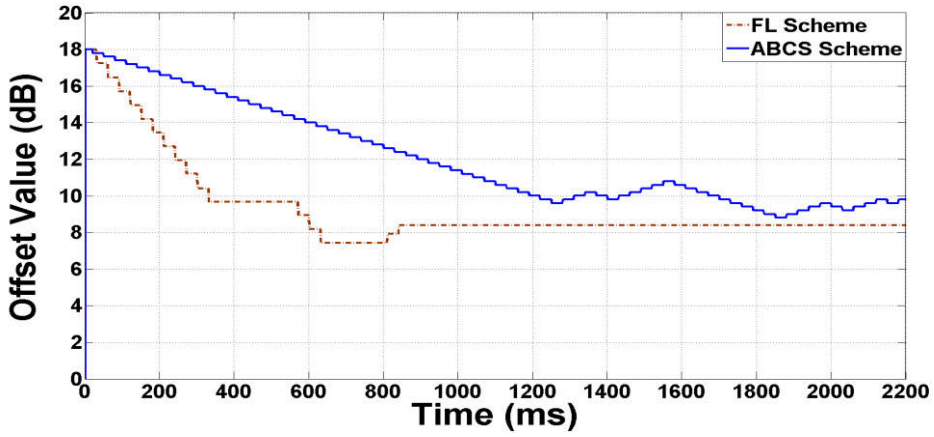

Figure 6.6. The dynamic offset value for the center cell using FL for FB

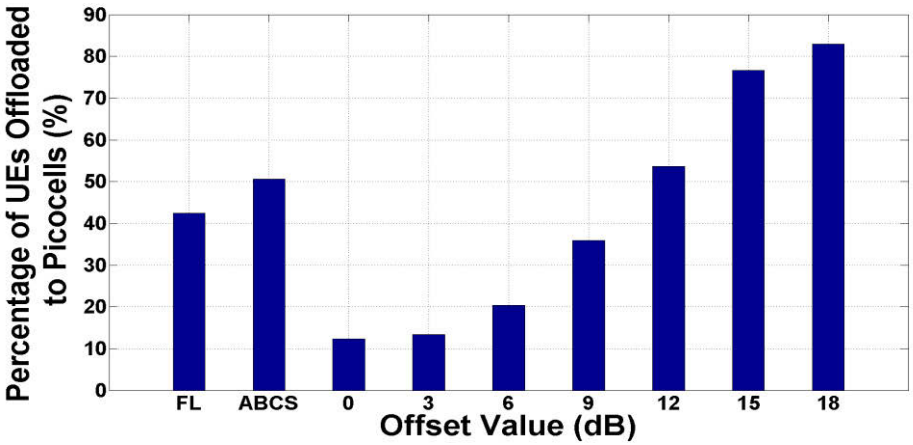

Figure 6.7. The percentage of UEs offloaded to picocell for different schemes for FB

When the CRE offset value is deployed, fewer UEs are connected to the macro eNB and hence more PRBs can be allocated to each macro UEs. Therefore, the throughput of macrocell improves at the cost of decreasing picocell throughput. As shown in Figure 6.10, using large offset value (i.e., 15 dB and 18 dB) can lead to a reduction of total cell throughput because most UEs experience too low SINR. However, the ABCS and the

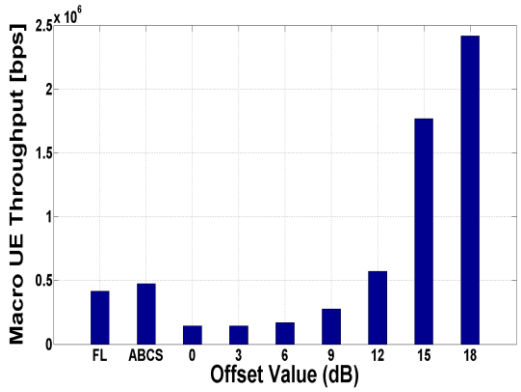

Figure 6.8. Average macro UE throughput

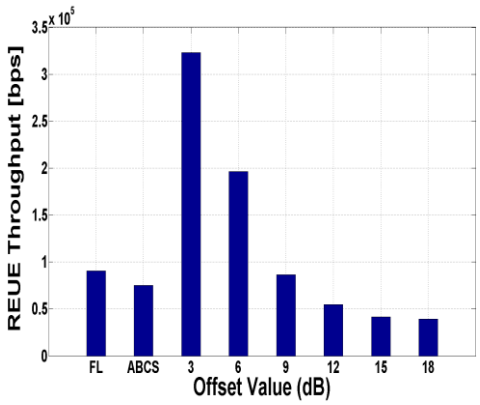

Figure 6.9. Average RE UE throughput

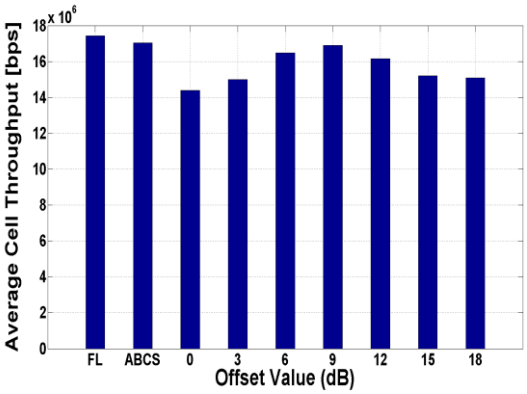

Figure 6.10. Average cell throughput

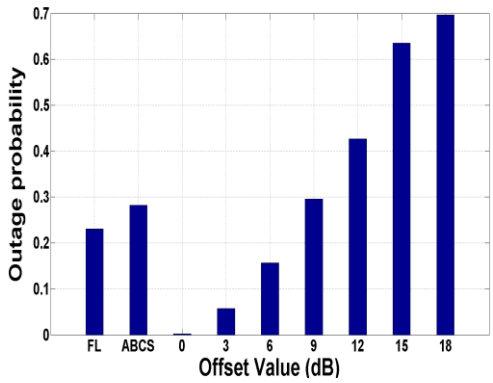

Figure 6.11. The outage probability

proposed CRE schemes can outperform the static offset values in terms of total throughput because these two schemes can find the best offset value for different situations.

6.4.1.3. Outage Probability

Figure 6.11 illustrates the outage probability for different offset values. The outage probability is an increasing function of offset value. This is because UEs far away from pico eNBs are offloaded to picocell by increasing of offset value while these UEs suffer severe interference from the macro eNB. It causes that the SINRs of more RE UEs become smaller than the outage threshold. Figure 6.11 shows that the smallest outage probability was achieved by max-RSRP scheme because only UEs located in the basic coverage of pico eNB are served by the picocell. Moreover, Figure 6.11 shows the proposed CRE scheme produces a smaller outage probability than ABCS scheme. The reason is that the proposed CRE scheme considers the SINR of RE UEs as an input, and then can change the offset value faster than ABCS scheme when SINR decreases.

6.4.2. Performance Analysis of Dynamic eICIC Scheme

In this subsection, the performance of the proposed eICIC which combines the dynamic CRE and ABS schemes is analysed. The eICIC schemes reviewed in literature were compared with some of (ABS, CRE) combinations. However, these schemes were only compared with limited numbers of (ABS, CRE) combinations while it is possible the proposed schemes cannot overcome all (ABS, CRE) combinations. This is because there is a trade-off between the macro UE throughput and RE UE throughputs. In addition, the number of subfarems in each frame is constant then an increase of ABS can lead to a decrease of macro UE throughput for smaller CRE offset value or vice versa. Therefore, in this chapter and next chapter, the proposed eICIC schemes are compared with the following three schemes.

1) Static schemes which are the fixed (ABS, CRE) combinations across the entire network as shown in Table 6.1.

2) A dynamic ABS scheme with static CRE offset value proposed in [99] where the computed number of ABSs is dynamically changed based on the macro load, pico load and pico CRE load and using a minimization approach.

3) A dynamic ABS and CRE scheme proposed in [108] which used a utility function based on the throughput of macrocell, edge and centre throughput of picocell, number of picocell and macrocells, and the number of UEs.

Table 6.1. (ABS, CRE) Combinations Used in This Thesis

	ABS value							
Offset Value	**10%**	**20%**	**30%**	**40%**	**50%**	**60%**	**70%**	**80%**
9 dB	✓	✓	✓	✓	✓	✓	✓	✓
12 dB	✓	✓	✓	✓	✓	✓	✓	✓
15 dB	✓	✓	✓	✓	✓	✓	✓	✓

6.4.2.1. Percentage of the Offloaded UEs

Figure 6.12 shows the ABS value determined by the proposed eICIC scheme for the centre cell. The blue (solid) line is the value calculated by the proposed eICIC scheme and the red line represents the ABS value used by macrocell which converged to 40% after 200 ms. The reason is that the number of ABSs must be a factor of 10 due to 10 subframes in each frame. In addition, the CRE offset value computed by the proposed scheme converges to 12.62 dB as shown in Figure 6.13. Figure 6.14 shows when the offset value is small, fewer UEs are connected to the pico eNB, while more UEs are

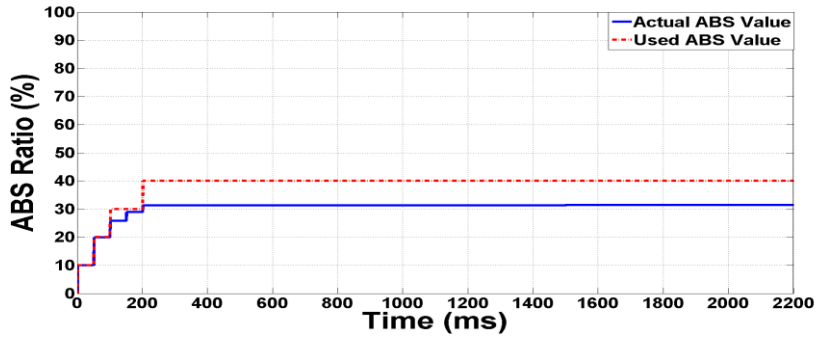

Figure 6.12. The ABS value obtained by FL for centre cell (4 picos/macro)

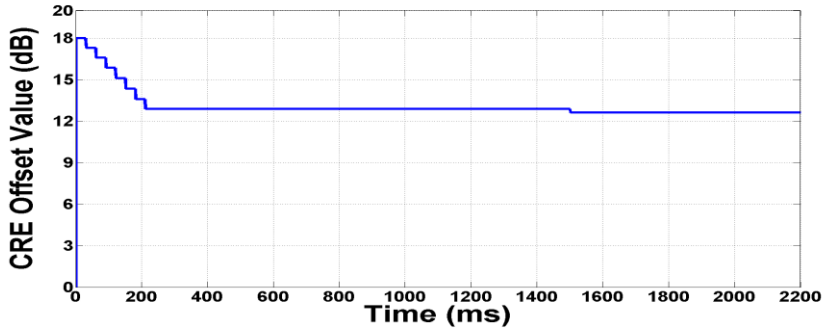

Figure 6.13. The offset value obtained by FL for centre cell (4 picos/macro)

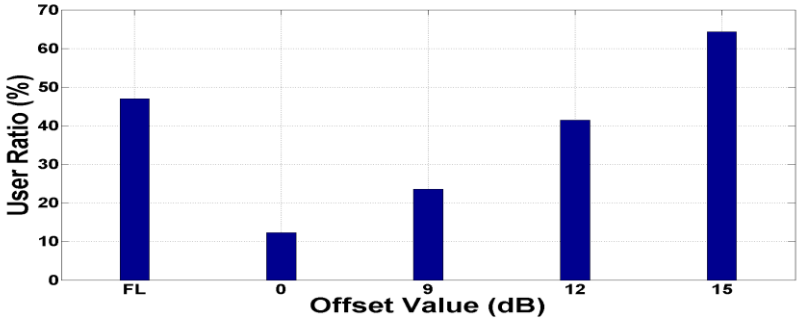

Figure 6.14. Number of the offloaded UEs from macrocell to picocells (4 picos/macro)

offloaded to picocell for larger offset values. For instance, the Number of the offloaded UEs to picocells is 23% when offset value is set to 9 dB because more UEs are connected to macro eNBs due to a higher RSRP from the macro eNB. This ratio goes up to 64% by increasing the CRE offset value to 15 dB. Since the proposed eICIC scheme changed the offset value based on several metrics such as number of RE UEs, 47% of UEs are offloaded to picocells.

In order to study the effect of membership functions on system performance, another types of membership function called Gaussian function is used given by (6.2).

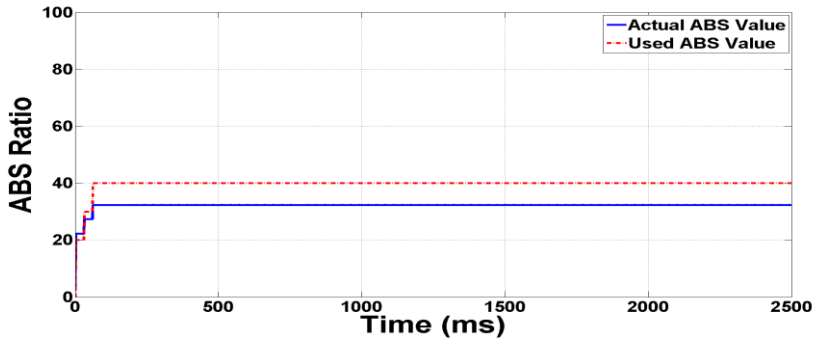

Figure 6.15. The ABS value obtained by FL for centre cell (4 picos/macro)

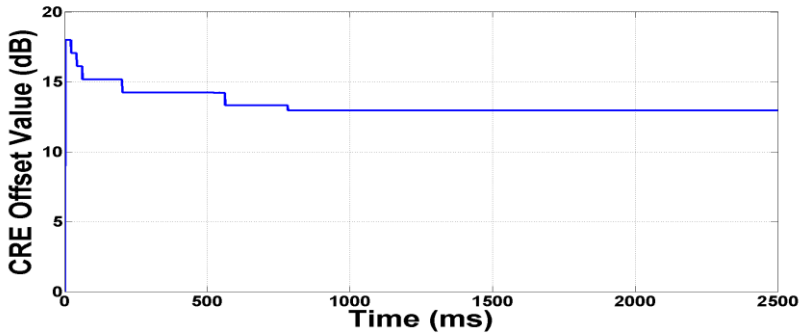

Figure 6.16. The offset value obtained by FL for centre cell (4 picos/macro)

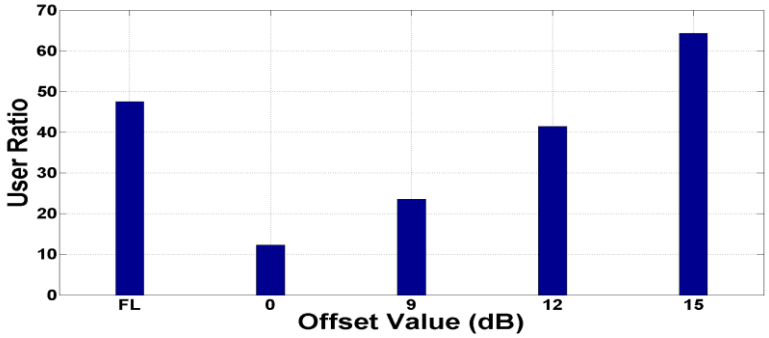

Figure 6.17. Number of the offloaded UEs from macrocell to picocells (4 picos/macro)

$$f(x;\sigma,d) = e^{\frac{-(x-d)^2}{2\sigma^2}} \tag{6.2}$$

where d indicates the central value and σ is the Gaussian standard deviation. When compared to Triangular membership function, the ABS value obtained by Gaussian membership function converges to the same value as shown in Figure 6.15. Moreover, the offset value obtained by Gaussian membership function converges to 12.96 dB (see

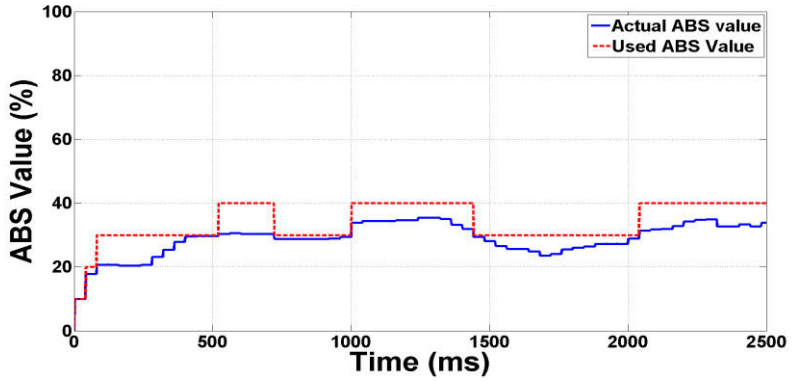

Figure 6.18. The ABS value obtained by FL for centre cell (2 picos/macro)

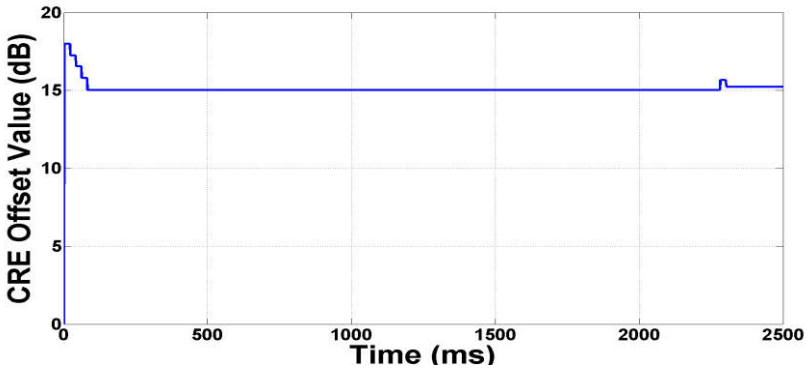

Figure 6.19. The offset value obtained by FL for centre cell (2 picos/macro)

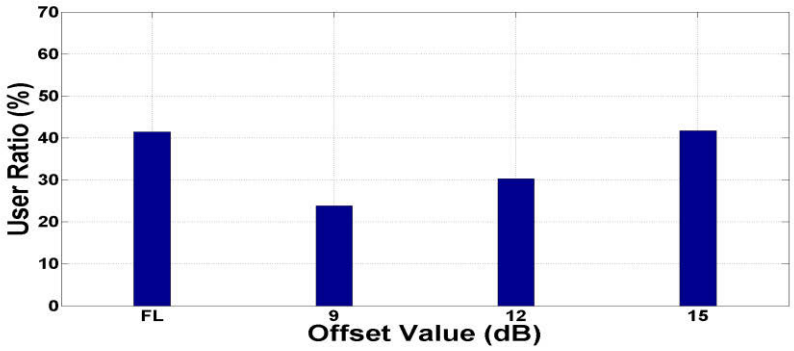

Figure 6.20. Number of the offloaded UEs from macrocell to picocells (2 picos/macro)

Figure 6.16) which is not much larger than Triangular membership function and therefore number of the offloaded UEs is approximately same for both types of membership functions.

By decreasing the picocell density from four to two picocell per macrocell, the offset value obtained by the proposed scheme increases as shown in Figure 6.19. This is because when the number of picocell decreases, a lower number of UEs is offloaded to picocells and hence a larger offset value is needed to increase number of UEs offloaded to picocells. Figure 6.20 shows that 41% of UEs are offloaded to picocells when density of picocells reduces to two picocells per macrocell.

6.4.2.2. Outage Probability

Figure 6.21 compares the outage probability of the proposed eICIC scheme with schemes with different CRE offset and ABS. The outage probability reduces when the ABS is used because UEs that receive higher interference are scheduled on ABSs. Since the proposed eICIC scheme takes into account the SINR value, hence the outage probability can be maintained within an acceptable range as shown in Figure 6.21. By changing the SINR's membership functions, the outage probability can be changed to reach the new system requirements. By decreasing of the picocell density, the outage probability reduces as shown in Figure 6.22. This is because the number of offloaded UEs to picocell decreases and hence more UEs far away from the pico eNBs are connected to the macro eNB instead of the pico eNB.

6.4.2.3. Throughput Performance

When the ABS value is small, more non-ABS can be allocated to macro UEs while the number of ABSs assigned to RE UEs is low. Therefore, the throughput of macro UEs improves at the expense of reduction of RE UEs' throughput as shown in Figures 6.23 and 6.24. In contrast, by increasing the ABS value, more subframes can be allocated to RE UEs. Since the macro eNB has to be muted on the ABSs, the interference decreases which can lead to increase of the RE UE throughput at the expense of reduction of macro UE throughput. There is a trade-off between macro UE and RE UE throughputs when ABS scheme is used. Moreover, the increase of RE UE throughput can lead to an

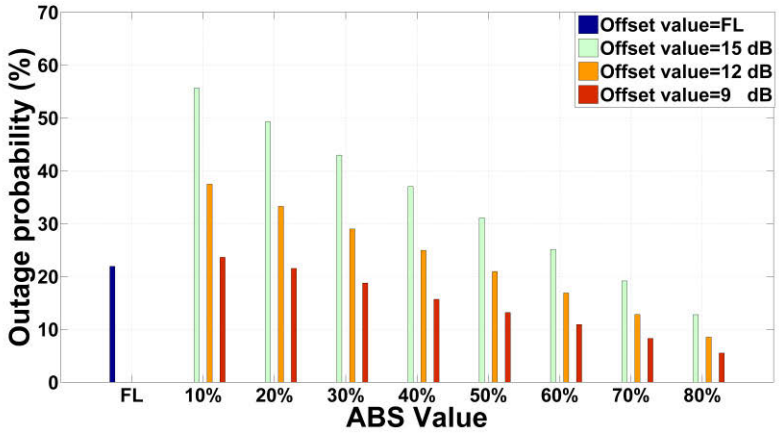

Figure 6.21. The outage probability for difference ABS values and CRE offset values (4 picos/macro)

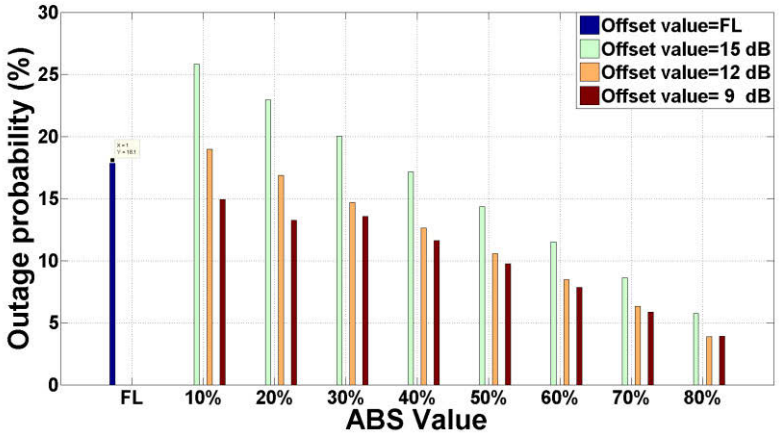

Figure 6.22. The outage probability for difference ABS values and CRE offset values (2 picos/macro)

increase of picocell throughput as shown in Figure 6.25. However, using larger ABS values results in a significant reduction of the macro UEs throughput and macrocell throughput (see Figure 6.26). On the other hand, by increasing the offset value to 15 dB, more UEs are offloaded to range expanded area and hence the average RE UE throughput decreases as these UEs suffer high interference from macro eNB. In this case, if the small ABS value is used (e.g., 10%), the number of ABS cannot support all of RE UE and then pico eNB schedules them on non-ABS. Since the interference on non-ABS is high for RE UEs particularly for RE UEs far away from pico eNB, the RE UE throughput and picocell throughput reduces as depicted in Figures 6.24 and 6.25. Consequently, the ABS configuration must maintain the trade-off between throughput of macro UEs and RE UEs while the required throughput for macro UEs is satisfied.

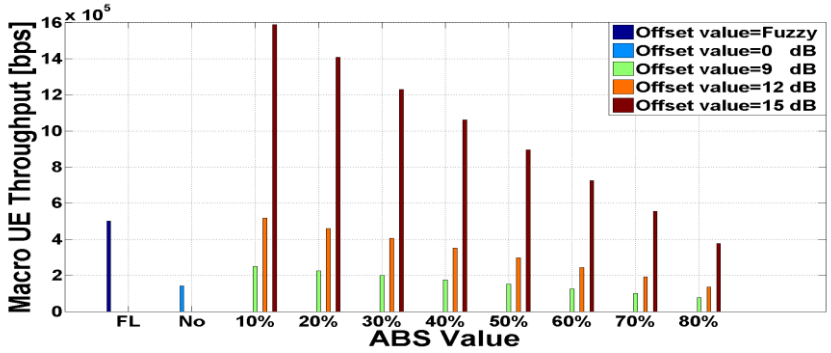

Figure 6.23. Average macro UE throughput (4 picos/macro)

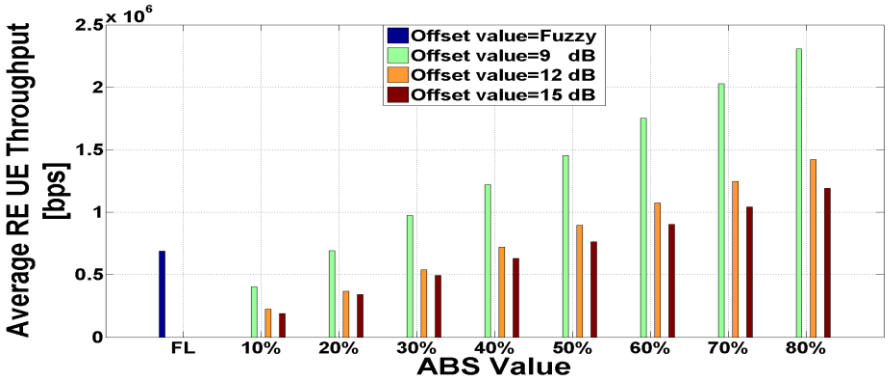

Figure 6.24. Average RE UE throughput (4 picos/macro)

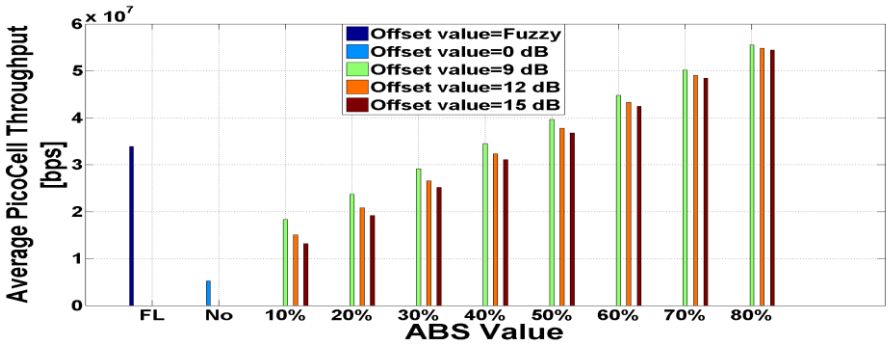

Figure 6.25. Average picocell throughput (4 picos/macro)

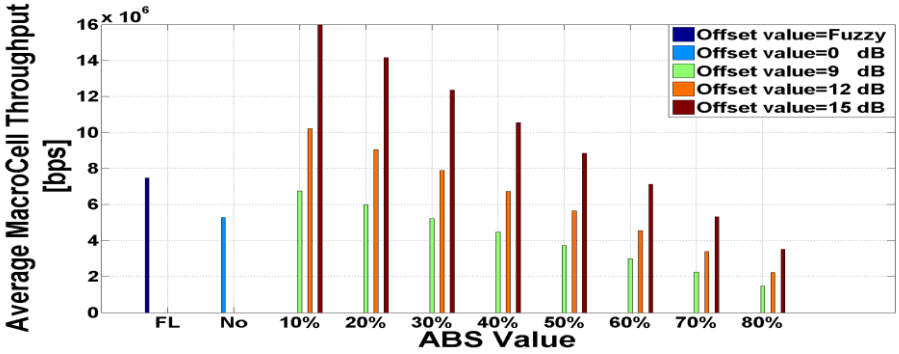

Figure 6.26. Average macrocell throughput (4 picos/macro)

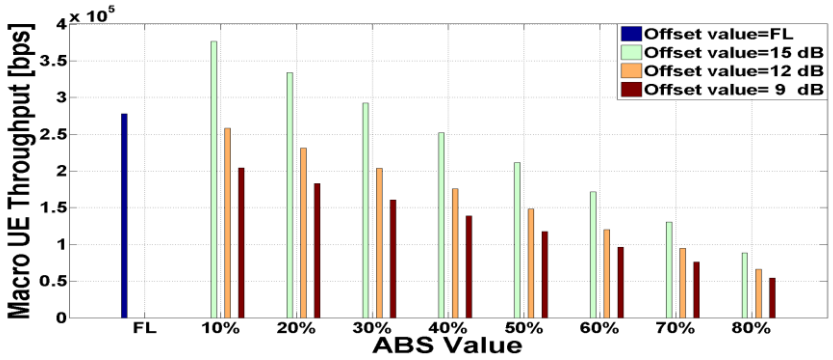

Figure 6.27. Average macro UE throughput (2 picos/macro)

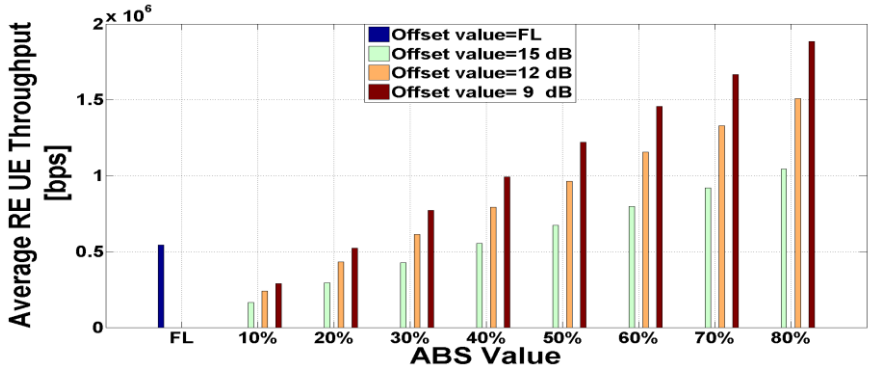

Figure 6.28. Average RE UE throughput (2 picos/macro)

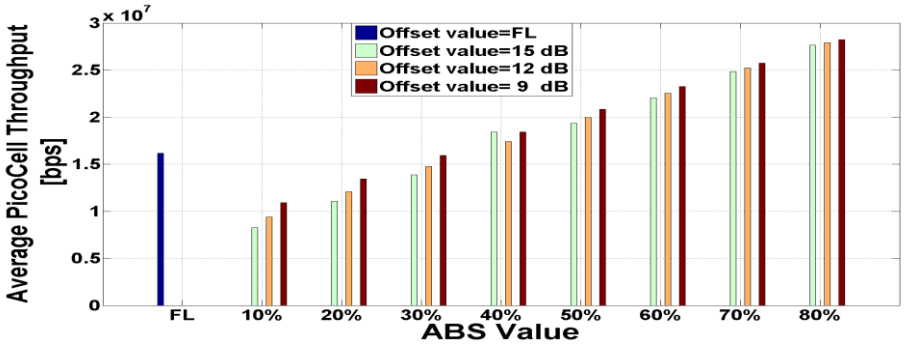

Figure 6.29. Average picocell throughput (2 picos/macro)

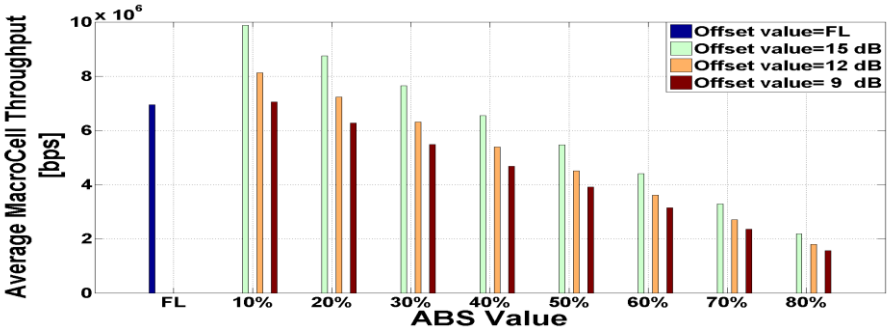

Figure 6.30. Average macrocell throughput (2 picos/macro)

Moreover, the number of UEs connected to the pico eNBs and the macro eNB must be controlled. In order to satisfy the above requirements, the proposed eICIC scheme set ABS value and offset value to 40% and 12.62 dB, respectively, such that the average throughput of macro UEs is satisfied while the average throughput of RE UE is acceptable as shown in Figures 6.23 and 6.24.

In order to investigate the influence of picocell density on throughput, the throughputs are obtained when the picocell density is set to two picocells per macrocell. Based on Figure 6.27, the throughput of macro UEs decreases because more UEs are served by macro eNB when compared to throughput for four picocells per macrocell (see Figure 6.23). In addition, by decreasing the picocell density, each picocell has to serve more offloaded UEs which leads to a decrease of RE UEs' throughput as shown in Figure 6.28.

6.4.2.4. Result Comparison

Table 6.2 compares the proposed eICIC based on FL with the proposed schemes [99] and [108] in literature. Based on this Table, the proposed FL base scheme and [108] converged to ABS value of 40 % and 60% respectively, whereas [99] oscillated between 50%-60%. In addition, the proposed scheme and [108] obtained the same offset value. However, the proposed scheme could maintain the trade-off between macro UE and RE throughputs while [99] and [108] sacrificed the macro UE throughput to increase the RE UE throughput. Although [108] considered the macro cell and picocell throughputs, it only used the total sum of macro cell and pico cell throughputs to find the best ABS and CRE offset values. Therefore, it is possible the total cell throughput obtained for a particular combination of ABS and offset values becomes large because only the macro cell throughput or pico cell throughput is high while the RE UE throughput or macro UE throughput has been sacrificed (see Table 6.2). Moreover, [108] requires much more time than FL based scheme to find the best (ABS, CRE) combination. The outage probabilities of all schemes are approximately same between 20% and 24%.

Table 6.2. System Performance Comparison for FL based Scheme for 4 picos/macro

eICIC Scheme	Offset Value (dB)	ABS Value (%)	Outage (%)	Throughput			
				Macro UE (kbps)	RE UE (kbps)	Macrocell (Mbps)	Picocell (Mbps)
FL based	12.98	40	22	735	598	7.10	34.12
Ref.[99]	13	Oscillated between 50-60	20.62	341	970	4.81	41.31
Ref.[108]	13	60	24.49	297	1065	5.29	42.9

6.5. Summary

This chapter proposed a dynamic CRE scheme for LTE-A heterogeneous networks based on fuzzy logic system. The fuzzy logic system monitored the number of UEs, SINR and throughputs and then modified the CRE offset value using a set of rules. This process was performed for each cell independently. Thereafter, the proposed dynamic CRE scheme has been combined by a dynamic ABS scheme to introduce a dynamic eICIC scheme to overcome the co-channel interference problem in heterogeneous networks. The proposed eICIC scheme calculated the CRE offset value and ABS value based on the historical system performance using a fuzzy logic system. The simulation results illustrated the number of UEs offloaded to picocell was controlled by the dynamic CRE offset value. Moreover, the balance between throughput of macro UEs and RE UEs was maintained such that the minimum required throughputs of macro UEs and RE UEs could be satisfied. Furthermore, the simulation results showed the outage probability was maintained at an acceptable level.

Chapter 7

ENHANCED ICIC SCHEME IN LTE-A HETEROGENEOUS NETWORKS FOR VIDEO STREAMING TRAFFIC

As mentioned in Chapter 6, the static ABS value cannot support the dynamically changing network conditions. In addition, the suitable number of offloaded UEs cannot be controlled by the static CRE offset value. In this chapter, two dynamic eICIC schemes are proposed.

The first eICIC scheme is based on fuzzy Q-learning algorithm (FQL) and can find the optimum ABS and CRE offset values based on the system requirements for the full buffer and video streaming traffics. The difference between the proposed scheme based on FQL and the scheme proposed in Chapter 6 is that the new scheme assumes that there is no prior knowledge about the consequent part of the rules. Moreover, the proposed eICIC scheme can support the video streaming traffic.

The second proposed eICIC scheme is based on Genetic Algorithm (GA) where the number of ABSs and locations of ABSs in each frame are determined for static CRE offset value. This scheme is executed for video streaming traffic to improve the system throughput and decrease the delay and interference when macrocell and picocells share the bandwidth.

The rest of the chapter is organized as follows. Section 7.1 provides a description of the proposed dynamic eICIC scheme based on FQL. Section 7.2 introduces the dynamic ABS configuration scheme based on Genetic Algorithm. Section 7.3 contains the simulation results and a discussion. The conclusion is given in the final section.

7.1. Proposed eICIC Scheme based on Fuzzy Q-Learning

Q-learning approach is one type of reinforcement learning technique in which the learner, known as an agent, creates a table of q-values using a q-function approach [120]. By exploring the environment, the q-function estimates the discounted future costs when the agent applies an action in the current state. The q-value is then stored in the table for each state and each possible action. However, each agent has to store q-values in a table which is quite complex and impracticable for large state-action space and continuous state space. In order to overcome these problems, fuzzy logic system [82], [121] can be added to q-learning approach to discretise the continuous variables and this is known as Fuzzy Q-Learning (FQL) [122]. Consequently, in FQL the continuous states and actions are transformed into a finite number of fuzzy variables using fuzzy membership functions such that the overall rewards are maximized.

7.1.1. Fuzzy Q-Learning Controller Components

Since the basics of FQLs used in both modules of CRE offset value and ABS value are same, the deployed FQLs are described together. During each iteration, each agent observes the complete state of the system (such as important downlink metrics) and then applies an action which causes the system to move into a new state. After that, the action receives an instantaneous reward which indicates the quality of this transition. The basic components of FQLs including state input, action and rewards are described as follows.

1) State Variables

In order to indicate how the system is performing, several metrics can be measured in each state. As described in Chapter 6, the offset value has a direct influence on throughputs of UEs connected to macro and pico eNBs. Moreover, if the number of ABS and non-ABS are not corresponding to number of macro and pico UEs, the throughputs of macro UEs and pico UEs will significantly decrease. Therefore, the input state vectors considered for the modules are represented by S_{CRE} and S_{ABS}, respectively.

$$S_{CRE} = [Offset\_value \quad N_{UE} \quad Thr_m \quad SINR_{RE}] \tag{7.1}$$

$$S_{ABS} = [ABS\_value \quad N_{UE} \quad Thr_m \quad SINR_{RE}] \tag{7.2}$$

where o*ffset_value* is the current offset value added to RSRP received from pico eNBs. *ABS_value* is the current ABS value applied on the macrocell and its picocells. N_{UE} indicates the ratio of RE UEs to macro UEs. Thr_m represent the average throughput of macro UEs and $SINR_{RE}$ is 5 % of CDF of SINR of pico UEs. Thr_m and $SINR_{RE}$ ensure that the minimum required data rate of macro UEs is satisfied and the throughput of UEs with lower SINR is improved. Figure 7.1 shows how the inputs of FLQs are extracted from the system performance.

2) Fuzzifier

A finite number of fuzzy labels are defined based on the system requirements to fuzzify the state variables. Each label is assigned to a membership function with a membership degree within the interval [0, 1]. Note that the dimension of the input state vector and the number of its corresponding fuzzy labels establishes a trade-off between the network accuracy and the convergence speed of the learning procedure. In the proposed scheme, input and outputs variables are fuzzified using the specified fuzzy label sets called T_{offset_value}, $T_{ABS\text{-}value}$, T_N, T_{thr}, T_{SINR}, $T_{\Delta offset\_value}$, and $T_{\Delta ABS\_value}$ as shown in Table 7.1

Table 7.1. Fuzzy Label Sets Defined for Input and Output Variables

Inputs/Outputs	Fuzzy Label Set
offset_value	{Low, Medium, High}
ABS_value	{Low, Medium, High}
N_{UE}	{Small, Medium, Large}
Thr_m	{Low, Medium, High}
$SINR_{RE}$	{Low, Medium, High}
Δ_{offset_value}	{Decrease, Constant, Increase}
Δ_{ABS_value}	{Decrease, Constant, Increase}

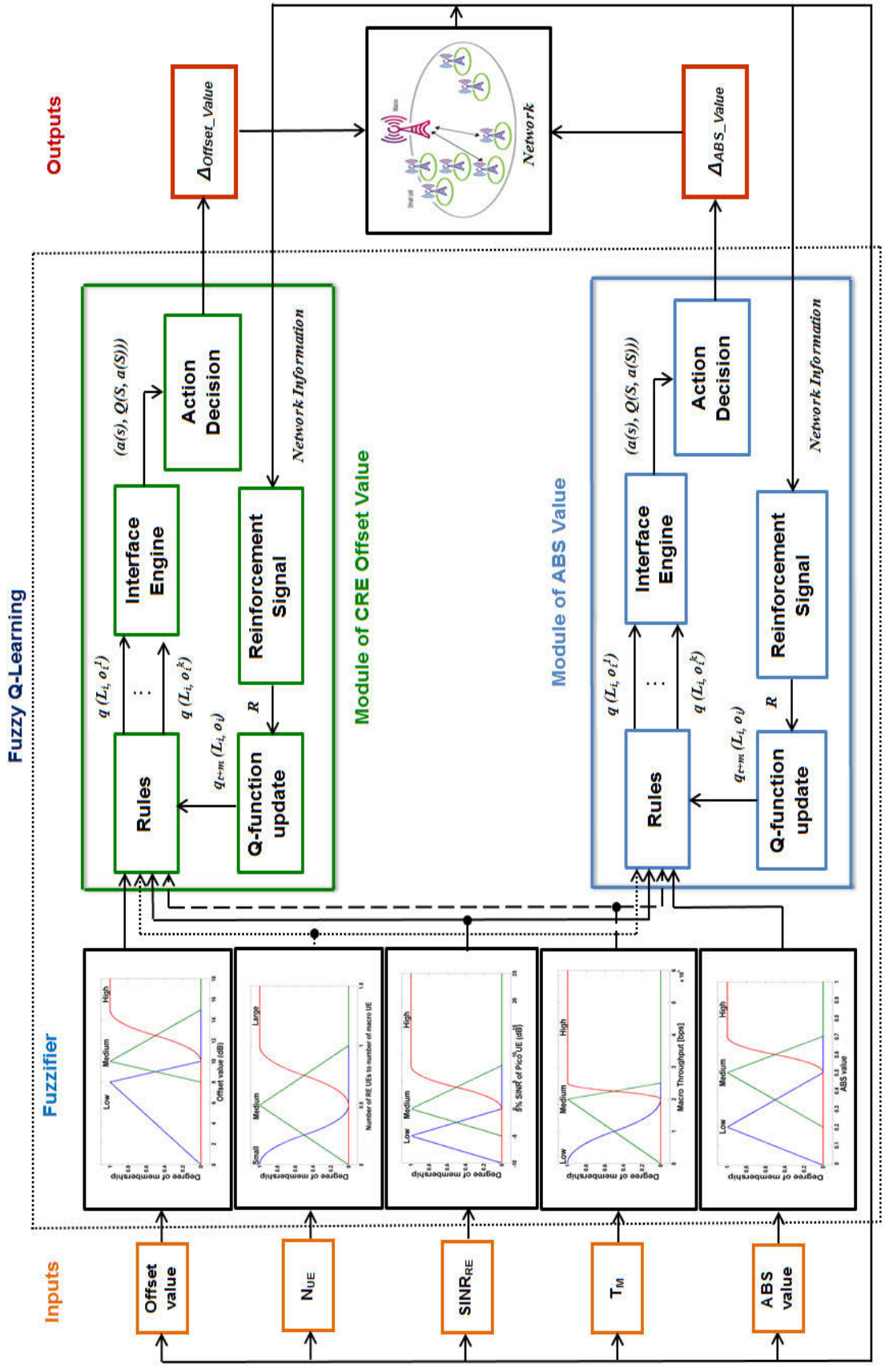

Figure 7.1. Block diagram of the proposed eICIC scheme based on FQL

3) Interface Stage

In the inference stage, inputs are mapped to outputs using a set of "IF-Then" rules to control the output value. Two fuzzy rule sets are defined for the proposed scheme independently. The fuzzy rule in FQL for each module is represented by:

$$\text{IF } (S^1 \text{ is } L_i^1) \text{ AND } (S^2 \text{ is } L_i^2) \ldots \text{ AND } (S^N \text{ is } L_i^N)$$
$$\text{THEN} \quad a = o_i^1 \text{ with } q\,(L_i, o_i^1)$$
$$\text{or} \quad a = o_i^2 \text{ with } q(L_i, o_i^2)$$
$$\vdots$$
$$\text{or} \quad a = o_i^k \text{ with } q(L_i, o_i^k)$$

where L_i^n is the fuzzy label corresponding to a distinct fuzzy set defined in the domain of the n^{th} component of the state vector $S = [S^1, S^2, \ldots, S^n, \ldots, S^N]$ and o_i^k is the k^{th} output action for rule i which also is called the consequent part of rule. The vector $L_i = [L_i^1, L_i^2, \ldots, L_i^n, \ldots, L_i^N]$ is named the modal vector of rule i which specifies one state of controller. $q\,(L_i, o_i^k)$ is the q-value function of the state L_i and action o_i^k of rule i. the initial values of all q are set to zero. Moreover, it is assumed that the actions of rules are to be same for all eNBs.

4) Action

The actions of FQLs are to find the Δ_{offset_value} and Δ_{ABS_value}. The Δ_{offset_value} and Δ_{ABS_value} are fuzzified with three labels as shown in Figures 7.2 and 7.3. The selected range ensures that the changes are not abrupt. Then Δ_{offset_value} and Δ_{ABS_value} are added to last offset value and ABS value, respectively. Each macro eNB performs local actions to find its optimum offset value and ABS value and then uses these values for itself and its picocells.

The number of actions depends on the prior knowledge in the consequent part of the rules. If the knowledge about a rule is sufficient then one action is sufficient in the consequent part of that rule. When the knowledge about a rule is imprecise, a subset of

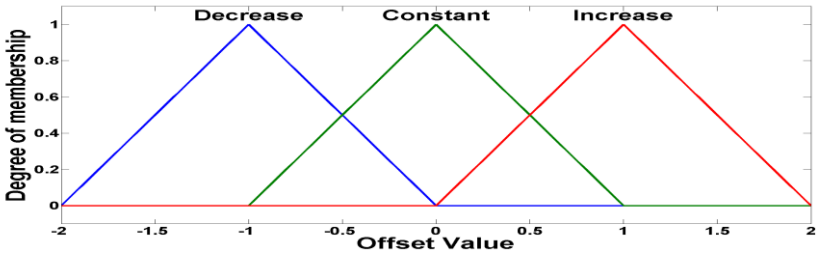

Figure 7.2. Membership functions of Δ_{offset_value}

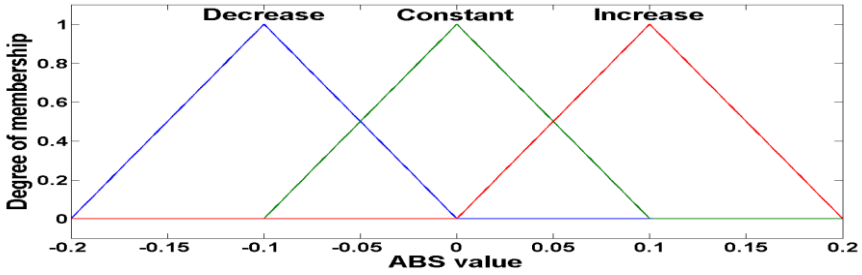

Figure 7.3. Membership functions of $\Delta_{ABS\ value}$

possible actions is considered for that rule. For a system without any prior knowledge, all the possible actions are taken into account to define the rule. In this chapter, it is assumed that there is no prior knowledge (the worst case) and then all actions are considered in all rules with equally probability in all states.

5) Instantaneous Rewards

A reinforcement learning reward R is defined for each module to inform the controller about the result of its previous actions. If R is correctly defined, the best consequent can be selected for each rule. R is calculated to characterize the results of actions when the controller transits from State S_t to State S_{t+m}. If the selected action leads to a good result, a positive reward is considered for that action while the negative reward is assigned for poor result. In this scheme the good result must lead to the improvement of system performance in terms of delay and throughput of RE UEs and macro UEs. R has the same form in these two modules to let q-values in two modules have a similar degree of reward and punishment. An expression for R for each type of traffic is described as follows:

$$R = \left(\frac{\gamma - SINR}{\gamma}\right) + \left(\frac{T^* - T_m}{T^*}\right) \qquad \textit{for full buffer} \qquad (7.3)$$

$$R = \left(\frac{\gamma - SINR}{\gamma}\right) + \left(\frac{T^* - T_m}{T^*}\right) + \left(\frac{D^* - D}{D^*}\right) \qquad \textit{for video streaming} \qquad (7.4)$$

where *SINR*, T_m, and D are the values of 5% CDF of pico UEs' SINR, macro UE throughput and delay extracted from system performance under the state-action pair. Moreover, γ, T^*, and D^*, are the outage threshold, the required throughput of macro UEs and the maximum allowable delay for sending data. Moreover, m is set to 10 to investigate the average effect of ABS value during each frame.

7.1.2. FQL Algorithm

At the first step for each module, the current state of the agent is specified using the truth degree of each FLS rule. The degree of truth of rule i equals the product of membership degrees of each inputs for the rule i as follows:

$$\alpha_i(S) = \prod_{n=1}^{N} \mu_{L_i^n}(S^n) \tag{7.5}$$

where N represents the number of FLS inputs and $\mu_{L_i^n}$ is the membership function for the n^{th} FLS input and the rule i. At the next step, an action is selected for each activated rule based on the greedy exploration/exploitation policy [122] given as follows:

$$\begin{aligned} a_i &= \arg_{k\in K} \max q(L_i, o_i^k) \quad \text{with probability } \varepsilon \\ a_i &= random\,\{o_i^k\}_{k\in K} \quad\quad \text{with probability 1-}\varepsilon \end{aligned} \tag{7.6}$$

where ε sets a trad-off between exploration and exploitation in the algorithm. When ε increases over the time, a slow transition occurs from exploration to exploitation. After determining the action of each activated rule, the inferred action which should be applied by the FQLC is calculated by the following equation:

$$a(S) = \sum_{i\in P} \alpha_i(S) \times o_i \tag{7.7}$$

where P is the set of rules. The q-value for the input state vector is computed using an interpolation among the current q-values of the activated rules:

$$Q(S,a(S)) = \sum_{i \in P} a_i(S) \times q(L_i, o_i) \tag{7.8}$$

When the selected action is applied by FQLC, the agent transits from the current State S_t to the new State S_{t+m}. Moreover, a reinforcement learning reward is given to the agent because of this transition. The value of the new state is calculated as follows:

$$V(S_{t+m}) = \sum_{i \in P} \alpha_i(S_{t+m}) \times \max_{k \in K} q(L_i, o_i^k) \tag{7.9}$$

Then, the q-values are updated using a quantity ΔQ which is defined as the difference between the old and new values of $Q(S, a(S))$.

$$\Delta Q = R_{t+m} + \vartheta V(S_{t+m}) - Q(S_t, a(S_t)) \tag{7.10}$$

$$q_{t+m}(L_i, o_i) = q_t(L_i, o_i) + \chi \alpha_i(S_t) \Delta Q \tag{7.11}$$

Algorithm 1. Fuzzy Q-learning

1. Initialize the $q(L_i, o_i^k)$ for all $i \in P$ and $k \in K$
2. Select an action for each activated rule based on ε-greedy policy (Equation (7.6)).
3. Calculate the inferred action using Equation (7.7).
4. Estimate the Q-function from the current q-values and the degree of truth of the rules (Equation (7.8))
5. Apply the inferred action and observe new State S_{t+m}.
6. Extract the reinforcement learning reward based on performance results.
7. Compute the value of the new state represented by $V(s_{t+m})$ in Equation (7.9).
8. Calculate the difference between the old and new values of Q(S, $a(S)$) using Equation (7.10).
9. Update the q-values for each activated rule based on Equation (7.11).
10. Repeat the process starting from Step 2 until the convergence is attained.

The parameters ϑ and χ are the discount factor and the learning rate, respectively, with a range of [0 1].

7.2. Proposed eICIC Scheme based on Genetic Algorithm

The second eICIC scheme proposed in this chapter aims to find the optimal number of ABSs and the best locations of ABSs in each frame when the static CRE scheme is used. For this purpose, some requirements of video streaming traffic are considered as the objective functions of GA [123] including throughput, interference, delay and Packet Loss Rate (PLR). The objective functions monitor the system performance until it reaches an optimal performance. Minimizing the PLR can guarantee the reliability of transmission while minimizing the delay guarantees packet delay requirements for on-going video streaming. Moreover, the level of interference is minimized between macrocell and picocells while the maximization of throughput guarantees the minimum required data rate of macro UEs and pico UEs are satisfied. The output parameter of this optimization method is the ABS configuration used in each macrocell and its picocells. The ABS configuration includes the number of ABSs and the locations of ABSs in each frame.

7.2.1. Maximizing Throughput

The objective function of throughput can be given by (7.12)

$$T = \frac{1}{N_u}\frac{1}{T_s}\sum_{k=1}^{N_u}\sum_{t=1}^{T_s} R_i(t) \tag{7.12}$$

where $R_i(t)$ is the total size of the received packets (in bits) of UE_k at time t, T_s is the total simulation time and N_u is the total number of UEs in a macrocell and its picocells. Since a trade-off between macro and pico UE throughputs is needed to optimize the performance of macrocell and picocell, two sub-functions are defined as follows.

$$f_1 = \frac{1}{R_m^*}\left(\frac{1}{N_m}\frac{1}{T_s}\sum_{k=1}^{N_m}\sum_{t=1}^{T_s} R_i(t)\right) \tag{7.13}$$

$$f_2 = \frac{1}{R_p^*}\left(\frac{1}{N_p}\frac{1}{T_s}\sum_{k=1}^{N_p}\sum_{t=1}^{T_s} R_i(t)\right) \tag{7.14}$$

where f_1 and f_2 are the objective function of throughputs for macrocell and picocell, N_m and N_p represent the total number of macro UEs and pico UEs, respectively. R_m^* and R_p^* indicate the minimum required data rate of macro UEs and pico UEs, respectively.

7.2.2. Minimizing Interference

The interference between macrocell and picocells can limit the throughputs particularly for RE UE. The objective function for minimizing interference level on pico UEs can be defined as follows:

$$f_3 = \frac{1}{N_p}\sum_{k=1}^{N_p}\delta_k \frac{P_k H_k}{P_l H_l} \tag{7.15}$$

where P_l and P_k are transmission powers of serving eNB$_l$ and interfering eNB$_k$ on PRB$_n$, respectively. H_l and H_k represent channel gains of serving eNB$_l$ and interfering eNB$_k$ on RB$_n$, respectively. δ_k is set to 1 or 0 to indicate whether the interfering cell k allocates PRB$_n$ to its UEs.

7.2.3. Minimizing PLR

In the wireless network, PLR is defined as the percentage of the discarded packets to transmitted packet for a service. Minimizing the PLR is one of the most important functions in real time services which can guarantee the reliability of packet transmission. Note that, the PLR has to be maintained below a threshold in order to satisfy the QoS requirement.

$$f_4 = 1 - \frac{1}{P^*}\left(\frac{1}{N_u}\sum_{k=1}^{N_u}\frac{p_d}{p_s}\right) \tag{7.16}$$

where p_d is the total size of discarded packets (in bits) of UE_k and p_s is the total size of all packets (in bits) arrived into the eNB's buffer of UE_k. P^* is the maximum packet loss tolerance for video streaming traffic. F_4 indicates whether average PLRs of all UEs is lower than the maximum packet loss tolerance.

7.2.4. Minimizing Delay

Delay is an important parameter affecting system performance for real time services. If the packet is not received by UE within a delay threshold it will be lost. Delay can be defined as the average delay of Head-of-Line (HOL) packets of all UEs. The HOL packet of a UE is the packet that has the longest resided time in the buffer of eNB.

$$f_5 = 1 - \frac{1}{D^*}(\arg\max_{k \in N_u}(\max(d_{p,k}))) \tag{7.17}$$

where $d_{p,k}$ is the delay of the p^{th} packet of UE_k and D^* is the maximum packet delay tolerance for video streaming traffic. F_5 indicates whether maximum packet delay of the system is lower than the maximum packet delay tolerance.

7.2.5. Optimize Multi-Objectives

In multi-objective optimization problems, the challenge is to find an optimal solution such that all desired objectives are satisfied. One of the most popular and simplest approaches to solve multi-objective optimization problem is Weighted Sum Method [124], where multiple objective functions are combined into a single composite function using (7.18):

$$f(x) = \sum_{1}^{5} w_i f_i(x) \tag{7.18}$$

where $w_i \geq 0$ represents the relative importance of the objectives and it is assumed that $\sum_{1}^{j} w_i = 1$, $f_i(x)$ is desired objective functions and $[x_1, x_2, \ldots, x_j]$ are the vector of decision variables. The results are changed when the weighting coefficients change, hence the

weighting coefficients can be allocated to objective functions based on objective functions' roles in improvement of system performance. Based on this approach, systems can instantaneously change its aim by adjusting the weighting coefficients.

7.2.6. ABS Configuration using Genetic Algorithm (GA)

GA is one type of population-based search algorithms in which an optimized solution is obtained using recombination and selection strategies. GA can be used to optimize the objective functions without much mathematical requirements. In GA, the specified variables of a problem are represented as genes in a chromosome, and the chromosomes are evaluated based on fitness values including some measurement functions. For this purpose, a set of chromosomes are randomly selected as the initial population that encodes a set of possible solutions. For the initialized population, some genes may show better performance in one chromosome while at the same time another chromosome may have some genes that are better than others. In order to combine best genes from different chromosomes, the crossover operator and mutation operators are used to produce new chromosomes named offspring. Finally, GA converges to the best solution after creating several generations. The GA is terminated when a termination condition is satisfied.

7.2.6.1. Population Initialization

The initial population is obtained by randomly initializing variables. In order to reduce the computer memory overhead and computation cost, the population is scaled to a small size. In the proposed algorithm, the population is shown in Figure 7.4 where each frame distribution is coded as one chromosome (ch) and indicates which subframes (S_n) are identified as ABS. In Figure 7.4, 1 indicates the subframes that are labelled as ABS and 0 indicates the subframes which are used as non-ABSs. For example, Ch_n represents that $\{S_1, S_2, S_3, S_5, S_7, S_8, S_9\}$ are non-ABSs while $\{S_4, S_6, S_{10}\}$ are used as ABSs.

	S_1	S_2	S_3	S_4	S_5	S_6	S_7	S_8	S_9	S_{10}
Ch_1	1	0	0	1	1	1	0	1	0	0
Ch_2	0	1	1	1	0	0	1	1	1	1
						.				
						.				
						.				
Ch_n	0	0	0	1	0	1	0	0	0	1

Figure.7.4. Initialized population of GA

7.2.6.2. Fitness Evaluation

Each chromosome in the population has a corresponding fitness value. The fitness value is directly related to the objective function and is used to determine which chromosomes will be selected for the next generation. The chromosome with the greater fitness value has more chances to survive. In this scheme, the weighted sum of five objective functions, $f(x)$, is considered as the fitness value.

7.2.6.3. Crossover Operator

For the generated population, the crossover is an important operator to find the optimal solution. The crossover helps genes of parents to be combined and passed to its offsprings. Moreover, it may produce new offsprings to expose a new search area. Single-point is one type of crossover operation where parents are divided into two parts at a single-point and then offsprings are generated by combining of first part of one parent and second part of another parent. Figure 7.5 (a) shows an example of single-point crossover where $\{S_1, S_2, S_3, S_4\}$ of parent 1 are combined with $\{S_5, S_6, S_7, S_8, S_9, S_{10}\}$ of parent 2 and vice versa.

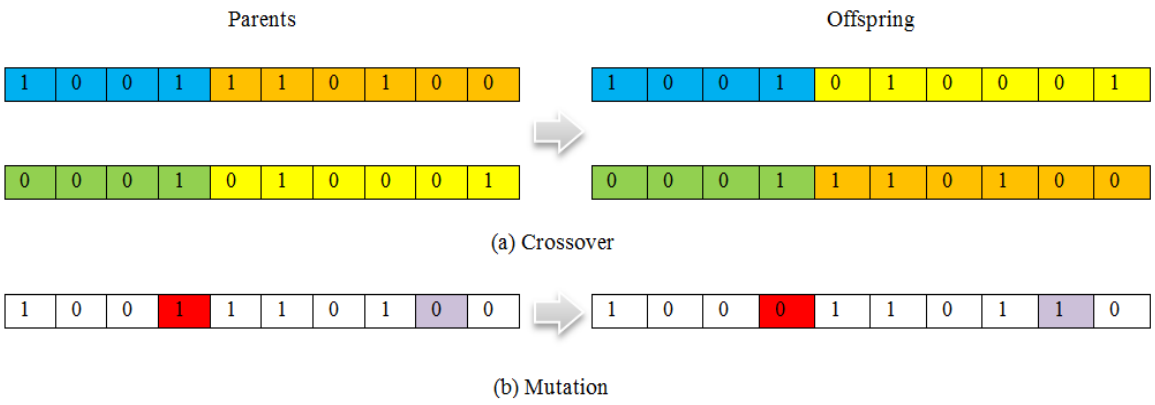

Figure.7.5. Examples of (a) crossover and (b) mutation operators

7.2.6.4. Mutation Operator

In order to find the optimal solution and avoid a suboptimal solution, the mutation operation is required in which some modification is performed to provide possible variation in the offspring. Mutation operation changes one or more genes in a chromosome of parent to prevent the population from stagnating at any local optimum. Using a normal distribution, one or more genes are selected and then its value is changed from 0 to 1 or 1 to 0. Figure 7.5 (b) shows that the value of S_4 and S_9 were changed using mutation operator.

7.2.6.5. Selection

The selection step determines which of the chromosomes will be retained for the next generation. It guaranties that the better chromosomes have more chances to be selected. In this algorithm, the roulette wheel method is used as the selection operator. The first step of selection is to compute the cumulative fitness of the total population using the sum of the fitness of all chromosomes. Then, probability of each chromosome is computed using (7.19) given as follows:

$$P\{x_i\} = \frac{f(x_i)}{\sum_{j=1}^{m_{ch}} f(x_j)} \tag{7.19}$$

Where m_{ch} is number of chromosomes and $f(x)$ is the fitness value of each chromosome. Thereafter, an array is constructed using cumulative probabilities of the chromosomes. Moreover, a vector is generated containing n normalised random numbers. Finally, the surviving chromosomes will be selected by comparing the elements of these two vectors based on the $P\{x_i\}$.

7.2.6.6. Termination

A termination criterion needs to be set for the GA to stop iterating. The termination condition can be selected as the total number of iterations or a threshold of desired fitness values. In the proposed scheme, the termination condition was set to total number of iterations to reduce the computing time.

Algorithm II. Genetic Algorithm

Input: At each time window, the macro eNB collects

1. *Throughputs*
2. *Interference*
3. *Delay*
4. *PLR*

Output: ABS configuration for each macrocell and its picocells.

while *stopping conditions are met* **do**

Formulate the GA to do ABS assignments.

Randomly generate the first population. **Repeat**

- Compute the fitness value of each chromosome based on the objective functions.
- Apply the crossover operation on the parents to produce a new generation.
- Apply mutation operation to enhance the new generation.
- Compute the fitness of the new offspring.
- Apply selection method

end While

ABS configuration

7.3. Simulation Results and Discussion

This section evaluates the proposed schemes using a system level simulation. The simulation parameters were given based on parameters specified in Chapter 2. In addition, the required simulation values of FQL and GA are outlined in Table 7.2. The performance of the proposed schemes were evaluated in terms of number of the offloaded UEs, RE UE throughput, average macro UE throughput, and outage probability, and delay (as described in Section 2.5). In this subsection, the proposed eICIC schemes were benchmarked with respect to Table 6.1 for two traffic models to evaluate the results obtained by the proposed schemes from prior known results.

7.3.1. Performance Analysis of FQL based Scheme

The performance of the proposed eICIC scheme based on FQL is evaluated for both full and video streaming traffics.

Table 7.2. Simulation Parameters

Parameter	Value
Minimum required throughput for FQL	200 Kbps
Time window of ABS value	50 TTI
total number of GA iterations	20
D^*	150 ms
P^*	10^{-3}
R_p^*	256Kbps
R_m^*	256Kbps
w_1, w_2, w_3, w_4, w_5	0.20

7.3.1.1. Performance of Full Buffer Traffic

In this subsection, the performance of FQL based eICIC scheme is analysed for full traffic.

7.3.1.1.1. Percentage of the Offloaded UEs

The ABS value calculated by the proposed scheme for the centre cell is depicted in Figure 7.6. Since there are 10 subframes in each frame, the ABS is a factor of 10. For the defined inputs, ABS value converged to 40% after a time interval of 1856 ms as shown in Figure 7.6. Moreover, the FQL used in the CRE offset value module converged to the offset value of 10.88 dB as shown in Figure 7.7. When compared to the proposed eICIC scheme based of FL, the two schemes converged to the same ABS value while the FQL based scheme converged slower than FL based scheme. This because it was assumed there is no knowledge about the consequent part of rules. As a result, FQL needs more time to converge. Moreover, Figure 7.7 shows that there is not a significant difference between the CRE offset values. In Figure 7.8, since the proposed fuzzy scheme changes the offset value based on the ratio of UEs, average throughput and SINR, 45.6% of UEs are offloaded to picocells.

7.3.1.1.2. Outage Probability

The outage probability of the proposed scheme is compared for different offset values with different ABS values in Figure 7.9. Based on this figure the outage probability

increases by increasing the offset value. When the offset value increases UEs far away from pico eNBs are offloaded to picocell while UEs' SINRs are low.

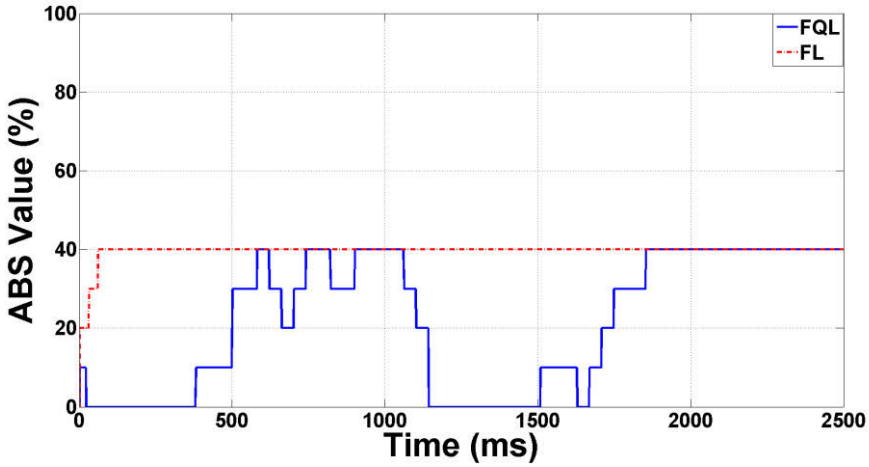

Figure 7.6. The optimum ABS value for centre cell using FQL for FB

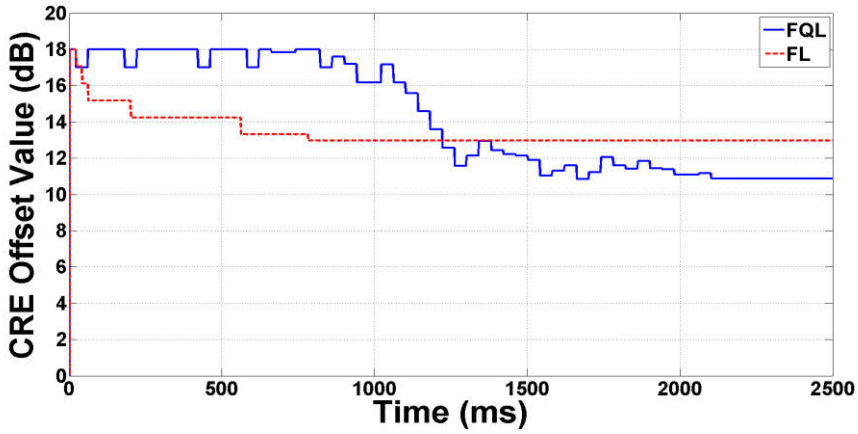

Figure 7.7. The optimum offset value for centre cell using FQL for FB

On the other hand, using ABS value causes the outage probability reduces because UEs with high received interference are scheduled on ABSs. Note that the max RSRP scheme has the lowest outage probability because in this scheme the offset value is set to 0 dB and hence the UE which are closer to pico eNB are offloaded to picocells. Since the proposed scheme considers the SINR value, it can maintain the outage probability on the acceptable range as shown in Figure 7.9. By changing the SINR's membership functions, the outage probability can be changed based on the system requirements.

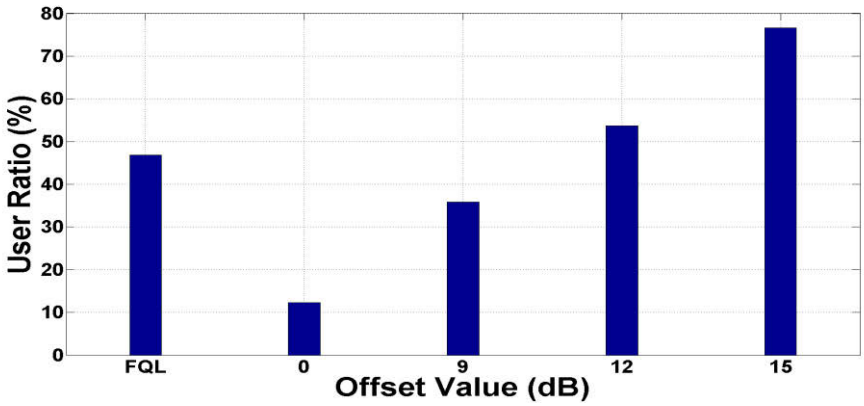

Figure 7.8. Number of the offloaded UEs from macrocell to picocells for FB

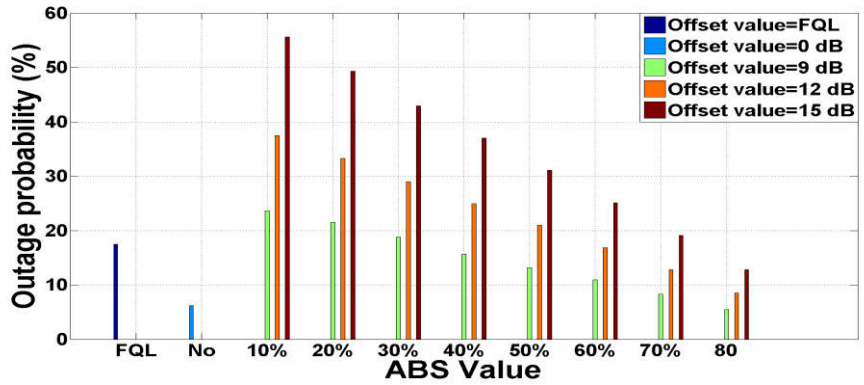

Figure 7.9. The outage probability for difference ABS values and CRE offset values for FB

7.3.1.1.3. Throughput Performance

When the offset value is low (i.e., 9dB), more UEs are connected to macro eNBs and hence the macro UEs throughput is low as shown in Figure 7.10. A large offset value can be used to improve the macro UE throughput. However, Figure 7.12 shows that the RE UE throughput reduces with increasing the offset value because UEs far away from the picocells are connected to the pico eNB. This results in more interference for RE UEs and then a lowering of throughput. The proposed scheme based on FQL set the offset value and ABS value based on system requirements such that the throughputs of macro UEs and RE UEs are not sacrificed as depicted in Figure 7.10 and 7.12.

On the other side, when a small ABS value is used, more non-ABS are assigned to macro UEs while the number of ABSs that can be allocated to RE UEs is low. Consequently, the throughput of macro UEs increases while the throughput of RE UEs is degraded as shown in Figure 7.10 and 7.12. In contrast, if the ABS value increases,

the number of subframes that can be allocated to macro UE will decrease and the number of ABS assigned to RE UEs will increases. Since the macro eNB is muted on the ABSs, the interference decreases which can lead to increase of the RE UE throughput at the expense of reduction of macro UE throughput.

Moreover, the increase of RE UE throughput can increase the picocell throughput (see Figure 7.13). However, for larger ABS values, the throughput of macro UEs reduces significantly which lead to decrease of macrocell throughput as shown in Figure 7.11. By increasing of offset value to 15 dB, more UEs are located in the range expanded area. As a result, the average RE UE throughput reduces because UEs far away from the pico eNB are connected to the pico eNB while these UEs suffer high interference from macro eNB.

In this case, if the ABS value is set to a small value such as 10%, the number of ABS cannot support all of RE UE and the pico eNB has to schedule them on non-ABS. Since the interference on non-ABS is high for RE UEs particularly for RE UEs far away from pico eNB, the RE UE throughput and picocell throughput decrease for low number of ABSs as shown in Figures 7.12 and 7.13.

As a result, the trade-off between throughput of macro UEs and RE UEs must be maintained while the required throughput for macro UEs is satisfied. Moreover, the number of UEs connected to pico eNBs and macro eNB must be considered. In order to satisfy the above requirements, the proposed scheme based on FQL set ABS value to 40%. Using the selected ABS value, the average throughput of macro UEs is satisfied while the average throughput of RE UE is still good as shown in Figures 7.10 and 7.12.

7.3.1.1.4. Result Comparison

Table 7.3 summarizes outage and throughputs of different schemes for full buffer traffic to compare the system performance of the proposed FQL based eICIC scheme with the proposed schemes [99] and [108] in literature. The proposed eICIC schemes based on FL and FQL could maintain the trade-off between RE UE and macro UE throughputs better than other schemes while its outage value is still small.

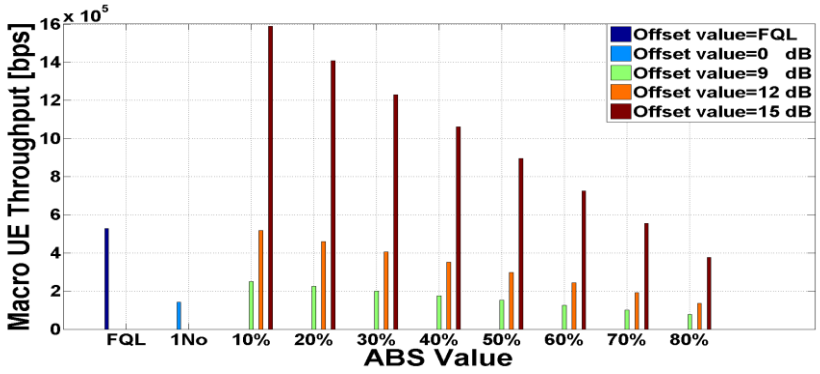

Figure 7.10. Average macro UE throughput for FB

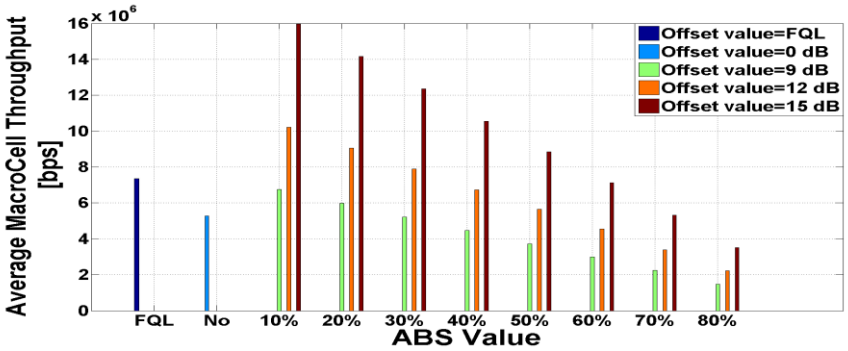

Figure 7.11. Average macrocell throughput for FB

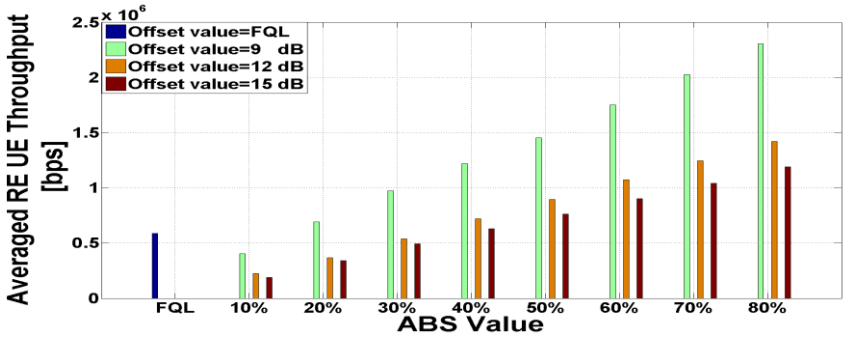

Figure 7.12. Average RE UE throughput for FB

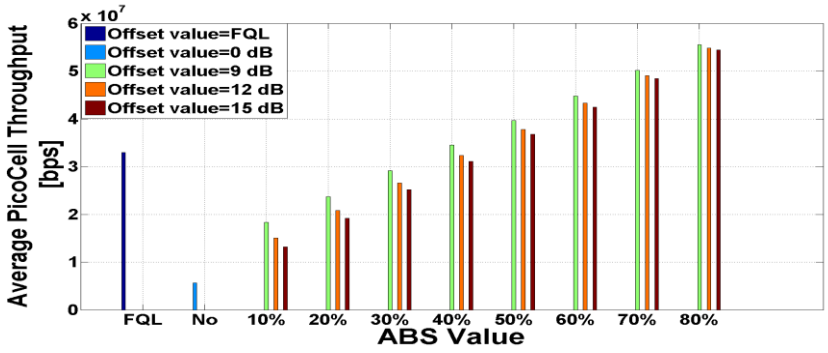

Figure 7.13. Average picocell throughput for FB

This balance is maintained better by FQL because the FQL based scheme determined the consequent part of fuzzy rules through the system monitoring. Although [108] considered the macrocell and picocell throughputs, it only used the total sum of macrocell and picocell throughputs to find the best ABS value. Therefore, it is possible the total cell throughput obtained for a particular combination of ABS and offset values becomes large because only the macrocell throughput or picocell throughput is high while the RE UE throughput or macro UE throughput has been sacrificed. Furthermore, [108] needs much more time than the proposed schemes to find the best ABS and offset values. This is because the total throughputs for all combination of (ABS, CRE) are calculated at the first step and then the combination that obtains the maximum total throughput is selected as the optimal combination.

Table 7.3. System Performance Comparison for FB

eICIC Scheme	Offset Value (dB)	ABS Value (%)	Outage (%)	Throughput			
				Macro UE (kbps)	RE UE (kbps)	Macrocell (Mbps)	Picocell (Mbps)
FQL	10.88	40	17.5	528	581	7.26	32.9
FL	12.98	40	22	735	598	7.30	34.12
Ref.[99]	11	Oscillated between 40-50	20.80	253	1040	4.42	37.8
Ref.[108]	13	60	24.49	297	1065	5.29	42.9

7.3.1.2. Performance of Video Streaming Traffic

Referring to metrics introduced in Chapter 2, the proposed scheme is evaluated for the video streaming traffic in this sub-section.

7.3.1.2.1. Trends of ABS and Offset Values

The ABS value and CRE offset value calculated by the proposed eICIC scheme based on FQL are presented in Figures 7.14 and 7.15 for the video streaming traffic. The

figures demonstrate that the ABS value converges to 40% when the FQL is applied. This is because the requirement of system is satisfied for this ABS value based on inputs defined for ABS value module. Moreover, the FQL used for the CRE offset value module selects 12.2 dB as the optimum offset value. By considering the optimum offset value, 63.2% UEs are offloaded to picocells as shown in Figure 7.16.

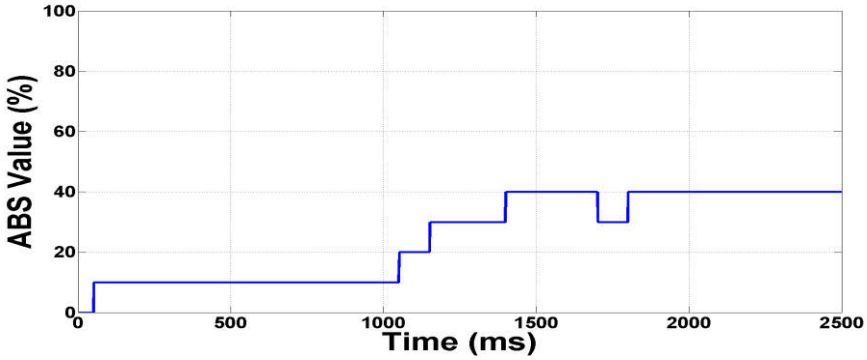

Figure 7.14. The optimum ABS value for centre cell using FQL for VS

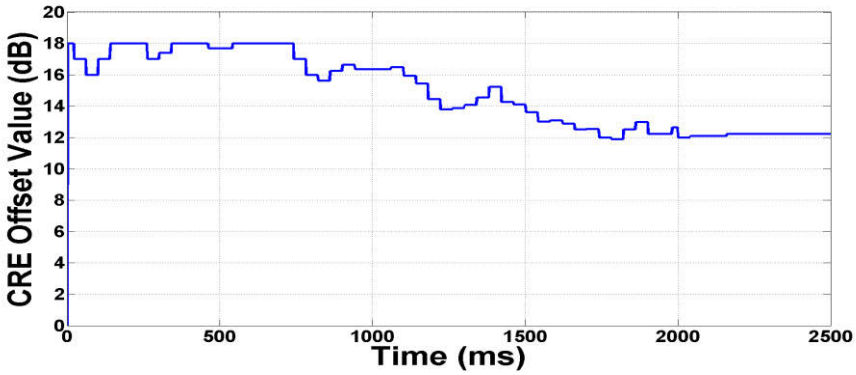

Figure 7.15. The optimum offset value for centre cell using FQL for VS

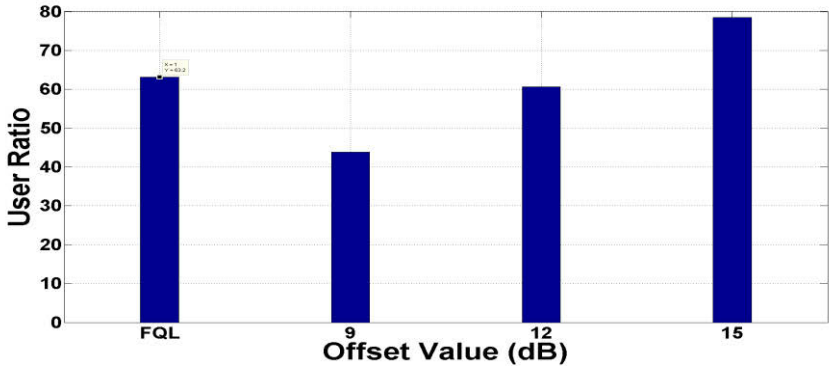

Figure 7.16. Number of the offloaded UEs from macrocell to picocells for VS

7.3.1.2.2. Throughput Performance

As mentioned in Chapter 6, when the offset value is low (i.e., 9dB), the macro UEs throughput is low due to large number of UEs located in macrocell while using the large value leads to improve the macro UE throughput as shown in Figure 7.17. On the other hand, although using large offset value can improve the macro UE throughput, the throughput of RE UEs decreases due to experience of low SINR.

Based on the simulation results shown in Figures 7.17 and 7.19, the proposed scheme can maintain the balance between the macro UE and RE UE throughputs by deploying the optimum ABS and offset values for video streaming traffic. In contrast to full buffer traffic, the average macrocell throughput decreases by increasing the offset value due to difference in nature of traffic models. When the full buffer is used as the traffic model, it is assumed that eNB always contains data to transmit and hence all PRBs are used in scheduling process.

Therefore, when the number of macro UEs decreases, more PRB can be allocated to each macro UE which results in an increase of both macro UE throughput and macrocell throughput. However, for the video streaming traffic, this scenario can change. Since the packets arrive at a regular interval with 256 kbps source video rate, all of PRBs may be not used for UEs.

When the number of UEs increases, the number of PRB used for scheduling increases which leads to increase of total macrocell throughput as shown in Figure 7.18. This scenario can occur for RE UE throughput and picocell throughput (see Figure 7.20). The throughputs shown in Figures 7.17 and 7.19 illustrate that the proposed eICIC scheme can maintain the trade-off between macro UE and RE UE throughputs and satisfy the system requirements for video streaming traffic.

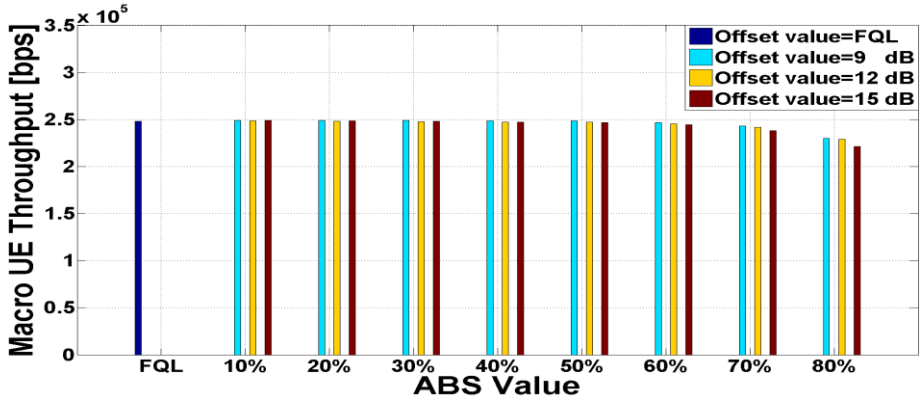

Figure 7.17. Average macro UE throughput for VS

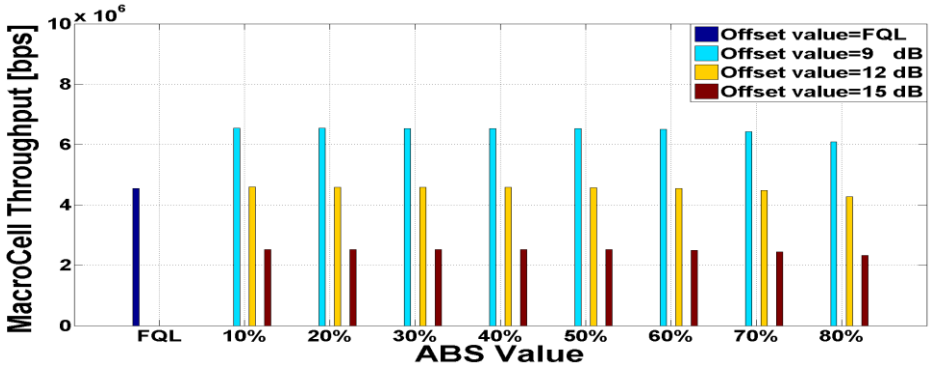

Figure 7.18. Average macrocell throughput for VS

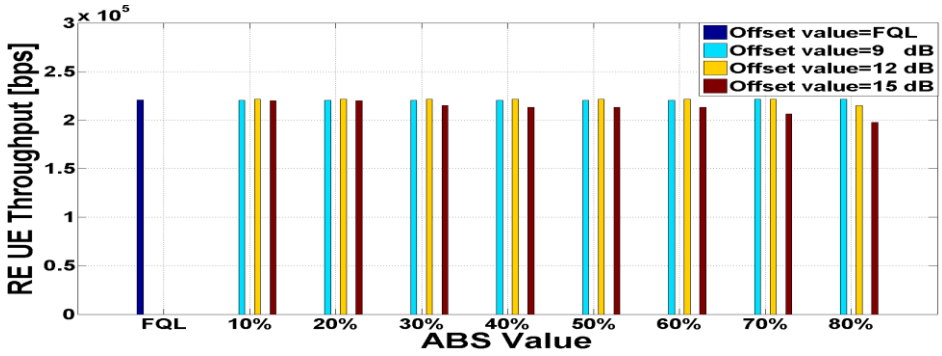

Figure 7.19. Average RE UE throughput for VS

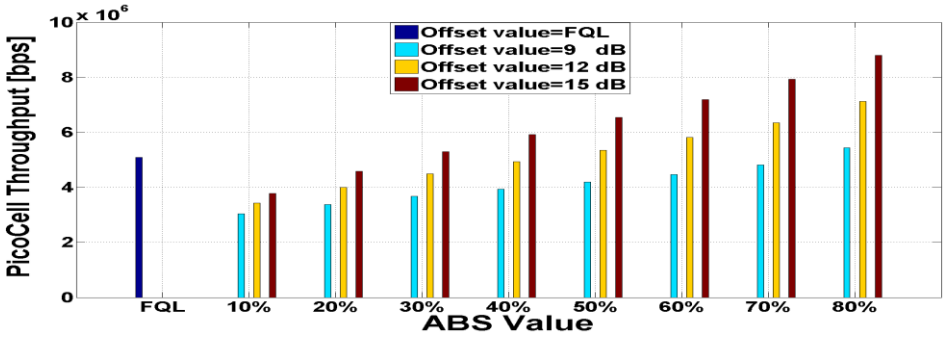

Figure 7.20 Average picocell throughput for VS

7.3.1.2.3. Delay

When the ABS configuration and offset value change, the number of PRBs allocated to each UE changes. For different SINR, an appropriate MCS is selected which results in a changing throughput. For example, for low SINR, a lower order modulation is used which provides a lower transmission bit rate. Therefore, if the number of the allocated PRBs and the selected MCS cannot support the amount of the received data, data are transmitted with delay. Since delay is considered as the one metric in generating the reinforcement learning reward, the proposed scheme updates the q-values by considering the delay. Figure 7.21 shows that the proposed scheme has an acceptable delay in compared to other schemes while the other requirements of system are satisfied.

7.3.1.2.4. Outage Probability

Figure 7.22 shows that the outage probability is still at an acceptable level compared with other schemes when the video streaming traffic is used. This is because the proposed scheme considers the SINR value for input as well as the reinforcement learning reward.

7.3.1.2.5. Result Comparison

Table 7.4 compares the proposed eICIC based on FQL with other proposed schemes [99] and [108] in literature for video streaming traffic. According to this table, the offset values obtained from FQL based scheme and [108] converged to 12.22 dB and 9 dB, respectively. For these offset values, the proposed scheme and [108] converged to ABS value of 40 % and 20 % respectively, whereas [99] oscillated between 50%-70%. The proposed FQL based scheme could maintain the trade-off between macro UE and RE throughputs while satisfied the required throughput of all UEs. Moreover, it outperformed [99] and [108] in term of delay. This is because the proposed FQL based scheme considered delay while [99] and [108] only used the macro and pico loads and the total cell throughput to determine the ABS value.

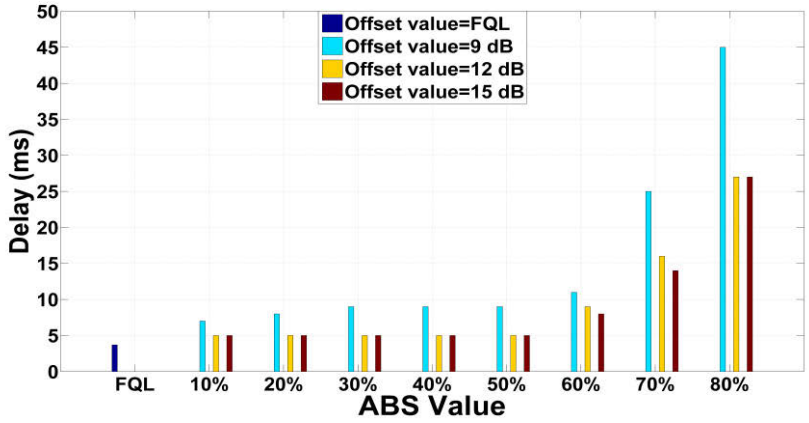

Figure 7.21. Delay for difference ABS values and CRE offset values for VS

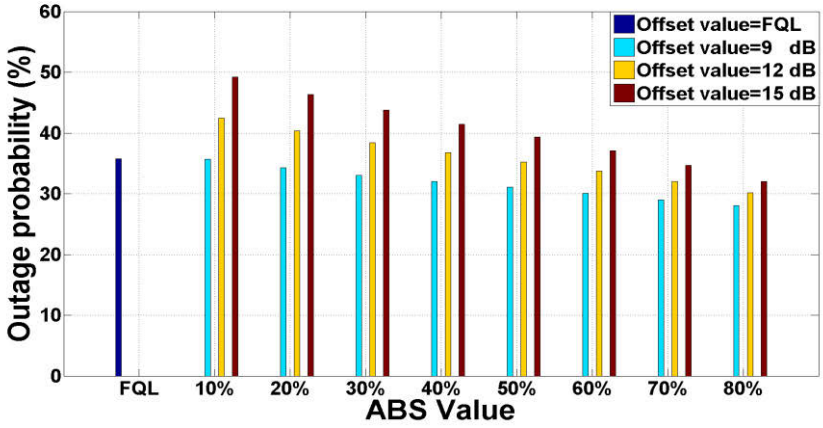

Figure 7.22. The outage probability for difference ABS values and CRE offset for VS values

Although [108] could maintain the trade of between throughputs similar to the proposed FQL based scheme, the number of offloaded UEs is only 42%. However, 63 % of UEs are offloaded to picocells using the proposed FQL based scheme while the balance between throughputs is maintained and delay is small. Moreover, the scheme proposed in [108] takes much more time than the proposed scheme to find the best ABS and offset values because [108] calculates the total throughputs of all combination of (ABS,CRE) and then selects the combination that obtains the maximum total throughput as the optimum ABS and offset values.

Table 7.4. System Performance Comparison for VS

eICIC Scheme	Offset Value (dB)	ABS Value (%)	Outage (%)	Delay (ms)	Throughput			
					Macro UE (kbps)	RE UE (kbps)	Macrocell (Mbps)	Picocell (Mbps)
FQL	12.22	40	35.7	3.59	248	221	4.54	5.09
Ref.[99]	12	Oscillated between 50-70	37.76	8.33	215	251	4.06	5.67
Ref.[108]	9	20	34.3	8	238	220	6.53	3.38

7.3.2. Performance Analysis of GA based Scheme

Since the main goal of the proposed eICIC scheme based on GA was to improve the system performance of video streaming traffic, the proposed scheme is evaluated for the video streaming traffic in this chapter.

The ABS value and its configuration obtained by the proposed eICIC scheme are presented for different CRE offset values in Table 7.5. Observation demonstrates that the best ABS values are 10%, 50% and 70% for CRE offset values of 9 dB, 12 dB and 15 dB, respectively. This is because the requirement of system is satisfied for this ABS value based on the defined fitness values. Moreover, the locations of ABSs are shown for different CRE offset values in Table 7.5. In addition, Figure 7.23 shows the convergence of the fitness values of different offset values.

Table 7.5. ABS Configuration Obtained by GA based Scheme for VS

Offset Value	ABS Value	ABS configuration									
9 dB	**10%**	0	0	0	1	0	0	0	0	0	0
12 dB	**50%**	1	0	1	0	1	0	0	0	1	1
15 dB	**70%**	0	0	1	1	0	1	1	1	1	1

Based on Figures 7.24 and 7.25, the macro UE and RE UE throughputs of the ABSs obtained for different static CRE offset values can approximately satisfy the required

data rate (i.e., 250 kbps). In Figure 7.25, it can be seen that the RE UE throughput for offset value of 15 dB is lower than the required data rate. This is because the number of UEs offloaded to pico UEs is large and then the average RE UE throughput is decreases.

Figure 7.26 and 7.27 illustrates the outage probability and delay, respectively. When compared to Figure 7.21, the delay is higher using GA and this is due to configuration of ABSs in each frame. Based on Table 7.5, some subframes are sequentially allocated to ABS/non-ABSs and this can lead to an increase of delay for macro UEs/RE UEs. However, delay is still on the acceptable level.

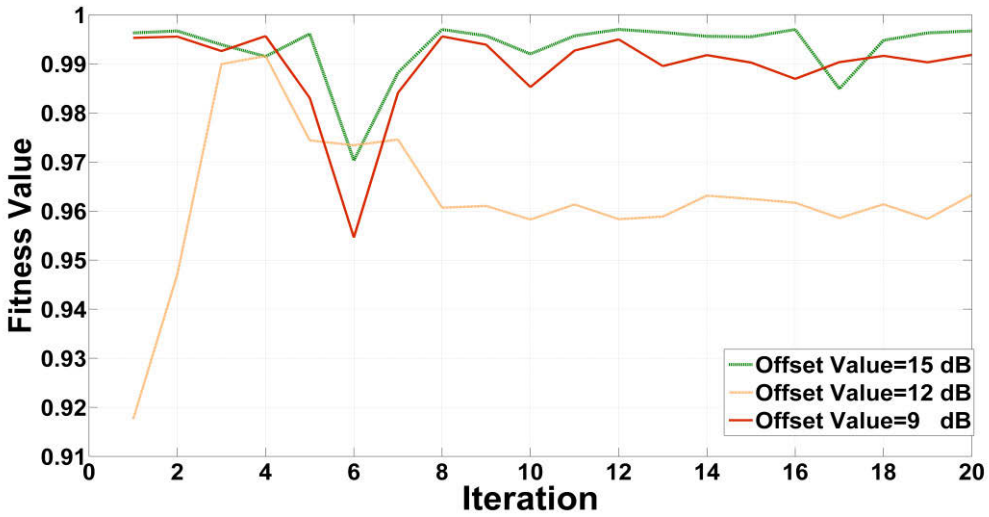

Figure 7.23. Fitness value of GA

7.3.2.1. Result Comparison

The system performances of different eICIC schemes were compared in Table 7.6 to evaluate the results of GA based algorithm. It was assumed that CRE offset value is set to 9 dB and traffic model is video streaming traffic. The reason for selecting 9 dB is that [108] selected the offset value of 9 dB as its optimum offset value. Therefore, all schemes are compared for 9 dB in order to compare results in the same situation.

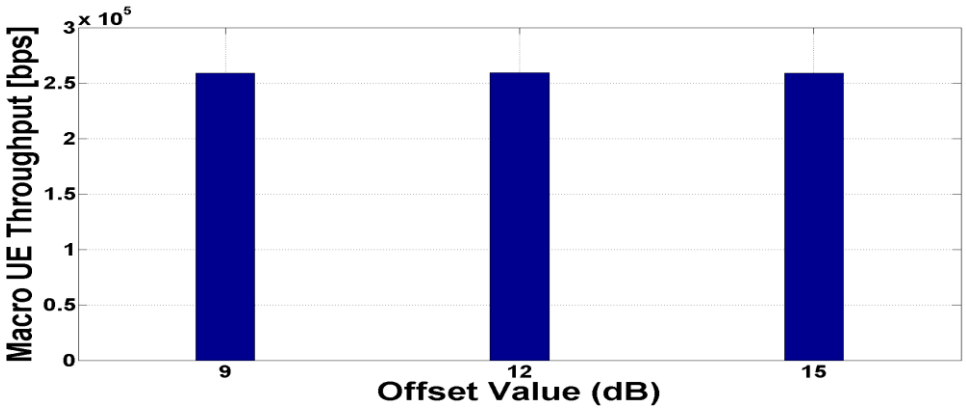

Figure 7.24. Average macro UE throughput using GA for VS

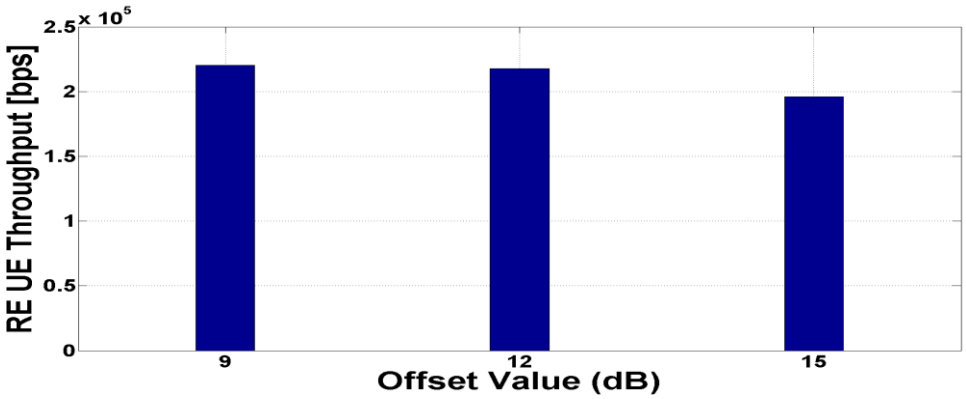

Figure 7.25. Average RE UE throughput using GA for VS

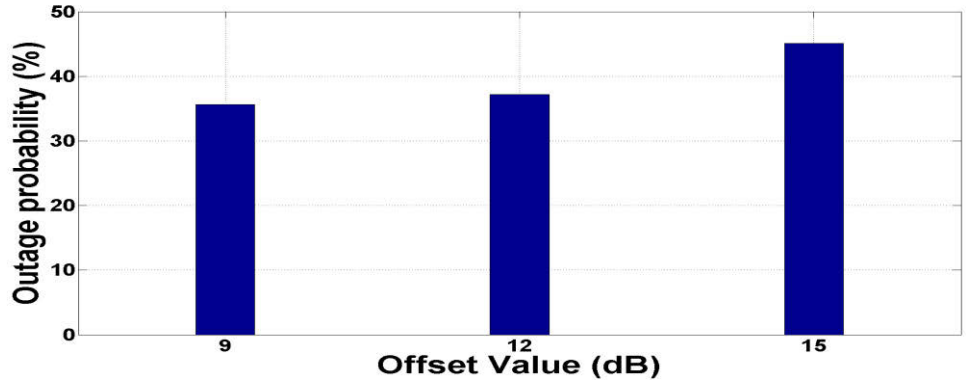

Figure 7.26. The outage probability using GA for VS

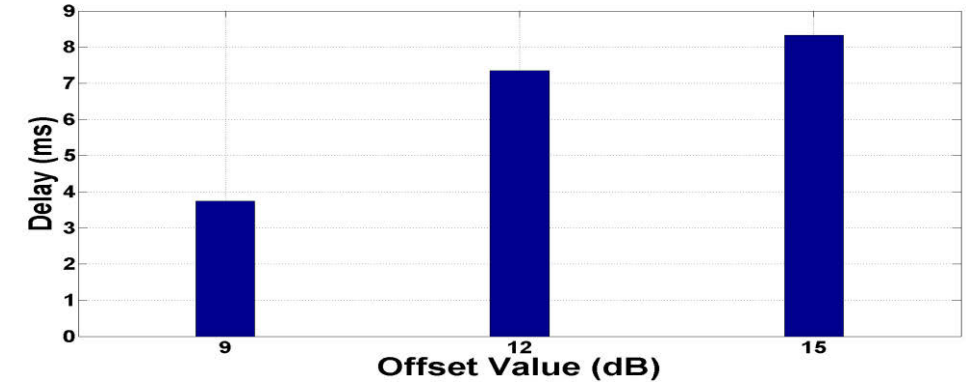

Figure 7.27. Delay using GA for VS

The proposed GA base scheme and [108] converged to ABS value of 10 % and 20% respectively, whereas [99] oscillated between 50%-60% for an offset value of 9 dB. However, the proposed schemes based on GA could maintain the trade-off between macro UE and RE throughputs while [99] sacrificed the macro UE throughput to increase the RE UE throughput. Moreover, the proposed scheme outperforms [99] in terms of outage and delay. This is because the proposed GA based scheme considered the throughput of RE UEs, macro UE throughout, interference level and delay to find the best ABS configuration.

Although the GA based scheme and [108] obtained similar results for macro UE and RE UE throughputs, the scheme proposed in [108] takes much more time than the proposed GA based scheme to find the best ABS and offset values because it calculates the total throughput for all combination of (ABS, CRE) and then selects the combination that achieves the maximum total throughput.

Table 7.6. System Performance Comparison for GA based Scheme

eICIC Scheme	Offset Value (dB)	ABS Value (%)	Outage (%)	Delay (ms)	Throughput			
					Macro UE (kbps)	RE UE (kbps)	Macrocell (Mbps)	Picocell (Mbps)
GA	9	10	35.6	3.47	248	220	6.54	3.04
Ref.[99]	9	Oscillated between 50-60	39.7	11.608	210	253	4.55	5.61
Ref.[108]	9	20	34.3	8	238	227	6.23	3.38

7.4. Summary

This chapter proposed an eICIC scheme based on fuzzy Q-learning approach to overcome the co-channel interference problem in heterogeneous networks. The FQL-eICIC scheme combined the fuzzy logic system and Q-learning approach to intelligently select the optimum ABS value and CRE offset value using two separate modules. By considering the SINR, macro UE throughput and number of UEs as inputs,

an excellent balance could be achieved between the macro UE and RE UE throughputs. The system level simulation has been developed to support the analysis for both full buffer and video streaming traffics. Simulation results showed the required throughput of macro UEs and RE UEs were guaranteed while the outage probability was at an acceptable level. Moreover, the delay for the video streaming traffic was low using the proposed eICIC scheme. Furthermore, the number of UEs offloaded to picocell could be appropriately controlled by the CRE offset value. Thereafter, the ABS configuration was determined using Genetic Algorithm (GA) to support the video streaming traffic. For this purpose, the macro UE throughput, pico UE throughput, interference level, delay and PLR were considered as the objective functions and then the best configuration was obtained after several iterations. The GA based scheme was compared with other dynamic ABS schemes in literature. The simulation results demonstrated that the proposed GA scheme could find the best ABS value and ABS locations such that the balance between macro UE and RE UE throughputs were maintained while the delay and outage were kept within acceptable ranges.

Chapter 8

ANALYTICAL CALCULATION OF OPTIMUM CRE OFFSET VALUE AND ABS VALUE USING STOCHASTIC GEOMETRY ANALYSIS

Since the CRE approach affects the downlink signal quality of the offloaded users, these users experience high interference from macro eNB on both the control and data channels. Therefore, an intercell interference mitigation technique is needed to realize the promised capacity and coverage in co-channel HetNets. Several techniques have been proposed to solve these issues mathematically. The optimal offset value was obtained in [125] using different regions defined based on pathloss and UE density. A tractable analytical framework for evaluating coverage probability in heterogeneous networks for frequency domain has been presented in [126]. Semi-analytical methods have been presented in [127-128] where the optimal offset value was determined through simulation. In [129], a load-aware model is proposed to find the average load per macro and pico eNBs using stochastic geometry but it did not consider the ABS. In addition, offloading and resource partitioning was described in [130-131] for a heterogeneous network and the number of ABSs has been derived in [132]. However these papers did not consider the minimum required throughput for macro UEs and pico UEs.

This chapter presents a mathematically tractable macrocell-picocell HetNet framework. For this purpose, the network model proposed in [133] is extended for a two tier HetNet consisting of pico eNBs and macro eNBs. The optimum offset value and its minimum and maximum values are obtained under constraints on the outage probability. After that, the required number of ABSs will be formulated. The number of ABSs is analytically derived based on the ergodic rate and the minimum required throughput of users through stochastic geometry tool.

The rest of the chapter is organized as follows. The system model is provided in Section 8.1. Section 8.2 calculates the downlink outage probability in each tier and then obtains the CRE offset value. The ergodic rate of each tier is obtained in Section 8.3. The optimal number of ABS is obtained in Section 8.4. The results are shown in Section 8.5. The conclusion is given in the final section.

8.1. System Model

A two tier HetNet is considered where picocell is overlaid with macrocell. Tier 1 consists of macro eNB modelled as homogeneous Poisson Point Process (PPP) with density λ_m and pico eNBs are located in tier 2 modelled as homogeneous PPP with density λ_p [133]. In this model, all UEs are modelled as PPP of density λ_u. Each eNB in tier i operates at a fixed transmission power $\{P_p, P_m\}$. The log-distance pathloss model is considered with a path loss exponent α where $\alpha > 2$. Furthermore, it is assumed that UE only experience fast fading power gain presented by h such that the received power at the UE with distance R from its serving eNB is $P_j h R^{-\alpha}$, ($j = m, p$).

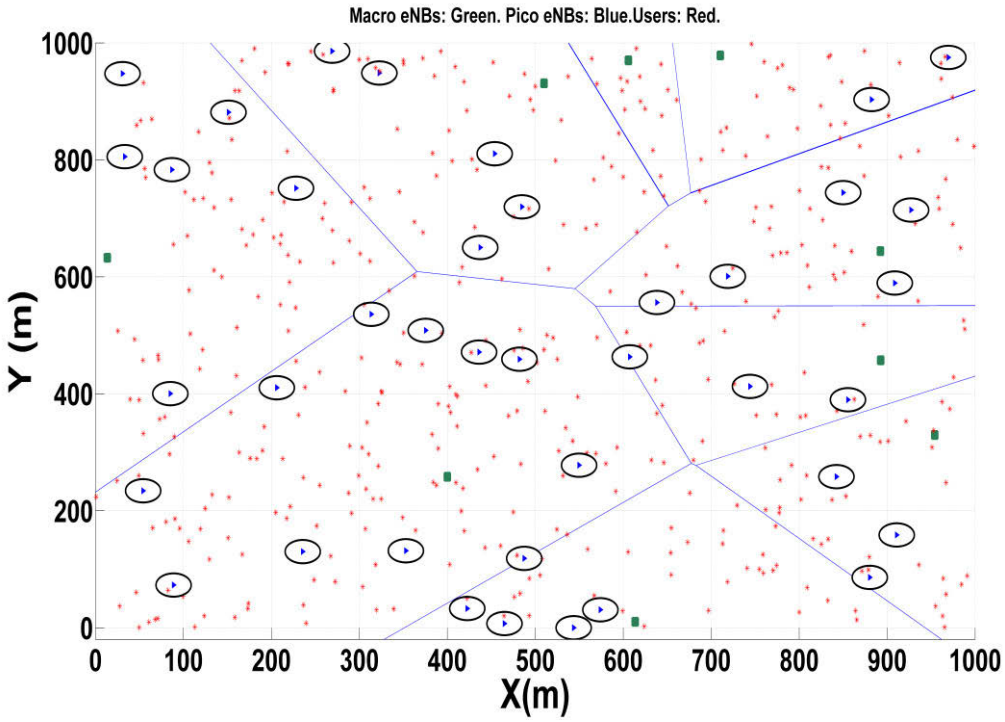

Figure 8.1. Example of the network model

8.1.1. User Association

In the CRE method, a UE is connected to tier 1 or 2 based on maximum long-term average received power when the offset value β is used as follows:

$$j = \arg \max_{j = p, m} (\beta_j \, RSRP_j) \tag{8.1}$$

The offset value is used for pico eNBs (β_p=β) while for macro eNBs, the offset is set to one (β_m=1). The offset value is broadcast by the pico eNB to help UEs make the accurate association decision. In order to investigate the impact of offset value, the network is divided into three regions: 1) the basic coverage area of macro eNB, 2) the basic coverage area of pico eNB, and 3) the range expanded area of pico eNB. The following open access policy is assumed for UE association in each region:

- UE is a pico UE if $RSRP_p > RSRP_m$
- UE is a RE UE, if $RSRP_p < RSRP_m$ and $\beta \, RSRP_p > RSRP_m$
- UE is a macro UE if $\beta \, RSRP_p < RSRP_m$

8.1.2. The Average Number of UEs per Tier

The average number of UEs located in each region is derived from [133] as follows.

$$N_m = (1 + \frac{\lambda_p (p_p \ \beta)^{2/\alpha}}{\lambda_m (p_m)^{2/\alpha}})^{-1} \frac{\lambda_u}{\lambda_m} \tag{8.2}$$

$$N_p = (1 + \frac{\lambda_m (p_m)^{2/\alpha}}{\lambda_p (p_p)^{2/\alpha}})^{-1} \ \frac{\lambda_u}{\lambda_p} \tag{8.3}$$

$$N_{RE} = (1 - (1 + \frac{\lambda_p (p_p \beta)^{2/\alpha}}{\lambda_m (p_m)^{2/\alpha}})^{-1} - (1 + \frac{\lambda_m (p_m)^{2/\alpha}}{\lambda_p (p_p)^{2/\alpha}})^{-1}) \ \frac{\lambda_u}{\lambda_p} \tag{8.4}$$

where N_m, N_p and N_{RE} represent the number of macro UEs, pico UEs and RE UEs, respectively.

8.1.3. Statistical Distance to Serving eNB

The probability density functions (PDF) $f_R(r)$ of UE at the distance of R from its serving eNB is given as follows [129].

$$f_R^m(r) = \frac{2\pi\lambda_m}{A_m} r \exp(-\pi r^2 (\lambda_p (\frac{\beta P_p}{P_m})^{2/\alpha} + \lambda_m)) \tag{8.5}$$

$$f_R^p(r) = \frac{2\pi\lambda_p}{A_p} r \exp(-\pi r^2 (\lambda_m (\frac{P_m}{P_p})^{2/\alpha} + \lambda_p)) \tag{8.6}$$

$$f_R^{RE}(r) = \frac{2\pi\lambda_p}{A_{RE}} r \{\exp(-\pi r^2 (\lambda_m (\frac{P_m}{\beta P_p})^{2/\alpha} + \lambda_p)) - \exp(-\pi r^2 (\lambda_m (\frac{P_m}{P_p})^{2/\alpha} + \lambda_p))\} \tag{8.7}$$

where

$$A_m = (1 + \frac{\lambda_p (p_p \beta)^{2/\alpha}}{\lambda_m (p_m)^{2/\alpha}})^{-1} \tag{8.8}$$

$$A_p = (1 + \frac{\lambda_m (p_m)^{2/\alpha}}{\lambda_p (p_p)^{2/\alpha}})^{-1} \tag{8.9}$$

$$A_{RE} = 1 - (1 + \frac{\lambda_p (p_p \beta)^{2/\alpha}}{\lambda_m (p_m)^{2/\alpha}})^{-1} - (1 + \frac{\lambda_m (p_m)^{2/\alpha}}{\lambda_p (p_p)^{2/\alpha}})^{-1} \tag{8.10}$$

8.2. Downlink Outage Probability

In this section, the downlink outage probabilities of macro UEs, pico UEs, and RE UEs on ABS and non-ABS are derived. The SINR of a UE at a distance of R from its serving eNB can be expressed as:

$$SINR = \frac{P_j h_j R_j^{-\alpha}}{\sum_{i \in \Omega, i \neq j} P_i g_i R_i^{-\alpha} + \sigma^2} \tag{8.11}$$

where Ω is the set of interferers eNBs, P_j and P_i are the transmission powers of the serving eNB_j and interferer eNB_i, respectively. h_j and g_i are the fast fading power gains from the serving eNB and interferer eNB, respectively, and σ^2 is noise power.

The outage probability, O_k, represents a probability that SINR is less than an outage threshold, γ_0, which means the rate supported by the random fading channel is less than the threshold value for the UE to function appropriately. The outage probability for a typical UE_k at a distance r from its serving eNB_j is formulated as:

$$O_k \triangleq \mathbb{E}_r[\mathbb{P}[SINR_k(r) \le \gamma_0]\} \tag{8.12}$$

In HetNet, it can be assumed that the density of eNB is usually high which results in an increase of interference power such that the interference power can dominate thermal noise. Therefore, by ignoring thermal noise (interference limited scenario, $\sigma^2 \to 0$), the outage probability for each region can be defined as follows when the ABS scheme is considered. Based on (8.12), the outage probability of UEs in each region on non-ABS and ABS is derived as follows when ABS scheme is applied.

1) Outage probability of RE UE on non-ABSs: Given that a RE UE is associated with tier 2 and based on the definition of PPP, the outage probability is given by (8.13) when there are macro and pico interferers around a randomly selected RE UE:

$$\begin{aligned} O_{RE}^{N_s-N_a} &= 1-\mathbb{P}_{\mathrm{RE}}\{SIR > \gamma_0\} \\ &= 1-\int_0^\infty \mathbb{P}\{\frac{P_p h r^{-\alpha}}{I_p + I_M} > \gamma_0\} f_r^{RE}(r)\, dr \end{aligned} \tag{8.13}$$

where N_s and N_a are the total number of subframes in a frame and number of ABS, respectively. I_p and I_M represent the interferences from pico eNBs and macro eNBs, respectively. Using the fact h follows an exponential distribution with mean of one (i.e., $h \sim \exp(1)$), the outage probability can be expressed as:

$$O_{RE}^{N_s-N_a} = 1-\int_0^\infty \mathbb{E}_I\{\exp(\frac{-\gamma_0 r^{-\alpha}}{P_p}(I_p + I_M))\}\, f_R^{RE}(r)\, dr \tag{8.14}$$

The inner probability from (8.14) can be calculated as:

$$\mathbb{E}_I\{P\{\frac{P_p h r^{-\alpha}}{I_p + I_M} > \gamma_0\}$$

$$= \mathbb{E}_I\{P\{h > \frac{\gamma_0(I_p + I_M)}{P_p r^{-\alpha}}\}\}$$

$$= \mathbb{E}_I\{\exp(\frac{-\gamma_0 r^\alpha}{P_p}(I_p + I_M))$$

$$= \mathbb{E}_{I_p}\{\exp(\frac{-\gamma_0 r^\alpha}{P_p} I_p)\}\, \mathbb{E}_{I_M}\{\exp(\frac{-\gamma_0 r^\alpha}{P_p} I_M)\}$$

$$\overset{(a)}{=} \mathcal{L}_{I_p}\{\frac{-\gamma_0 r^\alpha}{P_p} I_p\}\, \mathcal{L}_{I_M}\{\frac{-\gamma_0 r^\alpha}{P_p} I_M\} \tag{8.15}$$

where (a) is obtained through the Laplace transform in [134],

$$\mathcal{L}_{I_p}\{\exp(\frac{-\gamma_0 r^\alpha}{P_p} I_p\} = \exp(-\pi r^2 \lambda_p \rho(\gamma_0, \alpha, 1)) \tag{8.16}$$

$$\mathcal{L}_{I_M}\{\exp(\frac{-\gamma_0 r^\alpha}{P_p} I_M\} = \exp(-\pi r^2 \lambda_m (\frac{P_m}{P_p})^{2/\alpha} \rho(\gamma_0, \alpha, 1/\beta)) \tag{8.17}$$

where

$$\rho(\gamma, \alpha, \beta) = (\gamma)^{2/\alpha} \int_{(\beta/\gamma)^{2/\alpha}}^{\infty} (\frac{1}{1 + x^{\alpha/2}}) dx \tag{8.18}$$

The proof of Laplace transform of I_M is provided in below:

$$\mathcal{L}_{I_M}(s) \overset{\Delta}{=} \exp(-\lambda \int (1 - f(x)).dx)$$

$$= \exp(-2\pi\lambda \int_{r/k_2}^{\infty} (1 - \frac{1}{1 + sP_m\, v^{-\alpha}}) v.dv \tag{8.19}$$

By replacing $s = \gamma_0 (P_p)^{-1} r^\alpha$,

$$\exp(-2\pi\lambda \int_{r/k_2}^{\infty} (1 - \frac{1}{1 + \gamma_0 (\frac{P_m}{P_p}) r_x^\alpha v^{-\alpha}}) v\, dv$$

$$= \exp(-\pi\lambda \int_{r/k_2}^{\infty} (\frac{(\frac{P_m}{P_p})}{\gamma_0(\frac{P_m}{P_p}) + (v/r)^{\alpha}}) v\, dv$$

$$= \exp(-\pi\lambda \int_{r/k_2}^{\infty} (\frac{1}{1 + (\frac{v}{r(\gamma_0(\frac{P_m}{P_p}))^{1/\alpha}})^{\alpha}}) v\, dv \quad (8.20)$$

Employing a change of variable $u = (\frac{v}{r\,(\gamma_0 \frac{P_m}{P_p})^{1/\alpha}})^2$ and plugging $k_2 = (\beta\, P_p / P_m)^{1/\alpha}$ into (8.20) results in

$$\mathcal{L}_{I_M}\{\frac{-\gamma_0 r}{P_p} I_M\} = \exp(-\pi\lambda_m r^2 (\frac{P_m}{P_p})^{2/\alpha} \rho(\gamma_0, \alpha, 1/\beta)) \quad (8.21)$$

The similar method is used to find the I_p.

Plugging (8.15), (8.16), (8.17), (8.18) and (8.21) into (8.14), the outage probability of a UE on non-ABS is obtained:

$$O_{RE}^{N_s - N_a} = 1 - \frac{\lambda_p}{A_{RE}} \left(\frac{1}{\lambda_p\,(1 + \rho(\gamma_0, \alpha, 1)) + \lambda_m ((\frac{P_m}{\beta\, P_p})^{2/\alpha} + (\frac{P_m}{P_p})^{2/\alpha} \rho(\gamma_0, \alpha, 1/\beta))} - \frac{1}{\lambda_p (1 + \rho(\gamma_0, \alpha, 1)) + \lambda_m (\frac{P_m}{P_p})^{2/\alpha} (1 + \rho(\gamma_0, \alpha, 1/\beta))} \right) \quad (8.20)$$

2) Outage probability of RE UE on ABSs: Since RE UEs are only scheduled on ABS, there is no interference from macro eNB (I_m) . Therefore, only the interference term from other pico eNBs (I_p) that schedule its RE UEs on ABSs is considered. Consequently, for a typical RE UE associated with tier 2 based on definition of PPP, the outage probability on ABS is given by:

$$O_{RE}^{N_a} = 1 - \int_0^{\infty} \mathbb{P}\{\frac{P_p h r^{-\alpha}}{I_p} > \gamma_0\}\, f_R^{RE}(r)\, dr$$

$$= 1 - \frac{\lambda_p}{A_{RE}} \left(\frac{1}{\lambda_p (1 + \rho(\gamma_0, \alpha, 1)) + \lambda_m \left(\frac{P_m}{\beta P_p} \right)^{2/\alpha}} - \frac{1}{\lambda_p (1 + \rho(\gamma_0, \alpha, 1)) + \lambda_m \left(\frac{P_m}{P_p} \right)^{2/\alpha}} \right) \quad (8.21)$$

3) Outage probability of macro UE on non-ABSs: The macro UE's outage probability on non-ABS is given by:

$$O_m^{Ns-N_a} = 1 - \int_0^\infty \mathbb{P}\left\{ \frac{P_m h r^{-\alpha}}{I_p + I_M} > \gamma_0 \right\} f_R^m(r)\, dr$$

$$= 1 - \frac{\lambda_m}{A_m} \left(\frac{1}{\lambda_m (1 + \rho(\gamma_0, \alpha, 1)) + \lambda_p \left(\left(\frac{\beta P_p}{P_m} \right)^{2/\alpha} + \left(\frac{P_p}{P_m} \right)^{2/\alpha} \rho(\gamma_0, \alpha, \beta) \right)} \right) \quad (8.22)$$

4) Outage probability of pico UE on non-ABSs: the outage probability of a random selected pico UE on non-ABS is derived as follows:

$$O_p^{Ns-N_a} = 1 - \int_0^\infty \mathbb{P}\left\{ \frac{P_p h r^{-\alpha}}{I_p + I_M} > \gamma_0 \right\} f_R^p(r)\, dr$$

$$= 1 - \frac{\lambda_p}{A_p} \left(\frac{1}{\lambda_p (1 + \rho(\gamma_0, \alpha, 1)) + \lambda_m \left(\frac{P_m}{P_p} \right)^{2/\alpha} (1 + \rho(\gamma_0, \alpha, 1/\beta))} \right) \quad (8.23)$$

The total outage probability when a UE is located in the pico basic coverage area or the range expanded area is given by (8.24) when the ABS scheme is applied:

$$O_P^T = \frac{A_p}{A_p + A_{RE}} O_p^{N_s - N_a} + \frac{A_{RE}}{A_p + A_{RE}} \left((1 - \eta) O_{RE}^{N_s - N_a} + \eta\, O_{RE}^{N_a} \right) \quad (8.24)$$

In this paper, the ratio of RE UE scheduled on ABS to RE UE scheduled on non-ABS is represented as η where $0 \leq \eta \leq 1$. For a specified η, the suitable offset value can be obtained under a constraint as follows:

$$O_P^T \leq O_T \quad (8.25)$$

where O_T is an acceptable outage probability for the UE served by pico eNB. Based on (8.24) and (8.25), the maximum and minimum outage probability for picocell can be calculated by setting η=0 and η=1, respectively:

$$O_P^{\min} \le O_P^T \le O_P^{\max} \tag{8.26}$$

where

$$O_P^{\max} = \frac{A_p}{A_p + A_{RE}} O_p^{N_s - N_a} + \frac{A_{RE}}{A_p + A_{RE}} O_{RE}^{N_s - N_a} \tag{8.27}$$

$$O_P^{\min} = \frac{A_p}{A_p + A_{RE}} O_p^{N_s - N_a} + \frac{A_{RE}}{A_p + A_{RE}} O_{RE}^{N_a} \tag{8.28}$$

8.3. Average Ergodic Rate

In this section, the average ergodic rate is derived for a random UE in each tier in order to obtain the required number of ABS and non-ABS. The average ergodic rate is calculated with a similar method as the outage probability in Section 8.2. The unit of average ergodic rate is assumed as nats/sec/Hz (1bit=ln(2)=0.693 nats) to simplify the analysis. The general result of average ergodic rate of a UE at distance r from its serving eNB$_j$ in the downlink is derived as [133-134]:

$$\begin{aligned}
\tau(\lambda,\alpha) &\overset{\Delta}{=} \mathbb{E}[\ln(1+SINR)] \\
&= \int_{r>0}^{\infty} \mathbb{E}[\ln(1+SINR(r)]\, f_R^l(r) dr \\
&= \int_{r>0}^{\infty} \int_{t>0}^{\infty} \mathbb{P}[\ln(\frac{P_j h r^{-\alpha}}{I_p + I_M}) > t]\, dt\, f_R^l(r)\, dr \\
&= \int_{r>0}^{\infty} \int_{t>0}^{\infty} \mathbb{P}[h > \frac{r^{\alpha}}{P_j}(I_p + I_M)(e^t - 1)]\, dt\, f_R^l(r)\, dr \\
&= \int_{r>0}^{\infty} \int_{t>0}^{\infty} \mathcal{L}_{I_p}[\frac{r^{\alpha}}{P_j}(e^t - 1) I_p]\, \mathcal{L}_{I_M}[\frac{r^{\alpha}}{P_j}(e^t - 1) I_M]\, dt\, f_R^l(r)\, dr
\end{aligned} \tag{8.29}$$

where $j=\{p, m\}$ and $l=\{p, m, RE\}$. Now the ergodic rates are calculated for UEs located in the basic coverage area of macro eNB, basic coverage area of pico eNB, and range expanded area of pico eNB when ABS scheme is used to mitigate interference.

1) Average ergodic rate of RE UE on non-ABSs: the average ergodic rate of a typical UE in the range expanded area is given by (8.30) when it is scheduled on non-ABS.

$$E_{RE}^{N_s-N_a} = \int_{r>0}^{\infty} \int_{t>0}^{\infty} P[\ln(\frac{P_p h r^{-\alpha}}{I_p + I_M}) > t]\, dt\, f_R^{RE}(r)\, dr$$

$$= \int_{r>0}^{\infty} \int_{t>0}^{\infty} \mathcal{L}_{I_p}[\frac{r^{\alpha}}{P_p}(e^t-1)I_p]\, \mathcal{L}_{I_M}[\frac{r^{\alpha}}{P_p}(e^t-1)\, I_M]\, dt\, f_R^{RE}(r)\, dr \tag{8.30}$$

where

$$\mathcal{L}_{I_p}\{\frac{-(e^t-1)\, r^{\alpha}}{P_p} I_p\} = \exp(-\pi r^2 \lambda_p \rho((e^t-1),\alpha,1)) \tag{8.31}$$

$$\mathcal{L}_{I_M}\{\frac{-(e^t-1)\, r^{\alpha}}{P_p} I_M\} = \exp(-\pi r^2 \lambda_m (\frac{P_m}{P_p})^{2/\alpha} \rho((e^t-1),\alpha,1/\beta)) \tag{8.32}$$

plugging (8.31) and (8.32) into (8.30), the average ergodic rate of a UE on non-ABS is obtained:

$$E_{RE}^{N_s-N_a} = \int_{t>0}^{\infty} \frac{\lambda_p}{A_{RE}} \Big(\frac{1}{\lambda_p(\rho((e^t-1),\alpha,1)+1) + \lambda_m((\frac{P_m}{P_p})^{2/\alpha}\rho((e^t-1),\alpha,1/\beta) + (\frac{P_m}{\beta P_p})^{2/\alpha})} - \frac{1}{\lambda_p(\rho((e^t-1),\alpha,1)+1) + \lambda_m(\frac{P_m}{P_p})^{2/\alpha}(\rho((e^t-1),\alpha,1/\beta)+1)} \Big) dt \tag{8.33}$$

In the particular case of α=4,

$$\rho((e^t-1),4,\beta) = (e^t-1)^{1/2} \int_{(\beta/(e^t-1))^{1/2}}^{\infty} (\frac{1}{1+x^2}) dx = \sqrt{(e^t-1)}\, \tan^{-1}(\sqrt{(e^t-1)/\beta}) \tag{8.34}$$

As a result, the average ergodic rate can be expressed to a single simple numerical integration as follows:

$$E_{RE}^{N_s-N_a} = \frac{\lambda_p}{A_{RE}} \int_{t>0}^{\infty} \left(\frac{1}{\lambda_p \left(1+\sqrt{(e^t-1)}\tan^{-1}\left(\sqrt{(e^t-1)}\right)\right) + \lambda_m \left(\left(\frac{P_m}{P_p}\right)^{2/\alpha}\sqrt{(e^t-1)}\tan^{-1}\left(\sqrt{\beta(e^t-1)}\right) + \left(\frac{P_m}{\beta P_p}\right)^{2/\alpha}\right)} - \frac{1}{\lambda_p \left(\sqrt{(e^t-1)}\tan^{-1}\left(\sqrt{(e^t-1)}\right)+1\right) + \lambda_m \left(\frac{P_m}{P_p}\right)^{2/\alpha}\left(\sqrt{(e^t-1)}\tan^{-1}\left(\sqrt{\beta(e^t-1)}\right)+1\right)} \right) dt \quad (8.35)$$

2) Average ergodic rate of RE UE on ABSs: Given that a RE UE is associated with tier 2, the average ergodic rate of a typical RE UE on ABS is expressed by:

$$E_{RE}^{N_a} = \int_{r>0}^{\infty}\int_{t>0}^{\infty} P\left[\ln\left(\frac{P_p h r^{-\alpha}}{I_p}\right) > t\right] dt\, f_R^{RE}(r)\, dr$$

$$= \frac{\lambda_p}{A_{RE}} \int_{t>0}^{\infty} \left(\frac{1}{\lambda_p \left(1+\sqrt{(e^t-1)}\tan^{-1}\left(\sqrt{(e^t-1)}\right)\right) + \lambda_m \left(\frac{P_m}{\beta P_p}\right)^{2/\alpha}} - \frac{1}{\lambda_p \left(\sqrt{(e^t-1)}\tan^{-1}\left(\sqrt{(e^t-1)}\right)+1\right) + \lambda_m \left(\frac{P_m}{P_p}\right)^{2/\alpha}} \right) dt \quad (8.36)$$

3) Average ergodic rate of macro UE on non-ABSs: The average ergodic rate of a macro UE scheduled on non-ABS is derived from (8.37):

$$E_m^{N_s-N_a} = \int_{r>0}^{\infty}\int_{t>0}^{\infty} P\left[\ln\left(\frac{P_m h r^{-\alpha}}{I_p + I_M}\right) > t\right] dt\, f_R^{m}(r)\, dr$$

$$= \frac{\lambda_m}{A_m} \int_{t>0}^{\infty} \left(\frac{1}{\lambda_m \left(1+\sqrt{(e^t-1)}\tan^{-1}\left(\sqrt{(e^t-1)}\right)\right) + \lambda_p \left(\left(\frac{P_p}{P_m}\right)^{2/\alpha}\sqrt{(e^t-1)}\tan^{-1}\left(\sqrt{(e^t-1)/\beta}\right) + \left(\frac{\beta P_p}{P_m}\right)^{2/\alpha}\right)} \right) dt \quad (8.36)$$

4) Average ergodic rate of pico UE on non-ABSs: for a typical UE located in the basic coverage area of pico eNB, the average ergodic rate on non-ABS can be given by:

$$E_p^{N_s-N_a} = \int_{r>0}^{\infty} \int_{t>0}^{\infty} P[\ln(\frac{P_p h\, r^{-\alpha}}{I_p + I_M}) > t]\, dt\, f_R^p(r)\, dr$$

$$= \frac{\lambda_p}{A_p} \int_{t>0}^{\infty} \left(\frac{1}{\lambda_p (1+\sqrt{(e^t-1)}\tan^{-1}(\sqrt{(e^t-1)})) + \lambda_m (\frac{P_m}{P_p})^{2/\alpha} (\sqrt{(e^t-1)}\tan^{-1}(\sqrt{\beta(e^t-1)})+1)} \right) dt \tag{8.37}$$

8.4. Required Number of ABS and non-ABS

When a small number of ABS is used, more non-ABS are assigned to macro UEs while the number of ABSs that can be allocated to RE UEs is small. Consequently, the data rate of macro UEs increases while the data rate of RE UEs is degraded. In contrast, if the number of ABS increases, the number of non-ABS that can be allocated to macro UE decreases and the number of ABS assigned to RE UEs will increase. Since the macro eNB transmission is muted on the ABSs, the interference decreases which can lead to an increase of the RE UE's data rate at the expense of reduction of macro UE's data rate. It can be concluded that there is a trade-off between macro UE and RE UEs' data rates when ABS scheme is applied. The number of required ABS and non-ABS are derived while the minimum required data rate of UE per tier is satisfied. For this purpose, it is assumed that the equal time slots are allocated to each UE on a round robin basis by the scheduler. In this scenario, the RE UE can be scheduled on both ABS and non-ABS while pico and macro UEs have only access to non-ABS. The average ergodic rates for all regions are given as:

$$\tau_{RE}(\lambda_p, \alpha) = (\frac{N_s - N_a}{N_s})\, E_{RE}^{N_s-N_a}(\lambda_p, \alpha) + (\frac{N_a}{N_s})\, E_{RE}^{N_a}(\lambda_p, \alpha) \tag{8.38}$$

$$\tau_p(\lambda_p, \alpha) = (\frac{N_s - N_a}{N_s})\, E_p^{N_s-N_a}(\lambda_p, \alpha) \tag{8.39}$$

$$\tau_m(\lambda_m,\alpha)=(\frac{N_s-N_a}{N_s})\,E_m^{N_s-N_a}(\lambda_m,\alpha) \tag{8.40}$$

The average data rate of UEs located in each region can be defined as:

$$\overline{\tau_{RE}}(\lambda_p,\alpha)=\frac{\tau_{RE}(\lambda_p,\alpha)}{N_{RE}} \tag{8.41}$$

$$\overline{\tau_p}(\lambda_p,\alpha)=\frac{\tau_p(\lambda_p,\alpha)}{N_p} \tag{8.42}$$

$$\overline{\tau_m}(\lambda_m,\alpha)=\frac{\tau_m(\lambda_m,\alpha)}{N_m} \tag{8.43}$$

In order to satisfy the minimum required data rate for UEs in each tier, the constraints on the average user data rate of each tier are given by,

$$\begin{cases}\overline{\tau}_{RE}\geq\theta_{RE}\\ \overline{\tau}_{p}\geq\theta_{p}\\ \overline{\tau}_{m}\geq\theta_{m}\end{cases} \tag{8.44}$$

where θ_{RE}, θ_p and θ_m are the minimum required data rate for each region with units nats/sec/Hz. Plugging (8.41), (8.42), and (8.43) into (8.44), three limitations on required number of ABS and non-ABS are obtained. Finally, the minimum value of (N_a)s is selected as the number of ABSs.

$$N_a\geq\min(\max(\left\lceil\frac{N_{RE}\theta_{RE}-E_{RE}^{N_s-N_a}}{E_{RE}^{N_a}-E_{RE}^{N_s-N_a}}N_s\right\rceil,0),N_s) \tag{8.45}$$

$$N_a\leq\min(\max(\left\lceil(1-\frac{N_p\theta_p}{E_p^{N_s-N_a}})N_s\right\rceil,0),N_s) \tag{8.46}$$

$$N_a \le \min(\max(\left\lceil (1-\frac{N_m\theta_m}{E_m^{N_s-N_a}})N_s \right\rceil,0), N_s) \tag{8.47}$$

where $\lceil x \rceil$ means the smallest integer greater than x.

8.5. Results and Discussions

In this section, results are shown using simulation where eNBs and UEs are deployed in each tier based on the given model in Section 8.1. The simulation parameters were given based on parameters specified in Chapter 2. In addition, the required simulation parameters specified for this chapter are given in Table 8.1 [17].

Table 8.1.Simulation Parameters

Parameter	Value	Parameter	Value
Carrier frequency	2 GHz	Pathloss α	4
Carrier bandwidth	5MHz	Macro eNB intensity λ_m	$10^{-5}m^{-2}$

8.5.1. Outage Probability and Offset Value

An expression for outage probability of picocell is derived with respect to offset value and pico eNB density. The variation of outage probabilities for picocell with the density of $\lambda_p=4\lambda_m$ for different offset values are shown in Figure 8.2. The pathloss exponent is $\alpha=4$ and the respective outage threshold is set to -5 dB. This figure shows the outage probability of picocell decreases when η increases. The reason is that when η increases, more RE UE are scheduled on ABS. Moreover, the maximum outage probability demonstrates that all RE UE are scheduled on non-ABSs while the minimum outage probability is achieved if all RE UE are scheduled on ABS. This is because when RE UEs are scheduled on non-ABS, these RE UEs suffer severe interference from macro eNB which leads to a decrease of their SINR. On the other hand, when RE UEs are only scheduled on ABS, there is a minimal interference and hence the UE experiences very good link quality. However, if more ABSs are used for RE UE, the number of non-ABS that can be allocated to macro UE will decrease which can lead to a reduce of macro UE throughput.

In order to study the effect of density of pico tiers, the outage probability of picocell is shown for η =0.4 and different λ_p in Figure 8.3. When the density of picocell increases, the outage probability of picocell is reduced. The average load per picocell decreases which results in a decrease of interference.

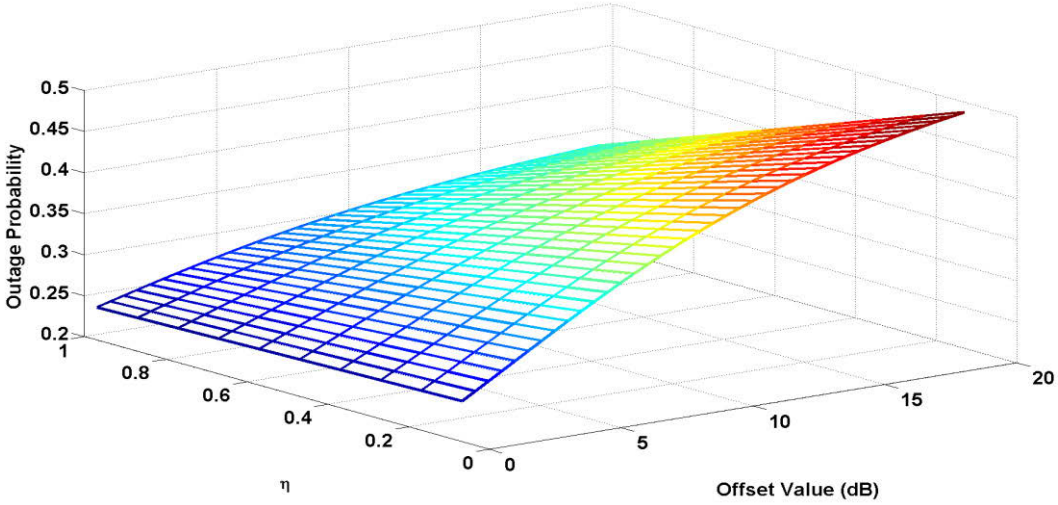

Figure 8.2. Outage probability of picocell for different η

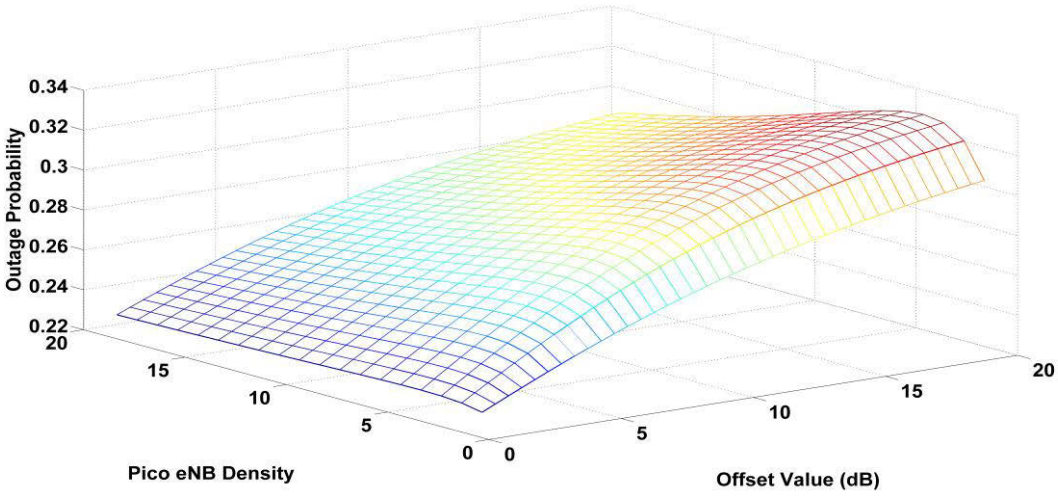

Figure 8.3. Outage probability for UEs connected to pico tier

Table 8.2 illustrates the maximum offset value that can be used to maintain the system under the desired outage probability (O_T) using (8.25). For example, when all RE UEs are scheduled on non-ABS (η=0), the maximum offset value can be set to 3.22 dB and 7.70 dB for O_T =0.3 and O_T =0.4, respectively. Moreover, for η=1, there is no limitation on offset value and then the maximum offset value (i.e., 20 dB) can be used for O_T =0.4.

Therefore, it can be concluded that when the RE UEs are scheduled on non-ABS, small offset value must be used to keep the outage under the threshold while by scheduling RE UEs on ABS larger offset value can be deployed and hence more UEs can be offloaded to picocells.

Table 8.2. Maximum Allowable Offset Value (dB) for Different Desired Outage Probability (λ_p=4 λ_m)

O_T \ η	**0**	**0.2**	**0.4**	**0.6**	**0.8**	**1**
0.3	3.22	3.61	4.47	5.44	7.24	11.81
0.4	7.70	9.08	11.39	16.17	No Limitation	No Limitation

8.5.2. Required Number of ABSs

As discussed in Section 8.4, there is a trade-off between macro UE and RE UEs' data rate when ABS scheme is applied, and therefore, the data rate of each tier should be consider to obtain the ABS number. Figures 8.4 demonstrates the number of ABS derived by (41), (42) and (43) for different offset values, λ_p and λ_u. It is assumed that $\theta_{RE}=\theta_p=\theta_m=\theta$ to simplify the figure descriptions. In the following figures, four different curves are used defining as follows:

1. The maximum number of ABSs allowed by macrocell is defined as the maximum number of subframes that macrocell can be muted on them and hence pico eNBs can use them as ABSs.

2. The maximum number of ABSs allowed by picocell demonstrates the maximum number of subframes that picocell does not schedule the pico UE on them and then these subframes can be used as ABSs for scheduling RE UEs. Note that it is assumed that the UE located in the basic coverage area of picocell are only scheduled on non-ABS.

3. The required number of ABS represents the number of ABS that is needed for scheduling REUE in order to satisfy the θ_{RE} in (8.44).

4. Number of the allocated ABSs which is the minimum N_a obtained by (8.45), (8.46) and (8.47) and illustrates the number of ABS that can be used in the network to satisfy the required UE's data rate in all tiers. Since there are 10 subframes in each frame, then the ABS is a factor of 10.

As shown in Figure 8.4 (a), for $\lambda_u=4\times10^{-4}$ m^{-2}, the maximum number of ABSs allowed by macrocell increases by increasing the offset value because the number of UE connected to the macro eNB decreases and hence smaller number of non-ABS is needed to support macro UEs. Moreover, since the number of UE located in basic coverage area of picocell is usually fixed, the number of non-ABS required for pico UE remains fixed or change in a narrow range. However, the increase of offset value leads to increase of number of RE UEs offloaded to picocell. As a result, more ABSs are required to support the RE UEs. Since the required number of ABS is smaller than the maximum ABS allowed by picocell and macrocell, the number of the allocated ABSs is same as required number of ABS. By increasing the number of UEs (i.e., $\lambda_u=6\times10^{-4}$ m^{-2}), more UEs will be located in each tier, therefore, the maximum numbers of ABSs allowed by picocell and macrocell decrease because picocell and macrocell need more non-ABSs to schedule UEs. In contrast, the required number of ABSs for RE UEs increases. Consequently, more ABSs are allocated to RE UEs as shown in Figure 8.4 (b). For large offset value, the maximum number of ABS permitted by macrocell and picocell is less than the required number of ABSs. Therefore, the number of the allocated ABSs is limited by macrocell and picocell.

In order to investigate the effect of θ, the results for θ=0.027 nats/sec/Hz are shown in Figures 8.4 (c) and (d). Based on these figures, more ABS and non-ABS are needed to satisfy the required θ. For small offset value, the required number of ABSs is limited by the maximum number of ABS allowed by macrocell. Moreover, for the large offset value, the number of the allocated of ABS will be truncated by picocell. It can be concluded that the requirements of pico UE and macro UE are important factors to obtain the ABS. Figures 8.5 (a) and (b) depict the effect of picocell density on number of ABSs. When the density of picocell increases, the average load in each cell is reduced which results in decrease of the number of non-ABSs required for pico UE and macro UE. Moreover, the average number of RE UE offloaded to each picocell is also reduced which leads to decrease of the required number of ABS.

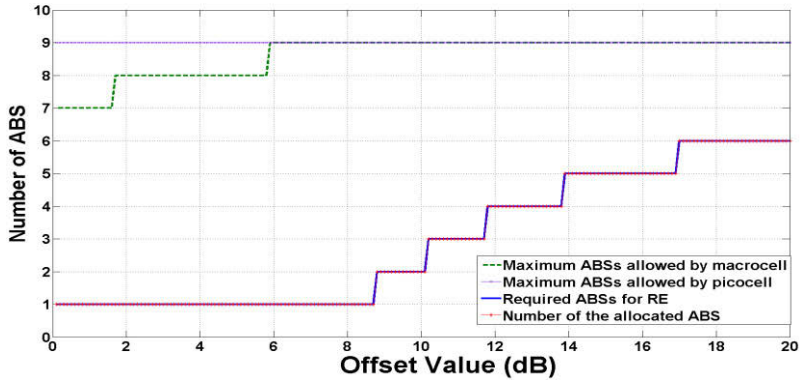

(a) λ_u= 4×10^{-4} m^{-2}, θ_{RE}=θ_p=θ_m=0.013 nats/sec/Hz

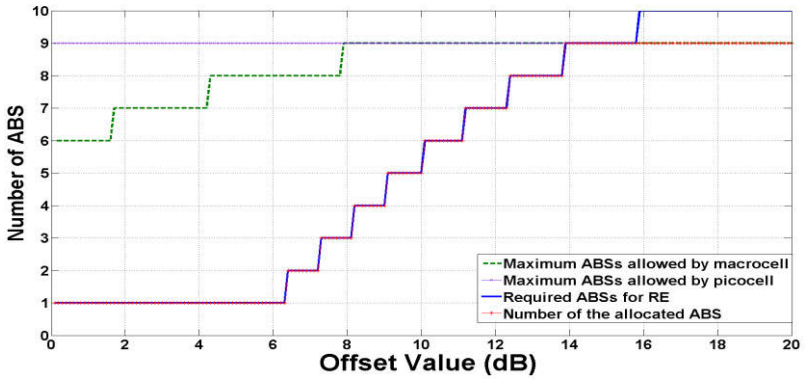

(b) λ_u= 6×10^{-4} m^{-2}, θ_{RE}=θ_p=θ_m=0.013 nats/sec/Hz

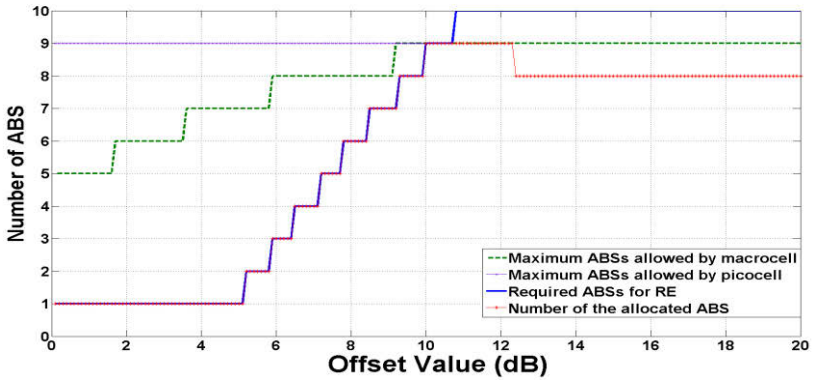

(c) λ_u= 4×10^{-4} m^{-2}, θ_{RE}=θ_p=θ_m=0.027 nats/sec/Hz

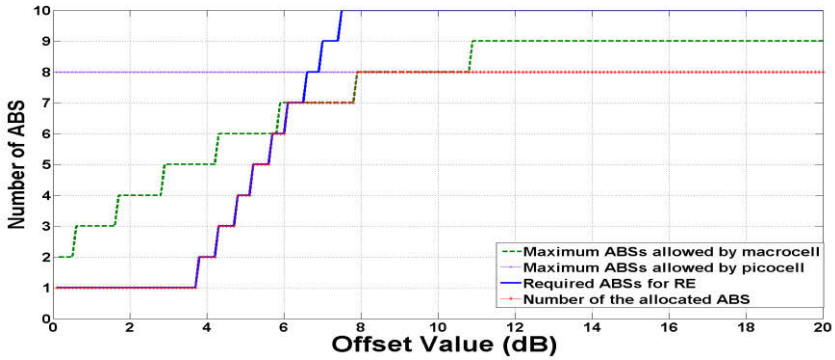

(d) λ_u= 6×10^{-4} m^{-2}, θ_{RE}=θ_p=θ_m=0.027 nats/sec/Hz

Figure 8.4. Number of ABS for different offset values when λ_p=4 λ_m

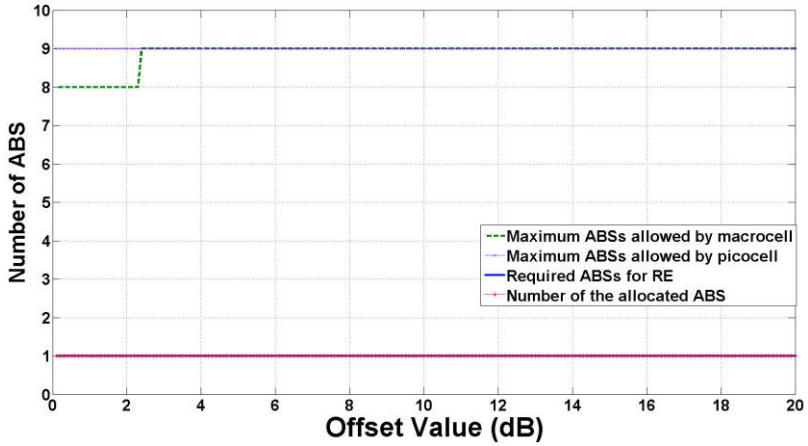

(a) $\lambda_u = 4\times10^{-4}$ m^{-2}, $\theta_{RE}=\theta_p=\theta_m=0.013$ nats/sec/Hz

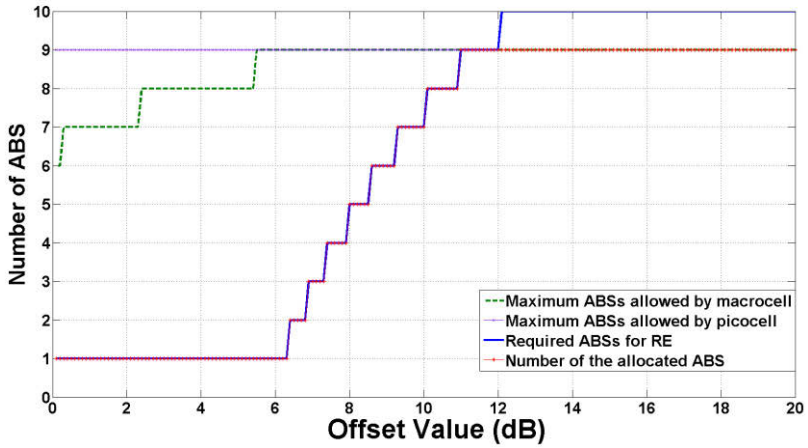

(b) $\lambda_u = 4\times10^{-4}$ m^{-2}, $\theta_{RE}=\theta_p=\theta_m=0.027$ nats/sec/Hz

Figure 8.5. Number of ABS for different offset values when $\lambda_p=10\ \lambda_m$

8.5.3. Result Comparison

This sub-section compares the scheme proposed in this chapter with algorithm in [132], represented as 'Literature', where the number of the allocated ABS was calculated based on the outage throughputs of RE UE on ABS and non-ABSs.

Figure 8.6 (a) shows that the proposed scheme selected larger ABS values when the offset value increased while [132] allocated the same ABS value for offset values greater than 6 dB. By increasing θ form 0.013 nats/sec/Hz to 0.027 nats/sec/Hz, the number of the allocated ABS value increases in both schemes as shown in Figure 8.6 (b). However, algorithm in [132] assigned all subframes as ABS when the offset value becomes greater than 14 dB.

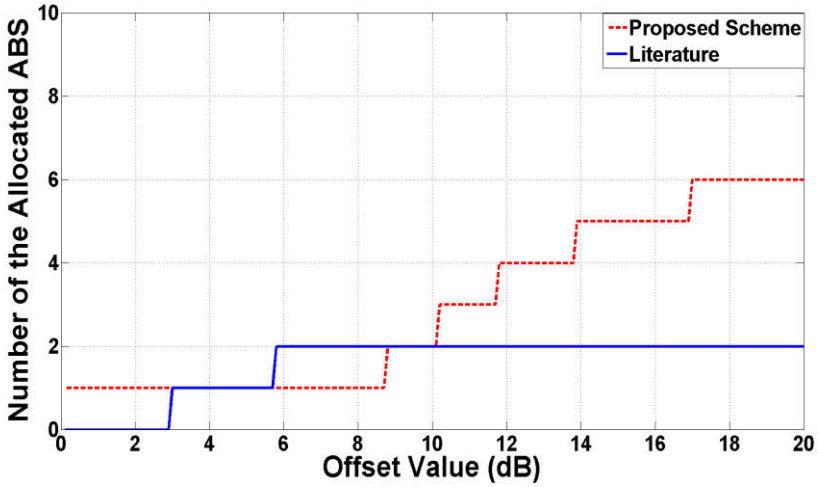

(a) $\lambda_u = 4\times10^{-4}$ m^{-2}, $\theta_{RE}=\theta_p=\theta_m=0.013$ nats/sec/Hz

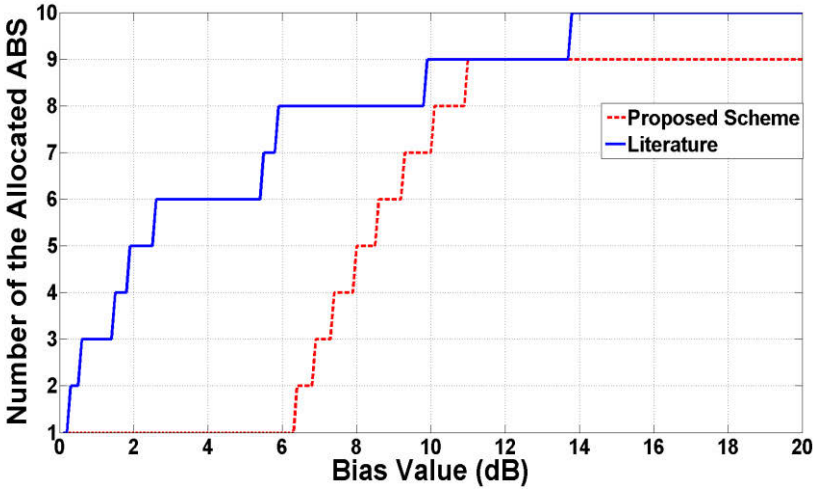

(b) $\lambda_u = 4\times10^{-4}$ m^{2}, $\theta_{RE}=\theta_p=\theta_m=0.027$ nats/sec/Hz

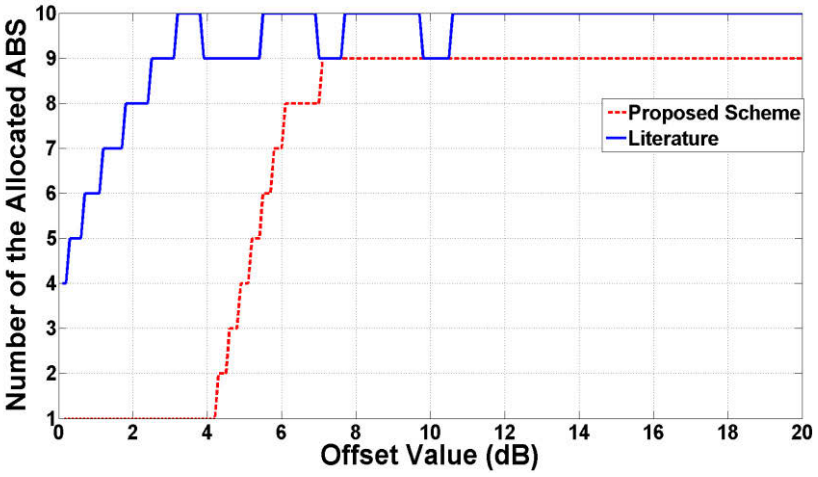

(c) $\lambda_u = 6\times10^{-4}$ m^{2}, $\theta_{RE}=\theta_p=\theta_m=0.027$ nats/sec/Hz

Figure 8.6. Number of ABS for different schemes when $\lambda_p=4\,\lambda_m$

This is because [132] did not consider the requirements of UE located in the macro coverage area and the pico basic coverage area. Therefore, the macro eNB and pico eNB cannot transmit any data to macro UEs and pico UEs. Since the proposed scheme in this chapter is based on the ergodic rate of all UEs in all coverage areas, 9 subframes are used as ABS for larger offset values and 1 subframe is labelled as non-ABS for macro UEs and pico UEs. The scheme proposed in [132] will be more underutilized when the UE density increases. As shown in Figure 8.6 (c), [132] marked all subframes as ABSs. However, the proposed scheme always reserved some of subframes for non-ABS to support UEs located in macro coverage area and pico basic coverage area.

Table 8.3. Throughput Comparison between the Proposed Scheme and [132] in Literature for $\lambda_u = 4\times10^{-4}$ m^2, $\theta_{RE}=\theta_p=\theta_m=0.027$ nats/sec/Hz

Scheme	Offset Value	ABS Value	RE UE Throughput (kbps)	Macro UE Throughput (kbps)	Average UE Throughput (kbps)
Proposed Scheme	9 dB	6	227.6	159.49	156.78
Ref. [132]		8	377.1	141.57	140.57
Proposed Scheme	12 dB	9	380.4	177.42	168.85
Ref. [132]		9	380.4	177.42	168.85
Proposed Scheme	15 dB	9	237.7	208.72	195.92
Ref. [132]		10	493.3	0	0

Based on Table 8.3, the proposed scheme could maintain the balance between UEs better than [132]. For example, the proposed scheme allocated 6 subframes as ABS for offset value of 9 dB while the [132] selected 8 subframes as ABS which causes that the throughput of macro UEs is sacrificed more than the proposed scheme in this chapter. In addition, the proposed scheme set the ABS value to 9 for offset value of 15 dB whereas the algorithm in [132] marked all UEs as ABS. Therefore, the macro eNB cannot send data to macro UE when offset value is 15 dB. Consequently, the proposed scheme could outperform [132] because of considering the ergodic rates of all UEs in all tiers.

8.6. Summary

This chapter provided a mathematically tractable macrocell-picocell heterogeneous network framework to obtain the maximum offset value using the stochastic geometry to reach an acceptable outage probability. Based on the extensive numerical results, it was observed that the number of RE UE scheduled on ABS and non-ABS directly affect the outage probability of picocell. Moreover, this chapter proposed a mathematical method to approximate the number of the ABS in respect to requirements of macro UEs, pico UE and RE UEs when the macrocell and picocells share the bandwidth. The analysis showed that number of UEs, picocell density and system requirements directly affect the number of ABS allocated to RE UEs.

Chapter 9

CONCLUSIONS AND FUTURE RESEARCH DIRECTIONS

This thesis studied intercell interference challenges in LTE and LTE-A systems and a number of contributions were provided in this thesis to improve downlink system performance by mitigating the intercell interference in macrocell-macrocell and macrocell-picocell scenarios. The final chapter summarises the research contributions of this thesis in Section 9.1 and then discusses directions for future relevant research in Section 9.2.

9.1 Summary of Thesis Contributions

The original contributions of this thesis can be divided into three major parts as follows:

9.1.1 Intercell Interference Mitigation in LTE Macrocell-Macrocell Scenario

The intercell interference problem is one of the main challenges in the LTE downlink system. In order to deal with this problem, a novel downlink ICIC scheme for LTE was presented in Chapter 4 to address the first part of research question described in Section 1.4.1 (i.e., How to design a new ICI mitigation schemes to increase the cell throughput, the user throughput and cell-edge throughput in the macrocell-macrocell?).

In this scheme, a dynamic priority based scheme is considered in which the resource allocation for each subband was performed using a user priority that was based on the interference level, Quality of Service and Head of Line delay. UEs could be scheduled based on this priority on the specified sub-bands. Therefore, the network changes and traffic model could be considered in this scheme. In addition, the transmission power of each PRB was dynamically determined through a fuzzy logic system. Consequently, the proposed scheme could jointly optimize PRB and power allocations for each cell, while in the traditional methods, the spectrum allocation or the power allocation is fixed in each cell. In addition, the proposed scheme is a decentralized scheme in which each

eNB specified its PRB allocation and transmission power by exchanging messages with neighbouring eNBs over X2 interface.

Under the assumption described in Chapter 2, the proposed ICIC scheme based on user priority could outperform SFR and RF1 schemes in terms of average system performance around 12% and 28.7% respectively for video streaming traffic. This is because it dynamically adjusts the transmission power of each PRB based on SINR, throughput and achievable data rate through the FLS while the system traffic loads and system changes were taken into account for PRB allocation. Furthermore, the proposed ICIC scheme based on priority obtained higher cell edge user throughput compared to RF1 and SFR schemes.

9.1.2 Intercell Interference Mitigation in Macrocell-Picocell Scenario in LTE-A HetNet

As discussed in Chapter 5, picocell is one of the important low power nodes in HetNet that can be used to enhance the overall system capacity and coverage. However, the transmission power difference between macro eNB and pico eNB results in new challenges in cell selection technique and intercell interference management. Based on these challenges, Chapters 6 and 7 addressed the second goal of the research question: "How to design new ICI mitigation schemes to increase the cell throughput and cell-edge throughput in the macrocell-picocell configurations while decreasing the outage probability?".

In chapter 6, initially, a novel dynamic CRE offset value was proposed to determine the offset value dynamically based on the historical system performance using a fuzzy logic system to control the number of offloaded UEs while the system requirements are satisfied. It was evaluated via system level simulation that the proposed CRE scheme outperformed the static CRE scheme in terms of total throughput. In addition, since the proposed CRE scheme calculated the offset value dynamically based on the throughputs of macro UEs and pico UEs, it could maintain a good trade-off between macro UEs and pico UEs throughputs while the outage probability was maintained at an acceptable level.

At the next step, a new dynamic ABS scheme was suggested to mitigate interference without reducing the throughput of macro UEs when the radio resources were shared between macrocell and picocell. Similar to the proposed CRE scheme, a fuzzy logic system was used to obtain the required ABS value based on the historical system performance. Thereafter, the proposed dynamic CRE offset was combined with the proposed dynamic ABS value scheme for further improvements of the system performance as described in Chapter 6. In this scheme, each macrocell could simultaneously change the ABS and CRE offset values of all picocells under its control to reach the expected system performance. The proposed eICIC scheme was simulated for different membership functions and picocell densities. The simulation result showed that ABS and CRE offset values converged to 40% and 12.62 dB, respectively for membership function represented by Triangular shape for 4 picocells per macrocells and 47% of UEs were offloaded to picocells. By using the Gaussian membership function, the ABS value converged to the same value as Triangular function and the offset value was not much higher than Triangular function. However, by decreasing of number of picocells from four to two, the offset value increased using the proposed eICIC scheme based on FL. In addition, the average throughput of macro UEs was satisfied while the average throughput of RE UE and the outage probability could be maintained within the acceptable range. In addition, by decreasing the picocell density, each picocell served more offloaded UEs which result in a decrease of RE UEs' throughput. In contrast to the proposed schemes in literature, the proposed dynamic eICIC scheme based on FL simultaneously determined both CRE offset value and ABS value. Moreover, the proposed eICIC scheme could maintain a trade-off between macro UE and RE UE throughputs better than other schemes in the literature.

In the proposed eICIC scheme based on fuzzy logic system, it was assumed that all rules are defined using the experience of operator about effects of ABS and CRE offset values on the system performance. In order to evaluate the consequent part of rules, fuzzy logic system was added to q-learning approach and this was known as fuzzy q-learning (FQL) in Chapter 7. It was assumed that there was no prior knowledge (the worst case) and hence all actions were evaluated to find the best consequent parts of rules. Moreover, both full buffer and video streaming traffics were considered in this scheme. The simulation results showed that the ABS value converged to 40% and the CRE offset value converged to 10.87 dB. Based on this offset value, 45.6% of UEs were

offloaded to picocells. Therefore, there was no a significant difference between the proposed scheme using FL and the proposed scheme based on FQL. In contrast to full buffer traffic, the average macrocell throughput decreased by increasing the offset value due to decreasing of the number of UEs. In addition, by increasing the number of UEs, the number of PRB used for scheduling increased which result in an increase of total picocell/macrocell throughputs. The simulation results demonstrated that the proposed eICIC scheme could keep the trade-off between RE UE and macro UE throughputs and satisfy the system requirements for video streaming traffic within an acceptable delay when compared to other static and dynamic schemes.

The proposed schemes only require the information about important downlink metrics which can be measured directly from the system. Therefore, sharing such information in the network does not result in the noticeable overhead. Given such information, each eNB can execute the same algorithms to improve its performance. Moreover, fuzzy logic systems used in the proposed schemes, are simple, flexible, with low complexity and computation. In addition, it works on real time systems and can handle problems with imprecise and incomplete data, and also can model nonlinear functions of arbitrary complexity.

Genetic Algorithm was used to determine the best location of ABSs in each frame. This algorithm aimed to find the optimized solution through recombination and selection strategies without high mathematical computation. The proposed eICIC scheme based on GA considered the macro and pico UE throughputs, interference level, delay and PLR as the objective functions and then combined these objective functions using a weighted sum algorithm. The value obtained from weighted sum algorithm was used as the fitness value for each chromosome. In each iteration, new offsprings were generated through crossover and mutation operators and then the better offsprings is selected as the parents for next generations via a selection method. After several iterations, the best offspring was selected as the ABS configuration. The simulation results demonstrated that the proposed eICIC scheme based on GA could satisfy the requirements of video streaming traffic for different CRE offset values when the macrocell and picocells shared the bandwidth.

9.1.3. Mathematical Analysis of Downlink Intercell Interference in LTE HetNet using Stochastic Geometry

An important contribution of this thesis was the development of a mathematically tractable framework for macrocell-picocell HetNet. Based on the mathematical model, the optimum offset value was obtained for each outage threshold when the ABS scheme was applied. Moreover, the minimum and maximum offset values were formulated. Thereafter, the network model proposed in [133] was extended for a two tier heterogeneous network consisting of pico eNBs and macro eNBs to formulate the number of the required ABSs based on the ergodic rate and the minimum required throughput of UE through stochastic geometry tool. The mathematical expressions were derived for outage probability, offset value and number of ABS with respect to different pico eNB densities, outage threshold and minimum required data rate for each tier. The numerical analysis showed the outage probability of picocell decreased when number of RE UE scheduled on ABS increased due to decrease of interference which result in an increase of the maximum allowable offset value. In addition, the outage probability of picocell decreased when the density of picocells increased because of decrease of the average load per picocell. Moreover, the required data rate of UE located in the macrocell and basic coverage area of picocell affected directly on number of ABSs used by RE UE particularly for higher data rates. Consequently, the requirement of both macro and pico tiers should be considered when the ABS is configured. Simulation results demonstrated that the proposed scheme could outperform the algorithm in [132] in terms UE throughputs in all tiers particularly when higher data rate is required in each tier.

9.2 Future Research Directions

By growing the demand for 4G technology, new features are added to LTE/LTE-A systems to enhance the system performance. However, new challenges could arise by adding new features and hence, new research areas will be open which can be taken into account by researchers. Based on the study of intercell interference challenges in mobile cellular networks, a number of important issues have been identified for future research work. Some of the issues are briefly discussed as follows:

- In HetNet, different types of nodes with different transmission power are deployed and when the number of low power nodes increases, the manual operations may be costly. Therefore, one optimal solution for the radio resource allocation (in same or different bands) can be the autonomous interference management technique which does not need synchronization. Moreover, the amount of information which is exchanged will be minimized by autonomous technique.

- A subsequent interest research area is to consider the interference between uplink and downlink in TDD which occurs between eNB-eNB and UE-UE. Moreover, when different operators use different carriers in the same band or different uplink-downlink configurations, the interference problem can come up in the adjacent channel and co-channel. In addition, the semi static mechanism which has been used to design the uplink-downlink configuration may not be able to track the instantaneous traffic conditions. Therefore, working on the dynamic subframe allocation for uplink and downlink can be another open research area [134-136].

- Due to increasing use of internet and smart devices, the demand for mobile data services with different traffic requirements is dramatically growing. In order to overcome the new demands, the 5G is being developed. The small cells can play an important role to satisfy the 5G requirement such as frequency efficiency, energy reduction and capacity. However, new challenges can arise for interference management in uplink and downlink by introducing the CA, CoMP and direct communication among UEs (D2D communication). Therefore, the development of new interference management techniques that can overcome these crucial challenges will be a subject in future studies [137-140].

REFERENCES

[1] I.F. Akyildiz, D. M. G. Estevez., E.Ch.Reyes, "The Evolution to 4G Cellular Systems: LTE-Advanced,"*Physical Communication*, vol.3, no.4, December 2010, pp.217-244.

[2] F. Khan, "LTE for 4G Mobile Broadband - Overview of Inter-Cell Interference Coordination in LTE," United States of America by Cambridge University Press, 2009.

[3] D. Astely, E. , Dahlman, A. Furuskar, Y. Jading, M. Lindstrom, and S. Parkvall, "LTE: the Evolution of Mobile Broadband,"*IEEE Communications Magazine*, vol.47, no.4, 2009, pp.44-51.

[4] S. Sesia, I. Toufik, and M. Baker. LTE - The UMTS Long Term Evolution: From Theory to Practice,*Wiley*. 2011,pp. 1-648.

[5] C. Gessner, UMTS Long Term Evolution (LTE) Technology Introduction*: Rohde & Schwarz Products*, 2008.

[6] M. Rinne, O. Tirkkonen, " LTE, The Radio Technology Path Towards 4G," *Computer Communications*, vol.33, no.16, October 2010, pp.1894-1906.

[7] M. S. Sharawi, (2010). RF Planning and Optimization for LTE Networks. In L. S. a. J. Shen (Ed.), Evolved Cellular Network Planning and Optimization for UMTS and LTE, *CRC Press*, pp. 399–432.

[8] D.M.Sacristán, J. F. Monserrat, J.C.Peñuelas, D.Calabuig, S.Garrigas and N.Cardona, "On the Way towards Fourth-Generation Mobile: 3GPP LTE and LTE-Advance," *EURASIP Journal on Wireless Communications and Networking*, vol. 2009, no.4, March 2009, pp.1-10. doi: 10.1155/2009/354089

[9] S.Kumar, "Final Techniques for Efficient Spectrum Usage for Next Generation Mobile Communication Networks : An LTE and LTE-A Case Study," PhD Thesis, Aalborg University, Radio Access Technology Section, 2009.

[10] M. Rumney, "3GPP LTE: Introducing Single-Carrier FDMA". BSc, C. Eng, MIET, May 2010, http://cp.literature.agilent.com/litweb/pdf/5989-7898EN.pdf.

[11] 3GPP TS 36.211: "Evolved Universal Terrestrial Radio Access (E-UTRA); Physical Channels and Modulation", Version 8.8.0 Release 8, 2009.

[12] 3GPP TR 36.913, "Requirements for Further Advancements for Evolved Universal Terrestrial Radio Access (E-UTRA) (LTE-Advanced), Technical Report," December 2009.

[13] 3GPP R1 084026, "LTE-Advanced Evaluation Methodology," October 2008.

[14] S. Brueck, "Heterogeneous Networks in LTE-Advanced," *8th International Symposium on Wireless Communication Systems*, 2011, Aachen, pp.171-175.

[15] www.radiocomms.com.au

[16] 3GPP TS 36.423, "evolved Universal Terrestrial Radio Access Network (E-UTRAN); X2 Application Protocol (X2AP) (Release9)," 2010.

[17] A. Damnjanovic, J. Montojo, W. Yongbin, J. Tingfang, L. Tao, M. Vajapeyam and D. Malladi, "A Survey on 3GPP Heterogeneous Networks," *IEEE Wireless Communications*, vol, 18, no.3, February.2011, pp.10-21.

[18] J. C.Ikuno, M.Wrulich, and M. Rupp, " System Level Simulation of LTE Networks," *IEEE 71stVehicular Technology Conference (VTC 2010-Spring),* May 2010, pp.1-5.

[19] 3GPP TR 36.931, "LTE; Evolved Universal Terrestrial Radio Access (E-UTRA); Radio Frequency Requirements for LTE Pico NodeB", May. 2011.

[20] L. Jiang and M. Lei, "CQI Adjustment for eICIC Scheme in Heterogeneous Networks," *IEEE 23rd International Symposium on personal, Indoor and Mobile Radio Communications* (*PMRC*), September 2012, pp.487-492.

[21] 3GPP TR 25.942 "Universal Mobile Telecommunications System (UMTS); Radio Frequency (RF) system scenarios (version 11.0.0 Release 11)," October 2012.

[22] M. Masihpour and J. I. Agbinya, *Planning of WiMAX and LTE Networks (Part III): WiMAX and LTE Link Budget Planning and Optimisation of 3G and 4G Wireless Networks,* 2010, pp. 105 – 136, Denmark, River Publishers.

[23] M. Patzold, U. Killat, and F. Laue, "A Deterministic Digital Simulation Model for Suzuki Processes with Application to a Shadowed Rayleigh Land Mobile Radio Channel," *IEEE Transactions on Vehicular Technology,* vol. 45, no. 2, pp. 318-331, 1996.

[24] Wikipedia, "Rayleigh Fading," in http://en.wikipedia.org/wiki/Rayleigh_fading, accessed: 4 September 2011.

[25] Y.Chen, X. Wen, X.Lin, and W. Zheng, "Research on the Modulation and Coding scheme in LTE TDD Wireless Network," *International Conference onIndustrial Mechatronics and Automation* (*ICIMA*)*,* 2009, pp.468-471.

[26] A. Alexiou, Ch. Bouras, V.Kokkinos, A.Papazois, and G.Tsichritzis, "Multimedia Broadcasting in LTE Networks,"*Wireless Multi-Access Environments and Quality of Service Provisioning, IGI Global,* January 2012,pp.269-289.

[27] I.B. Aban, M.M. Meerschaert, and A.K. Panorska, "Parameter Estimation for the Truncated Pareto Distribution," *Journal of the American Statistical Association*, vol. 101, no. 473, March 2006, pp. 270-278

[28] G. Roche, A. Alayón Glazunov, and B. Allen, *LTE-Advanced and Next Generation Wireless Networks: Channel Modelling and Propagation*, Wiley, November 2012, 566 pages, ISBN: 978-1-1199-7670-7.

[29] 3GPP TR 36.942, "E-UTRA Radio Frequency (RF) System Scenarios," V8.3.0, September 2010.

[30] 3GPP R1-100350, "Downlink CCH Performance Aspects for Co-channel Deployed Macro and HeNBs," TSG RAN WG1 Meeting #59bis, Nokia Siemens Networks, Nokia, January 2010.

[31] D. Kimura, Y. Harada, and H. Seki, "De-Centralized Dynamic ICIC Using X2 Interfaces for Downlink LTE Systems," *IEEE 73rd Vehicular Technology Conference* (*VTC*), 2011, pp.1-5.

[32] F.Khan, *LTE for 4G Mobile Broadband: Air Interace Technologies and performance*. Cambridge University Press, 2009.

[33] G.D.Gonz´alez, M. G. ozano., S.Ruiz, and J.Olmos, "Static Inter-Cell Interference Coordination Techniques for LTE Networks A Fair Performance Assessment," *3th International Conference on Multiple Access Communications,* 2010, pp. 211-222

[36] S. E. Elayoubi,O.B.Haddada,and B. Fourestie, "Performance Evaluation of Frequency Planning Schemes in OFDMA-based Network," *IEEE Transactions on Wireless Communications,* vol.7, no.5, 2008, pp.1623-1633.

[37] X. Zhang,Ch. He, L. Jiang, and J. Xu , "Inter-cell Interference Coordination based on Softer Frequency Reuse in OFDMA Cellular Systems," *International Conference on Neural Networks and Signal Processing*, June 2008, pp.270 – 275.

[38] 3GPP R1-060135, "Interference Mitigation by Partial Frequency Reuse," RAN WG1#42, Siemens, London, UK, January 2006.

[39] 3GPP R1-050507, "Soft Frequency Reuse Scheme for UTRANLTE," RAN WG1#41, Huawei, Athens, Greece, May 2005.

[40] R. Kwan,and C. Leung, " A Survey of Scheduling and Interference Mitigation in LTE," *Journal of Electrical and Computer Engineering,* 2010, pp.1-10.

[41] R. Ghaffar and R. Knopp, "Fractional Frequency Reuse and Interference Suppression

for OFDMA Networks," *8th International Modelling and Optimization in Mobile, Ad Hoc and Wireless*, June 2010, pp. 273 – 277.

[42] F. B. Mugdim, "Interference Avoidance Concepts," WINNER II project, 2007.

[43] E. Haro, S. Ruiz, D. Gonzalez, M.G-Lozano, and J. Olmos, "Comparison of Different Distributed Scheduling Strategies for Static/Dynamic LTE Scenarios," Technical University of Wien, 2009

[44] IEEE 802.16 Broadband, "Fractional Frequency Reuse in Uplink," *LG Electronics*, 2008.

[45] M. Porjazoski and B. Popovski, "Analysis of Intercell Interference Coordination by Fractional Frequency Reuse in LTE," *Software, Telecommunications and Computer Networks (SoftCOM) Conference*, 2010, pp. 160-164.

[46] M. Porjazoski and B. Popovski, "Contribution to Analysis of Intercell Interference Coordination in LTE: A Fractional Frequency Reuse Case," *Global Mobile Congress (GMC)*, 2010, pp. 1-4.

[47] A. Mills, D. Lister and M. De Vos, "Understanding Static Inter-cell Interference Coordination Mechanisms in LTE," *Journal of Communications*, vol.6, no.4, July.2011, pp.312-318.

[48] S. Kumar, G. Monghal, J. Nin, I. Ordas, K. I. Pedersen, and P. E. Mogensen, "Autonomous Inter Cell Interference Avoidance under Fractional Load for Downlink Long Term Evolution," *IEEE 69th Vehicular Technologies Conference (VTC),* April 2009, pp.1-5.

[49] L. Liu, G. Zhu, D. Wu, "A Novel Fractional Frequency Reuse Structure Based on Interference Avoidance Scheme in Multi-cell LTE Networks," 6th *International ICST Conference on Communications and Networking in China* (*CHINACOM*), August 2011, pp.551 – 555.

[50] L. Liu, D. Qu, and T. Jiang, "Dynamic Fractional Frequency Reuse based on Interference Avoidance Request for Downlink OFDMA Cellular Networks," *6th International Wireless Communications and Mobile Computing Conference* (*IWCMC*), July 2010, Caen, France, pp.381-386.

[51] Z. Xie and B. Walke, "Resource Allocation and Reuse for Inter-cell Interference Mitigation in OFDMA based Communication Networks," 5th *Annual ICST Wireless Internet Conf.* (*WICON*), 2010, pp. 1-6.

[52] L. Dong, and W.Wenbo, "A Novel Semi-Dynamic Intercell Interference Coordination

Scheme based on UE Grouping," *IEEE 70th Vehicular Technology Conference*, 2009, pp.1-5.

[53] G. Li and H. Liu, "Downlink Radio Resource Allocation for Multi-Cell OFDMA System," *IEEE Transactions on Wireless Communications*, vol. 5, no.12, 2006, pp. 3451-3459.

[54] A. Triki and L. Nuaymi, "Intercell Interference Coordination Algorithms in OFDMA Wireless Systems," in *Proc. IEEE 73rd Vehicular Technology Conference* (*VTC Spring*), 2011, pp. 1-6.

[55] Ch.You, Ch.Seo, Sh.Portugal, G.Park, T. Jung, H.Liu and I.Hwang, "Intercell Interference Coordination using Threshold-Based Region Decisions," *Wireless Personal Communications*, vol. 59, no.4, 2011, pp.789-806.

[56] M. Qian, W. Hardjawana, Y. Li, B. Vucetic, J. Shi, and X. Yang, "Inter-cell Interference Coordination through Adaptive Soft Frequency Reuse in LTE Networks," *IEEE Wireless Communication and Networking Conference: MAC and Cross-Layer Design*, 2012, pp.1618-1623.

[57] Y. Yu, E. Dutkiewicz, X. Huang, and M. Mueck, " A Resource Allocation Scheme for Balanced Performance Improvement in LTE Networks with Intercell Interference," *IEEE Wireless Communication and Networking conference: MAC and Cross-layer Design*, 2012, pp. 1630-1635.

[58] M. Osborne and A. Rubinstein, *A Course in Game Theory*. MIT Press, 1994.

[59] M. Iturralde, A. Wei, T. Ali Yahiya, and A.L. Beylot, "Resource Allocation for Real Time Services using Cooperative Game Theory and a Virtual Token Mechanism in LTE Networks," *IEEE Conference on Consumer Communications and networking* (*CCNC*), January 2012, pp.879-883.

[60] L.Shuhui, C.Yongyu, Y.Ruiming, and Y.Dacheng, "Efficient Distributed Dynamic Resource Allocation for LTE Systems," *IEEE Vehicular Tecnology conference (VTC)*, 2011, pp.1-5.

[61] H. Kwon, and B.G. Lee, "Distributed Resource Allocation through Non-Cooperative Game Approach in Multi-cell OFDMA Systems," *IEEE International Conference on Communications* (*ICC*), 2006, pp. 4345-4350.

[62] M. Rahman, and, H. Yanikomeroglu, "Enhancing Cell-edge Performance: A Downlink Dynamic Interference Avoidance Scheme with Intercell Coordination," *IEEE Transaction on Wireless Communications*, vol.9, no.4, 2010, pp.1414-1425.

[63] M. Rahman, H. Yanikomeroglu, and W. Wong, "Interference Avoidance with Dynamic Inter-Cell Coordination for Downlink LTE System," *IEEE Wireless Communications and Networking Conference (WCNC)*, 2009, pp.1-6.

[64] H.W. Khun, "The Hungarian Method for the Assignment Problem," *Naval Research Logistic Quarterly*, vol. 2, 1955, pp. 83-97,

[65] P.Vlacheas, E. Thomatos, K. Tsagkaris, and P. Demestichas, "Autonomic Downlink Inter-cell Interference Coordination in LTE Self-Organizing Networks," 7th *International Conference on Network and Service Management* (*CNSM*), 2011, pp.1-5.

[66] S. Boyd and L. Vandenberghe, *Convex Optimization*, Cambridge University Press, 2004.

[67] A. Giovanidis, Q. Liao, and S. Stanczak, "A Distributed Interference-aware Load Balancing Algorithm for LTE Multi-Cell Networks," *International ITG Workshop on Smart Antenna* (*WSA*), 2012, pp.28-35.

[68] M.C. Necker, " Scheduling Constraints and Interference Graph Properties for Graph-based Interference Coordination in Cellular OFDMA Networks," *Mobile Networks and Applications,* vol. 14, no.4, 2009, pp.539-550.

[69] M.C. Necker, "Towards Frequency Reuse 1 Cellular FDM/TDM Systems," *9th ACM/IEEE international symposium on modeling, analysis and simulation of wireless and mobile system* (*MSWiM*), October 2006, pp.338-346.

[70] Y.J. Chang, Z. Tao, J. Zhang and C.C. J. Kuo, "A Graph-Based Approach to Multi-Cell OFDMA Downlink Resource Allocation," *IEEE GLOBECOM*, December 2008, pp. 1 – 6

[71] I. Karla, " Distributed Algorithm for Self Organizing LTE Interference Coordination," *Mobile Networks and Management*, Springer Berlin Heidelberg, vol. 32, 2010, pp.119-128.

[72] T. Szymanski, "Interference and Power Minimization in TDMA-OFDMA Infrastructure Wireless Mesh Networks," *5th International Conference on Systems and Networks Communications (ICSNC),* August.2010, pp. 348 –355.

[73] D. Br´elaz, "New Methods to Colour the Vertices of a Graph," *Communications ACM*, vol. 22, no.4, April 1979, pp. 251–256.

[74] E. Aarts and J. K. Lenstra, Eds., *Local Search in Combinatorial Optimization*, 1st ed. New York, NY, USA: John Wiley & Sons, Inc.,1997.

[75] Ch.Y. Yu, C. Jie, and Y.D. Cheng, " A Novel Inter-Cell Interference Coordination Scheme based on Dynamic Resource Allocation in LTE-TDD Systems," *IEEE 71st Vehicular Technology Conference* (*VTC*) , May 2010, pp.1-5.

[76] Q. Ai, P. Wang, F. Liu, Y. Wang, F. Yang and J. Xu, "QoS-Guaranteed Cross-Layer Resource Allocation Algorithm for Multiclass Services in Downlink LTE System," *International Conference on Wireless Communications and Signal Processing* (*WCSP*), October. 2010, pp.1-4.

[77] Z.Bingbing, C.Liquan, Y.Xiaohui, and W.Lingling, "A Modified Inter-Cell Interference Coordination Algorithm in Downlink of TD-LTE," 6th *International Conference on Wireless Communications Networking and Mobile Computing* (*WiCOM*), 2010, pp.1-4.

[78] G. Fodor, Ch. Koutsimanis, A. Racz, N. Reider, A. Simonsson, and W. Muller, "Intercell Interference Coordination in OFDMA Networks and in the 3GPP Long Term Evolution System," *Journal of Communications*, vol.4, no.7, August 2009, pp.445-453.

[79] G. Boudreau, J. Panicker, N. Guo, R. Chang, N. Wang, and S. Vrzic, "Interference Coordination and Cancellation for 4G Networks," *IEEE Communications Magazine,*vol.47, no.4, April 2009, pp. 74 – 81.

[80] A.S. Hamza, S.S. Khalifa, H.S. Hamza, and K. Elsayed,,' A Survey on Inter-Cell Interference Coordination Techniques in OFDMA-Based Cellular Networks' , *IEEE Communications Surveys & Tutorials*, vol. 15, no. 4, Fourth Quarter 2013, pp.1642-1670.

[81] 3GPP, TS 23.203, "Digital Cellular Telecommunications System (Phase 2+); Universal Mobile Telecommunications System (UMTS); LTE; Policy and Charging Control Architecture", V10.6.0., 2012.

[82] L. Zadeh, (1965)"Fuzzy sets", *Information Control*, Vol. 8,No.3, pp.338–353.

[83] T. Ross, (1995). *Fuzzy Logic with engineering application*, McGraw-Hill.

[84] S. Sesia, I. Toufik, M. Baker, (2011). *LTE - The UMTS Long Term Evolution: From Theory to Practice*, Wiley, pp. 1-648.

[85] H. Holma, and A.Toskala. *LTE for UMTS, OFDMA and SC-FDMA based Radio Access*. Wiley, 2009.

[86] J. G. Andrews, "Seven Ways that HetNets Are a Cellular Paradigm Shift," ," *IEEE Communications Magazine*, vol.51, no.3, March.2013, pp.136-144.

[87] 3GPP, "Mobile Broadband Innovation Path to 4G: Release 9,10 and Beyond," February, 2010, www.3GAmericas.org.

[88] 3GPP TR 36.871, "Evolved Universal Terrestrial Radio Access (E-UTRA); Downlink Multiple Input Multiple Output (MIMO) Enhancement for LTE-Advanced." December 2011.

[89] Ch. Kosta, B. Hunt, A. U. Quddus, and R. Tafazolli, "On Interference Avoidance through Inter-Cell Interference Coordination (ICIC) based on OFDMA Mobile Systems," *IEEE Communications Survey & Tutorials*, vol.15, no.3, Third Quarter 2013, pp. 973-995

[90] S. Deb, P. Monogioudis, J. Miernik, and J.P. Seymour, "Algorithms for Enhanced Intercell Interference Coordination (eICIC) in LTE HetNets," *IEEE/ACM Transactions on Networking*, 99, March 2013, pp. 1-13.

[91] 3GPP TS 136.300, "Evolved Universal Terrestrial Radio Access (E-UTRA) and Evolved Universal Terrestrial Radio Access Network (E-UTRAN); Overall Description; Stage 2 (Release 10)," 2011.

[92] B. Soret, and K.I. Pedersen, "Macro Transmission Power Reduction for HetNet Co-Channel Deployments," *IEEE Globcom, Wireless Communication Symposium*, 2012, pp.4126-4130.

[93] A. Morimoto, N. Miki, and Y. Okumura "Performance Evaluation of Reduced Power Inter-cell Interference Coordination for Downlink in LTE-Advanced Heterogeneous Networks," *European Wireless*, Guildford, UK, April 2013, pp.1-6.

[94] A. Damnjanovic, J. Montojo, Y.Wei, Ti.Ji, T. Luo,Ma.Vajapeyam, T.Yoo, O.Song, and D.Malladi, "A Survey on 3GPP Heterogeneous Networks", *IEEE Wireless Communications*, vol.18, no.3, June.2011, pp. 10-21.

[95] 3GPP TS 36.104, "Technical Specification Group Radio Access Network; Evolved Universal Terrestrial Radio Access (E-UTRA); Base Station (BS) Radio Transmission and Reception", December 2011.

[96] S. Ye, Sh.H. Wong, and Ch. Worrall, "Enhanced Physical Downlink Control Channel in lTE Advanced Release 11," *IEEE Communications Magazine*, vol.51, no.2, February 2013, pp.82-89.

[97] 3GPP R1-104968, "Summary of the Description of Candidate eICIC Solutions," Madrid, Spain, August2010.

[98] M. Shirakabe, A.Morimoto, and N. Miki, " Performance Evaluation of Inter-cell Interference Coordination and Cell Range Expansion in Heterogeneous Networks for LTE-Advanced Downlink" *8th International Symposium on Wireless Communication Systems* (*ISWCS*), November 2011, pp. 844 - 848.

[99] S.N.S. Kshatriya, S. Kaimalettu, S.R. Yerrapareddy, K. Milleth, and N. Akhtar, "On Interference Management based on Subframe Blanking in Heterogeneous LTE Networks," *Fifth International Conference on Communication Systems and Networks* (*COMSNETS*), Bangalore, January 2013, pp.1-7.

[100] K. Okino, T. N., C. Yamazaki, H. Sato, and Y. Kusano, "Pico Cell Range Expansion with Interference Mitigation toward LTE-Advanced Heterogeneous Networks," *IEEE International Conference on the In Communications Workshops* (*ICC*), June 2011, pp.1-5.

[101] J. Pang, J. Wang, G. Shen, Q. jiang, and J. Liu, "Optimized Time-Domain Resource Portioning for Enhanced Intercell Interference Coordination in Heterogeneous Networks," *IEEE Wireless Communication and Networking Conference: MAC and Cross-Layer Design*, April 2012, pp.1613-1617.

[102] J. Wang, J. Liu, D. Wang, J. Pang, and G. Shen, "Optimized Fairness Cell Selection for 3GPP LTE-A Macro-Pico HetNets," *IEEE 74th Vehicular Technology Conference* (*VTC-Fall*), San Francisco, United States, September 2011, pp.1-5.

[103] L. Jiang and M. Lei, "Resource Allocation for eICIC Scheme in Heterogeneous Networks," *IEEE 23rd International Symposium on Personal, Indoor and Mobile Radio Communications* (*PMRC*), September 2012, pp.464-469.

[104] J. Nash, "The Bargaining Problem", *Econometrica*, vol. 18, no. 2, April 1950, pp. 155-162

[105] Z. Han, Z. Ji, and K.J. Liu, "Fair Multiuser Channel Allocation for OFDMA Networks using Nash Bargaining Solutions and Coalitions," *IEEE Transactions on Communications*, vol. 53, 2005, pp. 1366-1376.

[106] S. Deb, P.Monogioudis, J. Miernik, J.P. Seymour, "Algorithms for Enhanced Inter-Cell Interference Coordination (eICIC) in LTE HetNets," *IEEE/ACM Transactions on Networking*, vol.22 , no. 1, February 2014,pp. 137 – 150.

[107] A. Nedic and A. E. Ozdaglar, "Sub-gradient Methods in Network Resource Allocation: Rate Analysis," *42nd Annual Conference on Information Sciences and Systems* (*CISS*), Princeton, 2008, pp. 1189–1194.

[108] Rawi, M. Simsek, and R. Jantti, "Utility-based Resource Allocation in LTE-Advanced Heterogeneous Networks," *9th International Wireless Communications and Mobile Computing Conference* (*IWCMC*), Sardinia, July 2013,pp. 826 – 830.

[109] M. Al-Rawi, J. Huschke, and M. Sedra, "Dynamic Protected-Subframe Density Configuration in LTE Heterogeneous Networks," *21th international Conference on Computer Communication and Networks* (*ICCCN*), August 2012, pp.1-6.

[110] J. Wang, X. She, and L. Chen, "Enhanced Dynamic Inter-cell Interference Coordination Scheme for LTE-Advanced," *IEEE 75th Vehicular Technology Conference* (*VTC spring*), May 2012, pp.1-6.

[111] L. Jiang and M. Lei, "CQI Adjustment for eICIC Scheme in Heterogeneous Networks," *IEEE 23rd International Symposium on Personal, Indoor and Mobile Radio Communications* (*PMRC*), September 2012, pp.487-492.

[112] 3GPP R1-110103, "Consideration on Periodic CSI Reporting and RLM in eICIC," TSG-RAN WG1 # 63bis, January 2011.

[113] D. Lopez-Perez, and C.Xiaoli, "Inter-Cell Interference Coordination for Expanded Region Picocells in Heterogeneous Networks," *20th International Conference on the Computer Communications and Networks* (*ICCCN*), July.2011, pp.1-3.

[114] J. Huang, P. Xiao, and X.Jing, "A Downlink ICIC Method based on Region in the LTE-Advanced System," *IEEE 21st International Symposium on the Personal, Indoor and Mobile Radio Communications Workshops* (*PIMRC Workshops*), September 2010, pp.420-423.

[115] L. *Qiming, D. Xiao, and D.Yang, "*A Downlink ICIC Method based on Priority in LTE-Advanced Systems,*" Proc. of IEEE IC-BNMT,* 2011, pp.498-501..

[116] L.Bo, and Y.Da-cheng, "Inter-cell Downlink Co-channel Interference Management through Cognitive Sensing in Heterogeneous Network for LTE-A," *The Journal of China Universities of Posts and Telecommunications,* vol.18, no.2, April 2011, pp. 25–32.

[117] V. Capdevielle, A. Feki, and E.Temer, " Enhanced Resource Sharing Strategies for LTE Picocells with Heterogeneous Traffic Loads," *IEEE 73rd Vehicular Technology Conference* (*VTC Spring*), May 2011, pp.1-5.

[118] Ch.S.Chiu, and Ch.Ch. Huang, " An Interference Coordination Scheme for Picocell Range Expansion in Heterogeneous Networks," *IEEE 73rd Vehicular Technology Conference* (*VTC Spring*), May 2012, pp. 1-6.

[119] P. Tian, H. Tian, J. Zhu, L. Chen, and X. She, "An Adaptive Bias Configuration Strategy for Range Extension LTE-Advanced Heterogeneous Networks", *IET International Conference on Communication Technology and Application* (*ICCTA*), 2011, pp. 336 – 340,

[120] A. Gosavi, "Reinforcement Learning: A Tutorial Survey and Recent Advances", *INFORMS Journal on Computing Spring*, vol.21, no.2, pp.178-192, 2009.

[121] E. H. Mamdani, and S. Assilion, "An Experiment in Linguistic Synthesis with a Fuzzy Logic Controller," *International Journal of Man-Machine Studies* , 1974, vol. 7, no.1, pp.1-13.

[122] H.R. Berenji, "Fuzzy Q-Learning: A New Approach for Fuzzy Dynamic Programming," *IEEE World Congress on Computational Intelligence Fuzzy Systems*, 1994, pp. 486-491.

[123] R.L. Haupt, S.E. Haupt, *Practical Genetic Algorithms*. Second Edition, New Jerey, Wily, 2004.

[124] K. Deb, *Multi-Objective Optimization using Evolutionary Algorithms Chichester [u,a]*: Wiley, 2002.

[125] D. L´opez-P´erez, X. Chu, and I. Guvenc, "On the Expanded Region of Picocells in Heterogeneous Networks," *IEEE Journal of Selection Topics Signal Processing*, vol. 6, June 2012, pp. 281–294.

[126] T. D. Novlan, R. K. Ganti, A. Ghosh, and J. G. Andrews, "Analytical Evaluation of Fractional Frequency Reuse for Heterogeneous Cellular Networks," *IEEE Transaction on Communications*, vol. 60, July 2012, pp. 2029 –2039.

[127] I. Guvenc, "Capacity and Fairness Analysis of Heterogeneous Networks with Range Expansion and Interference Coordination," *IEEE Communications Letter*, vol. 15, October 2011, pp. 1084–1087.

[128] Q. Ye, B. Rong, Y. Chen, M. Al-Shalash, C. Caramanis, and J. G. Andrews, "User Association for Load Balancing in Heterogeneous Cellular Networks," *IEEE Transactions on Wireless Communication*, vol. 12, no. 6, 2013, pp. 2706– 2716.

[129] H. Tang, J. Peng, p. Hong, and K. Xue, "Offloading Performance of Range Expansion in Picocell Networks: A Stochastic Geometry Analysis," *IEEE Wireless Communications Letters*, vol.2, No.5, October 2013, pp. 511-514.

[130] S. Singh, and J.G. Andrews, " Joint Resource Partitioning and Offloading in

Heterogeneous Cellular Networks," Available: http://arxiv.org/abs/1303.7039.

[131] S. Singh, H. S. Dhillon, and J. G. Andrews, "Offloading in Heterogeneous Networks: Modelling, Analysis, and Design Insights," *IEEE Transaction on Wireless Communication*, vol. 12, no. 5, May 2013, pp. 2484–2497.

[132] M. Cierny, H. Wang, R. Wichman, Zh. Ding, and C. Wijting, "On Number of Almost Blank Subframes in Heterogeneous Cellular Networks," *IEEE Transactions on Wireless Communication*, vol.12, no.10, October 2013, pp. 5061-5073.

[133] H. S.Jo, Y.J. Sang, P.Xia, and J.G. Andrew, "Heterogeneous Cellular Networks with Flexible Cell Association: A Comprehensive Downlink SINR," *IEEE Transactions on Wireless Communication*, vol.11, no. 10, October 2012, pp.3484-3494.

[134] A. Khoryaev, A. Chervyakov, M. Shilov, S. Panteleev, and A. Lomayev, "Performance Analysis of Dynamic Adjustment of TDD Uplink-Downlink Configurations in Outdoor Picocell LTE Networks," *4th International Congress on Ultra-Modern Telecommunications and Control Systems and Workshops* (*ICUMT*), October. 2012, pp.2157-0221.

[135] Y. Wang, Y.Chang, and D.Yang, "An Efficient Inter-Cell Interference Coordination Scheme in Heterogeneous Cellular Networks," *IEEE Vehicular Technology Conference* (*VTC Fall*), Quebec City, September 2012, pp.1 – 5.

[136] J. Hyoungju, K. Younsun, Ch.Seunghoon, Ch. Joonyoung, and L. Juho, "Dynamic Resource Adaptation in beyond LTE-A TDD Heterogeneous Networks," *IEEE International Conference on Communications Workshops* (*ICC*), Budapest, June 2013, pp. 133 - 137

[137] S. Hong, J. Brand, J.I. Choi, .ain, J. Mehlman, S. Katti, and P. Levis, "Applications of Self-Interference Cancellation in 5G and Beyond," *IEEE Communications Magazine,* vol.52, no.2, February 2014, pp.114 – 121.

[138] W. Nam, D. Bai, J. Lee, and I. Kang, "Advanced Interference Management for 5G Cellular Networks," *IEEE Communications Magazine*, vol.52, No.5, May 2014, pp.52 – 60.

[139] S. Chen, and J. Zhao, "The Requirements, Challenges, and Technologies for 5G of Terrestrial Mobile Telecommunication," *IEEE Communications Magazine,* vol.52 , no.5 , May 2014, pp.36 – 43.

[140] E. Hossain, M. Rasti, H. Tabassum, And A. Abdelnasser, "Evolution toward 5G Multi-Tier Cellular Wireless Networks: An Interference Management Perspective," *IEEE*

Wireless Communications, vol.21, no.3, June 2014, 118 – 127.